Climate Change and Energy Systems

Impacts, Risks and Adaptation in the Nordic and Baltic countries


norden

Climate Change and Energy Systems

Impacts, Risks and Adaptation in the Nordic and Baltic countries

Edited by Thorsteinn Thorsteinsson and Halldór Björnsson

TemaNord 2011:502

Climate Change and Energy Systems
Impacts, Risks and Adaptation in the Nordic and Baltic countries

Edited by Thorsteinn Thorsteinsson and Halldór Björnsson

TemaNord 2011:502
ISBN 978-92-893-2190-7

Print: Arco Grafisk A/S
Copies: 1.200

Cover photo: B-Line

Printed in Denmark

This publication has been published with financial support by the Nordic Council of Ministers. But the contents of this publication do not necessarily reflect the views, policies or recommendations of the Nordic Council of Ministers.

Nordic co-operation

Nordic co-operation is one of the world's most extensive forms of regional collaboration, involving Denmark, Finland, Iceland, Norway, Sweden, and Faroe Islands, Greenland, and Åland.

Nordic co-operation has firm traditions in politics, the economy, and culture. It plays an important role in European and international collaboration, and aims at creating a strong Nordic community in a strong Europe.

Nordic co-operation seeks to safeguard Nordic and regional interests and principles in the global community. Common Nordic values help the region solidify its position as one of the world's most innovative and competitive.

Nordic Council of Ministers
Ved Stranden 18
DK-1061 København K
Phone (+45) 3396 0200

www.norden.org

Content

Preface

The project *Climate and Energy Systems: Risks, Potential and Adaptation (CES),* was one of 16 research projects selected to form part of Nordic Energy Research´s 2007–2010 strategy and action plan. Involving nearly 100 scientists at 33 institutions in all Nordic and Baltic countries, the CES project contributed to NER's purpose of adding Nordic value to national research programs and activities within the energy sector. The main goal of the project was to study the impacts of projected climate change on renewable energy sources in the Nordic and Baltic region up to 2050 and assess the development of the Nordic electricity system until 2020.

The total budget of the *Climate and Energy Systems* project amounted to 18,235,000 NOK. With a contribution of 10 million NOK, Nordic Energy Research contributed more than 50% of the funding. Nordic energy companies, i.e. the National Power Company in Iceland, Statkraft in Norway, DONG Energy in Denmark, Elforsk in Sweden and the Finnish Energy Industries provided funds amounting to 5,800,000 NOK. The participating research institutes financed the remaining part of the budget.

This final report of the CES project starts with a Summary of main results and describes project aims and structure in Chapter 1. The present use of renewable energy resources in the Nordic and Baltic countries and near-future prospects are outlined in Chapter 2. These chapters were written by the report editors and project administrators. Chapters 3–11 present main results from the research carried out by CES working groups; on climate scenarios, time-series analysis, hydropower, wind power, bio-fuels, energy systems and risk analysis. The lead authors of these chapters coordinated the working group activities within the project on the national and international level. The report concludes with an update of recent developments in the global climate system (Appendix 1) and finally lists CES participants who contributed to this report (Appendix 2). At the end of Chapters 3–11, scientific papers produced in the course of the project are listed. Not all of these works are cited in the text. More detailed information on publications resulting from the project is given on the project webpage: http://en.vedur.is/ces.

The recent development and implementation of the Top-level Research Initiative (TRI) by the Nordic Council of Ministers, managed by *NordForsk, Nordic Innovation Centre* and *Nordic Energy Research* shows the serious approach taken by the Nordic Council of Ministers regarding a Nordic response to the impact of climate change. Partners in *Climate and Energy Systems* took part in formulating two projects funded by TRI. These are (i) *ICEWIND*, led by the Risø National Laboratory in Denmark and funded under the TRI program *Integration of large-scale wind pow-*

er; and (ii) *SVALI*, led by the University of Oslo and the Icelandic Meteorological Office and funded by the TRI program *Interaction between climate change and the cryosphere.*

The success in obtaining funding for these new projects demonstrates the positive results of long-term Nordic investment in the buildup of capabilities, technology transfer and research innovation within research sectors that are essential in addressing future challenges in the adaptation to climate change.

Summary

Introduction

This report summarises results from the recently completed research project *Climate and Energy Systems* (CES), which delivered a new assessment of the future development of renewable energy resources in the Nordic and Baltic Regions. The project focused on climate impacts within the energy sector, addressing both the positive aspects as well as the increased risks associated with expected climate change up to the mid-21st century. Main results produced by CES working groups are briefly summarised in this chapter.

Statistical analysis of hydrological and meteorological time series

The research group focusing on statistical analyses of hydrological and meteorological time series within the CES project made use of data from the Nordic stream-flow database, which consists of 160 series of daily discharge data from Denmark, Finland, Iceland, Norway and Sweden, to analyse long-term trends at individual stations within the Nordic region. Long-term trends in regional series have also been analysed based on precipitation, temperature and discharge records available in the individual countries.

The regional series analyses undertaken all point towards a positive anomaly in annual temperature in recent years, relative to the reference period 1961–1990. Results for precipitation and runoff are much more variable, both between countries and between regions in individual countries. An increase in annual precipitation occurred in Denmark, Norway and southern Iceland and annual runoff increased up to the year 2000 in these same areas and as well as in northern Sweden. Seasonal analysis of runoff anomalies for the Baltic countries indicates a marked increase in winter runoff throughout the region, and a decrease in summer runoff.

A strong negative trend in the timing of spring snowmelt (i.e. earlier snowmelt) is found for many of the stations in the Nordic Region. Analysis of the occurrence of peak flow events exceeding the mean annual maximum flood suggests a pattern of spatial variability, with some stations (for example, in western Norway and in Denmark) exhibiting an increase in the total number of events, and other stations (in Sweden, Finland and parts of Denmark) exhibiting a decrease. For the Baltic re-

gion, the analysis of the timing of the spring flood maximum discharge suggests an earlier spring flood due to an earlier spring snowmelt.

Climate scenarios for the Nordic and Baltic region

Regional climate models (RCMs) were used in CES to produce high-resolution (25x25 km) climate scenarios for the Nordic and Baltic region. From an ensemble consisting of 15 RCM climate change simulations, three were selected for use in targeted studies within CES, with focus on the period 2021–2050. Some of the working groups in CES have used scenarios for the entire 21st century in their modelling studies. All three models project a summer temperature increase of at most 2°C over most of the region for the period 2021–2050, in comparison with the control period 1961–1990. Increases in winter temperatures will be more variable and most pronounced (up to 4°C) in the eastern and northern areas. In particular, there is a strong response to the general warming over the northernmost oceans where feedback mechanisms associated with retreating sea-ice come into play. The largest precipitation increase will generally be seen in winter. In summer, there is a larger uncertainty and the possibility that precipitation will decrease in southern parts of the region cannot be excluded, although several regional simulations indicate that summertime precipitation could increase over the Baltic Sea. Wind speed changes are generally small with the exception of areas that will see a reduction in sea-ice cover, where wind speed is projected to increase.

The analysed RCM scenarios sample only a part of the full uncertainty range for the future climate. This is true both for the 15 selected scenarios and even more so for a subset of 3 scenarios used in most of the impact studies within the project. In order to characterize the full spread in a better way probabilistic climate change signals were calculated based on a larger ensemble of general circulation models (GCMs). It was found that the selected RCM-scenarios in general fit well within the distributions inferred from the wider range of GCM climate scenarios. However, for some variables, regions and seasons there are deviations where the RCM scenarios deviates from the general picture. The results clearly indicate that one should be careful with drawing far-reaching conclusions based on individual model simulations.

CES climate modelers have also downscaled results from global climate models to higher resolution (1–3 km), producing spatially more detailed scenarios than the standard 25 km simulations. The largest differences are seen in mountainous areas, but coastal effects also come into play. Biases are observed in those high-resolution model outputs, when compared with observations, calling for the development and application of bias correction techniques.

Additional work done by the climate modeling group involved examination of the inter-annual variability of future climate, studies of the migration of climatic zones, assessment of 21st century precipitation trends in selected regions, studies of the characteristics of North Atlantic Cyclones, studies of storm statistics and future changes in surface geostrophic wind speeds, solar radiation projections and the possible future change in climate extremes in the CES area of interest, as determined by a range of General Circulation Models (GCMs).

Modelling future changes in glacier volumes and glacial runoff

Changes in glacier mass balance and associated changes in river hydrology are among the most important consequences of future climate change in Iceland, Greenland and some glaciated watersheds in Scandinavia. As an example, glaciers and ice caps cover 11% of the surface area of Iceland and hydropower plants harnessing the potential energy of glacial rivers produce 75% of the country´s electricity demand. Since 1995, the mass balance of all major ice caps in Iceland has been negative and runoff data from glaciated watersheds show a clear increase in glacial melt during this period. Within the CES project, the main focus has been on the period 2021–2050 in order to assess changes that affect decisions related to investments and operational planning of power plants and energy infrastructure that need to be made in the near future.

The snow and ice group used temperature and precipitation scenarios produced within CES and related projects to simulate changes in glacier volume and runoff up to 2050. The simulations were carried out with coupled mass-balance/ice-flow models and with mass-balance and hydrological models coupled to volume–area glacier-scaling models. Results indicate the most glaciers and ice caps in the Nordic countries, except the Greenland ice sheet, will be dramatically reduced in volume in the coming decades and are projected to essentially disappear in the next 100–200 years. Runoff from ice-covered areas in the period 2021–2050 may increase by on the order of 50% with respect to the 1961–1990 baseline. About half of this change has already taken place in Iceland. Furthermore, there will be large changes in runoff seasonality and the diurnal runoff cycle. The projected runoff change may be important for the design and operation of hydroelectric power plants and other utilisation of water.

Climate change impacts on hydrology and hydropower systems

The work of the hydrology group in CES focused on climate impacts on hydropower production and on dam safety studies based on ensembles of up-to-date regional climate scenarios. Catchment-scale modelling of river runoff was carried out for selected basins in Scandinavia, Iceland and the Baltic region. Uncertainties in simulations derived from ensembles of regional climate scenarios were explored and the need for improving the interface between climate models and hydrological models was addressed. An improved methodology to cope with impacts on lake and river regulation in a changing climate has also been studied, in particular for large lakes. Finally, a comparison of Nordic design flood standards under present and future climate conditions was carried out.

There is little doubt that the Nordic and Baltic hydropower systems will be affected strongly by the projected climate changes. In general, the potential for hydropower production is predicted to increase, although water shortage may become a problem in some locations for the summer season. Given earlier snowmelt and reduced snow storage, the occurrence of large snowmelt floods is likely to become more seldom. The combined effect of an increase in rainfall intensity, number of rainfall events and total rainfall volume will most likely provide conditions that may be expected to yield larger rain floods.

For Sweden, simulations focused on extreme floods, dam safety and design flood determination. For 100-year floods, hydrological results based on 16 regional climate scenarios show varying climate impacts in the period 2021–2050. In the central part of the country, 100-year floods are likely to decrease in size, mainly due to decreasing snowmelt floods in spring, while rain-fed floods in southern Sweden indicate the opposite tendency.

For watersheds in western Norway and Iceland, some of which are partially glacier-covered, simulations indicate a runoff increase of 3–40% in 2021–2050 when compared with the control period 1961–1990. For the five largest hydropower-producing rivers in Finland, a 5–10% increase in discharge is predicted, a clear increase in winter runoff and earlier occurrence of spring runoff peaks. For the Aiviekste river basin in Latvia, a 19–27% discharge increase is predicted for 2021–2050, whereas decreasing discharge is simulated for the river Nemunas in Lithuania after 2020. It is not clear to what extent these contrasting runoff changes in the Baltic rivers are caused by natural climate variability rather than a deterministic climate change trend.

Projecting future wind climates in the Nordic and Baltic region

The importance of wind energy is increasing, accounting for 39% of all new electricity-generating installations worldwide in 2009. The amount of wind power generated in the Nordic countries at the end of year 2010 was 3800 MW in Denmark, 2200 MW in Sweden, 400 MW in Norway and 200 MW in Finland. Wind power is currently not utilised in Iceland. The production of wind power is expected to grow significantly both on land and offshore in the Nordic and Baltic region in coming years.

The wind power group's contribution within the CES project was to project possible future wind climates and to assess the sources and magnitudes of uncertainties. Moreover, given that wind climates over the CES domain exhibit high year-to-year and decade-to-decade variability due to natural (or inherent) climate variability, efforts have been made to quantify how human-induced climate change due to increased greenhouse gas forcing might compare with changes resulting from natural variability. Specific focus points have been on changes in extreme wind speeds at 10 m height and 100 m height and on the assessment of strong wind statistics.

The analysis is based on scenario runs from the HIRHAM5 regional climate model with a 25 km horizontal resolution, using the control period 1958–2000. Two future scenarios for 50-year winds have been produced, for the periods 2001–2050 and 2051–2099. The projected wind patterns are similar to those observed in the control period and the difference is mostly within 5% over the entire domain studied. One scenario suggests a 20% increase in extreme winds in Denmark up to 2050, but results should be viewed with care due to the large uncertainty involved.

Effects of climate change on the production of bio-fuels

The objectives of this study were (i) to investigate the effects of climate and forest management on the potential production of bio-fuels (energy biomass from forests) along with timber, and on carbon sequestration and storage in forest ecosystems; and (ii) to assess carbon dioxide (CO_2) emissions of the management operations for energy biomass production in Finnish conditions. In this context, an ecosystem model (Sima) was utilised, integrated with an emission calculation tool, to simulate the studied factors during three 30-year periods (1991–2020, 2021–2050, 2070–2099). The results showed that changes both in climate and thinning regimes may increase substantially the production potential of energy biomass at energy biomass thinning and final felling over the whole of Finland. In addition, increased basal area thinning thresholds will enhance energy biomass production at final felling during 2021–2050

and 2070–2099 when compared with the current thinning regime. Increased thinning thresholds will also enhance timber production during the period 2021–2050 and carbon stocks over the whole simulation period (1991–2020). It was also found that an increase in initial stand density enhanced the energy biomass production at energy biomass thinning regardless of climate scenarios.

Under the climate scenarios employed, a concurrent increase in energy biomass and timber production as well as in carbon stocks would be possible in Finnish forests if thinning was performed at a higher thresholds level than currently. In addition, emission calculations for energy biomass production indicate that, depending on management regimes and species-specific site type, CO_2 emissions produced per unit of energy (kg CO_2 MWh^{-1}) could be reduced or increased up to 6% or 4%, respectively, compared with the current thinning regime. It is suggested that mitigation and adaptation in forest management and changes in forest policies need to be considered not only from the viewpoint of the forest productivity but also the ecological sustainability related to the carbon balance of the forest production system.

Simulating climate impacts on future electricity production

The operation of the NordPool electricity system was simulated using data on present and predicted climate conditions. The NordPool energy market includes Norway, Sweden, Finland and Denmark, but separate simulations were carried out for Iceland. The results show how generation, demand, and transmission characteristics, for a fixed system configuration, respond to expected changes in temperatures and inflow to hydropower reservoirs. Simulations have been carried out using SINTEF Energy Research's EMPS-model. Data from the period 1961–1990 are taken to represent present climate, whereas future climate is represented by regional climate model scenarios. The system model represents the electricity system in 2020 and is based on scenarios for production- and transmission capacities, electricity demand, input fuel costs, and CO_2-quota prices.

Model results are given for hydropower production in the reference climate and for two climate scenarios: HIRHAM5-ECHAM5-A1B (Echam) and HIRHAM-HadCM3-A1B (Hadam). The model simulates an average annual hydropower production of 214.9 TWh for the reference period and the two scenarios yield an increase of 11–12% until 2020. Both scenarios indicate much larger increase in reservoir inflow during winter and results from both models indicate that the major part of the winter increase will occur in Norway. The Hadam scenario predicts a summer decrease in Norway, Sweden and Finland. Warmer winters are predicted to reduce the electricity demand in the traditional high-load period,

which will contribute to less variation in reservoir levels. Combined with the reduction in demand, NordPool will have an excess supply of electricity. This will lead to a reduction in imports from and increase exports to continental Europe.

Separate simulations for Iceland indicate that increased glacial runoff will increase the potential energy in the total river flows to existing power stations by 20% (2.8 TWh) in 2050. The current production system is not designed to meet these changes in runoff and will, in 2050, only be able to utilize 38% of the increase. This calls for possible redesign and upgrades of currently operated power stations.

Analysing climate-related risks and opportunities in the Nordic energy sector

The goal of this working group was to assess the climate associated risks and opportunities of power and heat production systems in the Nordic countries for the next 20–30 years. The increased uncertainty of the future renewable resources with respect to climate change is a key issue for the energy sector. The main focus is often on minimizing negative impacts, but projected climate impacts may also create new opportunities for some power plants in future. Moreover, changes in seasonal and geographical variation of climate-related parameters may affect the productivity of current power plants. Disturbances in production due to extreme events such as floods, droughts, storms, increased wave heights *etc.* must also be taken into account. Uncertainty translates into riskier decisions at all levels within the energy sector, including operational and market issues, short-term responses, and investments.

This study focused on managing the risks and opportunities at the operational level with the aim of preventing adverse effects on current power systems. The methods being used can also be used to support decision-making in the preparatory phases for power-plant construction. Case studies were carried out for specific power plants in Finland, Sweden, Norway and Denmark, using a formal risk-analysis procedure that involves scope definition, data collection, risk/opportunity identification and risk/opportunity estimation.

Both risks and opportunities were identified in the case studies. Increased hydropower production due to inflow increase and longer-term springtime inflow was identified as a major opportunity. Identified risks included, for instance, an increase in autumn or wintertime inflow which might mobilise ice floes. In a worst case scenario, ice movement could create hazardous situations and endanger dams. Biomass-based CHP plants were found to benefit from a longer growing season and a subsequent increase in biomass growth. In the future, heating demands on district heating areas could be expected to decrease due to higher tem-

peratures, which will in turn necessitate changes in the power plants' heat and electricity production.

General conclusion

The Nordic and Baltic region is generally well positioned and sufficiently prepared to handle the impacts of projected climate changes on the energy systems of the region in the first half of the 21st century, and important adaptation measures are already being taken. Although the results presented in this report do not allow detailed comparisons of the effects of a warmer and slightly wetter future climate on the different sources of renewable energy, it seems clear that the effects on energy production in the region will be largely beneficial. Future planning of hydropower stations, wind farms and biomass-fired heat and power plants should take the expected changes in the natural environment into account.

The uncertainty in various scenarios and impact assessments is emphasised in several chapters in this report. Future development of regional climate scenarios with a higher resolution will help reduce such uncertainties, as will the advancement of models simulating hydrological systems, glaciological processes, ecosystems and energy systems. The CES project has demonstrated the Nordic added value of collaborative research on renewable energy sources, not least due to the important differences in these countries' energy sectors. Regional studies of impacts, adaptation and vulnerability will receive new impetus with the publication of the IPCC's Fifth Assessment Report (AR5), to be published in 2013–2014.

1. Climate and Energy Systems – Project structure

*Árni Snorrason, Jórunn Harðardóttir and Thorsteinn Thorsteinsson**

*Details on author affiliations are given in the Appendix

> "To know what you know and know what you don't know is the characteristic of one who knows"
>
> Confucius

1.1 Project overview

The Nordic project *Climate and Energy Systems* (CES) was initiated in 2007 with the aim of studying the impacts of projected climate change on the development of renewable energy systems in the Nordic region up to the mid-21st century. Special focus has been on the potential production and the future safety of the production systems as well as on uncertainties. The key objectives of the project are summarized below:

- To understand the natural variability and predictability of climate and climate-dependent renewable energy sources at different scales in space and time
- To continue development of increasingly detailed 21st century climate scenarios for the Nordic region
- To assess the risks resulting from changes in probabilities and nature of extreme events
- To identify risks and opportunities arising from changes in production of renewable energy
- To develop guiding principles for decisions under climate variability and change
- To develop adaptation strategies
- To conduct a structured dialog with stakeholders

Uncertainty about the future potential of renewable resources in a changing climate is a key issue for the energy sector. Uncertainty translates into riskier decisions within the sector, including operational and market issues, short term responses or investments. The productivity of some renewable energy resources will likely increase, but management will be needed in response to changes in the seasonal and geographical patterns of production and demand. Disturbances and costs due to pos-

sible changes in extremes such as floods, droughts or storms need to be dealt with. Uncertainty also calls for adaptation measures, e.g. adapting hydropower plants to increasing discharge and ensuring dam safety.

Climate and Energy Systems is the fourth in a series of Nordic project studying the impacts of climate change on Nordic energy resources and systems. The first project, *Climate Change and Energy Production* was initiated in 1991 (Sælthun *et al.*, 1998). It was funded by the Nordic Council of Ministers and focused on climate impacts on runoff and hydropower. In the early 2000s, an initiative by Nordic Energy Research led to the pre-project *Climate, Water and Energy* (Kuusisto, 2004; Árnadóttir, 2006), which paved the way for the larger, comprehensive research program *Climate and Energy* (2003–2006). The latter project provided long-term scenarios of climate change and associated impacts on energy systems up to 2100 for the Nordic and Baltic countries (Fenger, 2007).

1.2 Project organization and participants

The CES project was organized as a matrix structure with four working groups (WGs) focusing on renewable energy resources (horizontal bars in Figure 1.1). Cross-cutting issues were delegated to other working groups (vertical bars in Figure 1.1); e.g. the climate modeling group, which prepared climate scenarios used by the four above mentioned groups. Information management (including stakeholder involvement and public outreach) and workshop and conference organization were handled by separate WGs.

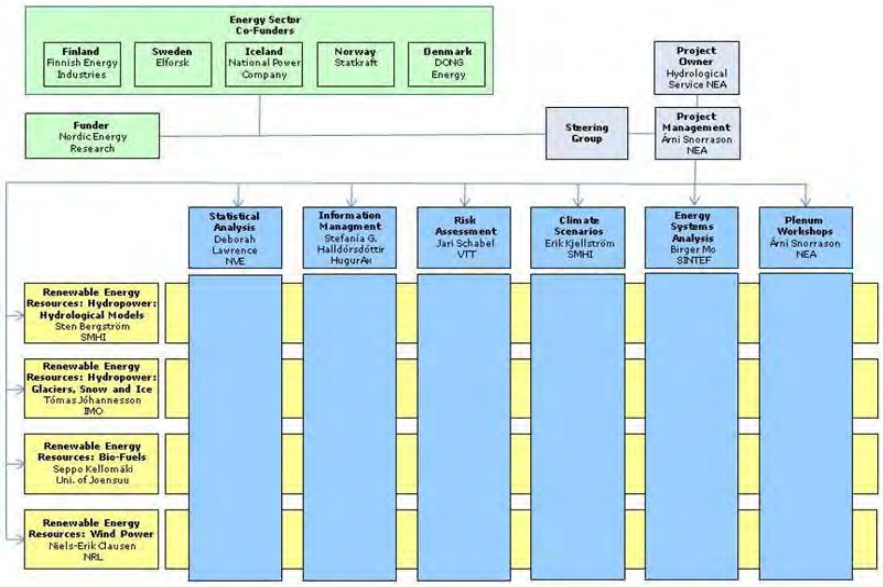

Figure 1.1. Organization of the project. The project manager was based at the Hydrological Service (HS) of Iceland´s National Energy Authority (NEA) at the inception of CES, but led the project from the Icelandic Meteorological Office (IMO) after a 2008 merger of the HS and the IMO.

The CES Steering Group consisted of the project manager, representatives of the co-financing Nordic energy companies and leaders of the individual working groups (WGs):

Project manager:	Árni Snorrason, NEA/IMO	Iceland
Co-financer:	Tom Andersen, Statkraft	Norway
Co-financer:	Christian Andersson, Elforsk	Sweden
Co-financer:	Kati Takala, Finnish Energy Industries	Finland
Co-financer:	Óli Grétar Blöndal Sveinsson, Landsvirkjun	Iceland
Co-financer:	Aksel Hauge Pedersen, DONG Energy	Denmark
Bio-fuels WG:	Seppo Kellomäki, University of Joensuu	Finland
Climate scenarios WG:	Erik Kjellström, SMHI	Sweden
Energy systems WG:	Birger Mo, SINTEF	Norway
Hydropower, hydrology WG:	Sten Bergström, SMHI	Sweden
Hydropower, snow and ice WG:	Tómas Jóhannesson, IMO	Iceland
Risk assessment WG:	Jari Schabel, VTT	Finland
Statistical analysis WG:	Hege Hisdal, NVE	Norway
Information management:	Stefanía G. Halldórsdóttir/Jórunn Harðardóttir, HugurAx/IMO	Iceland

A total of about 100 scientists at 33 institutions in the Nordic and Baltic countries contributed to the CES project (see Appendix 2). The CES Steering group met bi-annually during the period 2007–2010 to assess the development of the project. Working groups met annually and main results from the project were presented at the *Conference on Future Climate and Renewable Energy*, held in Oslo on May 31–June 2 2010 (Pikkarainen, 2010). Write-up of results in the form of individual chapters published in this volume was completed in spring 2011.

1.3 Working groups and their objectives

1.3.1 Climate Scenarios Working Group

The principal aims of the CES Climate Modeling and Scenarios group were:

- To provide climate scenario data for the CES groups for use in modeling applications.
- To provide a coherent and consistent analysis of ranges and conditional probabilities, for changes in mean climate and climate variability, with focus on the period of 2020–2050.
- To analyze regional climate scenarios in terms of impact-relevant indices defined in co-operation with the statistical analysis group.

Results are presented in Chapter 3. Regional climate simulations for the period until 2050 were conducted using the advanced regional climate models RCA and HIRHAM. The working group also conducted probability analysis, providing both decadal ranges and probabilities of climate variability and change in the Nordic region until 2050. The link between regional climate scenarios and the recent/ongoing climate behavior was

analyzed and customized regional climate scenarios for risk analysis were developed.

1.3.2 Statistical Analysis Working Group

Chapter 4 describes the results of the Statistical Analysis working group. This group evaluated trends and variability in long-term historical hydro-climatological time-series, such as precipitation and stream-flow, to determine if the effects of climate change are already found in these data. Comparisons were also made with expected future trends, based on simulated time-series from climate scenarios. Patterns of large-scale atmospheric circulation and weather types, both in the past and in the future were also studied, with emphasis on changes in the occurrence of extreme events, such as floods and droughts. An increased risk of flooding may have adverse consequences for dam safety, and these implications were analyzed using flood frequency analysis of historical and scenario data.

1.3.3 Hydropower–Snow and Ice Working Group

Changes in glacial runoff are one of the most important consequences of ongoing and future climate change in Iceland, Greenland and some glacierized watersheds in Scandinavia. Such changes have a strong impact on the hydropower industry as discharge volumes, seasonal variations and extreme discharge conditions change. The rapid retreat of glaciers also has other implications; for example changes in fluvial erosion from currently glaciated areas, changes in the courses of glacial rivers, which may affect roads and other infrastructures, and changes that affect travelers in highland areas and the tourist industry.

During historical times, glaciers and ice caps in Nordic countries have retreated and advanced in response to climate changes that are believed to have been much smaller than the greenhouse induced climate changes that are expected during the next decades to century. Therefore, the main focus of the Hydropower–Snow and Ice working group in CES was to analyze the effects of future climate change on glaciers and ice caps in Nordic countries and their implications for the hydrology of glacial rivers. Chapter 5 deals with results from this group.

1.3.4 Hydropower–Hydrology Working Group

Hydropower is the most important renewable energy source for electricity in the Nordic area. It is therefore of great interest to analyze the possible impacts of climate change on both the future production and the safety of the system. Building on earlier projects, the focus of the Hydropower–Hydrology group within CES can be summarized as follows:

- Assessments of the effects of climate change on hydropower production and dam safety were continued from earlier projects, using new and more diversified climate scenarios than in previous modeling efforts
- Improvement of the model interface between climate models and hydrological models
- Exploration of the uncertainties involved in the simulation of future conditions for hydropower production and safety
- Improvement of the methodology to cope with impacts of lake regulation in a changing climate
- Detailed dam safety analyses in comparative design studies across national borders
- Continuing development of an intensive user dialogue

Results are presented and discussed in Chapter 6.

1.3.5 Wind Power Working Group

The CES wind power group focused on investigating the conditions for production of electricity from wind energy in the Nordic countries and how they might change due to global warming during the coming decades. This relates both to the production potential and especially the design conditions for wind farms and their sensitivity to climate change. The wind power group analyzed historical data on extreme wind in the Nordic countries (50-year wind in 100 m height) and investigated climate change impacts on the extreme and strong winds, using CES scenarios. The approach used was to downscale results from Atmosphere-Ocean Global Climate Models (AOGCMs) using regional dynamical climate models (RCM and HIRHAM). Results are presented in Chapter 7.

1.3.6 Bio-fuels Working Group

The utilization of various sources of bio-energy is foreseen to increase in the Nordic countries in the future. This calls for studies of the present and future biomass production potential of forests and of the sustainability of bio-energy production. Furthermore, the complex relationships between climate, bio-energy production in forests and their management need further study. In addition, the sustainability of the production in the management of forests will be ensured by assessing the environmental side effects and risks of the production. This analysis identifies the management regimes optimal in production of forest biomass for energy, with minimizing risks and adapting the production systems to the climate change. By doing this, estimation of the total role of forest biomass in energy production and its effects in substituting fossil fuels and mitigating the climate change can be assessed. The key objectives are summarized as:

- Understanding of the natural variability and predictability of bio-energy production at different scales in space and time in the context of climate change
- Assessment of potential production of forest biomass for energy
- Assessment of the risks of the production of forest biomass for energy
- Assessment and development of forest management regimes to produce forest biomass along with timber to substitute fossil fuels and to mitigate climate change

Chapter 8 deals with results obtained from the CES bio-fuels working group.

1.3.7 Energy Systems Analysis Working Group

Climate change affects the electricity market in many ways. Increasing temperatures reduce the need for electrical heating, and altered wind-speeds may affect wind-power generation. Altered precipitation and changes in snow and glacier-ice melting will, however, have the largest climate-change related impact on the NordPool market (the Nordic energy market, see Chapter 9) because of the large share of hydropower in the region. Previous studies have shown that the geographical and seasonal distribution of precipitation as well as river runoff and the annual amount of inflow to reservoirs are affected by climate change. Using input from other working groups, the energy systems analysis group within CES worked on quantifying the variability of electricity production from renewable sources and its sensitivity to climate changes. The group carried out a detailed analysis of the NordPool electricity market for 2020 using SINTEF´s EMPS model (see Chapter 9) and studied the vulnerability of the system. The results show how generation, demand, and transmission characteristics, for a fixed system configuration, respond to expected changes in temperatures and inflow to hydropower reservoirs. The situation in Iceland was dealt with separately (Chapter 10), since the country's electricity system is not connected to the Nordic and European networks.

1.3.8 Risk Analysis Working Group

Chapter 11 discusses a key issue for the energy sector; i.e. the increased uncertainty of the future production levels and stability of renewable energy resources in a changing climate. The goal of the work carried out by the Risk Analysis group within CES was to assess the climate associated risks and opportunities of power and heat production systems in the Nordic countries over the next 20–30 years. An evaluation of risk under increased uncertainty in order to improve decision making in a changing climate was carried out through the following steps:

- Review of risk and uncertainty management approaches used in the energy sector
- Integration of risk and uncertainty in decision support tools. A risk management framework, developed by VTT of Finland in accordance with the interests of industrial partners, has been tested and applied in various energy sectors (e.g. hydro, CHP, bio and wind)

The target users of the decision support tools are decision makers operating various types of power plants. The tools can also be utilised by laymen as a first step in developing a strategy for dealing with changing weather patterns over the life time of existing and new power infrastructure investments.

1.3.9 Information Management Working Group

The Information management group was responsible for information dissemination, active stakeholder involvement and public outreach. The group also facilitated the establishment of working groups at the national level and maintained a project website (www.en.vedur.is/ces) which included a workspace for communication within each working group. The Information Management group organized project workshops and steering committee meetings. Together with NVE staff, this group was responsible for the CES final conference in Oslo 2010 and oversaw the publication of information leaflets, conference proceedings and the final report from the CES project.

1.4 Relevance for stakeholders in the energy sector

Studying the impacts of a changing climate on renewable energy sources is an important issue in the Nordic and Baltic Region with its heavy reliance on hydropower production, increasing development of wind power and large potential for bio-energy. Knowledge about past, present and future variability in climate and hydrology is therefore of vital importance to the energy sector. A change in hydro-climatological variability may lead to changes in the operation of reservoirs and wind turbines and in the energy production potential. In particular, the variability in hydropower is a great concern in the light of recent wet years and some sudden dry years, which have resulted in highly variable prices of electricity. The power industry and society in general need to make long term decisions, for example, regarding investments in new production capacity. The dam safety issue is also high on the agenda in the Nordic and Baltic countries and the industry requests guidance on how to cope with climate change in this respect. Thus, a major goal of the CES project was to contribute to improved decision making within the energy sector. A series of structured dialogs were held with representatives of energy

companies in order to assess the project's relevance for stakeholders (Gode and Thörn, 2010).

1.5 References

Árnadóttir, S., ed. (2006). *European Conference on Impacts of Climate Change on Renewable Energy Sources* (Abstract Volume), Reykjavík, Iceland, June 2006. Nordic Energy Research. 228 pp.

Fenger, J., ed. (2007). *Impacts of climate change on renewable energy sources: Their role in the Nordic energy system*. Nord 2007:003, Nordic Council of Ministers, Copenhagen. 190 pp.

Gode, J. and Thörn, P. (2010). Stakeholder relevance of the CES project. In: *Proceedings of the Conference on Future Climate and Renewable Energy: Impacts, Risks and Adaptation*, Oslo, 31 May–2 June 2010. pp. 74–75.

Kuusisto, E. (2004). *Climate, Water and Energy: a summary of a joint Nordic project 2002–2003*. Reykjavík, Climate, Water and Energy, Report CWE-4.

Pikkarainen, H., ed. (2010). *Proceedings of the Conference on Future Climate and Renewable Energy: Impacts, Risks and Adaptation.* Norwegian Water Resources and Energy Directorate, Oslo. 104 pp. Available at: http://www.vedur.is/media/ces/ces-oslo2010_proceedings.pdf

Sælthun, N.R., Aittoniemi, P., Bergström, S., Einarsson, K., Jóhannesson, T., Lindström, G., Ohlsson, P.-E., Thomsen, Th., Vehviläinen, B., Aamodt, K.O. (1998). *Climate change impacts on runoff and hydropower in the Nordic countries*. TemaNord 1998:552. 170 pp.

2. Renewable Energy in the Nordic and Baltic Countries

*Thorsteinn Thorsteinsson**

*Details on author affiliation are given in the Appendix

2.1 Introduction

The burning of non-renewable fossil fuels and the resulting emissions of greenhouse gases is one of the most pressing environmental issues facing the world today. The buildup of greenhouse gases, like carbon dioxide, methane, nitrous oxide and various industrial gases, changes the radiative balance of the atmosphere and is believed to be the main cause of the 0.74°C rise in mean atmospheric temperature during the 100-year period 1906–2005. Rising surface temperatures lead to changes in precipitation, cloud cover and wind patterns and affect the global hydrological cycle. Enhanced melting of glaciers and ice caps has been observed on all continents, leading to rising sea levels, and impacts on marine and terrestrial ecosystems are already substantial (IPCC, 2007).

Fossil fuels, which accounted for 81% of the global energy consumption in 2009, are a finite resource and their exploitation is increasingly expensive and damaging to the natural environment. In contrast, renewable energy sources derive their energy directly from the Sun or from the heat in the Earth´s interior and are thus constantly being replenished. Hydropower, wind power, bio-energy, geothermal energy, solar energy and ocean (tidal) energy are the most important renewable energy sources and their share in global energy consumption rose to 16% in 2009 (REN21, 2011). In 2010, renewables accounted for nearly 20% of the global electricity production (REN21, 2011). The EU Commission's *Climate Action and Renewable Energy Package,* published in 2008, sets the target of reducing greenhouse gas emissions by 20% in the period 1990–2020 and increasing the share of renewable energy to 20% of total energy consumption by 2020 (EC, 2010).

This chapter briefly summarizes the status of renewable energy use in the Nordic and Baltic countries and outlines future prospects. The share of renewable energy in total energy use in the Nordic and Baltic countries in 2008 and their 2020 targets are shown in Table 2.1.

Table 2.1. The percentage (%) share of renewable energy in final energy use[*] in the Nordic and Baltic countries in 2008 and targets for 2020.

Country	2008	2020
Denmark	19	30
Finland	30	38
Iceland	81	85[**]
Norway	62	66
Sweden	44	49
Estonia	19	25
Latvia	30	40
Lithuania	15	23

Sources: EU Facts Sheets (2008). See: http://www.energy.eu/http://www.nordicenergysolutions.org
Orkustofnun (2010). *Energy Statistics in Iceland 2009.*
Ruokonen *et al.* (2008) – see reference list.

[*] Here, terminology is taken up unchanged from the references used but it should be noted that terminology varies between the different national sources on energy statistics. *Primary energy* refers to energy found in nature that has not been subjected to any conversion or transformation process, e.g. coal, lignite, mineral oil, natural gas, uranium (nuclear energy), water (hydropower), solar radiation, wind. *Final energy* is a form of energy available to the user following the conversion from primary energy. Final forms of energy include gasoline or diesel oil, purified coal, purified natural gas, electricity, mechanical energy. [Source: www.isover.com].

[**] A specific 2020 target for Iceland has not been set. The figure is an estimate based on present aims to increase the share of renewable energy in the fisheries and transportation sectors (Á. Loftsdóttir, personal communication).

2.2 Denmark

Fossil energy is still the most important energy source in Denmark, but renewables like wind power, biogas, biomass and waste are steadily increasing in importance. Their share in the country's total energy production rose from 17% in 2005 to 19.7% in 2009 (Energistyrelsen, 2010a) and is targeted to rise to 30% by 2020 (Ruokonen *et al.*, 2008). Denmark has been a leader in the development of wind power and in an international comparison, the country's wind turbine industry is a major player. The most important onshore wind resources are located on the western coast of Jylland and on the southern and western coasts of Sjælland and other islands in the eastern part of Denmark. Offshore wind resources are very large and 12 wind farms were operational in 2010. In 2013, the *Anholt Offshore Wind Farm* will become operational and its 111 turbines are planned to produce 400 MW. By the end of 2010, installed wind power capacity stood at 3752 MW (Energistyrelsen, 2010b) and the share of wind power in the electricity supply was 21.9%. In February 2011, the Danish government announced the "Energy Strategy 2050", aiming for Denmark to become fully independent of fossil fuels by 2050 (Klima- og Energiministeriet, 2011).

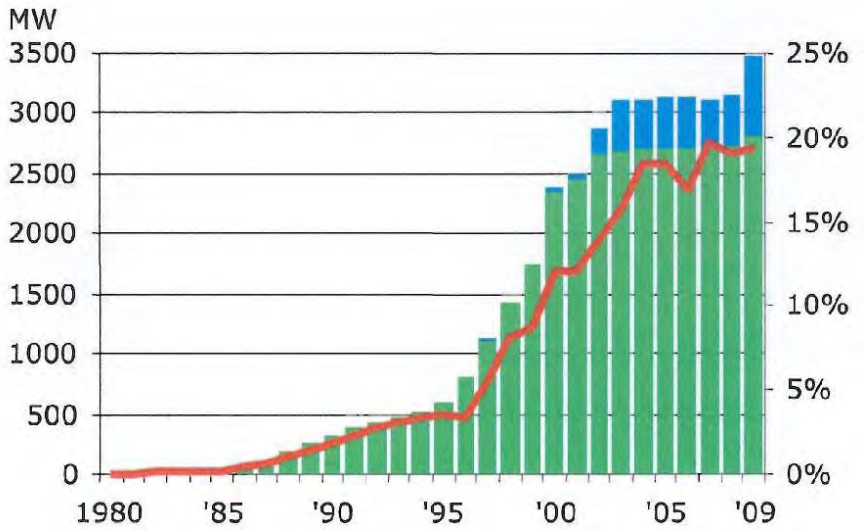

Figure 2.1. Development of the capacity of onshore (green columns) and offshore (blue columns) wind mills in Denmark 1980–2009 (vertical axis on the left). The red curve shows the percentage of electricity use in Denmark delivered by wind energy (vertical axis on the right).

Source: Energistatistik 2009. Danish Energy Agency.

2.3 Finland

In 2009, fossil fuels (coal, oil and gas) accounted for 46% of Finland's total energy consumption, whereas 20% were delivered by wood fuels, 19% by nuclear energy, 5% by peat, 3% by hydropower and the rest came from other sources, including imported energy (Statistics Finland, 2010). Of all the electricity consumed in Finland, 15% was imported in 2009. In April 2010, the Finnish government announced plans to build two new nuclear reactors as part of the country´s efforts to reduce Russian imports and meet the EU´s climate obligations (Euractiv, 2010).

By 2020, Finland aims to become independent of electricity imports and the share of renewable energy in the energy mix is then targeted to rise to 38% (up from 28.5% in 2005, see Ruokonen *et al.*, 2008). The forest industry uses 30% of all energy in Finland and waste from this industry (wood residues, black liquor) contributed 67% of the power generation from renewable energy sources in the country in 2005. Smaller contributions to renewable energy use come from biomass (wood pellets), hydropower, wind power, photovoltaics and solar heating.

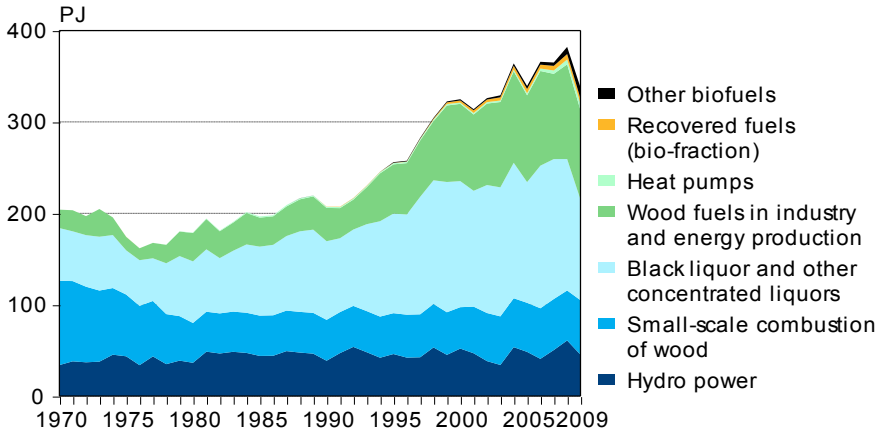

Figure 2.2. Energy production from renewable energy sources in Finland 1970–2009.

Source: Yearbook of Energy Statistics 2010. Statistics Finland.

2.4 Iceland

The Icelandic energy sector is unique in both its isolation from other European networks and the high share of renewable energy in the total primary energy budget. In 2009, geothermal energy provided about 66% of the total primary energy supply, the share of hydropower was 15%, and fossil fuels, mainly petroleum for transportation, provided the remaining 19%. The main use of the geothermal energy is for space heating and 90% of households in the country receive hot water from district-heating systems. Virtually 100% of electricity use in Iceland derives from renewable sources, hydropower plants producing 73% and geothermal plants 27% (Orkustofnun, 2010). Iceland has the world's highest hydropower production level per capita (52.500 kWh/person in 2009; see IEA/OECD, 2010), but ¾ of the electricity produced is used by power-intensive aluminium smelters operated in the country.

2.5 Norway

Norway has large resources of renewable energy, in the form of hydropower, onshore and offshore wind power and bio-energy from wood. The country's potential in developing energy production technologies like wave power and osmotic power is also substantial. Norway is Europe's largest producer of hydropower, which delivers 99% of the country´s electricity. On January 1 2008, Norway had a total installed capacity of 29030 MW at 699 hydropower stations larger than 1 MW. The Kvilldal hydropower station in Rogaland county is Norway's largest, with a maximum generating capacity of 1240 MW. About 60% of the country´s hydropower potential is already developed, whereas 22% are perma-

nently protected (Bogstrand, 2008). As a large exporter of oil and gas, Norway continues to put emphasis on increasing its share of renewable energy in order to meet climate protection obligations. In a recent study, the share of renewable energy in Norway's total energy consumption is predicted to rise to 66% by 2020 (Ruokonen *et al.*, 2008). Moreover, the Norwegian government has defined the target of reducing greenhouse gas emissions by 30% in the period 1990–2020 and making Norway carbon neutral by 2050 (Norwegian Ministry of the Environment, 2007).

Figure 2.3. Oddatjørndammen in Rogaland, Norways highest rock-filled dam (142 m) and the Blåsjø reservoir, which form part of the Ulla-Førre hydropower complex.

Source: Statkraft, Norway.

2.6 Sweden

Sweden is the largest producer and user of energy in the Nordic region. The country's total energy production in 2009 amounted to 568 TWh, derived from the following sources: Crude oil and oil products 32%, nuclear power 26%, biofuels 23%, hydropower 12%, coal 3%, natural gas 2%, heat pumps 1% and wind power 0.4%. Imports account for <1% (Statens Energimyndighet 2010, page 50).

Sweden leads the EU countries in the share of renewable energy production and the country´s 2020 target is to increase the share of renewables to 50% (up from 33.3% in 1990 and 44.7% in 2009) (Statens Energimyndighet 2010, page 57). The most important renewable energy sources in Sweden are (in order of production levels): Wood fuels and black liquors, hydropower, heat absorbed by heat pumps, organic waste, bio-based motor fuels and wind power. Hydropower delivers 49% of the electricity, nuclear power 37%, fossil- and bio-fuel- based production

12% and wind power 2% (Statens Energimyndighet 2010, page 79). In recent years, investments in wind power have grown notably slower than in bio-fuel-based electricity production (Ruokonen *et al.*, 2008), but a considerable increase in wind power utilization is expected in the coming decade.

The Swedish government's current climate and energy policy sets a target for the transport sector, requiring at least 10% of its energy use to be met from renewable sources by 2020. The long-term ambition is that vehicles in Sweden should be independent of fossil fuels by 2030. The vision for 2050 is that Sweden should by then have no net emissions of greenhouse gases to the atmosphere.

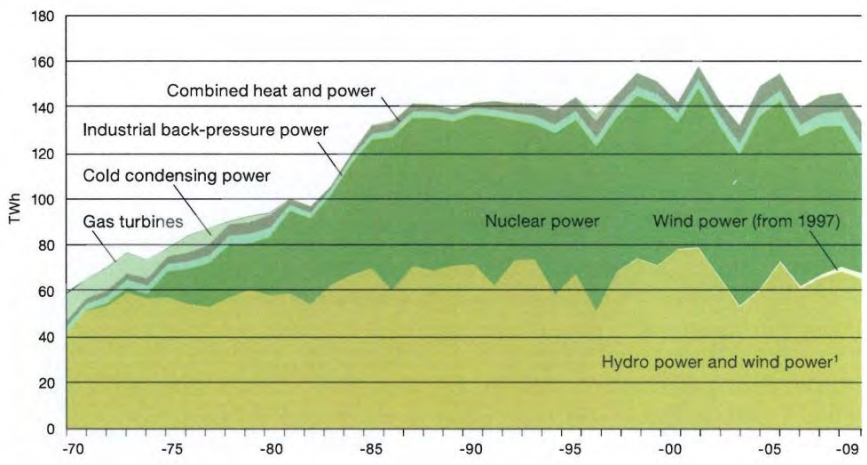

Figure 2.4. Electricity production in Sweden, by types of production plant, 1970–2009.

Source: Statistics Sweden and the Swedish Energy Agency.

2.7 The Baltic States

Estonia, Latvia and Lithuania cover part of their domestic electricity and heat usage by utilizing local sources of renewable energy and all three states are presently working to increase their share of renewable energy within the EU's current framework policies (see Table 2.1).

Estonia had an installed total electrical power capacity of 2977 MW in 2002, derived entirely from thermal power. Among the Baltic States, the country is distinguished by relatively high patterns of energy consumption per capita and a carbon intensive structure of the total primary energy supply (Streimikiene and Klevas, 2007). About 58% of the total primary energy supply (and 90% of the electricity production) is covered by a domestic fossil fuel source; oil shale (2002 figures, see Fammler *et al.*, 2003). Estonia's RES-potential lies mainly in biomass, biogas, wind and cogeneration from bio-fuels. Hydropower utilization on a small scale is also under development as only about half the potential

is currently exploited. The 2020 target is that renewables should by then deliver 25% of the primary energy supply.

Latvia had a total installed electrical power capacity of 2145 MW in 2002, of which hydroelectric plants delivered 1543 MW (Streimikiene and Klevas, 2007). Of the Baltic States, Latvia has the largest share of renewable energy sources in the total primary energy supply and 47% of the electricity was produced by renewables in 2004 (EU Fact Sheets, 2008). This is due to relatively high hydropower capacity within the country, most of which is delivered by the three large power plants Rigas, Kegums and Plavinas on the Daugava river. Latvia relies heavily on the import of fossil fuels and electricity from Estonia, Lithuania and Russia, but has considerable potential for wind power and bio-energy production in addition to hydropower. The country´s 2020 target is to produce 42% of the primary energy use from renewable energy sources.

Lithuania had a total installed electrical power capacity of 6156 MW in 2002 (Streimikiene and Klevas, 2007). By then, nearly one-third of the total primary energy supply was generated by the Ignalina Nuclear Power Plant, located at the eastern border of the country. Closedown of this plant was completed in 2009 as part of the country's accession agreement with the European Union. In order to reduce Lithuania's dependence on fossil fuel imports for energy production, plans call for the opening of a new nuclear reactor by 2016. Strong emphasis is also put on the development of renewable energy sources with focus on biomass for electricity generation, wind energy and use of waste for fuel production. Hydropower, geothermal energy and solar energy options are also being investigated. The 2020 target is that renewables should deliver 23% of the primary energy supply. In addition, the construction of a 440 km long submarine power link to Sweden, with a capacity of 700 MW, will be completed in 2015, thus opening up a connection between the Baltic and Nordic power systems (Lithuanian Energy Ministry, 2010).

2.8 References

Bogstrand, B., editor (2008). *Facts 2008: Energy and Water Resources in Norway*. Norwegian Ministry of Petroleum and Energy, Oslo. 144 pp.

EC (2010). See: http://ec.europa.eu/clima/documentation/package/index_en.htm

EU Facts Sheets (2008). See: http://www.energy.eu/

Euractiv (2010). http://www.euractiv.com/energy/finland-plans-more-nuclear-renewables-news-470763.

Energistyrelsen (2010a). *Energistatistik 2009.* Danish Energy Agency (www.ens.dk). 60 pp.

Energistyrelsen (2010b). See: http://www.ens.dk/da-DK/Info/TalOgKort/Statistik_og_noegletal

Fammler, H., Indriksone, D., Bremere, I., Köster, T., Morkvónas, Z., Simanovska, J. (2003). Renewable Energy Sources in Estonia, Latvia and Lithuania: Strategy and policy targets, current experiences and future perspectives. Baltic Environmental Forum, Riga. 56 pp.

IEA/OECD (2010). *Electricity information 2010.* Cited in: Energy in Sweden 2010, page 119.

IPCC (2007). *Climate Change 2007: The Physical Science Basis. Contribution of Working Group I to the Fourth Assessment Report of the Intergovernmental Panel on Climate Change*. Solomon, S., D. Qin, M. Manning, Z. Chen, M. Marquis, K. B. Averyt, M. Tignor, H. L. Miller, Jr., (*eds*). Cambridge University Press, Cambridge, UK, and New York, NY, USA, 996 pp.

Klima- og Energiministeriet (2011). See: http://www.energymap.dk/Newsroom/From-coal—oil-and-gas-to-green-energy.

Lithuanian Energy Ministry (2010). See: Lithuanian Energy Quarterly, 1, 2010 at: http://www.enmin.lt/en/activity/veiklos_kryptys/strateginiai_projektai/Lithuanian%20Energy%20Quarterly%20%282010Q1%29.pdf.

Norwegian Ministry of the Environment (2007). *Norwegian Climate Policy*. Report No. 34 (2006–2007) to the Storting. 44 pp.

Orkustofnun (2010). *Energy Statistics in Iceland 2009.* National Energy Authority, Reykjavík. 12 pp.

REN21 (2011). *Renewables 2011. Global Status Report.* Renewable Energy Policy Network for the 21st Century (REN21) Secretariat, Paris. 116 pp.

Ruokonen, J., Aronsen, G., Turkama, A.-M., Gautesen, K., Nilsson, M., Ollikainen, J., Middtun, A. (2008). *Promotion of renewable energy in the Nordic countries.* TemaNord 2008: 598. Nordic Council of Ministers, Copenhagen. 92 pp.

Statens Energimyndighet (2010). *Energy in Sweden 2010.* Swedish Energy Agency. Report ET 2010:47. 144 pp.

Statistics Finland (2010). See: http://www.stat.fi/til/ekul/2009/ekul_2009_2010-12-10_kuv_001_en.html.

Streimikiene, D. and Klevas, V. (2007). Promotion of Renewable Energy in Baltic States. *Renewable and Sustainable Energy Reviews,* 11, 672–687.

3. Climate scenarios

*Erik Kjellström, Jouni Räisänen, Torill Engen-Skaugen, Ólafur Rögnvaldsson, Hálfdán Ágústsson, Haraldur Ólafsson, Nikolai Nawri, Halldór Björnsson, Jussi Ylhäisi, Hanna Tietäväinen, Hilppa Gregow, Kirsti Jylhä, Kimmo Ruosteenoja, Igor Shkolnik, Sergey Efimov, Pauli Jokinen, Rasmus Benestad, Martin Drews and Jens Hesselbjerg Christensen**

*Details on author affiliations are given in the Appendix

3.1 Introduction

Climate scenarios from climate models lay the foundation for climate impact studies. In relatively small areas, like the Nordic and Baltic region, coarse-resolution global climate models (GCMs) fail to resolve important aspects of the regional climate. Downscaling techniques, including dynamical and statistical downscaling, can be used to arrive at a higher horizontal resolution. Here, in section 3.2, we present a number of climate scenarios for the Nordic and Baltic region produced by regional climate models (RCMs) run within the CES project in a joint effort with the European FP6-project ENSEMBLES (van der Linden and Mitchell, 2009). The large number of RCM-simulations generated in these two projects, forced by a range of GCMs, is unprecedented. However, even if the ensemble of RCM simulations is relatively large, it still covers only a part of the total uncertainty related to future climate change. Therefore, in section 3.3, we put the RCM scenarios in a wider context by comparing them to the output of a large number of GCM simulations. In particular, it is described how the regional scale information from the CES/ENSEMBLES RCMs can be added to the probabilistic climate change projections from the larger ensemble of GCMs. The RCM simulations described in section 3.2 and used in section 3.3 are undertaken at 25 km horizontal resolution. Even if this is state-of-the-art for today's large RCM ensembles, it may still not be sufficient for detailed impact studies at local scales. In section 3.4, we present two examples of further increasing the horizontal resolution: (1) by dynamical downscaling to 3 km in a few smaller areas in the Nordic domain, and (2) by statistical downscaling to 1 km horizontal resolution for Norway. In addition to the work reported on in sections 3.2–3.4 a number of other studies have been undertaken in the Climate Scenario group, these are briefly described in section 3.5 before concluding remarks are given in section 3.6.

The time period of interest to the CES project starts already at the present-day situation. Decadal climate prediction, in which actual predictions are made of the future climate starting from a known initial

state, is still in its infancy (Keenleyside and Ba, 2010). Therefore, it was decided that the work in the Climate Scenario group should be conducted on "classical" scenario periods. Consequently, most of the analyses concerns climate change comparing 2021–2050 to a control period 1961–1990. But, there are also exceptions to this due to a shortage of computing time (section 3.4.1) and a mismatch of timing with data in climate scenario archives, (sections 3.5.7 and 3.5.9). Another exception can be found in section 3.5.1 where we discuss the gradual climate change starting already in the late 20th century in a probabilistic manner. For the near future, the uncertainty in the future climate change signal is not primarily related to the future forcing as different emission scenarios do not lead to diverging climate scenarios in a significant way until the mid century. The presented analyses have been carried out based on the A1B scenario from the Special Report on Emission Scenarios (SRES, Nakićenović and Swart, 2000) unless otherwise noted.

3.2 Regional climate change scenarios

3.2.1 The CES/ENSEMBLES regional climate change scenarios

When the CES project was started, the larger European FP6-project ENSEMBLES was already running. As three of the modelling groups in CES were also participating in ENSEMBLES it was early on decided to try to benefit from that project by using also other regional climate model scenarios made available through that project. This was beneficial also to the ENSEMBLES project as we decided to make the scenarios produced within CES by the RCM groups available also to the wider ENSEMBLES community. We therefore adopted the common ENSEMBLES simulation protocol with a minimum domain covering Europe and thus including both the Nordic mainland and Iceland. Documentation of the simulation protocol can be found at http://ensemblesrt3.dmi.dk/.

Here we report on an ensemble consisting of 15 RCM climate change simulations available at the common ENSEMBLES/CES data base. Of these, seven are from the RCM groups active in the CES project. Table 3.1 gives a list of institutes performing the regional simulations, names of RCMs and driving GCMs.

Table 3.1. Regional climate change scenarios. For HadCM3, three different versions of the HadCM3 model from their so-called perturbed physics ensemble (Collins *et al.*, 2010) have been used. These are the reference version (ref), one with low climate sensitivity (low) and one with high climate sensitivity (high). A recommended subset of three simulations is indicated in italics face. RCM references can be found in Christensen *et al.* (2010).

No.	Institute	RCM	GCM	GCM reference
1	DMI	HIRHAM5	CNRM-CM3	Gibelin and Déqué (2003)
2	*DMI*	*HIRHAM5*	*ECHAM5/MPI-OM1*	*Jungclaus et al. (2006), Roeckner et al. (2006)*
3	*Met.No*	*HIRHAM*	*HadCM3Q0 (ref)*	*Collins et al., 2010*
4	*SMHI*	*RCA3*	*BCM*	*Déqué et al. (1994), Bleck et al. (1992)*
5	SMHI	RCA3	ECHAM5/MPI-OM1	Jungclaus *et al.* (2006), Roeckner *et al.* (2006)
6	SMHI	RCA3	HadCM3Q3 (low)	Collins *et al.* (2010)
7	VMGO	RRCM	HadCM3Q0 (ref)	Collins *et al.* (2010)
8	C4I	RCA3	HadCM3Q16 (high)	Collins *et al.* (2010)
9	CNRM	RM4.5	CNRM-CM3	Gibelin and Déqué (2003)
10	ETH	CLM	HadCM3Q0 (ref)	Collins *et al.* (2010)
11	KNMI	RACMO2	ECHAM5/MPI-OM1	Jungclaus *et al.* (2006), Roeckner *et al.* (2006)
12	Hadley Centre	HadRM3Q0	HadCM3Q0 (ref)	Collins *et al.* (2010)
13	Hadley Centre	HadRM3Q3	HadCM3Q3 (low)	Collins *et al.* (2010)
14	Hadley Centre	HadRM3Q16	HadCM3Q16 (high)	Collins *et al.* (2010)
15	MPI-M	REMO	ECHAM5/MPI-OM1	Jungclaus *et al.* (2006), Roeckner *et al.* (2006)

The ensemble holds 11 different RCMs downscaling seven different driving GCMs if the Hadley Centre perturbed physics members (ref, low and high) are counted separately. Some of the GCMs have been downscaled by more than one RCM making it possible to illustrate some of the uncertainties related to formulation of the RCM. All simulations were performed with the emission scenario SRES A1B (Nakićenović and Swart, 2000). Thus, the ensemble does not allow addressing uncertainties related to choice of emission scenarios, but as the time frame considered here (2021–2050) is relatively close in time this uncertainty is considered to be small. Also, uncertainties related uniquely to natural variability can not be studied as there are no simulations differing only in initial conditions.

3.2.2 A recommended subset of simulations

As some of the groups working on impact studies have been limited as to the maximum number of scenarios that can be considered, a smaller subset of three simulations has been recommended for use in CES (marked by italics face in Table 3.1). For this subset it was determined to use different RCMs and different driving GCMs assuring that there is spread in the resulting scenarios.

3.2.3 Results for a 15-member multi-model ensemble

Figure 3.1 shows seasonal changes in temperature at the 2m level, precipitation and wind speed at the 10m level for winter (DJF) and summer (JJA) respectively. All changes are calculated as 30-year averages comparing 2021–2050 to 1961–1990 as an average over the 15-member RCM ensemble in Table 3.1.

Changes in temperature are on average largest for the winter season and most so in the northern and eastern parts of the model domain, i.e.

including the domain of interest in CES. The 15-member multi-model mean changes in winter temperatures in this area are between 1 and 4°C. Simulated changes in summer are in general smaller than in winter and mostly less than 2°C for the CES domain. Precipitation is projected to increase in large parts of northern Europe in both winter and summer. In winter the increase is largest (10–20%) over parts of the Scandinavian region. Summertime precipitation is projected to have a weaker increase than in winter, and further to the south precipitation amount is projected to decrease. The relatively large summertime increase over parts of the Baltic Sea region is probably a result of a relatively strong warming of the Baltic Sea in many simulations. This is similar to what has earlier been found in the CE and PRUDENCE projects (e.g. Rummukainen *et al.*, 2007; Kjellström and Ruosteenoja, 2007). On average, projected changes in wind speed are small. However, in many simulations, and thereby also in the average, relatively large changes are seen in winter over parts of the northern oceans (Barents Sea, parts of the North Atlantic north of Iceland, the Baltic Sea). This is probably connected to changes in sea ice conditions with less sea ice leading to less stably stratified conditions which in turn imply that more momentum can be mixed down towards the surface and thereby generating higher wind speed.

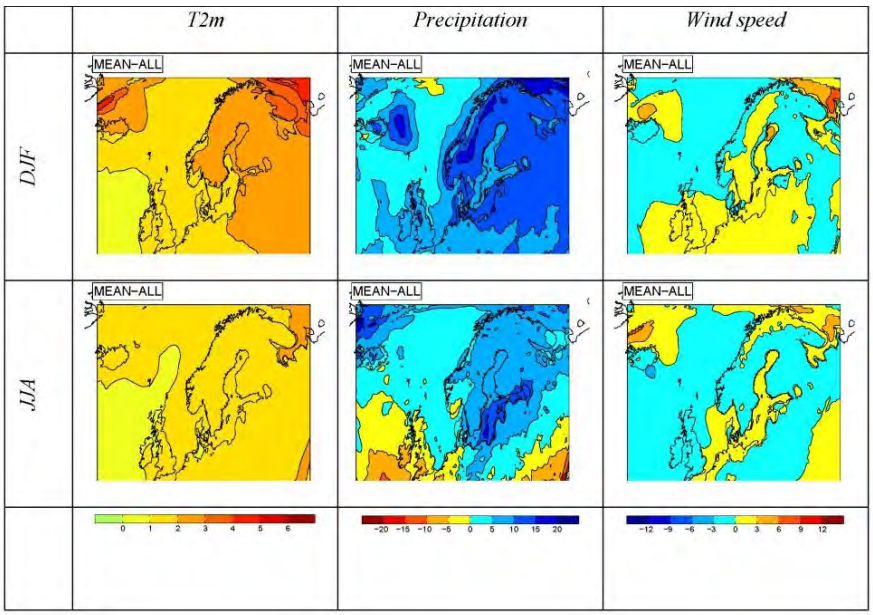

Figure 3.1. Change in 2m-temperature (°C), precipitation (%) and 10m-wind speed (%) comparing 2021–2050 with 1961–1990 for the 15-member multi-model ensemble mean.

3.2.4 Results for individual RCM scenarios

Differences between the individual RCMs are evident both in terms of magnitude and geographical pattern. As an example, large differences in the temperature increase over Iceland are evident between the three

recommended scenarios in both winter and summer (Figure 3.2). Many simulations, including the recommended ones, indicate that the warming in summer is as large as in winter over much of the Baltic Sea. We note here that none of the 11 RCMs used here included an ocean model. This implies that the Baltic Sea surface conditions (temperature and sea-ice) are given by the coarse scale ocean components of the GCMs. This may not be adequate for generating realistic conditions for the Baltic Sea (cf. Kjellström *et al.*, 2005; Kjellström and Ruosteenoja, 2007).

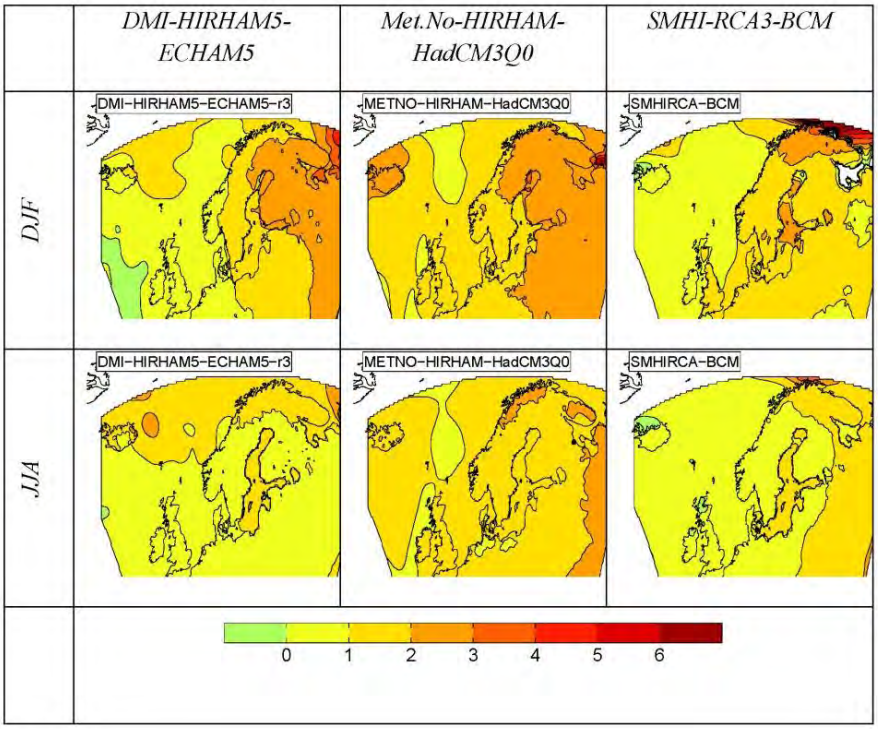

Figure 3.2. Change in 2m-temperature comparing 2021–2050 with 1961–1990 for the three recommended CES scenarios. Unit: °C.

All three recommended RCMs project precipitation increases in most of the areas in both winter and summer (Figure 3.3). However, the changes are relatively small compared with the multi-model mean in northern Fennoscandia (Figure 3.1). Analysis of all 15 simulations shows that there is a strong connection to the choice of forcing GCM. This can be exemplified by the larger precipitation increase averaged over the RCMs forced by HadCM3Q0 (ref) compared with that in those forced by ECHAM5/MPI-OM1 and CNRM-CM3 in summer (compare the DMI and Met.No simulations in Figure 3.3). In parts of the southern CES area, most notably in the Baltic States and in Denmark, precipitation is projected to decrease in several of the individual simulations. However, this is not the case in the three recommended scenarios.

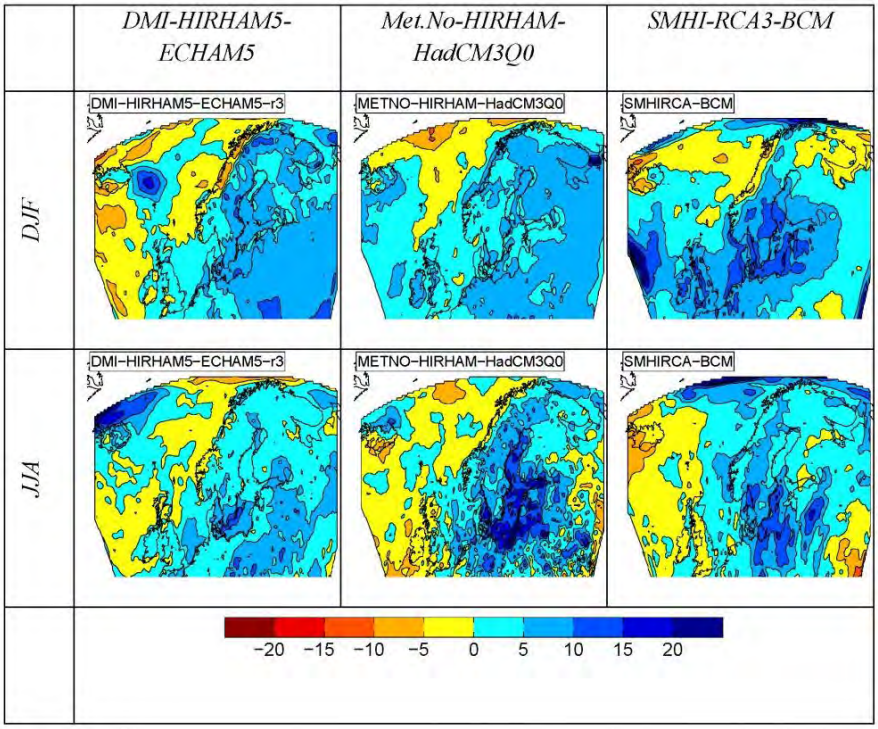

Figure 3.3. Change in precipitation comparing 2021–2050 with 1961–1990 for the three recommended CES scenarios. Unit: %.

For wind speed, there is also a strong dependency on the choice of GCM from which lateral boundary conditions are taken. In winter, relatively large changes are seen in the SMHI-RCA3-BCM simulation (Figure 3.4). The increase over the British Isles, the North Sea, Denmark and southern Sweden in the SMHI-RCA3-BCM simulation is connected to an increase in the north-south pressure gradient in this area in the BCM simulation as discussed by Kjellström *et al.* (2011). This simulation shows large changes over the northernmost sea areas in both summer and winter. Possibly this reflects the fact that the underlying BCM simulation shows a cold bias in this region with too extensive sea-ice cover in the control period. The climate change signal may therefore be augmented by an excessive warming as starting conditions are too cold.

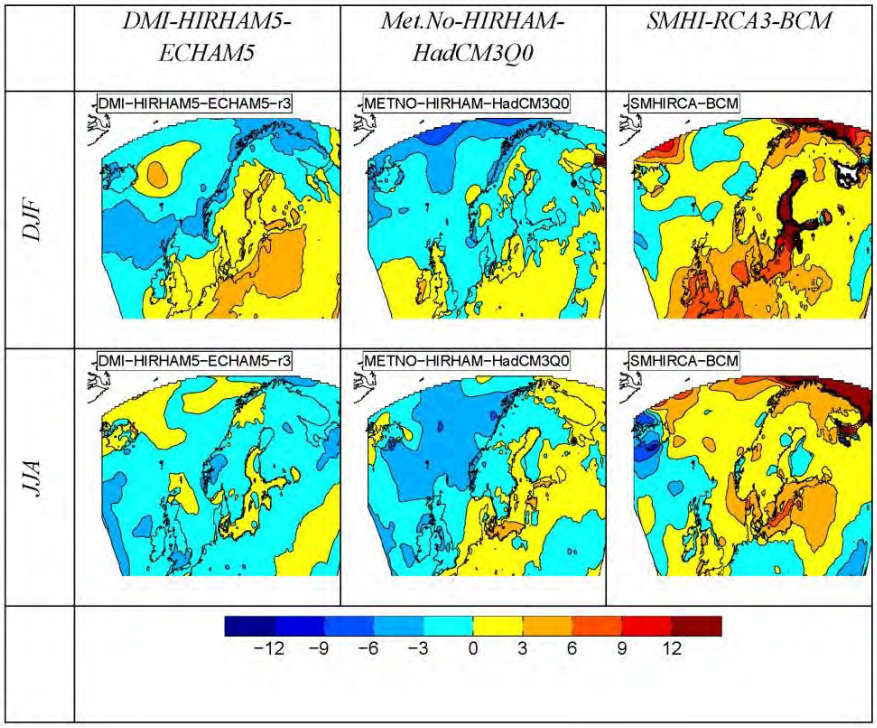

Figure 3.4. Change in wind speed comparing 2021–2050 with 1961–1990 for the three recommended CES scenarios. Unit: %.

3.2.5 Other climate change scenarios

Apart from the CES/ENSEMBLES RCM simulations a number of other climate change scenarios have also been analysed or used for subsequent climate impact related studies within the CES project. Most of these studies are based on the GCM simulations undertaken in the third climate model intercomparison project (CMIP3) used extensively in the Fourth Assessment Report (AR4) of the IPCC (Meehl *et al.*, 2007). Some of these GCM simulations have been downscaled in CES/ENSEMBLES as described above (Table 3.1), but also other GCM simulations have been used in various studies, either directly or further downscaled by statistical or dynamical techniques.

An additional relatively large ensemble of RCM simulations used in the CES project has been developed at the Rossby Centre. This involves the downscaling of 16 GCM simulations to 50km horizontal resolution over the ENSEMBLES minimum domain. This ensemble includes downscaling of: 8 different driving GCMs under a few different emission scenarios, 3 members from an ensemble with one GCM under one emission scenario only differing in initial conditions and 3 members from an ensemble with one GCM that is perturbed in its parameters. We do not present results from this ensemble here but refer to Kjellström *et al.* (2011) for a general description of the ensemble including changes in

seasonal mean conditions and to Nikulin *et al.* (2011) for changes in extremes based on daily data.

3.2.6 Reanalysis-driven RCM simulations

In addition to simulations of future climate, downscaling of ERA40 reanalysis data for the period 1961–2002 (Uppala *et al.*, 2005) has been carried out within the CES and ENSEMBLES projects, with the purpose of evaluating the RCMs in the recent past climate. Further documentation of these simulations and an evaluation of RCMs can be found in e.g. Christensen *et al.* (2010). They report on the RCMs ability to reproduce observed features of the climate including: the large-scale circulation, mesoscale variability, probability distributions of daily and monthly temperature and precipitation, extreme precipitation and temperature, seasonal cycles and long-term trends. A conclusion of that work is that no single RCM is best in reproducing all aspects of the climate in the ERA40 period. Further, models that are better than average in many variables and seasons show poor skill in other aspects implying that the use of an ensemble of simulations may be preferable even if the ensemble mean is not always better than the individual models.

3.3 Probabilistic projections of climate change based on a wider range of model simulations

The RCM simulations described in the previous section, and in particular the three simulations that were given the highest priority, only cover a part of the uncertainty space of plausible future climate changes. In this section, the temperature and precipitation changes as obtained from the three simulations are compared with probabilistic estimates based on a wider range of global and regional climate model simulations. Ideally, such probabilistic projections should answer the following question: if all possible RCMs were driven by boundary forcing from all possible GCMs and under all plausible emissions scenarios, then what would be the resulting distribution of climate changes, including the effects of natural variability?

3.3.1 Probabilistic forecasts of climate change on decadal time scales based on GCM simulations

As a first step, probabilistic forecasts of temperature and precipitation change for the four decades before the year 2050 were constructed by using output of 19 global climate models (Räisänen and Ruosteenoja, 2008). The expected anthropogenic warming was found to be quite strong compared with natural interdecadal temperature variability, whereas the corresponding change in precipitation is much weaker. In

most parts of northern Europe, this analysis indicates at least a 95% probability that the 10-year annual mean temperature will exceed the mean for 1971–2000 in the decade 2011–2020, but the corresponding probability of increasing precipitation is only 60–80%. In later decades, when the greenhouse gas forcing increases in magnitude, the sign of precipitation change also becomes more certain, but the quantitative uncertainty in the projections increases as the impact of climate model differences grows gradually larger. The sensitivity of the projections to differences between SRES emissions scenarios was found to be small prior to about 2040, but it increases substantially in the second half of the 21st century. As the emission scenario uncertainty is still relatively small for the period preceding 2050, we focus on climate change under the A1B scenario in the following.

3.3.2 Adding the RCM climate change signal to the probabilistic GCM-based forecasts

An approximate method for estimating the distribution of climate changes for "all" combinations of RCMs and driving GCMs was developed in Räisänen and Ruokolainen (2009). The method consists of three main steps:

1. The probability distribution of "large-scale" climate changes is estimated from available GCM simulations, using a previously developed resampling technique (Räisänen and Ruokolainen, 2006; Ruokolainen and Räisänen, 2007; Räisänen and Ruosteenoja, 2008) that serves to maximise the sampling of natural climate variability.
2. Available RCM simulations are used to find a statistical relationship between the large-scale and local climate change.
3. The relationships found in step 2 are combined with the distributions obtained in step 1, to estimate probability distributions of local climate change.

The method was applied using 19 GCMs from the CMIP3 intercomparison (Meehl *et al.*, 2007) and 13 RCM simulations from the ENSEMBLES data set (at the time this analysis was made, some of the 15 RCM simulations documented above were not yet available). "Large-scale" changes that were inferred directly from the GCMs were defined as area means over a 1500×1500 km square around the point of interest. As in Section 3.2 above, the focus was on 30-year mean climate changes from 1961–1990 to 2021–2050.

The resulting 5th, 50th and 95th percentiles of the distributions of annual mean temperature and precipitation change are shown in Figure 3.5. The best estimate (i.e., the 50th percentile) of warming varies from about 1.5°C in Iceland, Denmark and western Norway to more than 2°C in Finland and northern Scandinavia. The 95th percentile exceeds these values typically by at least 50%, whereas the 5th percentile of warming is

mostly less than half the best estimate but still above zero (although in Iceland, marginally so). The signal of precipitation change is more uncertain. Although the best estimate shows a precipitation increase exceeding 5% in most parts of northern Europe, the 5th percentile is negative in large areas, indicating more than 5% chance of less precipitation in 2021–2050 than in 1961–1990. The 95th percentile of annual mean precipitation change is typically about 15%.

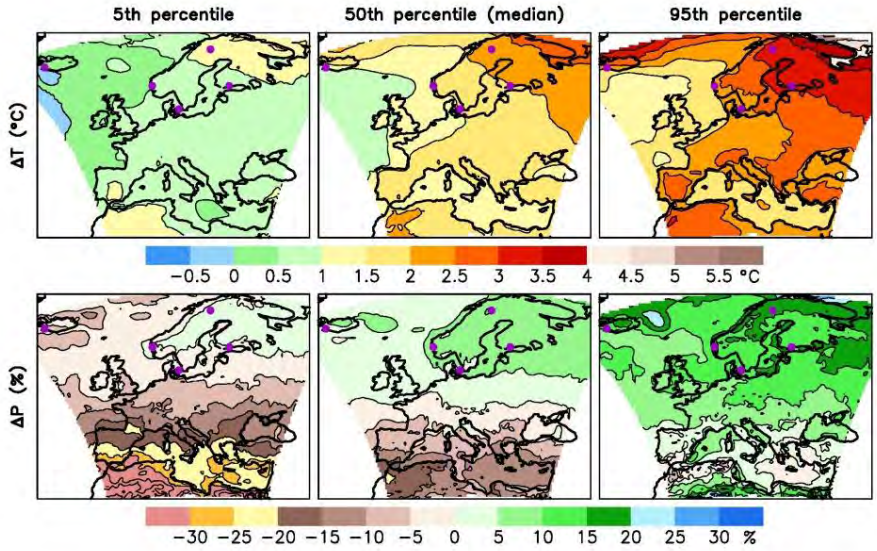

Figure 3.5. The 5th, 50th (median) and 95th percentiles of the probability distributions of annual mean temperature change (top) and precipitation change (bottom) from 1961–1990 to 2021–2050. The five purple dots indicate the locations used in Figure 3.6.

As illustrated for five locations in Figure 3.6, the uncertainty grows larger when individual months instead of annual mean values are considered. The models generally indicate a larger warming in winter than in summer, but the uncertainty in the magnitude of temperature change in winter months also tends to be particularly large. For precipitation, the larger uncertainty in monthly than annual mean changes is even more evident. With just a few exceptions mainly in winter months, the central 50% (25–75%) range of monthly precipitation changes intersects zero, indicating a large uncertainty in the sign of precipitation change in individual months. Much of this uncertainty is caused by the large natural variability of precipitation, which affects monthly mean values even more strongly than seasonal or annual means.

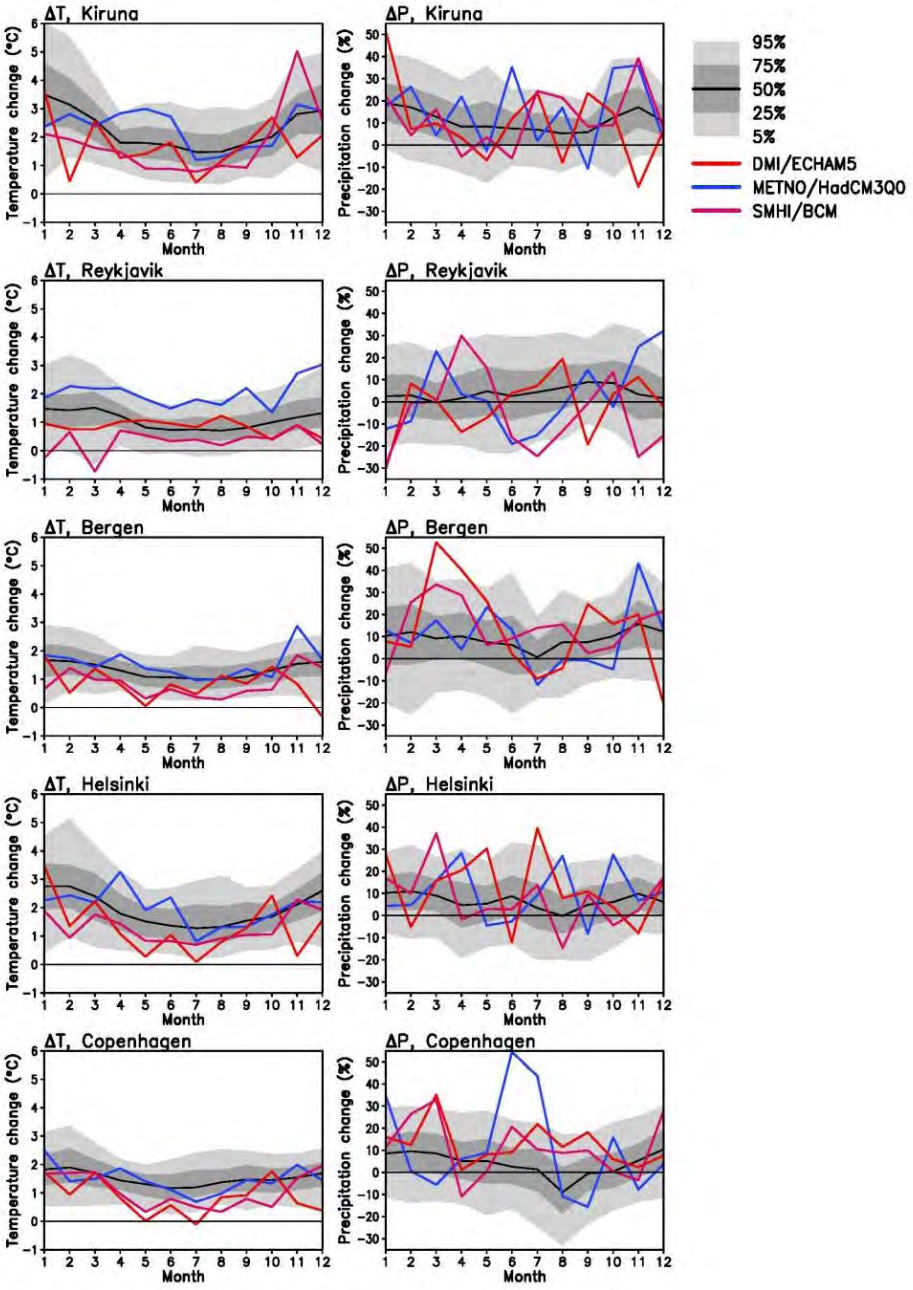

Figure 3.6. Comparison between probabilistic estimates of monthly mean temperature (left) and precipitation (right) change with the three recommended CES RCM simulations at the five locations indicated by the purple dots in Figure 3.5. The shading shows the 5th, 25th, 50th, 75th and 95th percentiles of the derived distributions, as indicated by the legend in the top-right corner of the figure. The three recommended RCM simulations are shown by coloured lines and are also identified in the legend.

3.3.3 Setting the recommended CES scenarios in a wider perspective

Also shown in Figure 3.6 are the temperature and precipitation changes in the three recommended RCM scenarios. In general, these fit well within the distributions inferred from the wider range of GCM and RCM simulations. However, the temperature change in both DMI-HIRHAM-ECHAM5 and SMHI-RCA3-BCM is mostly below the median estimate, and in some cases close to the lower bound from the wider distribution, whereas the warming in Met.No-HadCM3Q0 tends to exceed the median, particularly in Iceland. There are exceptions to these rules, including a very large warming in DMI-HIRHAM-ECHAM5 in northern Scandinavia in November.

Figure 3.6 reveals one major difference between the recommended RCM simulations and the probabilistic results, namely, a very large increase in precipitation in June and July in Met.No-HadCM3Q0 in the Copenhagen area. A partial explanation here is that Met.No-HadCM3Q0 was not yet available for the sample of RCM simulations used for the probabilistic analysis. On the other hand, Met.No-HadCM3Q0 is in this specific case an outlier compared with all other RCM simulations, possibly because of a too strong response to increasing sea surface temperature. This example further emphasises the danger of drawing far-reaching conclusions from the results of individual model simulations.

3.4 Downscaling to high spatial resolution

3.4.1 Dynamic downscaling of precipitation

In order to assess the impact of horizontal resolution on the simulated climate, the atmosphere has been simulated for selected areas at different resolutions (Figure 3.7). The simulations are carried out with the WRF model (Skamarock *et al*., 2008) with microphysics parameterized by the WSM3 scheme (Hong *et al*., 2004). The outermost domain is very large (400x200 grid-points) with a horizontal resolution of 27 km. There is one-way nesting to a 9 km domain (202x202 grid-points) covering Southern Scandinavia and parts of Finland (cf. Figure 3.7b). Within the 9 km domain, there are four domains (one-way nesting) with a 3 km horizontal resolution (cf. Figure 3.7c). The 3 km domains are as follows: W-Norway: 70x70 points (44.100 km^2), Central-Sweden: 142x142 points (181.500 km^2), Denmark: 70x94 points (59.200 km^2) and S-Finland: 55x70 points (34.650 km^2). The simulations are forced by a global simulation by the Arpège model (Déqué *et al*., 1994), run by the Bergen group (BCCR) on a T159c3 irregular grid. The simulation covers one year with forcing conditions representative of 1 September 2020 to 31 August 2021 from the SRES A1B scenario (Nakićenović and Swart, 2000). Values of sea surface temperature (SST) are calculated as ERA40 (Uppala *et al*., 2005) SSTs plus smoothed SST anomalies from ECHAM5/MPI-OM, cor-

rected for drift. Biases in the ice-edge are corrected to remove excessive ice cover in certain regions. The time varying forcing agents are varied, based upon observations. The varying forcing agents constitute CO_2, CH_4, N_2O, CFC11 (including other CFCs and HFCs), CFC12 and sulfate aerosols (Boucher data, only direct effect). Non-varying forcing agents include background aerosols such as black carbon, sea salt, desert dust, as well as stratospheric and tropospheric ozone, solar irradiance (1368 W/m^2) and the distribution of land cover types. No volcanic aerosols were included in the simulation. For more technical details, see Rögnvaldsson and Ágústsson (2009) and references therein.

Figures 3.7 and 3.8 show the accumulated one-year precipitation, simulated at different horizontal resolutions and Figure 3.9 gives the number of days per year when the grid-point precipitation, for each region and at various horizontal resolutions, exceeds different thresholds. In short, the highest horizontal resolution (3 km) yields highest precipitation and a maximum number of extremes. However, the sensitivity of accumulated precipitation to horizontal resolution is only moderate, except in the Norway region, where the 3 km domain results in about 50% more precipitation than the 9 km domain. The larger amount of precipitation in the mountainous regions of Norway in the high resolution simulation is expected as ascending motion above the mountains is not well resolved at the coarse resolutions. The larger precipitation over land is even larger than indicated by Figure 3.8, as approximately one fifth of the grid points of the Norwegian region are over sea, and as such not very sensitive to improved representation of the terrain. The precipitation extremes that appear at the fine resolutions (9 and particularly 3 km) are much more pronounced in Norway than elsewhere. This difference must be associated with strong winds and ascending motion over the mountains. In spite of mountains being present inside the Swedish domain, the total impact of increased resolution is much less in that region, than near the west coast of Norway. This difference is presumably related to the height and the spatial scale of the mountains. Mountains also cover a relatively larger part of the Norwegian domain than the Swedish domain and this is reflected in the smaller sensitivity of the total precipitation in the Swedish domain to horizontal resolution presented in Figure 3.8.

In spite of the land being relatively flat both in the Danish and Finnish regions, simulated precipitation increases with resolution. The sensitivity in Denmark is limited, but the signal is more evident in Finland. Figure 3.8 reveals that there is a precipitation maximum aligned with the coast of Southern Finland. This maximum becomes more pronounced when resolution is increased, indicating that increased resolution may enhance coastal convergence and that this effect may be important in a climate context. A similar feature can be detected in the Danish domain (Figure 3.7), but the size of that domain is such that this effect does not appear clearly in the accumulated precipitation in Figure 3.8.

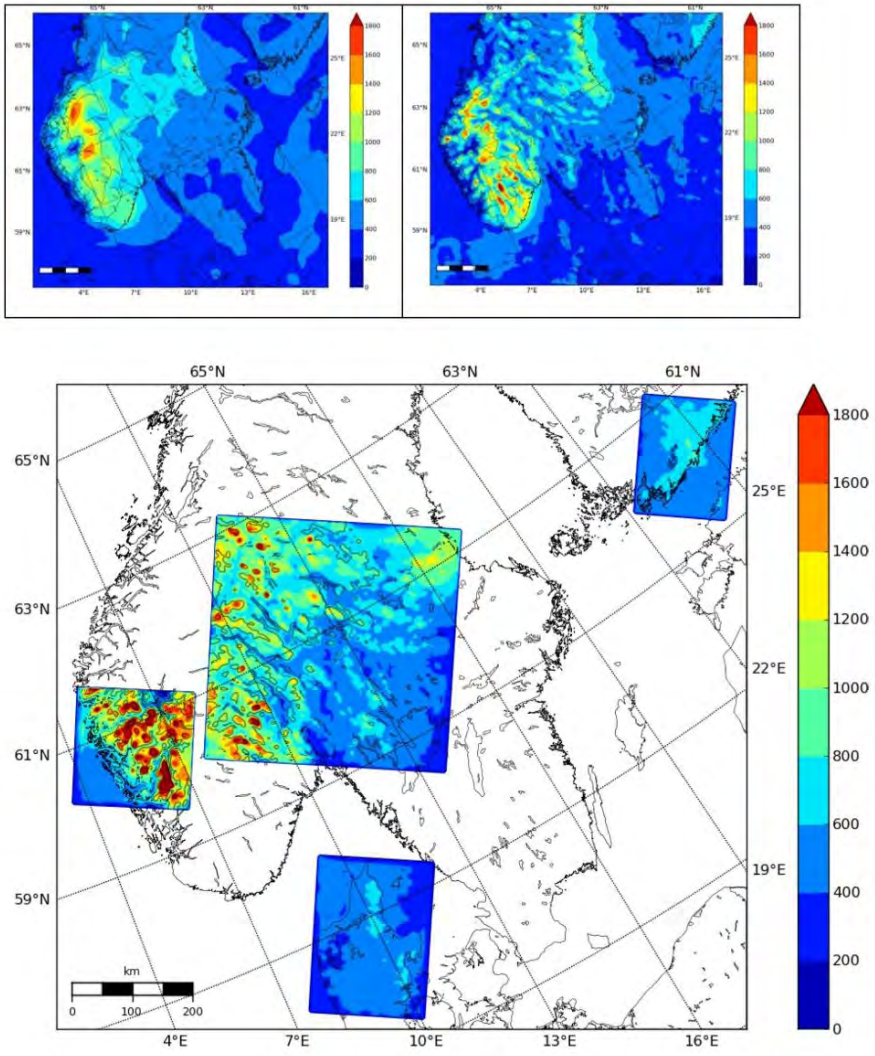

Figure 3.7. Accumulated stratiform precipitation simulated with the WRF model with boundaries from the Arpege T159c3 (SRES A1B) model simulated by the Bergen group (BCCR). The simulated period is September 2020 to September 2021 with horizontal resolution a) 27 km, b) 9 km and c) 3 km. Unit: mm.

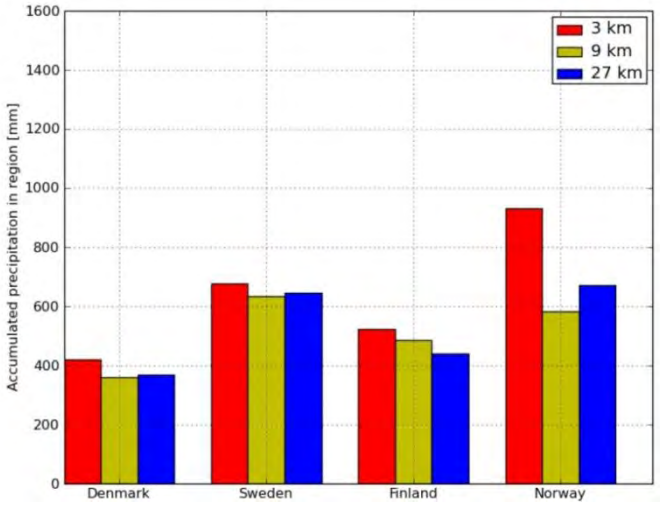

Figure 3.8. Accumulated precipitation in the regions in Figure 3.7 for different horizontal resolutions.

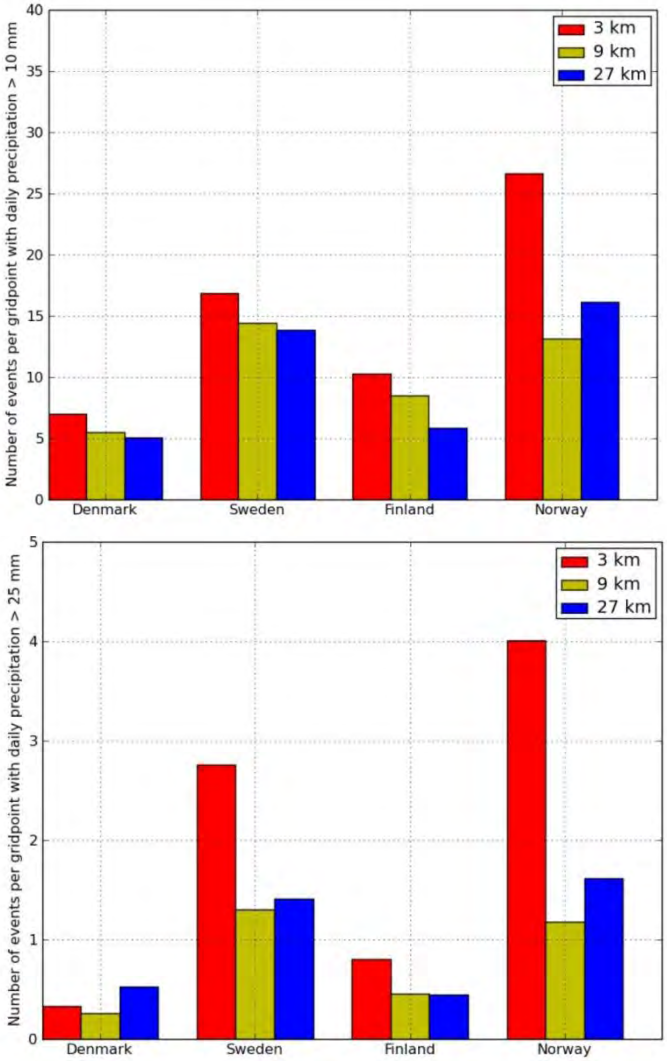

Figure 3.9. Number of days per year when the precipitation exceeds the limits of a) 10 mm and b) 25 mm in the areas in Figure 3.7.

3.4.2 High resolution climate projections for the Norwegian mainland

High resolution climate projections for the Norwegian mainland have been developed at the Norwegian Meteorological Institute (Met.No) as contributions to the CES project. As the spatial resolution in RCMs is rather coarse (the CES scenarios presented in sections 2 and 3 are all at 25 x 25 km horizontal resolution), and the output often shows biases, post processing of projections from RCMs is necessary to make them more useful when studying possible consequences of climate change. Examples of RCM biases as compared to local observational data include: erroneous monthly cycles of precipitation and temperature, too high or too low temperatures in winter and summer respectively, too large precipitation amounts, and wrong representation of the number of days with precipitation. Here we describe how temperature and precipitation obtained with RCMs are adjusted empirically to better represent the observed climate following the method given in Engen-Skaugen (2007).

Calculation of adjustment factors

Adjustment factors are calculated from observationally based fields with resolution 1 km^2 for "the control period" which in this case is 1961–1990. The observationally based gridded data sets of temperature and precipitation, which represent "present climate", are obtained by interpolating station values. Daily precipitation sum and mean daily temperature are interpolated to daily grids with spatial resolution of 1 km^2 covering the Norwegian mainland (Tveito *et al.*, 2005). The interpolation method used is triangulation on precipitation and residual interpolation on temperature (Tveito *et al.*, 2005). The precipitation values are corrected for altitude and for under-catch due to wind loss (Førland *et al.*, 1996). Time series in each 1 km^2 grid point of temperature and precipitation are available from 1957–present (see http://senorge.no).

The daily 1 km^2 observationally based grids contain uncertainties due to low density of available temperature and precipitation stations and because station measurements may not be representative for the 1 km^2 area. Uncertainty of the estimates follows the density of stations. In Norway, the density of temperature and precipitation stations increased from the beginning of measurements (before 1900) until ~1970. The number of stations was stable in the twenty-year period 1970–1990, but it has decreased after 1990. Another important aspect is that most of the stations are situated in low lying regions. High-elevation regions with complex terrain are therefore associated with larger uncertainty.

Empirical adjustment of RCM output

Daily temperature and precipitation projections from the three recommended RCM scenarios (No. 2–4 in Table 3.1) were interpolated to the 1 km^2 grid covering the Norwegian mainland (same lattice points as for the observationally based grids). Each grid point is considered as indi-

vidual time series in the subsequent adjustment procedure that involves the following steps:

1. The time series are normalised and standardised with mean value and standard deviation for the control period (1961–1990).
2. The residuals are then scaled up with mean value and standard deviation from observations during the same time period.
3. The climate signal from the RCM output is counted for in the scaling process for future time periods.

The procedure results in locally adjusted time series that maintain the monthly mean climate change signal as given by the RCMs.

An example of time series extracted from a grid point at the high mountain area Dovre in Norway, is presented in Figure 3.10. The figure shows accumulated frequency distribution curves of daily temperature during winter (DJF) for the time period 1961–1990 and the three projections for 2021–2050. It is clear that the projected temperature will increase for all days albeit not homogeneously as the change in very cold winter days tends to be larger. The mean change is largest in the met.no HadCM3-run, less in the SMHI BCM-run and smallest in the DMI ECHAM5-run. This is in accordance with the figures presented in Figure 3.2.

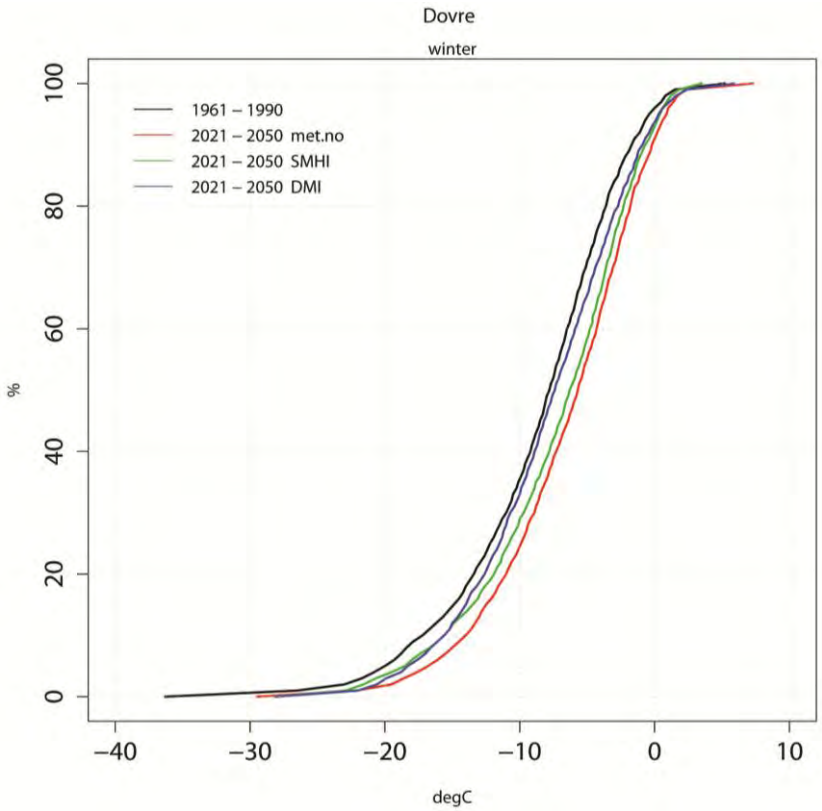

Figure 3.10. Accumulated frequency distribution curves of daily temperature for the reference period 1960–1990 and the future period focused on within the CES project (2021–2050). The three projections (met.no, SMHI and DMI) are listed as No. 2–4 in Table 3.1.

Another example of empirically adjusted projections of seasonal mean temperatures in southern Norway is given for the three selected model runs in Figure 3.11. The adjusted data have been used as input to the hydrological modelling in Norway (Bergström *et al.*, this volume).

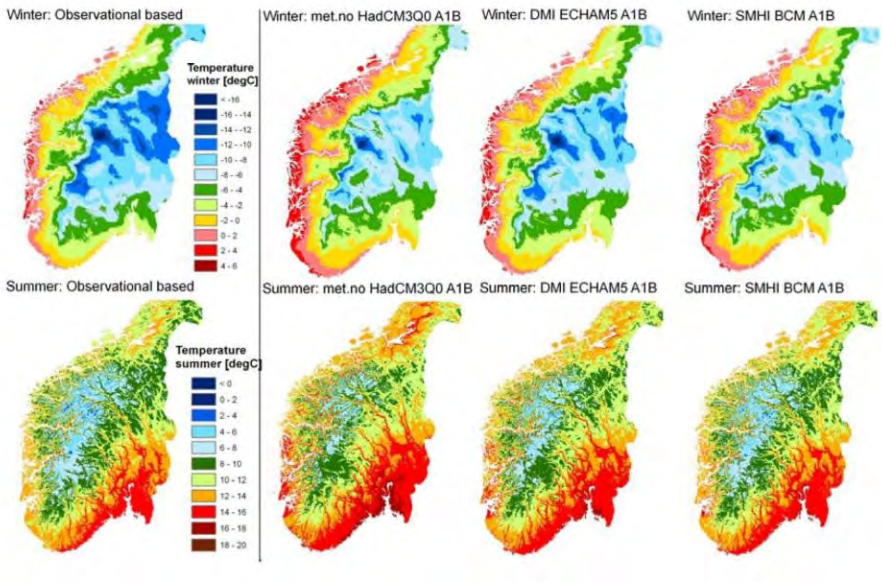

Figure 3.11. Winter and summer temperature projections for southern Norway for the time period 2021–2050 based on the three selected RCM runs.

3.5 Additional studies

3.5.1 Inter-annual variability of climate: observations alone do not tell what to expect for the future

Along with the expected gradual shift towards higher mean temperatures and generally slightly more precipitation, the inter-annual variability of weather conditions will continue. Over time, however, warm weather will become increasingly more common and cold weather less common. For temperature, the change that has already occurred means that observations from the commonly used reference period 1961–1990 no longer yield a good estimate of the present-day (year ~2010) climate.

A method for estimating the probability distributions of monthly, seasonal and annual means of temperature and precipitation in a changing climate was developed by Räisänen and Ruokolainen (2008), and was further refined and applied in the CES project by Räisänen (2009). The method starts from observed time series of climate variability, but modifies past observations attempting to make them representative of present or future climate conditions, by combining information from the observed evolution of the global mean temperature with model simulations of local and global climate change.

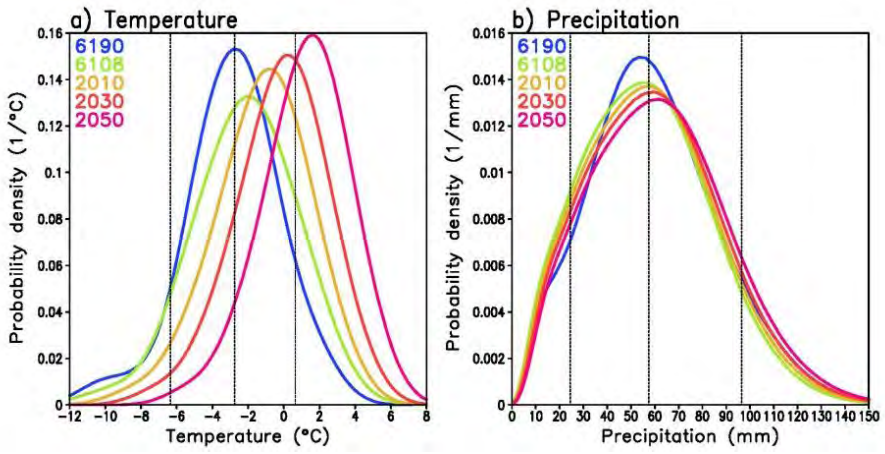

Figure 3.12. Probability distributions of (a) December mean temperature and (b) December precipitation sum in Helsinki, Finland. The blue and green lines represent the distributions derived from observations for 1961–1990 and 1961–2008, respectively, using Gaussian kernel smoothing. The yellow, red and purple lines give the model-based best estimates for the distributions around the years 2010, 2030 and 2050, respectively. The three vertical lines show the 10th, 50th and 90th percentiles of the distributions for the reference period 1961–1990.

As an example, the resulting distributions of December mean temperature and precipitation sum in Helsinki are shown in Figure 3.12. The blue and green lines show two observational estimates for the distributions, based on data for 1961–1990 and 1961–2008, respectively, and their differences reflect both climate change and sampling uncertainty. The other distributions, representing the present-day climate (2010) and the future (2030 and 2050), are built on observations from the longer and more recent period 1961–2008, but modifying these for the effects of climate change as outlined above. The main message from this analysis (which is also valid for other months and locations) is a much stronger effect of climate change on temperature than on precipitation variability. Already in the present-day climate, more than 70% of Decembers in Helsinki are estimated to be warmer than the median value for the reference period 1961–1990 (-2.8°C), and this fraction is projected to exceed 90% in the middle of the century. By contrast, the projected effect of near-term climate change on the distribution of December precipitation sum is modest, being comparable with the observed differences between the two overlapping periods 1961–1990 and 1961–2008. However, the impact becomes somewhat more pronounced when considering seasonal and annual sums of precipitation, which are less strongly affected by natural variability. A similar analysis has been repeated at 120 Nordic locations for temperature and 230 locations for precipitation, and the results have been made available on-line as described by Räisänen (2009).

3.5.2 Projected migration of climatic zones in Scandinavia and the Baltic Countries

The Köppen climate classification combines two climate parameters of high practical importance, namely temperature and precipitation. Many impacts of climate change on renewable energy resources are related to these two variables either directly or indirectly – through evaporation, soil moisture and runoff. Maps of the Köppen classification (Table 3.2) were produced, using regional climate model (RCM) simulations under the SRES A1B forcing for two future periods and the E-OBS v. 3.0 observed dataset for the reference period (Haylock *et al.*, 2008). The so-called delta change method was applied to account for bias in the RCM output, and the three scenarios recommended for use in CES were considered (No. 2–4 in Table 3.1).

According to the three RCMs, there is a general change in the CES study area towards milder winters as well as longer and warmer summers. The large-scale patterns are quite similar among the three RCMs as exemplified by DMI-HIRHAM5-ECHAM5 in Figure 3.13. However, Met.No-HIRHAM-HadCM3Q0 portrays more rapid zone shifts than the remainder (not shown).

- The climatic border line between cold, snowy winters (Df) and mild winters (Cf, with the mean temperature of the coldest month above -3°C) will penetrate north-eastward, particularly in the Baltic States.
- The tundra climate (ET, with the mean temperature of the coolest month below -3°C and of the warmest month below 10°C) will contract in the Scandinavian mountains, being replaced by Df, as well as in Iceland, being replaced by Cf.
- In areas of Fennoscandia where the climate type of seasonal snow cover (Df) will still prevail, the zone of long and warm summers (Dfb) will extend farther northward.

A separate investigation, conducted as a web-based questionnaire survey, indicated that the information regarding the migrating climatic zones, as disseminated by maps, was generally interpreted correctly (Jylhä *et al.*, 2010). This suggests that maps showing projected future climatic zones are an easily-comprehensible means to summarize climate change information and to compare results based on different RCMs.

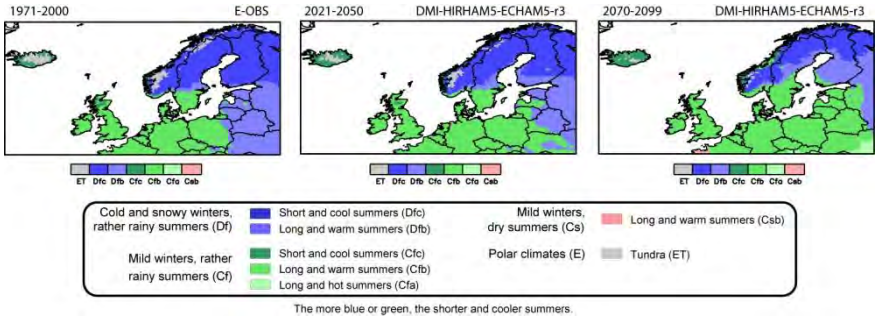

Figure 3.13. Köppen climate zones deduced from observations for the period 1971–2000 and from DMI-HIRHAM5-ECHAM5 simulations for two future periods, assuming the A1B scenario.

Table 3.2. Climatic zones prevailing in the study area and their criteria (based on Critchfield (1966) but modified for the border between ET and Cf, relevant for Iceland). It is additionally required that criteria for arid climates (not given here) are not fulfilled.

Zone	Description	Criteria
ET	Tundra	$T_{min} \leq -3^{\circ}C$ and $T_{max} \leq 10^{\circ}C$
Df	Cold and snowy winters, rather rainy summers	$T_{min} \leq -3^{\circ}C$ and $T_{max} > 10^{\circ}C$ $P_{min,s} \geq 40$ mm or $P_{min,s} \geq P_{max,w}/3$ and $P_{min,w} \geq P_{max,s}/10$
Dfc	Short and cool summers	$T_{4,max} < 10^{\circ}C$ and $T_{max} < 22^{\circ}C$
Dfb	Long and warm summers	$T_{4,max} \geq 10^{\circ}C$ and $T_{max} < 22^{\circ}C$
Cf	Mild winters and rather rainy summers	$-3^{\circ}C < T_{min} < 18^{\circ}C$ $P_{min,s} \geq 40$ mm or $P_{min,s} \geq P_{max,w}/3$ and $P_{min,w} \geq P_{max,s}/10$
Cfc	Short and cool summers	$T_{4,max} < 10^{\circ}C$ and $T_{max} < 22^{\circ}C$
Cfb	Long and warm summers	$T_{4,max} \geq 10^{\circ}C$ and $T_{max} < 22^{\circ}C$
Cfa	Long and hot summers	$T_{max} \geq 22^{\circ}C$
Cs	Mild winters and dry summers	$-3^{\circ}C < T_{min} < 18^{\circ}C$ $P_{min,s} < 40$ mm and $P_{min,s} < P_{max,w}/3$
Csb	Long and warm summers	$T_{4,max} \geq 10^{\circ}C$ and $T_{max} < 22^{\circ}C$

T_{min}	Average temperature of the coolest month
T_{max}	Average temperature of the warmest month
$T_{4.max}$	Average temperature of the 4th warmest month
$P_{min,s}$	Average precipitation in the driest one of the six warmest months
$P_{max,s}$	Average precipitation in the wettest one of the six warmest months
$P_{min,w}$	Average precipitation in the driest one of the six coolest months
$P_{max,w}$	Average precipitation in the wettest one of the six coolest months

3.5.3 Projected trends in summertime precipitation in Finland

Future evolution of mean precipitation in Finland in May–September (MJJAS) was projected based on the output of 13 regional climate model simulations developed in the ENSEMBLES project (Ylhäisi *et al.*, 2010). Two areas were considered, one located in the north-east (NE) and the other in the south-west (SW). Based on observations, the long-term (1908–2008) past MJJAS precipitation trends in those areas were either non-significant (SW) or increasing (NE). Model performance was evaluated by comparing the simulated precipitation sums during the baseline period 1961–2000 with those based on three observational data sets. The models appeared to commonly overestimate precipitation. A simple

scaling method was applied for each individual simulation to remove the mean bias; the ratio between the observed and simulated precipitation sums was assumed to stay constant also in the projected climate.

According to the multi-model mean (MMM) trends over the 140-year time period 1961–2100, precipitation will increase both in SW and NE (Figure 3.14). The mean MJJAS precipitation in 2021–2050 is 35 mm higher in NE and 37 mm higher in SW than in the baseline period 1961–2000. The long-term trend over the 140-year time period 1961–2100 in the MJJAS rainfall sum was 4.4 mm/10 years in NE and 3.2 mm/10 years in SW, corresponding to a rise per decade of 1.3% and 1.1%, respectively, relative to the baseline period. The MMM trends are statistically significant for both areas and time periods considered. The variation in the future trends between the individual simulations was quite large, particularly so for SW (Figure 3.14). Furthermore, the number of independent simulations in this study was fairly small, presumably resulting in an underestimate of the actual uncertainty in the future evolution of precipitation.

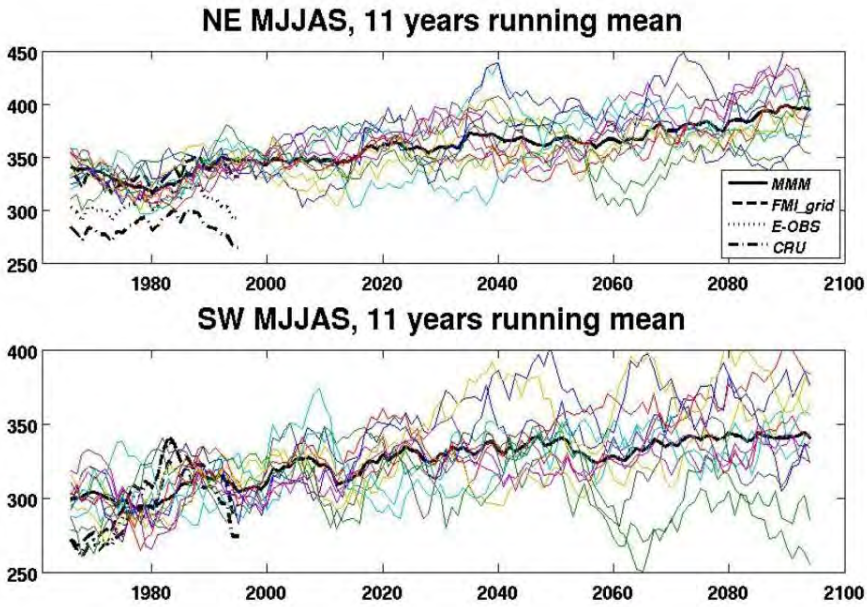

Figure 3.14. 11-year running means for the MJJAS precipitation sum for two study areas in Finland (NE and SW). Thin solid curves show individual simulations and the thick solid curve depicts the multi-model mean (MMM). Dashed and dotted curves represent observations in three gridded data sets. The model simulations are scaled so that the mean value in 1961–2000 corresponds with the mean value of the FMI grid (Ylhäisi et al., 2010).

3.5.4 Surface air temperature and total precipitation trends for Iceland in the 21st century

Nawri and Björnsson (2010) demonstrated by comparison between GCM fields on a 2°x2°-degree grid, ERA-40 reanalyses on a 1°x1°-degree grid, RCM simulations on a 0.25°x0.25°-degree grid, and high-density observations, that a spatial resolution above 1° in longitude and latitude is essential for an accurate representation of surface air temperature (SAT) and total precipitation (TP) over the complex terrain of Iceland. To further illustrate the impact and potential benefits of a higher spatial resolution, trends in SAT and TP over Iceland and the surrounding ocean area for a 10-member subset of the IPCC GCMs, as well as for the three recommended RCM scenarios (No. 2–4 in Table 3.1) were investigated. In all simulations the IPCC A1B emissions scenario was used.

Differences between land and ocean in linear trends of GCM ensemble mean SAT during the first half of the 21st century are small. The 10-model average warming rate is 0.30 K per decade over the ocean, and 0.32 K per decade over land. Differences in spatial patterns and amplitude of warming between different GCMs are, however, large leading to considerable differences between the three recommended RCM scenarios. The projected linear rates of RCM SAT increase per decade over the same period are 0.17 K and 0.20 K based on the SMHI-RCA3, 0.24 K and 0.32 K based on the MetNo-HIRHAM5, and 0.40 K and 0.44 K based on the DMI-HIRHAM5 over the ocean and land, respectively. Given the strong influence from the driving GCMs, RCMs provide little independent information beyond the GCM results over ocean and at low elevation. However, the higher spatial resolution of RCMs allows a more detailed analysis of linear SAT trends as a function of terrain elevation.

Taking into account GCM and RCM runs, average linear trends of total precipitation are 0.8% of the 1961–90 mean value per decade, or 2.5% per degree warming.

3.5.5 Characteristics of North Atlantic Cyclones in reanalysis and GCM data

Dominant daily low-pressure centres over the northern North Atlantic are mostly restricted to the open sea, and their geographical distribution is therefore limited by coastlines and the variable sea-ice edge. An analysis of ERA40-data (Nawri, 2010) shows that low-pressure centres on daily to seasonal time-scales tend to cluster in a region extending from the northern part of the Norwegian Sea into the Barents Sea, as well as in two regions southwest of Iceland: the Irminger Sea, associated with northward moving cyclones passing east of southern Greenland, and the Labrador Sea, associated with cyclones passing Greenland to the west and moving north into Davis Strait. 19 CMIP3 GCMs show different abilities of reproducing these low-pressure patterns. Three of these are shown together with ERA40 in Figure 3.15. As for the ERA40-reanalysis, GCM simulated

mean sea level pressure (MSLP) minima are also restricted to the ice free ocean. Consequently, the north-eastward spread of persistent wintertime cyclone centres is determined to a large extent by the sea ice cover over the Barents Sea. For a majority of the GCMs there is more extensive sea ice over the Barents Sea compared with the reanalysis, and correspondingly a reduced northward spread of dominant cyclone centres.

According to ERA40, linear trends in MSLP throughout the 1958–2009 period vary greatly across the North Atlantic region, as well as seasonally. In winter, negative trends occur north of 55°N, with a maximum decrease east of Greenland at a rate of 1 hPa per decade. In summer, trends are weaker but mostly positive around Greenland, with a maximum increase of 0.5 hPa per decade over the Labrador Sea. The wintertime trends towards lower pressure east of Greenland are strongly correlated with decreasing sea ice cover in that region. Some of the GCMs project a northward shift of the storm tracks over the North Atlantic (Yin, 2005). Contributing to this shift could be an excessive warming resulting from the cold bias in the Barents Sea in many GCMs in the 20th century.

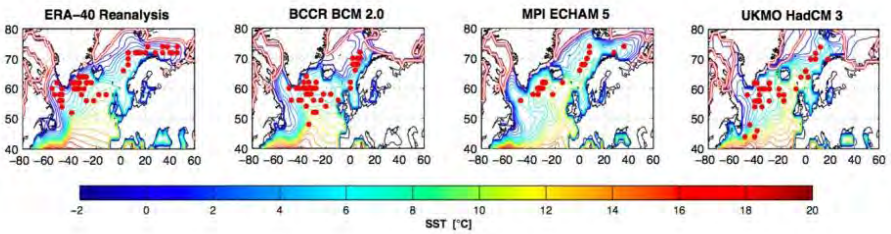

Figure 3.15. Distribution of wintertime (DJF) mean sea level pressure minima (red dots) during the 1957–1999 period, in relation to mean sea surface temperature (coloured contours) and the average 50% sea ice concentration contour (red double contour) for the same period.

3.5.6 Storm statistics

Storm statistics have been calculated from both re-analyses and RCM results (Benestad, 2010). These analyses included storm counts, estimates of the maximum gradient wind speed, spatial extent, and geographical distribution. The results suggests that there is no significant trend in the storm count or the maximum gradient wind speed over the period (1950–2050) simulated by the RCM, for which the SRES A1b emission scenario had been prescribed for the future. However, the model results had some biases compared with a similar analysis based on observations or re-analysis data, and there were indications of long-term increases in the frequency for the strongest storms over a larger region in a 20th century re-analysis data set. The 20th century re-analysis data also suggested a decrease in the maximum gradient winds over 1891–2008, but there is a concern that the mean sea level pressure fields in the re-analysis products are not homogeneous. Benestad (2010) expressed concerns that RCMs with a small spatial domain may be too constrained by the driving models, thus yielding too smooth spatial structures.

3.5.7 Surface geostrophic winds speed changes in global climate models

Ten global climate models (GCMs) are used to study future changes in surface geostrophic wind speeds (v_g) in northern Europe; a detailed report is given in Gregow and Ruosteenoja (2010, hereafter GR). Geostrophic rather than the true winds were analyzed, because the latter are sensitive to details in the surface parameterizations. We calculated percentage differences in the average v_g between the baseline period 1971–2000 and the scenario period 2046–2065 under the A1B scenario. The GCM-simulated baseline period mean v_g compares moderately well with the observation-based estimate (Figure 1 of GR).

According to the 10-GCM mean, the largest changes are simulated for autumn and winter. However, even in these seasons the average wind speeds will only change by a few percent (Figure 3.16). The most notable increase in wind speeds is seen in the southern part of northern Europe.

A closer look at the wind speed histogram was taken for the southern part of the Baltic Sea. We find that the increase in average v_g is associated with a decrease in the frequency of low wind speeds (by 3 percentage units when summing up all the frequencies with v_g < 10 ms^{-1}) and a corresponding increase of strong winds.

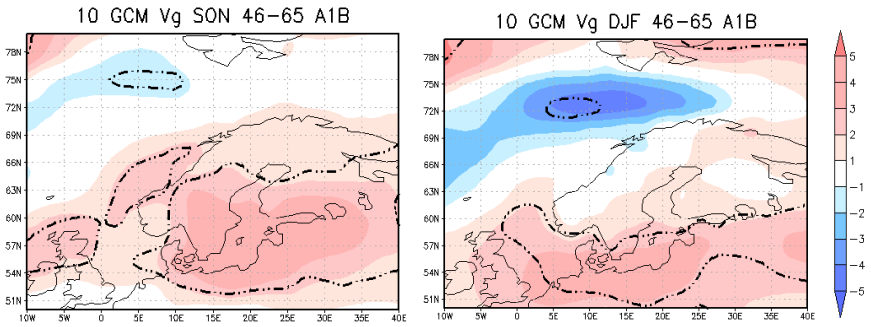

Figure 3.16. 10-GCM mean percentage changes in September-November (left panel) and December-February (right panel) mean geostrophic wind speeds (v_g) from 1971–2000 to 2046–2065. Areas where the response is statistically significant at the 5% level are marked by dashed contours.

3.5.8 Solar radiation projections

Projections for solar radiation focus here on the Nordic area and the period 2020–2049; for information for the entire Europe, see Ruosteenoja and Räisänen (2009, hereafter RR). Projections are based on simulations performed with 18 global climate models under the SRES A1B, A2 and B1 scenarios. For the baseline period 1971–2000, the mean of the 18 model simulations accords strikingly well with observations (Figure 1 of RR).

The geographical distribution of the projected insolation change (an average of 18 models) is depicted in Figures 3 (percentage) and 4 (in absolute terms) of RR. In the relative sense, largest changes occur in

central Scandinavia and southern Finland in winter, where more than 5% of incident radiation is lost. In the remaining three seasons, changes are quite modest, less than ±5%. When the radiation response is studied in absolute terms, the impression becomes somewhat different. In the winter months, changes in Nordic areas are very minor, less than 10 MJ m^{-2}. The largest changes occur in spring and summer, with the maximum decreases (increases) of about 40 MJm^{-2} in northern Lapland in spring (central Sweden in summer). In southern Europe, solar radiation is in general simulated to increase. There are areas where the annual insolation increases by more than 100 MJ m^{-2}. Considering the differences among the various model projections, the result indicating an insolation decrease in winter months in the Nordic area seems to be quite robust.

3.5.9 Changes in extremes as projected by a range of GCMs

To estimate a possible future change in climate extremes over the territories of Europe (EU) and European Russia (ER) Shkolnik and Efimov (2010) used results from an ensemble of 9 CMIP3 comprehensive global (coupled atmosphere-ocean) climate models. Two timeslices: 1980–1999 (baseline) and 2046–2065 (under the SRES A2 emission scenario) were considered. It was shown that the annual extreme temperature range, calculated as the difference between 20 yr mean absolute annual maxima and minima temperatures, tends to decrease in the future warmer climate over northern Europe by 2046–2065, mainly as a result of the strong warming in winter with cold extremes getting less severe. Changes in summertime heat waves (wintertime cold waves), defined as periods with a number of consecutive days with daily maximum (minimum) temperatures more than 5°C above (below) the 20-year summer (winter) daily maximum (minimum) averages for 1980–1999, were also investigated. It was found that the duration of summertime heat waves will be longer and wintertime cold waves shorter, by as much as 10 days in the CES area of interest. For extreme precipitation, the results show that the simulated fraction from daily precipitation events above baseline 90^{th} quantile in summer increases in northern Europe. At the same time there is no significant change in the dry spell length in the region.

In general, the changes in selected temperature indices are prone to moderate uncertainty due to inter-model differences at least for the particular modeling set and periods considered. For precipitation the uncertainty is larger. Over most of the region not only the magnitude of changes in precipitation extremes but even the sign of these changes cannot be estimated at a reasonable level of confidence.

3.6 Summary and concluding remarks

From a broad range of climate change scenarios it can be concluded that the Nordic and Baltic region will probably move in the direction of a warmer and wetter climate in the future. The projected future warming is most pronounced in the eastern and northern areas during winter. In particular, there is a strong response to the general warming over the northernmost oceans where feedback mechanisms associated with retreating sea-ice come into play. The largest precipitation increase will generally be seen in winter. In summer, there is a larger uncertainty, and the possibility that precipitation will decrease in southern parts of the region cannot be excluded. However, many RCM simulations show relatively strong increases in summertime precipitation over the Baltic Sea. The latter is probably a consequence of the strong increase in SSTs in this area in some coarse GCMs and we advocate use of high-resolution regional coupled atmosphere-ocean models in future climate change studies for this area. Wind speed changes are generally small with the exception of areas that will see a reduction in sea-ice cover, where wind speed is projected to increase.

The three recommended RCM scenarios (No. 2–4 in Table 3.1) fit well into the wider range of RCM simulations produced in the ENSEMBLES/CES matrix of RCM-GCM combinations and in an even wider context of CMIP3 simulations. Some of the uncertainties regarding future climate change can be inferred from the spread between the members of such an RCM-GCM matrix. The results show that the choice of forcing GCM is instrumental to the overall uncertainty, but also that choice of RCM leads to significant differences for some seasons and areas. The latter implies that the use of dynamical downscaling adds an additional level to the total uncertainty of the deduced climate change.

Downscaling to even higher horizontal resolution (1–3 km) shows resulting climatologies that contain many more features compared with the 25 km simulations being standard in ENSEMBLES/CES. The largest differences are seen in mountainous areas, but also coastal effects come into play. When compared to observations it is evident that climate model output is biased. These biases are problematic in further impact studies and in some cases it may be necessary to apply some kind of bias correction technique to obtain climate data that are representative locally in an adequate way. Different methods for bias correction of RCM runs are used in impact research communities (e.g. Yang *et al.*, 2010; Elshamy *et al.*, 2009; Engen-Skaugen, 2007). There is a need for comparison of different bias correction methods to evaluate the effect of the adjustment procedures on the statistical distribution of climate variables (e.g. extremes) to be able to give improved recommendations to end users of climate projections.

3.7 Acknowledgments

The production of ENSEMBLES data used in this work was funded by the EU FP6 Integrated Project ENSEMBLES (Contract number 505539) whose support is gratefully acknowledged. The modeling groups, the Program for Climate Model Diagnosis and Intercomparison and the WCRP's Working Group on Coupled Modelling are acknowledged for making available the CMIP3 dataset.

3.8 References

Benestad, R.E. (2010). A Study of Storms and Winds in the North-Atlantic. Met.no Report 07-2010.

Bleck, R., Rooth, C.,Dingming, H., Smith L. T. (1992). Salinity-driven thermocline transients in a wind- and thermohaline-forced isopycnic coordinate model of the North Atlantic. *J. Phys. Oceanogr.,* 22, 1486–1505.

Christensen, J.H., Kjellström, E., Giorgi, F., Lenderink, G., Rummukainen, M. (2010). Weight assignment in regional climate models. *Climate Research,* 44 (2–3), 179–194.

Critchfield, H.J., 1966. *General Climatology*. Prentice Hall, Englewood Cliffs, N.J., 2nd ed. 420 pp.

Collins, M., Booth, B. B., Bhaskaran, B., Harris, G. R., Murphy, J. M., Sexton, D. M. H., Webb, M. J. (2010). Climate model errors, feedbacks and forcings: A comparison of perturbed physics and multi-model ensembles. *Clim. Dyn.* doi:10.1007/s00382-010-0808-0.

Déqué M, Revetment, C, Braun, A., Cariotta, D. (1994) The ARPEGE/IFS atmosphere model: A contribution to the French community climate modeling. *Clim. Dyn.,*10, 249–266.

Elshamy M.E., Seierstad, I.A., Sorteberg, A. (2009). Impacts of climate change on Blue Nile flows using bias-corrected GCM scenarios. *Hydrology and Earth System Science*, 13 (5), 551–565.

Engen-Skaugen T. (2007). Refinement of dynamically downscaled precipitation and temperature scenarios. *Climate Change*, 84, 365–382, DOI 10.1007/s10584-007-9251-6.

Førland, E.J. (ed), Allerup, P., Dahlström, B., Elomaa, E., Jónsson, T., Madsen, H., Perälä, J., Rissanen, P., Vedin, H., Vejen, F. (1996). Manual for Operational Correction of Nordic Precipitation Data, DNMI-Report 24/96 KLIMA. 66 pp.

Gibelin, A. L. and Déqué, M. (2003). Anthropogenic climate change over the Mediterranean region simulated by a global variable resolution model. *Clim. Dyn.,* 20, 327–339.

Gregow, H. and K. Ruosteenoja (2010). Estimating the effect of climate change on surface geostrophic winds in Northern Europe. CES Climate Modelling and Scenarios Deliverable D2.4, task ii. Available from http://www.atm.helsinki.fi/~jaraisan/ces.html

Haugen, J.E. and Haakenstad, H. (2006). Validation of HIRHAM version 2 with 50 km and 25 km resolution. RegClim General Technical Report No. 9. pp 159–173. (http://regclim.met.no/results/gtr9.pdf).

Haugen, J. E. and Iversen, T. (2008). Response in extremes of daily precipitation and wind from a downscaled multi-model ensemble of anthropogenic global climate change scenarios. *Tellus,* 60A, 411–426

Haylock, M. R., Hofstra, N., Klein Tank, A. M. G., Klok, E. J., Jones, P. D., co-authors (2008). A European daily high-resolution gridded data set of surface temperature

and precipitation for 1950–2006. *J. Geophys. Res.*, 113, D20119, doi:10.1029/2008JD010201.

Hong, S. Y., Dudhia, J., Chen, S. H. (2004). A revised approach to ice microphysical processes for the bulk parameterization of clouds and precipitation, *Mon. Weather Rev.,* 132, 103–120.

Jungclaus, J.H., Botzet, M., Haak, H., Keenlyside, N., Luo, J.-J., Latif, M., Marotzke, J., Mikolajewitch, U., Roeckner, E. (2006). Ocean circulation and tropical variability in the coupled ECHAM5/MPI-OM. *J. Clim.,* 19, 3952–3972.

Jylhä, K., Tuomenvirta, H., Ruosteenoja, K., Niemi-Hugaerts, H., Keisu, K., Karhu, J. (2010). Observed and projected future shifts of climatic zones in Europe, and their use to visualize climate change information. *Weather, Climate, and Society,* 2, 148–167. (http://journals.ametsoc.org/doi/abs/10.1175/2010WCAS1010.1).

Keenlyside, N. S. and Ba, J. (2010). Prospects for decadal climate prediction. Wiley Interdisciplinary Reviews: *Climate Change*, 1, 627–635. doi: 10.1002/wcc.69

Kjellström, E. and Ruosteenoja, K. (2007). Present-day and future precipitation in the Baltic Sea region as simulated in a suite of regional climate models. *Climatic Change* , 81, 281–291. doi:10007/s10584-006-9219-y.

Kjellström, E, Döscher, R., Meier, H.E.M. (2005). Atmospheric response to different sea surface temperatures in the Baltic Sea: Coupled versus uncoupled regional climate model experiments. *Nordic Hydrology,* 36 (4–5), 397–409.

Kjellström, E., Nikulin, G., Hansson, U., Strandberg, G., Ullerstig, A. (2011). 21st century changes in the European climate: uncertainties derived from an ensemble of regional climate model simulations. *Tellus*, 63A (1), 24–40. DOI: 10.1111/j.1600-0870.2010.00475.x

Meehl, G.A., Stocker, T.F., Collins, W.D., Friedlingstein, P., Gaye, A.T., Gregory, J.M., Kitoh, A., Knutti, R., Murphy, J.M., Noda, A., Raper, S.C.B., Watterson, I.G., Weaver A.J., Zhao, Z.-C. (2007). Global Climate Projections. In: *Climate Change 2007: The Physical Science Basis.* Contribution of Working Group I to the Fourth Assessment Report of the Intergovernmental Panel on Climate Change [Solomon, S., D. Qin, M. Manning, Z. Chen, M. Marquis, K.B. Averyt, M. Tignor and H.L. Miller (eds.)]. Cambridge University Press, Cambridge, United Kingdom and New York, NY, USA. 996 pp.

Nakićenović, N. and Swart, R. (eds.) (2000). Special Report on Emissions Scenarios. A Special Report of Working Group III of the Intergovernmental Panel on Climate Change. Cambridge University Press, Cambridge, United Kingdom and New York, NY, USA. 599 pp.

Nawri, N. (2010). Characteristics of wintertime North Atlantic cyclones in ERA-40 reanalyses and IPCC 20th century control runs. In: Proceedings of the Conference on Future Climate and Renewable Energy: Impacts, Risks and Adaptation, Oslo, 31 May–2 June 2010. pp. 74–75.

Nawri, N. and Björnsson, H. (2010). Surface air temperature and precipitation trends for Iceland in the 21st century. Icelandic Meteorological Office Report. Available at: http://brunnur.vedur.is/pub/nikolai/Nawri_Bjornsson_CES_report.pdf

Nikulin, G., Kjellström, E., Hansson, U., Strandberg, G., Ullerstig, A. (2011). Evaluation and future projections of temperature, precipitation and wind extremes over Europe in an ensemble of regional climate simulations (in press). *Tellus A*, DOI: 10.1111/j.1600-0870.2010.00466.x

Roeckner, E., Brokopf, R., Esch, M., Giorgetta, M., Hagemann, S., Kornblueh, L., Manzini, E., Schlese, U., Schulzweida, U. (2006). Sensitivity of simulated climate to horizontal and vertical resolution in the ECHAM5 atmosphere model. *J. Clim.*, 19, 3771–3791.

Rögnvaldsson, Ó. and H. Ágústsson (2009). Status report for the dynamical downscaling part of the CES Project. Slemba, Reykjavík.

Räisänen, J. (2009). Probability distributions of monthly-to-annual mean temperature and precipitation in a changing climate, 32 pp. CES Climate Modelling and Scenarios deliverable D2.4, task i. Available from http://www.atm.helsinki.fi/~jaraisan/ces.html

Räisänen, J. and Ruokolainen, L. (2006). Probabilistic forecasts of near-term climate change based on a resampling ensemble technique. *Tellus,* 58A, 461–472.

Räisänen, J. and Ruokolainen, L. (2008). Estimating present climate in a warming world: a model-based approach. *Climate Dynamics,* 31, 573–585.

Räisänen, J. and Ruokolainen, L. (2009). Probabilistic forecasts of temperature and precipitation change by combining results from global and regional climate models, 36 pp. CES Climate Modelling and Scenarios deliverable D2.3. Available at: http:// www.atm.helsinki.fi/~jaraisan/ces.html

Räisänen, J. and Ruosteenoja, K. (2008). Probabilistic forecasts of temperature and precipitation change based on global climate model simulations, 46 pp. CES Climate Modelling and Scenarios deliverable D2.2. Available at: http://www.atm.helsinki.fi/ ~jaraisan/ces.html

Rummukainen, M., Ruosteenoja, K., Kjellström, E. (2007). Climate Scenarios. In: *Impacts of climate change on renewable energy sources: Their role in the Nordic Energy System*. Ed. J. Fenger. Nord 2007:003. ISBN 978-92-893-1465-7. pp. 36–57.

Ruokolainen, L. and Räisänen, J. (2007). Probabilistic forecasts of near-term climate change: sensitivity to adjustment of simulated variability and choice of baseline period. *Tellus,* 59A, 309–320.

Ruosteenoja, K. and Räisänen, J. (2009). Solar radiation projections derived from global climate models. CES Climate Modelling and Scenarios deliverable D2.4, task iii. Available at: http://www.atm.helsinki.fi/~jaraisan/ces.html

Shkolnik, I. and Efimov, S. (2010). Projections of selected temperature and precipitation extremes inferred by CMIP3 models. CES Climate Modelling and Scenarios deliverable D2.4, task iv. Available from http://www.atm.helsinki.fi/~jaraisan/ces.html.

Skamarock, W.C., Klemp, J.B., Dudhia, J., Gill, D.O., Barker, D.M. (2008). A description of the Advanced Research WRF version 3. NCAR Technical Note 475+STR.

Tveito, O. E., Bjørdal, I., Skjelvåg, A.O., Aune, B. (2005). A GIS-based agro-ecological decision system based on gridded climatology. *Meteorological Applications,* 12 (1), 57–68.

Uppala S. M. and 44 others (2005). The ERA-40 re-analysis. *Quart. J. R. Meteorol. Soc.*, 131, 2961–3012. doi:10.1256/qj.04.176.

van der Linden, P. and Mitchell, J. F. B., eds. (2009). ENSEMBLES: Climate change and its impacts: Summary of research and results from the ENSEMBLES project. Met Office Hadley Centre, FitzRoy Road, Exeter EX1 3PB, UK, 160 pp.

Yang, W., Andréasson, J., Graham, L.P., Olsson, J., Rosberg, J., Wetterhall, F. (2010). Distribution-based scaling to improve usability of regional climate model projections for hydrological climate change impacts studies. *Hydrology Research,* 41 (2–4), 211–229.

Yin, J.H. (2005). A consistent poleward shift of the storm tracks in simulations of 21st century climate. *Geophys. Res. Lett.,* 32, L18701.

Ylhäisi, J.S., Tietäväinen, H., Peltonen-Sainio, P., Venäläinen, A., Eklund, J., Räisänen, J., Jylhä, K. (2010). Growing season precipitation in Finland under recent and projected climate. *Natural Hazards and Earth System Sciences,* 10, 1563–1574, doi:10.5194/nhess-10-1563-2010.

Peer-reviewed publications resulting from work carried out during (or in conjunction with) the CES project, but not referenced in the chapter.

Arason, T, Rögnvaldsson, Ó., Ólafsson, H. (2010). Validation of numerical simulations of precipitation in complex terrain at high temporal resolution. *Hydrology Research*, 41 (3–4), 164–170.

Christensen, J.H., Boberg, F., Christensen, O.B. and Lucas-Picher, P. (2008). On the need for bias correction of regional climate change projections of temperature and precipitation. *Geophys. Res. Lett.*, 35, L20709, doi:10.1029/2008GL035694.

Elíasson, J., Rögnvaldsson, Ó., Jónsson, T. (2009). Extracting statistical parameters of extreme precipitation from a NWP model. *Hydrol. Earth Syst. Sci.*, 13, 2233–2240.

Gregow, H., Ruosteenoja, K., Pimenoff, N., Jylhä, K. (2011). Changes in the mean and extreme geostrophic wind speeds in Northern Europe until 2100 based on nine global climate models. *Int. J. Climatol.*, doi: 10.1002/joc.2398

Kilpeläinen, T., Tuomenvirta, H., Jylhä, K. (2008). Climatological characteristics of summer precipitation in Helsinki during the period 1951–2000. *Boreal Env. Res.*, 13, 67–80.

Kjellström, E., Boberg, F., Castro, M., Christensen, J.H., Nikulin, G., Sánchez, E. (2010). Daily and monthly temperature and precipitation statistics as performance indicators for regional climate models. *Climate Research,* 44, 135–150.

Peltonen-Sainio, P., Hakala, K., Jauhiainen, L., Ruosteenoja, K. (2009). Comparing regional risks in producing turnip rape and oilseed rape - Impacts of climate change and breeding. *Acta Agriculturae Scandinavica,* 59B:2, 129–138.

Pryor, S.C., Barthelmie, R.J., Clausen, N.E., Drews, M., MacKellar, N., Kjellström, E. (2010). Analyses of possible changes in intense and extreme wind speeds over northern Europe under climate change scenarios. *Climate Dynamics*, doi: 10.1007/s00382-010-0955-3.

Ruosteenoja, K., Räisänen, J., Pirinen, P. (2010). Projected changes in thermal seasons and the growing season in Finland. *Int. J. Climatology*, 31(10), 1473–1487.

Rögnvaldsson Ó, Jónsdóttir J.F., Ólafsson H. (2010). Dynamical downscaling of precipitation in Iceland 1961–2006. *Hydrology Research*, 41 (3–4), 153–163.

Tietäväinen, H, Tuomenvirta, H., Venäläinen, A. (2010). Annual and seasonal mean temperatures in Finland during the last 160 years based on gridded temperature data. *Int. J. Climatol*. 30 (15), 2247–2256.

Venäläinen A., Jylhä, K., Kilpeläinen, T., Saku, S., Tuomenvirta, H., Vajda, A., Ruosteenoja, K. (2009). Recurrence of heavy precipitation, dry spells and deep snow cover in Finland based on observations. *Boreal Env. Res.*, 14, 166–172.

Ylhäisi, J.S., Tietäväinen, H., Peltonen-Sainio, P., Venäläinen, A., Eklund, J., Räisänen, J., Jylhä, K. (2010). Growing season precipitation in Finland under recent and projected climate. *Nat. Hazards Earth Syst. Sci.*, 10, 1563–1574.

4. Analyses of historical hydroclimatological time series for the Nordic and Baltic regions

*Deborah Lawrence, Rebecca Barthelmie, Philippe Crochet, Göran Lindström, Tatjana Kolcova, Jurate Kriaučiūnienė, Søren Larsen, Sara Pryor, Alvina Reihan, Lars Roald, Hanna Tietäväinen and Donna Wilson**

*Details on author affiliations are given in the Appendix

4.1 Introduction

Climate change projections for the Nordic and Baltic Regions indicate a warmer and wetter future climate, together with a likely increase in the occurrence of extremes. Given that global temperature trends in recent years show some consistency with projections for the future, the question arises as to whether or not there also exists evidence of climate change in historical data at regional or local scales. A main objective of the statistical analysis group within the Climate and Energy Systems project has been to study patterns of change in historical data, with a particular emphasis on hydro-climatological variables of relevance to the renewable energy sector. In some cases, annual and seasonal anomalies have been considered, whilst in other work the focus has been on extreme events. Work on identifying connections between large-scale atmospheric processes and local phenomena has also been undertaken using, for example, weather type classifications and the North Atlantic Oscillation (NAO) index.

An overview of investigations analysing historical data is given in this chapter. The work is reported under three themes: i) analyses of regional series and trends for the individual countries; ii) analyses of local observations for determining changes in the occurrence of extreme events; and iii) analyses of links between atmospheric processes and local variables of interest to the energy sector, i.e. streamflow and wind. Some of this work has used data from the Nordic streamflow database, which consists of 160 records of daily data from Denmark, Finland, Iceland, Norway and Sweden (see Hisdal *et al.*, 2007). This database was updated to 2005 within the Climate and Energy Systems project. These data were also used to update the analysis of trends in streamflow in the Nordic

region (Wilson, *et al.*, 2010) undertaken in the previous CE project (Hisdal *et al.*, 2007; 2010).

4.2 Analysis of regional series and long-term trends

Long-term regional series of temperature, precipitation and runoff have been compiled and updated for the Nordic and Baltic countries. Because there are differences between the Nordic countries as to the most appropriate methods for estimating regional quantities given differences in local conditions, particularly topography, the compiled series are reported on a country-by-country basis for the Nordic region. For the Baltic countries, a combined analysis has been undertaken, although identified regions have also been further subdivided to reflect national boundaries. The emphasis within the project has been on comparisons relative to a 1961–1990 reference period, and most of the regional series have been standardised with respect to this baseline. Where sufficient data are available, anomalies relative to the reference period have been analysed for earlier periods, in addition to deviations in recent years.

4.2.1 Sweden

Regional series for the period 1901–2009 were compiled for four regions in Sweden. These regions comprise the land areas draining to the Bothnian Bay, the Bothnian Sea, the Baltic Proper and the Swedish west coast. This regional division has previously been used by Lindström and Alexandersson (2004) and Hellström and Lindström (2008). For each year, a mean deviation in temperature (in °C) and runoff (in %), relative to the 1961–1990 reference value, was estimated for each of the four regions. It is thus assumed that the year to year climatic signal is the same within each region. The regional temperature series were originally constructed by Alexandersson (2002) and have thereafter been extended annually. The runoff series in the present study are based on 16 long-term discharge series from the larger catchments within the regions.

The regional average deviations in temperature and runoff for the period 1901–2009 are illustrated for the four regions in Figure 4.1. The temperature signal is very similar in all four regions in Sweden. The main characteristics are the mild periods in the 1930's and from 1988 until the present, and a cooling period in between these two periods. The warmer periods are particularly evident in the Bothnian Bay region corresponding to northern Sweden. Subsequent to 1987, only one year has been colder than the 1961–1990 average. The past 20 years have been approximately one degree warmer than the 1961–1990 normal value. Runoff, however, varies more between the regions than does temperature, although some common characteristics can be seen in all four regions. For example, the 1970's represent the driest 10-year period in all regions, although this

anomaly is more evident in the two southern regions, the Baltic Proper and the West Coast. Within northern Sweden, runoff anomalies have been positive following this dry period. This period of high runoff culminated in the years 1998–2001, and runoff in more recent years has been more in line with the long term normal. All of the regions exhibit positive deviations in runoff during the 1920's, and in southeastern Sweden (Baltic Proper region), the largest positive deviations are found in that decade. It should be noted that the positive runoff anomalies in the 1920's are associated with a period of slightly cooler temperatures, i.e. they precede the positive temperature anomalies of the 1930's.

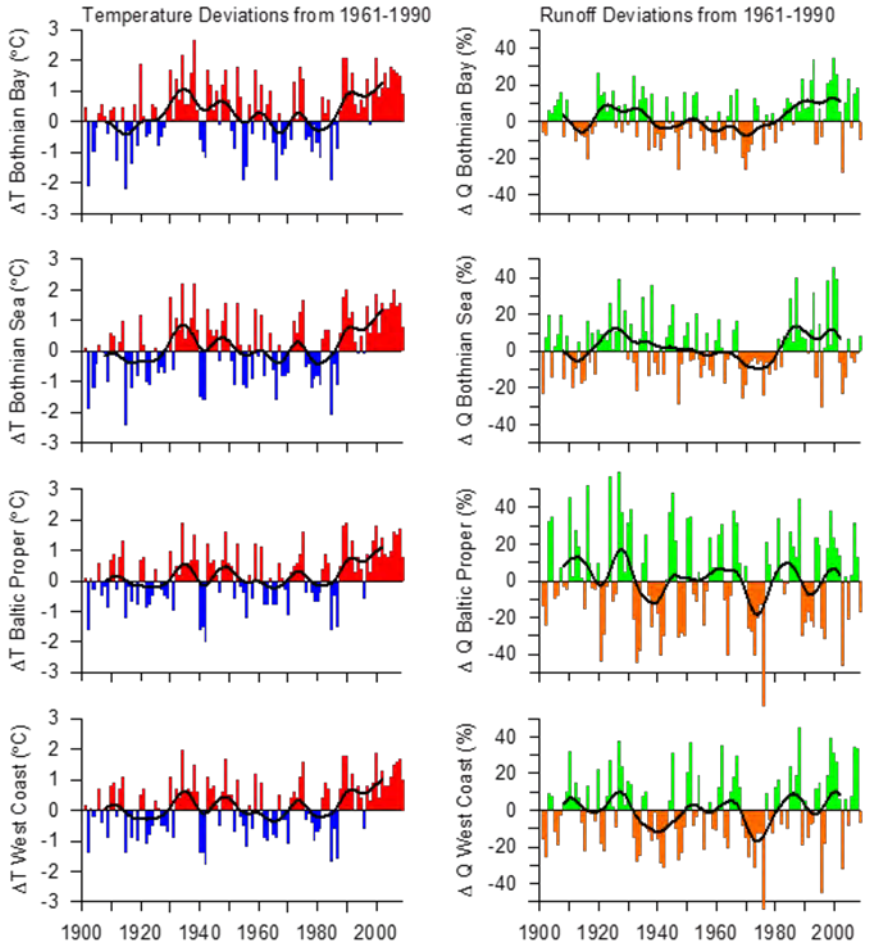

Figure 4.1. Regional average deviations in temperature and runoff 1901–2009 for four regions in Sweden, with respect to average values for 1961–1990. The thick black curve shows a smoothing obtained by a Gauss filter with a standard deviation of 3 years.

4.2.2 Finland

Regional series for the period 1901–2005 were compiled for northern and southern Finland. The regional series up to 2002 were originally compiled within the CE project (Lindström *et al.*, 2006), and were here extended

using discharge data from the CES database and temperature data from FMI. The Northern Finland region is comprised of land areas that drain to the Barents Sea, the Bothnian Bay and Ostrobothnia, and southern Finland of land areas draining to Ladoga, the Bothnian Sea and the Gulf of Finland. For each year a mean deviation in temperature (in °C) and runoff (in %), relative to the 1961–1990 reference value, was estimated for each of the regions, using the same methods as applied in Sweden.

The temperature signal is generally similar in northern and southern Finland (Figure 4.2). The temporal pattern of anomalies is characterised by mild periods in the 1930's and from 1988 until the present and a cool period in between these two periods. The positive deviation in temperature during the past 20 years is approximately one degree, similar to Sweden. Cold years in the beginning of the 1940's are very dominant in the southern Finland region, and pronounced negative deviations in runoff are also found during this decade. Two relatively wet periods are particularly notable in the southern Finland regional series, the 1920's and the 1980's. These periods share some similarities with the Swedish Baltic Proper regional series for these periods. The positive runoff deviations in the 1920's continue into the 1930's, but similar to the Swedish Bothnian Sea regional series, they begin during a period of normal to slightly cooler temperatures.

In addition to the regional analysis of temperature and runoff presented in Figure 4.2, monthly precipitation sums for the period May–September have been studied in two areas in Finland (Ylhäisi *et al.*, 2010). One of the areas considered is located in south-west (SW) Finland with a slight maritime influence, and the other area is in the north-east (NE) where the climate is more continental. Trends during the last 100 years were studied based on gridded data for Finland developed by FMI. Statistically significant long-term tendencies were found for June at SW and for May, July and the sum from May to September at NE, indicating increases in precipitation. For a shorter time period, 1961–2000, two other observational datasets (E-OBS gridded data (Haylock *et al.*, 2008); and CRU gridded data (Mitchell and Jones, 2005)) were also analysed. All three datasets indicated a tendency towards an increase in precipitation in June in the SW and a decrease in September in the NE. In many cases, however, the trends were not statistically significant and varied in sign from month to month and between the two study sites.

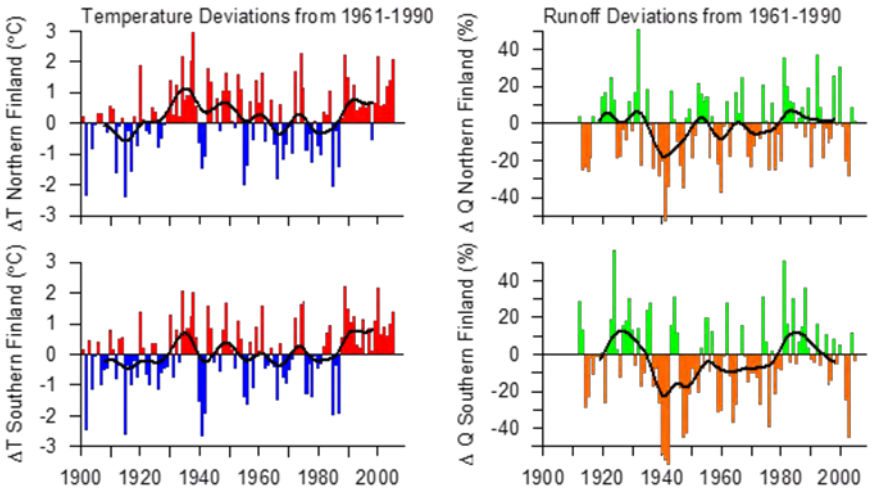

Figure 4.2. Regional average deviations in temperature and runoff 1901–2005 for northern and southern Finland, with respect to average values for 1961–1990. The thick black curve shows a smoothing obtained by a Gauss filter with a standard deviation of 3 years.

4.2.3 Norway

A new set of five regions has been compiled for Norway for use in estimating regional runoff series. These regions replace the 13 regions reported in Førland *et al.* (2000) and were identified based on annual runoff data from 82 stations for the period 1897 to 2009. Following normalisation of each station series (achieved by dividing annual values by the station mean for the period 1961–1990), cluster and correlation analyses were used to group stations with similar temporal behaviour. Station groupings, together with catchment boundaries and the boundaries of existing hydropower regions, were used to delimit the five regions illustrated in Figure 4.3. Temperature and precipitation regional series exist for Norway for the periods 1876–2003 and 1986–2004, respectively, for the six temperature and 13 precipitation regions described in Førland *et al.* (2000). These series were recalculated for the five runoff regions by areal weighting of each of the temperature and precipitation series, relative to the boundaries of the runoff regions.

The precipitation and runoff regional series were calculated as the mean of the normalised series for each region. Each individual temperature series, however, was normalised by subtracting the mean for the reference period 1961–1990 and dividing by the standard deviation. The method used to calculate the runoff and precipitation regional series is the same as that used for Sweden and Finland. However, there is a difference in derivation of the temperature regional series. In Sweden and Finland each individual series was standardised by subtracting the mean value only, prior to calculating the regional average of the station values. The results of the analyses indicate that all regions are characterised by relatively high temperatures within the recent period (1990–2003),

similar to the results for Sweden and Finland. Precipitation and runoff for individual years within the period 1990–2003 were more variable, but higher values were observed in all regions for both of these variables, relative to the 1961–1990 reference period. Figure 4.3 illustrates the percentage change in the average value between the reference and recent periods for the five regions. A 4–6% increase in precipitation is estimated for the four western and northern regions of Norway, whereas southeastern Norway has only experienced a small increase (1.5%) between the two periods. Runoff is observed to have increased by approximately 9% in the recent period, and the western mountainous region of Norway has experienced a moderate increase of 5.8%. The other three regions exhibit only a slight increase in the recent period. The increase in the northernmost region of Norway is consistent with the runoff deviations in northern Sweden, as illustrated by the regional series for the Bothnian Bay region in Figure 4.1. In that case, the smoothed series exhibits a positive anomaly of the order of 7–10% in recent years, whereas a negative anomaly for the period 1960–1980 is evident.

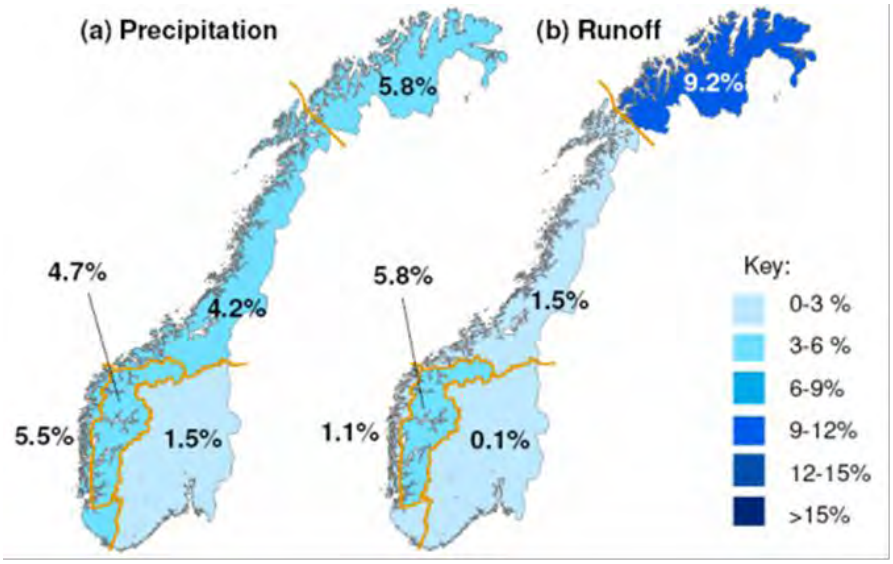

Figure 4.3. Percentage increase in the regional a) precipitation and b) runoff in Norway in the period 1990–2003, relative to the 1961–1990 reference period.

4.2.4 Iceland

Monthly, seasonal and annual regional series of temperature, precipitation and runoff were compiled for Iceland for the period 1961–2006 for three regions in Iceland. These regions are based on weather forecasting domains defined by Einarsson (1978), aggregated into three regions (Figure 4.4). Each individual series of temperature, precipitation and runoff was normalised using the same procedure described above for Norway. Gridded temperature and precipitation data were used for the

analysis. The temperature data set was produced using a spline interpolation method after elevation correction and the precipitation data set was produced with an orographic precipitation model (Crochet *et al.*, 2007; Jóhannesson *et al.*, 2007). Precipitation and temperature series were compiled for all regions while runoff series were compiled for two regions only (south and northwest). Two gauging stations corresponding to partially glacier-covered catchments were used to generate the regional series in the southern region (region 1), and five gauging stations were used for the northwestern region (region 3), one of which represents a partially glacier-covered catchment. In both regions, the total catchment areas corresponding to these gauging stations cover only a limited area within the respective regions, i.e. 19% of Region 1 and 7% of Region 3.

The annual regional series are illustrated in Figure 4.4, where mean annual values for the three 15-year periods between 1961 and 2006 are also indicated. The temperature series describe a similar signal in all regions and indicate that annual temperatures in the years subsequent to 1990 have been milder, on average, than during the 1961–1990 reference period. In particular, all years subsequent to 1995 have been systematically milder than the 1961–1990 reference value, in all regions, except for one year in Region 2 (NE). Seasonal analyses (not shown) indicate that the largest seasonal temperature increase in recent years is associated with the summer. Annual precipitation for the recent years has also been higher, on average, than the 1961–1990 reference value but differences exist between regions for individual years. In the southern region (Region 1), annual runoff has also been generally higher in recent years, particularly relative to the 1976–1990 15-year period, but has not increased as much as the precipitation. Within the northwestern region (Region 3), runoff was above the 1961–1990 average in the early 1990's, which is similar to what was seen in the early 1970's, but more recent years have generally been characterised by annual runoff below or close to the 1961–1990 reference value. A trend analysis of spring and autumn maximum precipitation and floods at Icelandic stations was undertaken by Jónsdóttir *et al.* (2008), identifying positive trends in the maximum one-, three- and five-day precipitation in spring and autumn at some stations. Trends in the magnitude of spring and autumn floods were mostly positive in the spring and negative in the autumn, although the results were generally not found to be statistically significant.

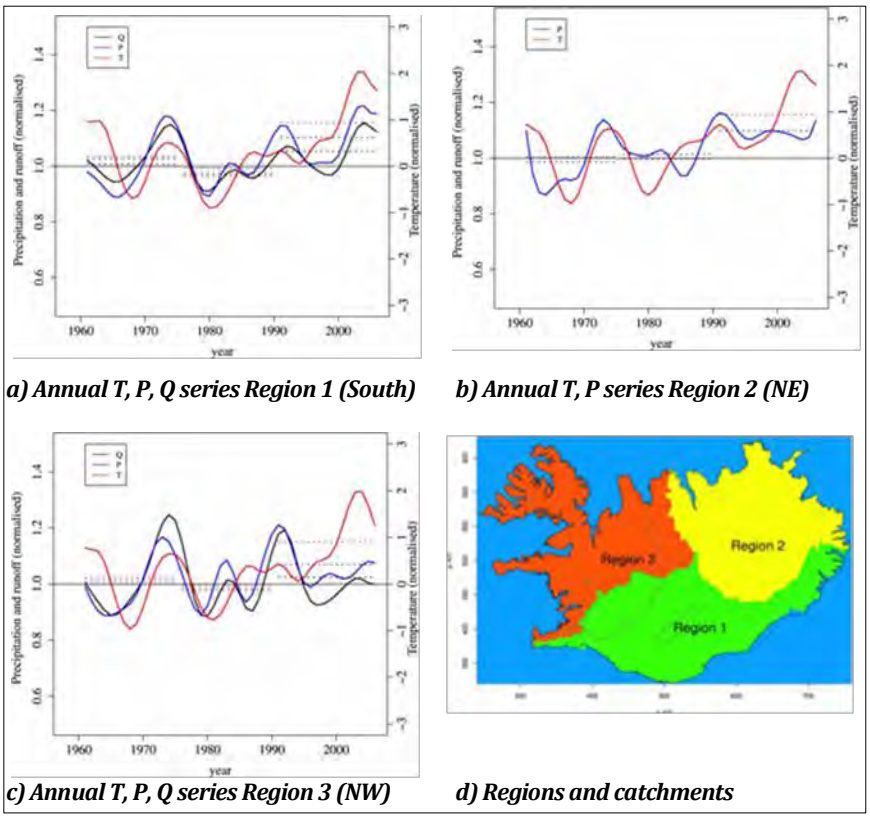

a) Annual T, P, Q series Region 1 (South)

b) Annual T, P series Region 2 (NE)

c) Annual T, P, Q series Region 3 (NW)

d) Regions and catchments

Figure 4.4. Normalised annual regional series of temperature (red lines), precipitation (blue lines) and runoff (black lines) in Iceland for (a) Region 1, (b) Region 2, (c) Region 3. The series have been Gauss-filtered with a standard-deviation of 3 years (solid lines), and mean annual values for the 1961–1975, 1976–1990 and 1991–2006 periods are also given (dashed lines).

4.2.5 Denmark

For Denmark, analyses of regional trends in precipitation and runoff have been conducted based on 8 climate and 18 discharge gauging stations distributed throughout the country (Figure 4.5). Analyses have considered changes in average annual precipitation, changes in monthly precipitation to assess seasonal trends, as well as changes in the annual and monthly average, maximum and minimum values. Yearly time series were analysed by applying the Mann-Kendall non-parametric trend test (Hirsch, *et al.*, 1982), and the Mann-Kendall seasonal trend test with correction for serial autocorrelation (Hirsch and Slack, 1984) was applied to the monthly data. The magnitude of the trend was estimated by the non-parametric Sen's slope estimator (Hirsch, *et al.*, 1982), which assumes that the trend is constant over the period analysed. Homogeneity of the seasonal trends was tested using the statistic introduced by van Belle and Hughes (1984).

Results indicate that the average annual precipitation has increased over the period 1917 to 2000 at seven of the eight stations considered. The increases at two of the stations (Broderup and Landbohøjskolen) are statistically significant. This agrees with an estimated change in average annual

precipitation of +1.3 mm per year for the whole of Denmark for the same period, based on area-weighted stations from the existing station network. The analysis of monthly precipitation for each of the 8 climate stations reveals large differences in the seasonal trends (Figure 4.6). The months of March and December have large and highly significant increases, whilst August is associated with decreases, which are significant at Nordby and Broderup. The overall pattern provides evidence for a trend towards wetter winter months and drier summer months at all of the stations considered.

The average annual runoff was found to have increased at all of the stations analysed over the period commencing with the first year of the station record (varying from 1917 to 1936 at individual stations) until 2000. This increasing trend was found to be significant at 10 of the 18 stations. The analyses of monthly average, maximum and minimum runoff at 10 of the stations show clear seasonal patterns in the trends (Figure 4.6). The largest positive trends in the monthly average runoff are associated with the winter half-year. In many streams, average runoff has increased significantly in the early spring to summer, most likely reflecting the increased winter recharge to these groundwater-dominated streams. The analyses also indicate that monthly maximum and minimum runoff have increased as well, implying an increased winter flood risk, particularly during winter periods.

Figure 4.5. The locations of the 18 Danish river gauging stations (blue) and the 8 climate stations (black) used for the analysis.

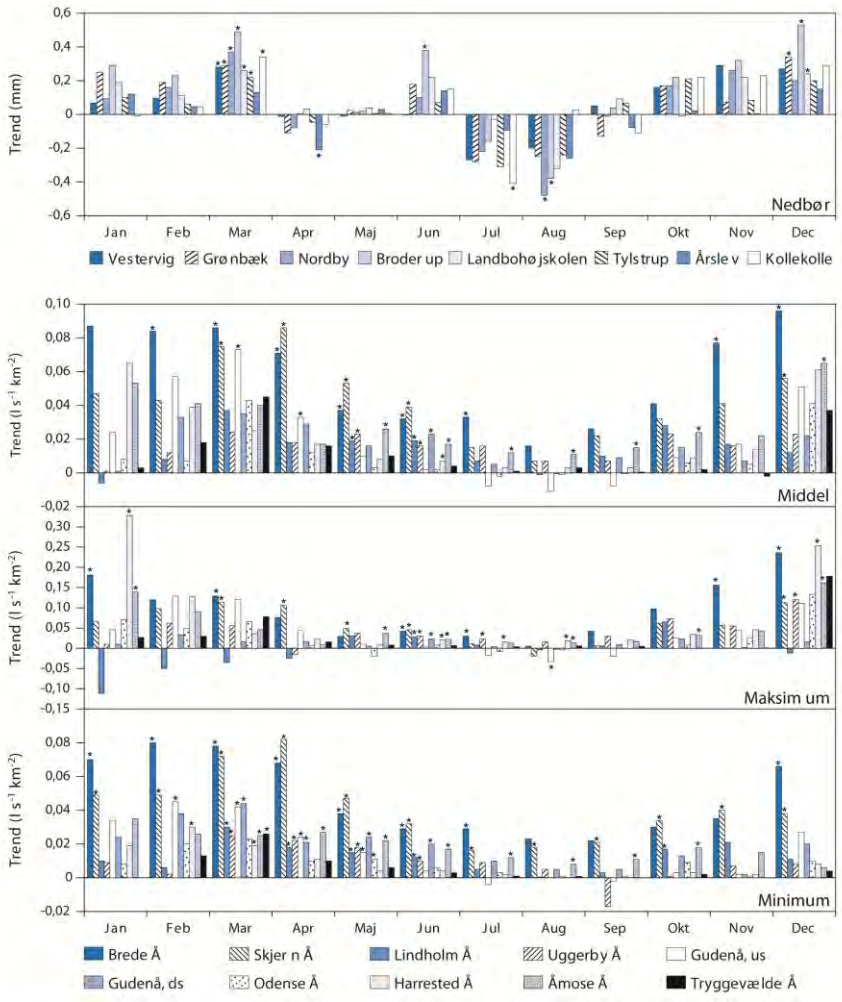

Figure 4.6. Trends in monthly precipitation at the 8 climate stations (upper diagram), and in the monthly average, maximum and minimum runoff at 10 of the river gauging stations (lower diagram) during a 75-year period. *Significant (P<0.05).

4.2.6 The Baltic countries

A combined analysis of regional series for temperature, precipitation and runoff for Lithuania, Latvia and Estonia was undertaken for the period 1961–2007, based on 10 hydrological regions (Figure 4.7) for the Baltic area. The series are based on 49 stations for temperature, 72 stations for precipitation and 64 stations for runoff. All series were normalised relative to the 1961–1990 reference period. Regional series were developed on monthly, seasonal and annual bases.

Comparisons between the temperature series in the recent period (1991–2007) relative to the reference period indicate an increase in annual and seasonal temperatures in all regions and all seasons. In Estonia, the annual temperature increased by 0.8 °C and in Lithuania by 1.1 °C relative to the reference value. Positive changes of air temperature occurred in all seasons (Figure 4.7a), with the largest anomalies observed

during the summer season and the smallest increases occurring during the autumn season. With respect to precipitation, an increase in precipitation was found for the winter season in recent years for all Baltic countries. In the western and central regions, precipitation increased by 10–16%, whilst in the eastern regions it increased by 15–29% during the winter season. Changes in precipitation during the spring season are variable between regions. Summer precipitation generally decreased, with the largest decreases associated with the western and central regions of Lithuania and the eastern region of Estonia. Anomalies in the regional runoff series vary with location and season. All regions exhibit an increase in runoff during the winter season during the period 1991–2007, with increases of 20 to 60% (Figure 4.7b). A decrease in spring runoff (of 10-20%) was found in the western regions, but no change of spring season runoff was found in the more inland regions. Long-term variability in temperature, precipitation and runoff from the 1925 until 2007 has also been evaluated for the Baltic countries in other work (Kolcova *et al.*, 2010), and large variations are observed over this time period.

4.2.7 Summary of regional series analyses

Although there are some differences in the methods used to develop the regional series described above and in the quantities presented, some common themes are apparent. Firstly, all of these studies report positive temperature deviations for all regions in recent years relative to the 1961–1990 reference period. The analyses illustrated for Sweden and Finland suggest that these anomalies are not necessarily unique in their magnitude within the past century, particularly when a comparison with the 1930s is made. However, the figures illustrated for Sweden and Finland, also suggest that the persistence of the temperature deviations in the period subsequent to 1990 possibly distinguish this period from the early warm period during the 1930s. The seasonal analyses presented for the Baltic countries further indicates that for this region, the largest seasonal increase in temperature in recent years is associated with the summer months.

With respect to runoff and precipitation, patterns during recent years relative to the reference period are much more variable, both between countries and between regions within individual countries. This is most likely related to the diversity of characteristics and associated rainfall and flow regimes which lead to variable responses at the catchment and the regional scale. Topography, for instance, will affect local and regional precipitation patterns differently depending on its location relative to atmospheric circulation patterns (for example, producing orographic enhancement *vs*. topographic blocking). In some regions (for example, northern regions in Norway and Sweden, and regions within Iceland), overall higher runoff values are observed for the period from 1990 to present. However, more detailed analyses of this period, for example in Sweden, suggest that the period of higher runoff possibly culminated

towards the end of the 1990s and that more recent years have been associated with runoff values more similar to the average for the 1961–1990 period. The seasonal analysis presented for the Baltic countries indicates a considerable increase in winter runoff in recent years in all of the 10 regions considered. Positive anomalies in annual precipitation have also been observed in Norway and Iceland in recent years, as well as increased winter precipitation in the Baltic countries.

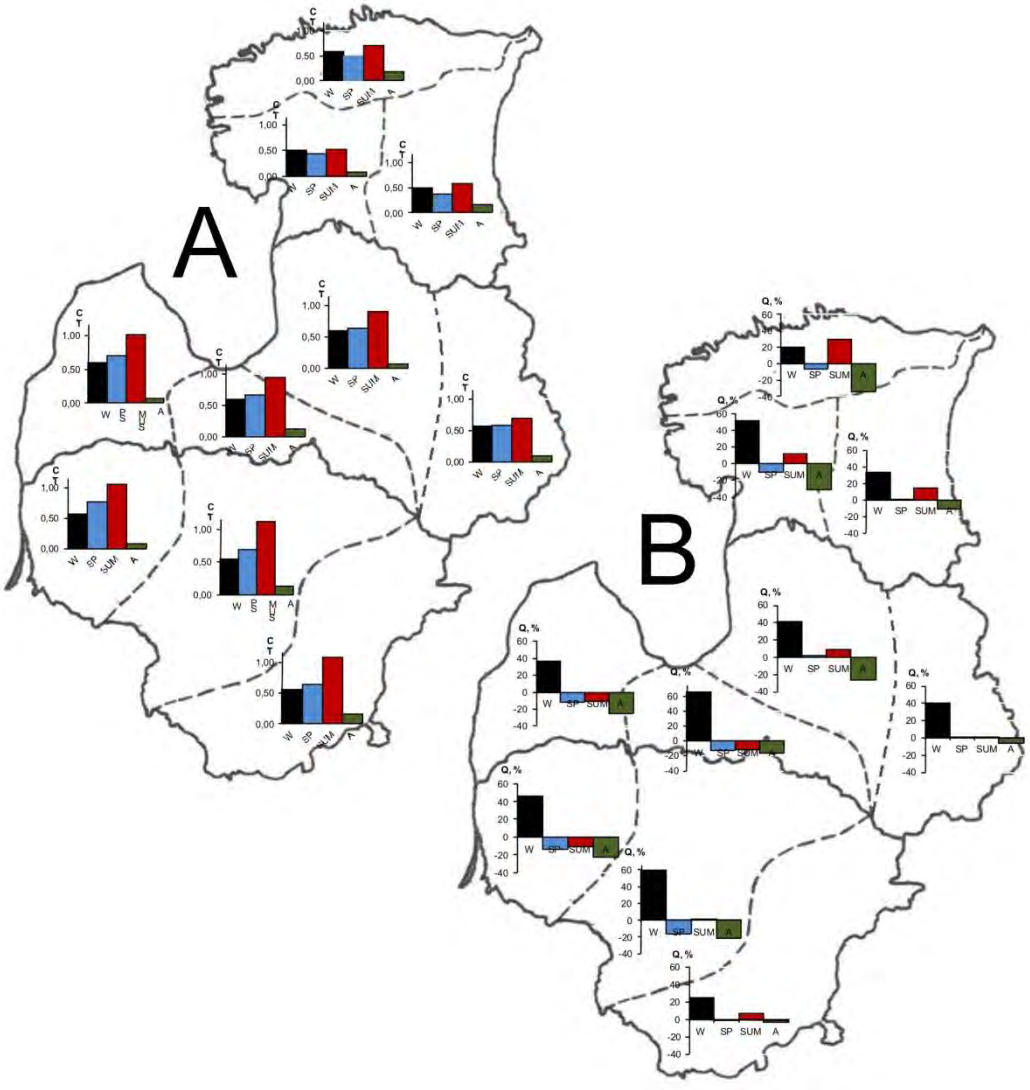

Figure 4.7. Seasonal anomalies for the period 1991–2007, relative to a 1961–1990 reference period for:
a) temperature in ℃, with the y-axis ranging from 0.00 to 1.00 ℃
b) runoff as a percentage, with the y-axis ranging from -40% to +60%. The seasons are indicated by colour: Dark blue – winter; light blue – spring; red – summer; green – autumn.

4.2.8 Summary of regional series analyses

Although there are some differences in the methods used to develop the regional series described above and in the quantities presented, some common themes are apparent. Firstly, all of these studies report positive temperature deviations for all regions in recent years relative to the 1961–1990 reference period. The analyses illustrated for Sweden and Finland suggest that these anomalies are not necessarily unique in their magnitude within the past century, particularly when a comparison with the 1930s is made. However, the figures illustrated for Sweden and Finland, also suggest that the persistence of the temperature deviations in the period subsequent to 1990 possibly distinguish this period from the early warm period during the 1930s. The seasonal analyses presented for the Baltic countries further indicates that for this region, the largest seasonal increase in temperature in recent years is associated with the summer months.

With respect to runoff and precipitation, patterns during recent years relative to the reference period are much more variable, both between countries and between regions within individual countries. This is most likely related to the diversity of characteristics and associated rainfall and flow regimes which lead to variable responses at the catchment and the regional scale. Topography, for instance, will affect local and regional precipitation patterns differently depending on its location relative to atmospheric circulation patterns (for example, producing orographic enhancement *vs*. topographic blocking). In some regions (for example, northern regions in Norway and Sweden, and regions within Iceland), overall higher runoff values are observed for the period from 1990 to present. However, more detailed analyses of this period, for example in Sweden, suggest that the period of higher runoff possibly culminated towards the end of the 1990s and that more recent years have been associated with runoff values more similar to the average for the 1961–1990 period. The seasonal analysis presented for the Baltic countries indicates a considerable increase in winter runoff in recent years in all of the 10 regions considered. Positive anomalies in annual precipitation have also been observed in Norway and Iceland in recent years, as well as increased winter precipitation in the Baltic countries.

4.3 Analyses of extreme events

Work within the statistical analysis group has also included investigations of changes in hydroclimatological extremes. Three of these studies are reported here, selected for presentation due to their use of combined regional data sets such that the results presented cover either the Nordic and/or Baltic regions, rather than referring only to individual countries within these regions. The first study considers the occurrence of dry spells based on precipitation data for stations in northern Europe. The

second study is based on an analysis of the updated Nordic streamflow database to consider changes in the occurrence of peak flows in runoff series. The third study presents a combined analysis of changes in the spring flood for stations within the Baltic region.

4.3.1 Dry spells in the Nordic and Baltic region

Temporal changes in meteorological drought in the Northern Europe during the 20th century were evaluated using daily precipitation data from 15 stations in the Nordic countries (Denmark, Finland, Sweden, Norway) and the Baltic countries (Estonia, Latvia, Lithuania) (Hohenthal *et al.*, 2010). Dry spell lengths were defined relative to 10, 100 and 400 mm thresholds for cumulative precipitation. The number of dry days at each station was calculated using 1.0 and 0.10 mm threshold values for daily precipitation. Both dry spell lengths and the number of dry days were calculated for the annual and the May – August (i.e. "summer") periods. The period of record varied between the stations, with most records beginning before 1910. (Two exceptions to this are the records for Riga in Lativa, which begins in 1943, and for Östersund in Sweden, which begins in 1918). Most of the analysed records extend until 2007, although some end a few years earlier.

The annual and summer dry spell lengths and number of dry days vary depending on the location of the stations with respect to mountain ranges and large water bodies, as well as with local air temperatures. Longer dry spells and higher number of dry days are found more often at the stations located in the cooler and more continental northern and eastern regions of Northern Europe than at stations located in the warmer and more maritime southern and western regions. The lengths of the longest 100 and 400 mm dry spells show more variation between the stations than do the 10 mm dry spells. The longest dry spells commencing during the summer months are generally shorter than dry spells beginning during other seasons. In Finland, Sweden and the Baltic countries, the 100 and 400 mm dry spells at the northern sites are longer than at the southern stations. In Norway, Sweden and Denmark, the eastern stations tend to be associated with longer dry spells relative to the western stations in those countries.

Trend analyses of the drought parameters were undertaken using both the parametric t-test and the non-parametric Mann-Kendall test. The Mann-Kendall test rejects the false null hypothesis (H_0 = no trend) more often when the distribution of the values is clearly skewed (Önöz and Bayazit, 2003), while t-test rejects the false null hypothesis more often when the values are normally distributed. The results indicate that meteorological drought occurrence has either remained the same or has decreased during the 20th century at most of the sites considered, particularly at the annual level. Highly significant ($p<0.01$) decreasing trends were found for the longest 100 and/or 400 mm dry spells in Copenhagen, Vestervig, Oslo, Jyväskylä, Riga and Vilnius, and for the <1.0

and/or <0.1 mm precipitation days in Bergen-Samnanger, Oslo and Riga (Figure 4.8). Increasing trends are the exception, but are found especially in the summer time series at stations located in the southern portions of the region. Significant ($p<0.05$) increasing trends were found in the longest 10 mm dry spells in Hammer, Odde and Copenhagen, and in the number of <0.1 mm precipitation days in Riga and Copenhagen.

4.3.2 Changes in the occurrence of peak over threshold floods in the Nordic region

Data from the Nordic streamflow database were used to investigate possible changes in the occurrence of high flows based on daily data from 84 discharge stations distributed throughout the Nordic region (Figure 4.8). Time series from these particular stations have been deemed to be suitable for daily analyses in previous work in the CE project (see Hisdal *et. al*, 2007). Peak over threshold floods were defined as the occurrence of discharge values exceeding the mean annual flood for the period 1961–1990 for a given daily discharge time series. Clusters of peaks were aggregated (to avoid sequent peaks from the same event) using 5-day and 70% recession criteria. The resulting peak over threshold series was then subdivided into fifteen-year periods for the period 1961–2005, and for stations where longer term series are available, also for the period 1931–1960. The number of events in each 15-year period were then tabulated, and the events for the entire series were ranked with reference to the period in which they occurred.

Results representing the change in the total number of events in the most recent 15-year period (1991–2005) relative to the two previous 15-year periods (1961–1975; 1976–1990) are illustrated in Figure 4.8. The change indicated represents the difference between the number of events occurring in 1991–2005 relative to the number of events occurring in each of the two fifteen-year periods. If the number of events in 1991–2005 was greater than (or less than) the number in each of the two previous periods, then the difference between the number in 1991–2005 and the largest (or smallest) number of occurrences in the two previous 15-year periods is illustrated. Otherwise, a station is reported as having no change. For stations with data records extending to 1931, comparisons were made between the number of events in 1991–2005 and all four 15-year periods between 1931 and 1990. The stations with the largest increases in the number of high flow events tend to be located on the western coast of Norway. Two Danish stations also exhibit this change. Stations in southern and eastern Norway and throughout most of Sweden, Finland and Denmark exhibit either no change or a decrease in the number of events. With respect to stations located in Iceland, one station located in southern Iceland (Maríufoss) was found to have an increase in the number of events in 1991–2005 relative to 1961–1990, and one station located in the northwest (Dynjandi) exhibits a decrease.

The statistical significance of the changes was tested using a χ^2 test for the number of events in each 15-year period, and a Mann-Whitney rank sum test to compare the relative magnitudes of the events in each 15-year period. In most cases, the tendencies illustrated in Figure 4.8 were not found to be significant. Exceptions to this include two stations located on the western coast of Norway which were found to have a significant increase in the number of events over the mean annual flood. Significant decreases in the number of events were found at one station in southern Sweden and two stations in Denmark.

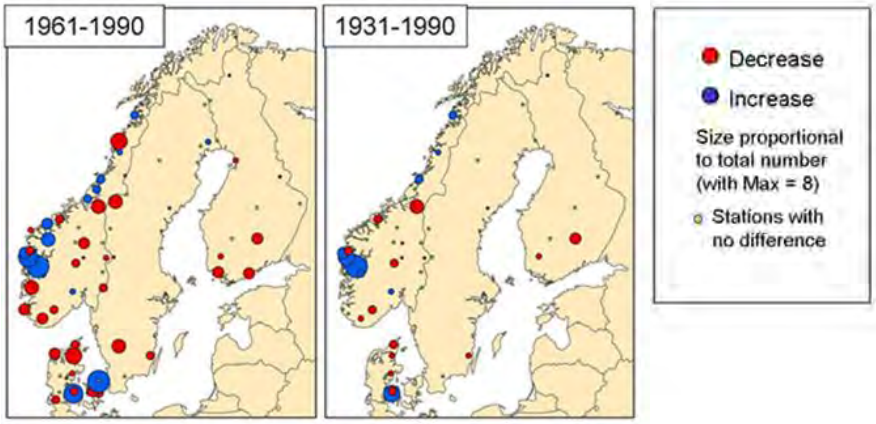

Figure 4.8. Change in the number of events in the period 1991–2005 which exceed the mean annual flood (1961–1990) relative to the periods 1961–1990 and 1931–1990. See text for further details.

4.3.3 Changes in spring flood in rivers of the Baltic States

Changes in parameters characterising the spring flood, including flood duration and frequency, runoff volume, peak discharge, and the timing of its occurrence were evaluated for 69 stations in the Baltic region. The Mann-Kendall trend test and the nonparametric Sen's method (Helsel and Hirsch, 2002) for the magnitude of the trend were used to detect trends in these quantities during three time periods (1923–2007, 1941–2007 and 1961–2007). Flood frequency estimation was based on the Gumbel distribution.

The results show a tendency towards a decrease in the spring flood maximum discharge and in its interannual variability at all stations considered, excepting three stations with positive trends and six stations with no trend. Significant and weakly significant negative trends were found for the periods, 1923–2007 (19 of 21 stations) and 1941–2007 (28 of 31 stations), respectively. The period 1961–2007 exhibited a negative tendency, but trends were not found to be significant, except in the western part of Lithuania, where out of 12 stations, 3 exhibited positive trends and 5 exhibited negative trends. In addition, no maximum discharges over 1% probability (return period = 100 years) have been observed during the last 70 years or over 5% probability (return period =

20 years) during the last 50 years, with the exception of rivers in Western Lithuania, where, for example, the spring flood in 1994 was the largest discharge recorded during the last 80 years.

For some time periods, the results also indicate that the spring flood peaks are now occurring earlier in the year. For the period 1923–2007, trends have been found to be negative, indicating earlier peak discharges. The tendency for an earlier spring maximum discharge timing has been reported for stations throughout the Baltic region (Meilutytė-Barauskienė and Kovalenkovienė, 2007; Klavins *et al.*, 2002; Reihan *et al.*, 2007). However, for the periods 1941–2007 and 1961–2007 trends in the timing of the spring flood were found to be insignificant. The spring flood duration is also observed to have decreased. The fraction of spring runoff to the annual runoff has decreased by 3–5% on average and by up to 10% in some regions. No significant trends were found for changes in spring flood volume, although the tendency was towards decreases in this quantity.

4.4 Analyses of links between atmospheric processes and hydroclimatological variables

In addition to studies which have analysed historical precipitation, temperature and runoff time series, work has been undertaken which considers links between atmospheric processes and variables directly relevant to the renewable energy sector, such as runoff and wind. The first study reported here evaluates the occurrence of rainfall floods in Norway with respect to the "weather type" responsible for the heavy rainfall. The second study evaluates connections between the North Atlantic Oscillation (NAO) and daily average streamflow and wind speeds in the Scandinavian countries and Finland. In addition, work on the relationship between regional hydrological droughts and associated weather types has also been undertaken (Fleig, *et al.*, 2010 a,b) with applications to Denmark and Great Britain. Long-term precipitation and discharge series in Iceland and their relationship to atmospheric circulation has also been investigated using an EOF analysis (Jónsdóttir and Uvo, 2009), in order to identify the principal patterns of variability in sub-regions within Iceland.

4.4.1 Rainfall floods and weather types in Norway

More than 900 rainfall events were identified based on 150 long-term daily precipitation series using a peak-over-threshold (POT) method, using a variable threshold to reflect the magnitude of rainfall in different regions within Norway. A number of floods were independently identified from daily flow series at 62 discharge stations located throughout Norway, also based on the exceedance of a threshold value (see Figure

4.9 for station locations). The runoff series included in this analysis are either unaffected by hydropower regulation or have been naturalised to take account of the effects of regulation. The date of the maximum daily rainfall was then compared with the date of the maximum daily mean discharge at nearby discharge stations. Events where the occurrence of the maximum rainfall *vs*. the maximum discharge differed by less than three days were defined as rainfall flood events for this analysis.

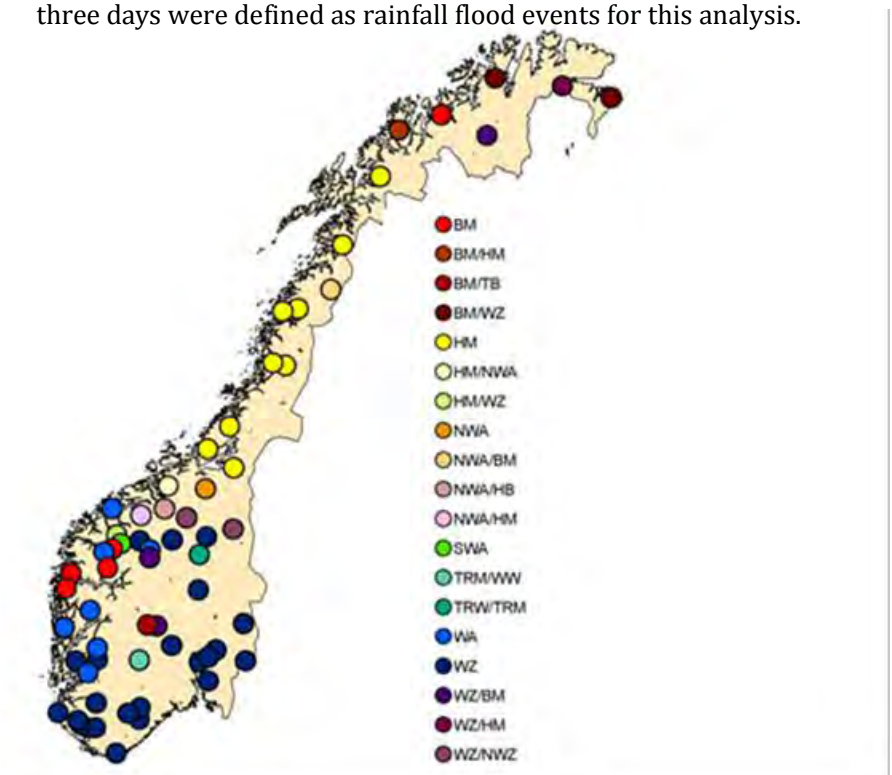

Figure 4.9. The most frequent rainfall flood generating weather type in Norway based on the Grosswetterlagen (GRW) classification. See text for description of the weather types illustrated.

The data set includes some events from the late 1890s, although most events occur after 1917, reflecting increases in the hydrological station network. In order to cover all of the rainfall flood events identified from the historical runoff data, it was therefore necessary to utilise weather type indices from two sources: Grosswetterlagen (GRW) (Gerstengarbe and Werner, 2005) and the Lamb-Jenkinson index (LWT) (Hulme and Barrow, 1997) rather than indices based on re-analysed data series, which begin in 1948. The Grosswetterlagen is focussed on Germany while the Lamb-Jenkinson index focuses on Great Britain. Both indices are available as daily indices, beginning in 1881. Each index comprises of approximately 30 classes, which can be grouped into three main weather types: Cyclonic, Anticyclonic and Zonal systems. The weather type associated with the date of the occurrence of the maximum rainfall in a given event was extracted for all rainfall floods for each discharge station. The total number of cyclonic, anticyclonic and zonal events was then calculated for each station, and the percentages of each type were

plotted for the two indices at each station. The most frequent rainfall flood generating weather type is shown for each station in Figure 4.9, based on the GRW-classification. Where a secondary weather type is also important in generating rainfall floods, this is indicated as the second type in the legend.

The weather type HM (yellow), "Hoch mittel", is characterised by anticyclonic systems over central Europe, and the well-defined region extending from Trøndelag to South Troms in central to north Norway represents an area where this weather type is quite dominant. The weather type BM (red), "Brücke mittel", is associated with a ridge extending from the continent to Britain, and is important in parts of western coastal Norway and, in this analysis, also appears in the northernmost catchments (although snowmelt dominates flooding there). The types WA (medium blue) and NWA (orange to pink) also reflect weather types in which anticyclones in the south force frontal systems to the north. Many events in southwestern Norway and in the inland and southeastern areas are linked to westerly weather types with zonal wind over Germany (WZ, indicated with dark blue to purple). Some rainfall floods in the southwest and along the southeast coast are linked to cyclones over the European mainland (TRM/TRW – light to medium blue). Catchments in western Norway draining northwards to the Trondheimfjord are shielded by mountains in the west and south, so that the NWA dominates there. Overall, the results illustrate the strong regional link between rainfall generating weather types and the Norwegian geography and topography.

Some of the largest floods in Norway have occurred as a result of meridional weather types, linked to blocking anticyclones in the Atlantic Ocean and over Finland/Russia. Warm and humid air masses originating from the Mediterranean or from subtropical part of the Atlantic are transported in a sector from southeast to southwest causing heavy rainfall and extreme floods in southern Norway. These events, however, occur too infrequently to be identified by the type of analysis presented here. The south-eastern type was responsible for the most extreme flood disaster on record in Norway, occurring in July 1789, which was caused by the Vb-low type storm trajectory (van Bebber, 1891). This weather type has caused many of the worst floods in Central Europe, such as the Oder flood in 1997 and the flood in the Elbe in August 2002. It can also contribute to large floods both in southern Sweden and southeast Norway.

4.4.2 Linking NAO with streamflow and wind

Variability in hydro- and wind energy parameters and their link to common climatological forcing via the North Atlantic Oscillation (NAO) has also been analysed. The NAO index is defined by the normalized pressure difference during the winter between a location in southwestern Europe and a station in Iceland (Pinto *et al.*, 2009). The NAO signal tends to be strongest during the winter (Cherry *et al.*, 2005). Therefore, correlations

between the daily NAO index and the i) average daily streamflow (based on station data held in the Nordic streamflow database); and ii) wind speed were assessed for that season. The results indicate that daily values of the wintertime NAO for 1950–2002 show some correlation with daily average streamflow in the region, with the highest correlations generally found in western Norway and at a few sites in southern Sweden, having values of up to 0.71 (Figure 4.10). Correlations with wind speed records are generally weaker, with the highest correlations associated with western Norway and with Denmark. Thus, a positive NAO index has a tendency to be linked with wetter, windier winters particularly in the southwestern region of the study domain.

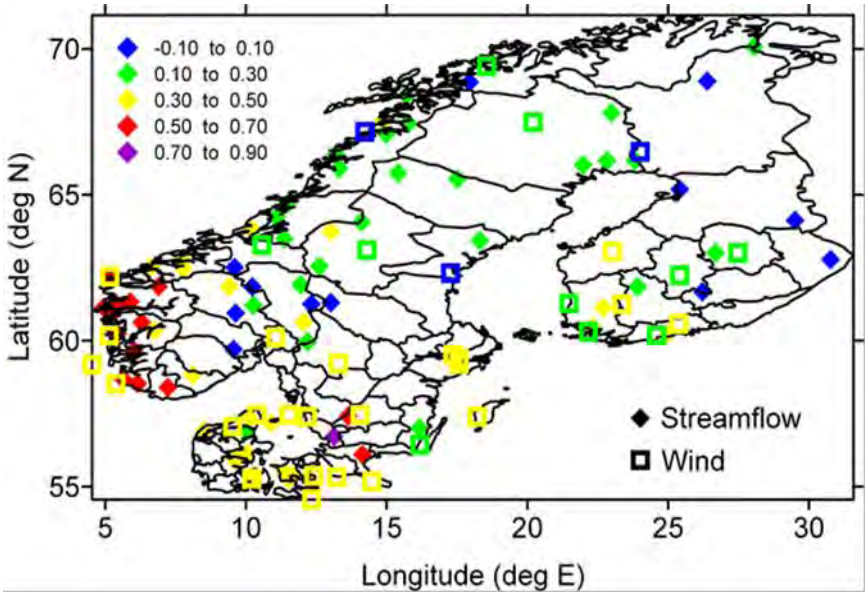

Figure 4.10. Correlation between winter NAO and wind speeds/stream flow (1980–2002)

4.5 Summary

The regional series analyses undertaken within the CES project all point towards a positive anomaly in annual temperature in recent years, relative to the 1961–1990 reference period. For countries where data are available and have been analysed (*i.e.* Figures 4.1 and 4.2 for Sweden and Finland, respectively), the magnitude of this anomaly is similar to that observed in the 1920's, although the length and persistence are more pronounced for the period subsequent to 1991. Results for precipitation and runoff are much more variable, both between countries and between regions in individual countries, and it is not feasible to draw general conclusions for the region. Notable features, however, include a) reported increases in annual precipitation in Denmark (Figure 4.5), Norway (Figure 4.3), and in the southern region of Iceland (Figure 4.4); and b) reported increases in annual runoff up to the year 2000 in these

same areas and also in the northern region of Sweden (Figure 4.1). In addition, the seasonal analysis of runoff anomalies for the Baltic countries indicates a marked increase in winter runoff throughout the region, and a decrease in summer runoff (Figure 4.7). The monthly analysis presented for Denmark (Figure 4.6) supports this tendency towards wetter winter and drier summer months.

Changes in extremes at individual stations throughout the Nordic and/or Baltic regions during recent years have also been considered in the CES project using differing approaches and methods. The analysis of trends in dry spells generally suggests that meteorological drought occurrence has either remained the same or has decreased during the 20th century, although some increasing trends were found for sites in Denmark and in Latvia. The analysis of the occurrence of peak flow events exceeding the annual maximum flood (Figure 4.8) also suggests a pattern of spatial variability, with some stations (for example, in western Norway and in Denmark) exhibiting an increase in the total number of events, and other stations (in Sweden, Finland and parts of Denmark) exhibiting a decrease. For the Baltic region, the analysis of the timing of the spring flood maximum discharge suggests an earlier spring flood due to an earlier spring snowmelt, which is consistent with previously published analyses for the Nordic region (Hisdal *et al.*, 2007; Wilson *et al.*, 2010).

The analyses of the connection between atmospheric circulation and hydroclimatological variables (Figures 4.9 and 4.10) demonstrate the potential fruitfulness of such an approach in identifying regional links between climate and runoff. It is, for example, noteworthy that the analysis of weather types contributing to rainfall flooding in Norway (Figure 4.9) has generated a spatial pattern which shares some similarities with the peak over threshold flood analysis (Figure 4.7), in that the stations associated with the largest increases in western Norway tend to be associated with particular weather types. Further work using this approach has a clear potential for contributing to a better understanding of the spatial variations observed in the response of runoff to changes in climate.

4.6 References

Alexandersson, H. (2002). Temperatur och nederbörd i Sverige 1860–2001. (Temperature and precipitation in Sweden 1860–2001, in Swedish). *Rapporter Meteorologi* Nr 104, SMHI, Norrköping.

van Bebber, W. J. (1891). Die Zugstrassen der barometrischen Minima nach den Banenkarten Deutsche Seewarte für den Zeitraum von 1875–1890. *Meteorol. Z.*, 8, 361–366.

Cherry, J., Cullen, H., Visbeck, M., Small, A., Uvo, C. (2005). Impacts of the North Atlantic Oscillation on Scandinavian Hydropower Production and Energy Markets. *Water Resources Managements,*19, 673–691.

Crochet, P., Jóhannesson, T., Jónsson, T., Sigurðsson, O., Björnsson, H. , Pálsson, F., Barstad, I. (2007). Estimating the spatial distribution of precipitation in Iceland using a linear model of orographic precipitation. *J. Hydrometeorol.,* 8, 1285–1306.

Einarsson, M.Á. (1978). Könnun á skiptingu Íslands í veðurspásvæði. (Division of Iceland into forecasting domains). Icelandic Meteorological Office Report, Reykjavik, 49pp. (in Icelandic).

Fleig, A., Tallaksen, L.M., Hisdal, H., Stahl, K., Hannah, D.M. (2010). Intercomparison of weather and circulation type classifications for hydrological drought development. *Physics and Chemistry of the Earth,* 35, 507–515.

Fleig, A., Tallaksen, L.M., Hisdal, H., Hannah, D.M. (2011). Regional hydrological drought in north-western Europe: linking a new Regional Drought Area Index with weather types. *Hydrological Processes,* 25 (7), 1163–1179.

Førland, E., Roald, L.A., Tveito, O.E. (2000). Past and future variations in climate and runoff in Norway. DNMI report No. 19/00 KLIMA, 77 pp.

Gerstengarbe. F.-W. and Werner, P.C. (2005). Katalog der Grosswetterlagen Europas (1881–2004) nach Paul Hess und Helmuth Brezowsky – 6. verbesserte und ergäntze Auflage. Potsdam, Offenbach a.M.

Haylock, M.R., Hofstra, N., Klein Tank, A.M.G., Klok, E.J., Jones, P.D., New, M. (2008). A European daily high-resolution gridded dataset of surface temperature and precipitation. *J. Geophys. Res. (Atmospheres)*, 113, D20119, 12 pp., doi:10.1029/2008JD010201.

Hellström, S. and Lindström, G. (2008). Regional analys av klimat, vattentillgång och höga flöden. (Regional analysis of climate, water resources and floods, in Swedish.) *SMHI Rapport Hydrologi* Nr. 110.

Helsel, D.R. and Hirch, R.M. (2002). Statistical Methods in Water Resources. Hydrological Analysis and Interpolation: Techniques of Water Resources Investigations of the US Geological Survey. Ch. A3, Book 4, pp. 266–274.

Hisdal, H., Barthelmie, R., Lindström, G., Kolcova, T., Kriauciunienè, J., Reihan, A. (2007). Statistical analysis. In: J. Fenger (ed.), *Impacts of Climate Change on Renewable Energy Sources,* Nord 2007:003. Nordic Council of Ministers, Copenhagen. pp. 58–73.

Hisdal, H., Holmqvist, E., Jónsdóttir, J.F., Jónsson, P., Kuusisto, E., Lindström, G., Roald, L. (2010). Has streamflow changed in the Nordic countries? Report No. 1 2010, NVE, Oslo, Norway.

Hohenthal J., Venäläinen A., Ylhäisi J., Käyhkö J. (submitted). Temporal development and variation of meteorological drought in Northern Europe during the 20th century. *Hydrology Research*. In revision.

Hirsch, R. M., Slack, J. R., Smith, R. A. (1982). Techniques of Trend Analysis for Monthly Water Quality Data. *Water Resources Research,* 18 (1), 107–121.

Hirsch, R.M. and Slack, J.R. (1984). A nonparametric trend test for seasonal data with serial dependence. *Water Resources Research,* 20, 727–732.

Hulme, M. and Barrow, E. (1997). Climates of the British Isles – present, past and future. Routledge, London and New York.

Jóhannesson T., Aðalgeirsdóttir, G., Björnsson, H., Crochet, P., Elíasson, E.B., Guðmundsson, S., Jónsdóttir, J.F., Ólafsson, H., Pálsson, F., Rögnvaldsson, Ó., Sigurðsson, O., Snorrason, Á. , Blöndal Sveinsson, O.G., Thorsteinsson, T. (2007). *Effect of climate change on hydrology and hydro-resources in Iceland*. Reykjavík, National Energy Authority, Report ISBN 978-9979-68-224-0, OS-2007/011, 91pp.

Jónsdóttir, J.F., Uvo, C.B., Clarke, R.T. (2008). Trend analysis in Icelandic discharge, temperature and precipitation series by parametric methods*. Hydrology Research, 39 (5–6), 425–436.*

Jónsdóttir, J.F. and Uvo, C.B. (2009). Long-term variability in precipitation and streamflow in Iceland and relations to atmospheric circulation*. Int. J. Climatol., 29, 1369–1380.*

Klavins, M., Briede, A., Radionov, V., Kokorite, I., Frisk, T. (2002). Long term changes of the river runoff in Latvia. *Boreal Environ. Res*., 7, 447–456.

Kolcova, T., Lizuma, L., Reihan, A., Kriaučiūnienė, J. (2010). Studies of cyclic behaviour of the air temperature, precipitation and water runoff time series in the Baltic states. In: H. Pikkarainen (ed.), *Proceedings of the Conference on Future Climate and Renewable Energy: Impacts, Risks and Adaptation.* Norwegian Water Resources and Energy Directorate, Oslo, pp. 64–65.

Lindström, G. and Alexandersson, H. (2004). Recent mild and wet years in relation to long observation records and climate change in Sweden. *Ambio*, vol XXXIII (4–5), 183–186.

Lindström, G., Hisdal, H., Holmqvist, E., Jónsdóttir, J.F., Jónsson, P., Kuusisto, E., Roald, L.A. (2006). Regional precipitation, temperature and runoff series in the Nordic countries. In: S. Árnadóttir (ed.), Proceedings of the EURENEW conference, Reykjavík 2006. CE-Report No. 2, 155–158.

Meilutytė-Barauskienė, D. and Kovalenkovienė, M. (2007). Change of spring flood parameters in Lithuanian rivers. *Energetika*, ISSN 0235-7208. Nr. 2, 26–33.

Mitchell, T.D. and Jones, P.D. (2005). An improved method of constructing a database of monthly climate observations and associated high-resolution grids. *Int. J. Climatol.,* 25, 693–712.

Pinto, J.G., Zacharias, S., Fink, A.H., Leckebusch, G.C., Ulbrich,U. (2009). Factors contributing to the development of extreme North Atlantic cyclones and their relationship with the NAO. *Climate Dynamics,* 32 (5), 711–737.

Reihan, A., Koltsova, T., Kriaučiūnienė, J., Lizuma, L., Meilutyte-Barauskiene, D. (2007). Changes in water discharges of the Baltic states rivers in the 21st century and its relation to climate change. *Nordic Hydrology,* 38 (4–5), 401–412.

van Belle, G. and J.P. Hughes (1984). Nonparametric Tests for Trend in Water Quality. *Water Resources Research,* 20 (1), 127–136.

Wilson, D., Hisdal, H., Lawrence, D. (2010). Has streamflow changed in the Nordic countries? Recent trends and comparisons to hydrological projections. *Journal of Hydrology,* 394 (3–4), 334–346.

Ylhäisi J. S., Tietäväinen H., Peltonen-Sainio P., Venäläinen A., Eklund J., Räisänen J., Jylhä K. (2010). Growing season precipitation in Finland under recent and projected climate. *Natural Hazards and Earth System Sciences,* 10, 1563–1574, doi:10.5194/nhess-10-1563-2010.

Önöz, B. and Bayazit, M. (2003). The power of statistical tests for trend detection. *Turkish Journal of Engineering and Environmental Sciences,* 27, 247–251.

Peer-reviewed publications resulting from work carried out during (or in conjunction with) the CES project, but not referenced in the chapter.

Jónsdóttir, J. F., Uvo, C. B., Clarke, R. T. (2008). Filling gaps in measured discharge series with model-generated series. Technical Notes. *Journal of Hydrological Engineering*, 13 (9), 905–909.

Lawrence, D. and Haddeland, I. (2011). Uncertainty in hydrological modelling of climate change impacts in four Norwegian catchments. *Hydrology Research,* 42 (6), 457–471.

Shkolnik I.M., Molkentin, E.K., Nadezhina, E.D., Khlebnikova, E.I., Sall, I.A. (2008). Temperature extremes and wildfires in Siberia in the 21st century: MGO regional climate model simulation. *Russ. Meteorol. Hydrol.*, 3, 5–15.

Tallaksen, L.M., Hisdal, H., van Lanen, H.A.J. (2009). Space-time modelling of catchment scale drought characteristics. *Journal of Hydrology*, 375, 363–372.

Tietäväinen, H. Tuomenvirta, H., Venäläinen, A. (2009). Annual and seasonal mean temperatures in Finland during the last 160 years based on gridded temperature data. *Int. J. Climatol.*, 30 (15), 2247–2256.

Venäläinen, A., Jylhä, K., Kilpeläinen, T., Saku, S., Tuomenvirta, H., Vajda, A., Ruosteenoja, K. (2009). Recurrence of heavy precipitation, dry spells and deep snow cover in Finland based on observations. *Boreal Environment Research*, 14, 166–172.

Veijalainen, N. and Vehviläinen, B. (2008). The effect of climate change on design floods of high hazard dams in Finland. *Hydrology Research,* 39 (5–6), 465–477.

5. Hydropower, snow and ice

*Tómas Jóhannesson, Guðfinna Aðalgeirsdóttir, Andreas Ahlstrøm, Liss M. Andreassen, Stein Beldring, Helgi Björnsson, Philippe Crochet, Bergur Einarsson, Hallgeir Elvehøy, Sverrir Guðmundsson, Regine Hock, Horst Machguth, Kjetil Melvold, Finnur Pálsson, Valentina Radić, Oddur Sigurðsson and Thorsteinn Thorsteinsson **

*Details on author affiliations are given in the Appendix

5.1 Introduction

Changes in glacier mass balance and consequent changes in glacier margins and land-ice volumes are among the most important consequences of future climate change in Iceland, Greenland and some glaciated watersheds in Scandinavia. Global sea level rise, observed since the beginning of the 20th century, is to a large extent caused by an increased flux of meltwater and icebergs from glaciers, ice caps and ice sheets. The increased flux of meltwater from land-ice has, apart from rising sea levels, potential global effects through the global ocean thermohaline circulation. It has also local effects on river and groundwater hydrology of watersheds adjacent to the glacier margins, with societal implications for many inhabited areas.

Changes in glacier mass balance and glacier geometry for several ice caps and glaciers in the Nordic countries have been modelled with mass balance and dynamic models within the CES project to estimate future response of glaciers to climate change as specified by the CES climate change scenarios. The main focus has been on the period 2021–2050 to assess changes that affect decisions related to investments and operational planning of power plants and energy infrastructure that need to be made in the near future. Some simulations were continued until the end of the 21st century to see the continued development for several decades after 2050. Natural climate variability is relatively more important for climate change simulations for the near future compared with the more distant future when the magnitude of the expected anthropogenic forcing has substantially exceeded the random background variability of the climate. Therefore, many different climate change scenarios where employed and used to assess the relative contributions of natural climate variability and deterministic greenhouse-gas induced climate trends in the simulated glacier changes.

Due to the importance of future glacier changes for the energy industry in Iceland, the most extensive CES glacier simulations were carried

out for the main Icelandic ice caps but studies with a somewhat more limited scope were also carried out for Greenland, Norway and Sweden. Glaciers and ice caps cover about 11% of the total area of Iceland and receive about 20% of the precipitation that falls on the country. They store the equivalent of 15–20 years of annual average precipitation over the whole country. Substantial changes in ice volume will, therefore, lead to large changes in the hydrology of glacier rivers with important implications for the energy industry and many other social sectors such as transportation and tourism. Glacier runoff affects most of the larger watersheds in Greenland and it is a large component in the water budget of several hydropower plants in Norway. Rapid changes are already taking place on the glaciers of the Nordic countries as the adjacent forefields bear witness to (Figure 5.1). As an example, Storbreen in Norway has retreated more than 500 m and lost 1/5 of its volume since mass balance measurements began in 1949 (Andreassen, 2009). In Iceland, all termini of non-surging glaciers that are monitored regularly have retreated since the beginning of this century. Many outlet glaciers of the Greenland ice sheet have been thinning and retreating at an accelerating rate during the last decade.

Figure 5.1. Left: The terminus region of the Greenland Ice Sheet near Paakitsoq on the western coast of Greenland (photo: Andreas Ahlstrøm 2003). The ice near the margin in this area is currently thinning by ~1 m per year. Centre: The former course of the Skeiðará river that drains the Skeiðarárjökull outlet glacier from the Vatnajökull ice cap, southeastern Iceland (photo: Ragnar Axelsson 2011). The Skeiðará river changed course in 2009 from the eastern side of the glacier to the Gígja river course close to the middle of the glacier tongue. This rendered the 1-km long Skeiðará bridge useless on dry land. Right: The Storbreen glacier in Jötunheimen in southern Norway (photo: Liss M. Andreassen 2008). The glacier has retreated by 500 m and lost one-fifth of its volume since 1949. Distinct end moraines extend down to the valley floor mark the post-glacial maximum of the glacier and bear witness to the large sensitivity of many glaciers to variations in climate. From its maximum extent in the 18th century, the glacier area has decreased by 25% and the length by almost 40%.

5.2 Climate scenarios for glacier modelling

The CES climate scenario group recommended three dynamically downscaled RCM scenarios (ECHAM5-r3/DMI-HIRHAM5, HadCM3/MetNo-HIRHAM, BCM/SMHI-RCA3) as described in Chapter 3 about climate scenarios. For Iceland and Greenland, a more recent downscaling of the ECHAM5-r3 global model with the RCAO regional model (Döscher *et*

al., 2010; Koenigk *et al.*, 2011) was used instead of the BCM/SMHI-RCA3 downscaling. The glacier simulations in Iceland also made use of a data set of 10 global AOGCM climate change simulations based on the A1B emission scenario submitted by various institutions to the IPCC for its fourth assessment report (IPCC, 2007). These 10 GCMs were chosen from a larger IPCC data set of 22 GCMs based on their surface air temperature performance compared with the ERA-40 reanalysis in the period 1958–1998 in an area in the N-Atlantic encompassing Iceland and the surrounding ocean (Nawri and Björnsson, 2010).

The recent warming in Iceland and Greenland has been particularly rapid, with a warming of ~1.25–2°C taking place at most weather stations in Iceland during the last 30 years (Figure 5.2). This rapid recent warming complicates the interpretation of climate change scenarios specifying a change in climate with respect to a past baseline period. The expected climate change during the next several decades with respect to the CES baseline period 1961–1990 depends crucially on how much of the rapid warming since the baseline period is viewed as a part of a deterministic warming trend and how much is viewed as a part of random climate variability. A temporary warming trend caused mainly by climate variability is likely to revert back to relatively cooler temperatures over a time period determined by the statistical autocorrelation of the temperature time-series.

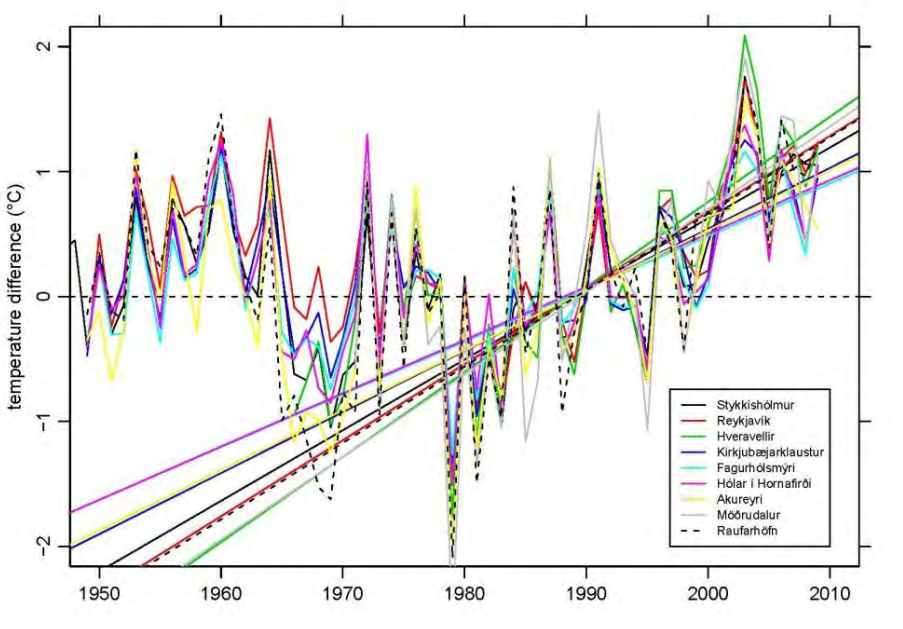

Figure 5.2. The difference of annual mean temperature with respect to the average of the period 1981–2000 for eight weather stations in Iceland from the middle of the 20th century to 2009. The period 1981–2000 is chosen as a reference because it is used in the spin-up of dynamic glacier models (see below). Straight lines show a least squares fit to the data from the last 30 years for each of the time-series, i.e. from the period 1980–2009.

There are many issues that need to be considered in the derivation of scenarios for short term climate change impact assessments. The most important are:

- *Type of scenario.* Typical δ-change scenarios have various flaws as described in the Chapter 3 about climate scenarios. Direct model output is, however, often difficult to use because of biases that make it unsuitable for hydrological and glaciological modelling
- *Baseline period.* The climate of any past baseline period such as 1961–1990 or 1971–2000 is characterised by a particular realisation of natural variability which is unlikely to be repeated in the future. In most cases, the climate of a (past) baseline period in a particular GCM simulation is characterised by internal "natural" variability of the respective GCM which has nothing to do with the actual climate during the same period in the real world. Using differences with respect to such a past baseline period unnecessarily introduces substantial uncertainties about past climate into the δ-change scenario. The use of the baseline period as a reference for comparison with a possible future climate needs to be separated from the use of the baseline period in the derivation of a climate change scenario
- *Recent climate changes.* A scenario needs to merge smoothly with the recent past climate, taking into account the effect of recent climate change that may partly be of anthropogenic origin and also the substantial internal autocorrelation of the climate. Past climate is in principle known and there is no reason to let internal "natural" variability of climate model simulations during already elapsed time periods introduce uncertainty into climate change scenarios
- *Seasonality of climate changes.* The annual cycle has a substantial effect on many aspects of the water cycle. There is large uncertainty regarding modelled changes in the seasonality of many climate variables. Modelled changes in seasonality need to be considered in detail and the deterministic component separated from the effects of random natural variability and, to the extent possible, model errors and biases
- *Surface characteristics.* The crude resolution of GCMs and some RCMs leads to an underestimate of the continentality of the climate at the location of many glaciers in the Nordic countries. The model cells nearest to the glaciers may contain large ocean areas that bring maritime effects far inland and into mountain areas where the climate is in reality to a large degree sheltered from maritime effects. It is particularly important to consider this problem when GCMs model results are directly used to derive climate change scenarios without downscaling
- *Choice of climate models.* There is considerable variation in the realism of different climate models regarding the present-day climate

in particular regions of the globe. Climate models need to be evaluated to detect serious biases and obvious errors that may degrade the quality of any scenarios derived from them
- *Internal consistency of climate variables.* Hydrological and glaciological simulations are based on several climate variables simultaneously. It is important that time-series of different climate variables in such modelling maintain their internal consistency when scenarios are derived. Precipitation has, for example, a tendency to fall on relatively warm days whereas cold periods have a tendency to be dry in some climate regions. It may be crucial to maintain such relationships in scenarios of future climate for simulations of future hydrological and glacier response to climate change to be meaningful

Based on the above considerations, climate change scenarios for the hydrological and glaciological modelling in Iceland were derived as follows (more details are given by Jóhannesson, 2010).

- The choice of RCM and GCM models was based on the analysis of Nawri and Björnsson (2010) and on the recommendations of the CES scenario group. This resulted in a total of 13 scenarios, 3 RCM-based and 10 based on IPCC GCM simulations. The choice of the GCM models was based on their surface air temperature performance for the present-day climate near Iceland as mentioned above
- For GCM-based scenarios, temperature change in the highland interior of Iceland, where the large ice caps are located, were increased by 25% based on the results of RCM downscalings (Nawri and Björnsson, 2010)
- Expected values for temperature and precipitation in 2010 were estimated by statistical AR (auto-regressive) modelling of past records, thereby taking into account the warming that has been observed in recent years as well as the inertia of the climate system so that the very high temperatures of the last few years have only a moderate effect on the derived expected values. These expected values are intended to represent the deterministic part of the recent variation in climate when short-term climate variations have been removed by the statistical analysis
- Scenarios of monthly mean temperature and accumulated precipitation were calculated from 2010 to the end of the climate simulation by fitting a least squares line to the monthly values simulated by the RCM or GCM from 2010 onwards and shifting the simulated time-series vertically so that the 2010 value of the least squares line matched the expected 2010 value based on the AR modelling of past climate. In this manner, the 1961–1990 CES baseline period was not directly used in the derivation of the future scenario. The CES baseline may nevertheless be used to express the scenario in terms of differences with respect to a baseline period if desired

The trend analysis of future climate eliminates the direct use of a past baseline period in the derivation of the scenarios and provides a consistent match with the recent climate development. The statistical matching of the past climate observations with the trend lines of the future climate, furthermore, provides an implicit bias correction. This is important near Iceland because the RCM and GCM simulations showed great biases with respect to observations in this area and the simulations of past variations in the climate were also quite different from the actual climate development, particularly with respect to the overall cold temperatures of the period 1961–1990 and the magnitude of the warming of the last several decades.

Figure 5.3 shows the 13 scenarios for annual mean temperature at the meteorological station Hveravellir in central Iceland together with a temperature time-series from Stykkishólmur, western Iceland, that extends back to the early half of the 19th century. The upper panel shows that, with the exception of the scenario based on the CSIRO_MK35 GCM model, the scenarios exhibit apparently random interannual to decadal variations, with a magnitude similar to past variations in the Stykkishólmur and Hveravellir records, superimposed on a general warming trend. The CSIRO_MK35 GCM model stands out with much greater interannual and decadal variations that appear to be substantially larger than past variations in temperature in spite of this model being one of the 10 models chosen from the set of 22 IPCC models with an overall realistic temperature performance in terms of bias and spatial variations in this area. One GCM model (MIUB_Echo_G) has somewhat smaller warming than the others, particularly near the end of the 21st century, whereas another (UKMO_HadCM3) indicates a greater rate of warming and comparatively large amplitude of interannual to decadal variations compared with the others. With the possible exception of the CSIRO_MK35 GCM model, this set of scenarios may provide an indication of the range of natural variability of the climate of the early 21st century as well as the magnitude of model uncertainties that may be expected in simulations with current GCM and RCM models. The lower panel of Figure 5.3 shows annual median values for different groups of the scenarios in order to highlight a more deterministic signal. It indicates a warming of close to 2°C near the end of the period 2021–2050 with respect to 1981–2000, about half of which has already taken place, and a warming of ~3–4°C by the end of the 21st century. Changes with respect to the CES baseline period 1961–1990 are very similar.

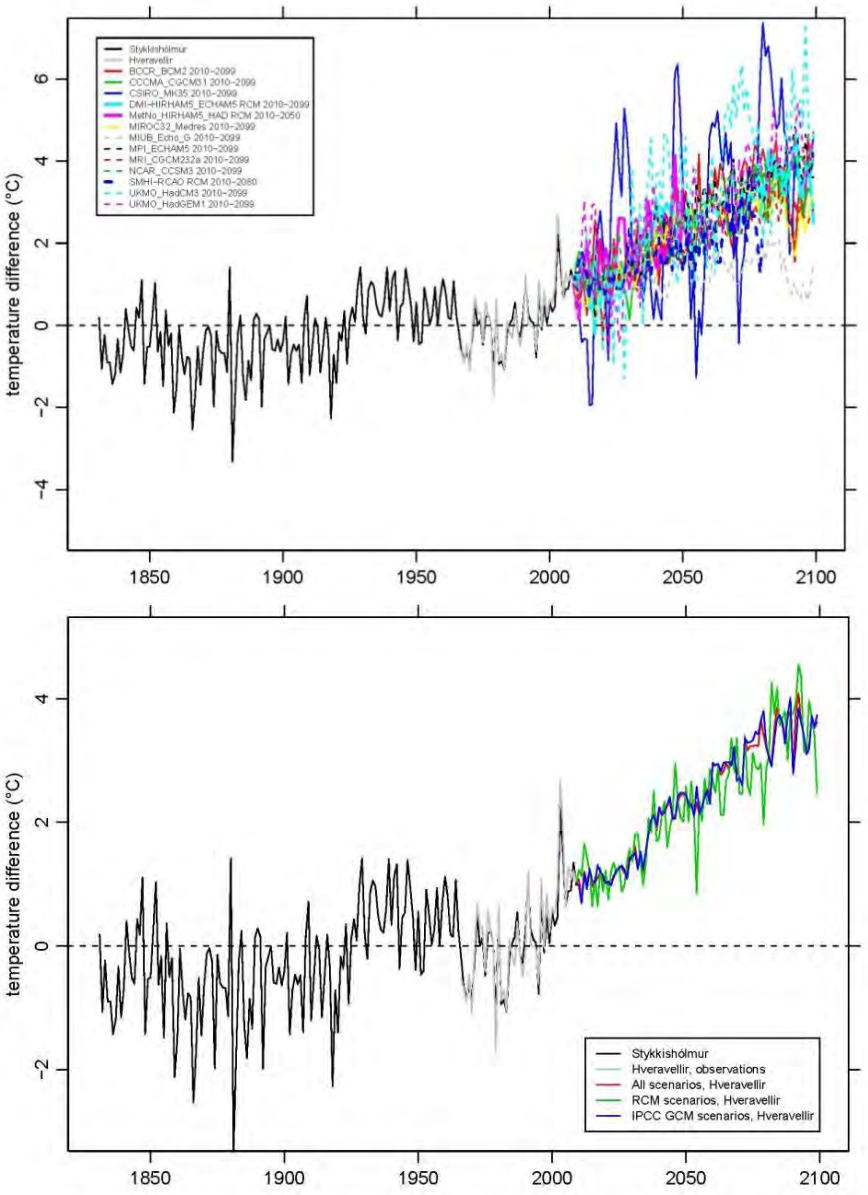

Figure 5.3. Future scenarios for annual mean temperature at Hveravellir, central Iceland. The longest temperature time-series from Iceland reconstructed for the Stykkishólmur meteorological station back to 1831 is also shown. Upper panel: All 13 scenarios (see text for explanations). Lower panel: Medians of several groups from the scenarios for each year. The figures show the difference of the mean annual temperature of glaciological years (starting in October of the previous year and ending in September of the respective year) with respect to the average of the period 1981–2000.

An analysis of the seasonality of the temperature changes shows that the warming is somewhat greater during the autumn and winter compared with the spring and summer. This is similar as found in earlier analyses of future climate change in Iceland (Björnsson *et al.*, 2008).

Precipitation changes were found to be dominated by the simulated "natural" climate variability. For some stations, including Hveravellir,

the AR statistical analysis of recent changes indicated an increase in precipitation in the last few decades but for others this was not the case. Typically, a slow increase of ~5–10% was found during the 21st century without a consistent seasonal variation.

For glacier simulations in Norway and Sweden, the three CES RCM-based scenarios were employed. The RCM results for Norway were further adjusted from the RCM grid points to a 1x1 km grid by the statistical downscaling method of Engen-Skaugen (2007) and for Sweden the RCM results were bias-corrected with ERA-40 using the metodology described by Radić and Hock (2006). The CES scenarios could not be used in Greenland because the RCM simulations did not reach far enough west to cover the Paakitsoq study area on the west coast of Greenland. Therefore, the glaciological modelling for Greenland had to be based on currently available simulations for that area from SMHI and DMI (see below).

5.3 Precipitation modelling

A linear theory of orographic precipitation (Smith and Barstad, 2004) has recently been used to produce a gridded daily precipitation data set for Iceland with 1 km horizontal resolution for the period 1958–2006 (Crochet *et al.*, 2007; Jóhannesson *et al.*, 2007). The LT-model combines airflow dynamics and cloud microphysics to calculate precipitation over complex terrain. The model was forced with large-scale atmospheric variables taken from the European Centre for Medium range Weather Forecasts (ECMWF). The data set is particularly suitable for creating forcing fields for glacier and hydrological modelling in remote mountainous areas where traditional precipitation time-series from precipitation gauges are few and far apart and where statistically based methods for spatial interpolation of station records are known to be inadequate. This precipitation data set is complemented by a data set of gridded daily temperature with the same horizontal resolution derived by spatial interpolation from the station network using a fixed vertical temperature lapse rate.

The present work explored whether several refinements in the methodology and parameterisation could improve the overall quality of the downscaled precipitation estimates at various temporal scales. Of particular importance was more physically-based and time varying estimation of several model parameters based on ambient atmospheric conditions. These parameters were previously determined with a statistical optimisation. With a physically-based parameter estimation, the application of the model for the downscaling of climate scenarios does not have to be based on an implicit, and perhaps unjustified, assumption of constant model parameter values under a changing climate.

An ensemble of simulations were performed over various periods ranging from 5 to 15 years, considering different strategies in the pa-

rameterization schemes and for estimating several input parameters. The best precipitation estimates of this ensemble were of similar quality in average, and sometimes better than previously obtained, but none of them resulted in a systematic improvement under all conditions. The resulting precipitation data sets are being used in mass balance and hydrological modelling of the Icelandic ice caps providing substantial improvements over earlier spatial precipitation distributions based on horizontal and vertical precipitation gradients. As an example Figure 5.4 shows the simulated distribution of accumulated precipitation on the Vatnajökull ice cap for January 1995.

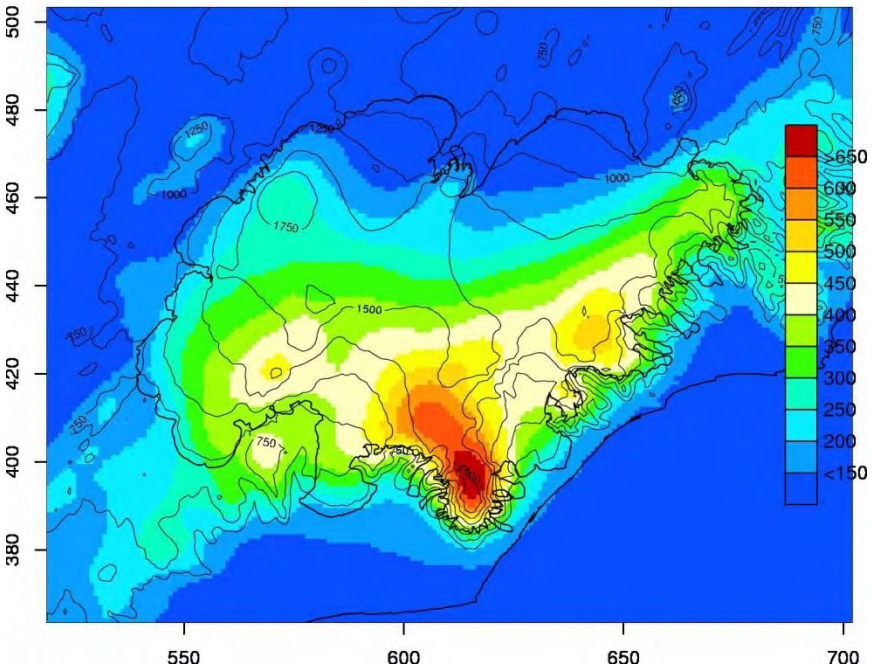

Figure 5.4. Distribution of accumulated precipitation on the Vatnajökull ice cap for January 1995 simulated with the LT-model of orographic precipitation. The 250-m contours show the shape of the ice surface and the surrounding terrain.

As a part of the CES project, the performance of the LT-model for precipitation modelling on the Svartisen ice cap in Norway was investigated (Schuler *et al.*, 2008) and the model was also tested for an area in Sweden encompassing Storglaciären and Mårmaglaciären. The model is, furthermore, being used in a glaciological context to model precipitation in mountainous areas in British Columbia in Canada. The model will be developed further based on the experience gathered in these widely separated areas.

5.4 Glacier mass balance and runoff simulation

5.4.1 Paakitsoq, western Greenland

Two downscaled simulations of the future climate of the Paakitsoq area near the western coast of Greenland (ECHAM5/SMHI-RCAO and ECHAM5/DMI-HIRHAM4, both based on the A1B emission scenario) were used to evaluate the quality of such simulations for glacier mass balance studies and to assess future glacier mass balance changes in this area (Machguth and Ahlstrøm, 2010). It was found that the output of both RCMs was characterised by considerable biases in modelled air temperature, global radiation and precipitation. Furthermore, RCAO seems to have an exaggerated variability of summer temperature in the neighbourhood of the Paakitsoq area resulting in an unrealistic spread of annual mass balance profiles as a function of altitude. A possible reason for this variability is that RCAO is a fully coupled RCM including an ocean module that may introduce unrealistic variations of ocean currents and sea-ice into the simulations in comparison with the GCM ocean state that is the lower boundary condition in HIRHAM4.

Estimating and correcting the RCM biases is not trivial because there are little meteorological and glaciological data to go from but this was nevertheless done resulting in reasonable present-day mass balance distributions from both RCMs. The future mass balance and mass balance changes were then calculated as functions of altitude using the same bias corrections (Figure 5.5). The mass balance changes were calculated as differences between the periods 2060–2080 and 1980–2000 in order to obtain a large difference compared with the underlying natural variability. Over this 80-year long period, the calculated change in mass balance below 1000 m a.s.l. is approximately -1 m/y which is about half of the estimate obtained by Ahlstrøm *et al.* (2008). The modelled change in mass balance diminishes rapidly with altitude above ~1000 m a.s.l. and is close to zero above ~1500 m a.s.l. The difference with respect to the earlier results of Ahlstrøm *et al.* is partly due to different mass balance models in the two studies (an energy balance model in the current study and a degree–day model in the study by Ahlstrøm *et al.*) and partly because the estimate presented by Ahlstrøm *et al.* includes the feedback effect arising from the lowering of the ice surface which is not included in the current study. Because of the large bias corrections, uncertainties in the simulated mass balance and mass balance changes must be considered large. The simulated future mass balance relies on the assumption that the RCM biases calculated for the present-day climate are valid in the future.

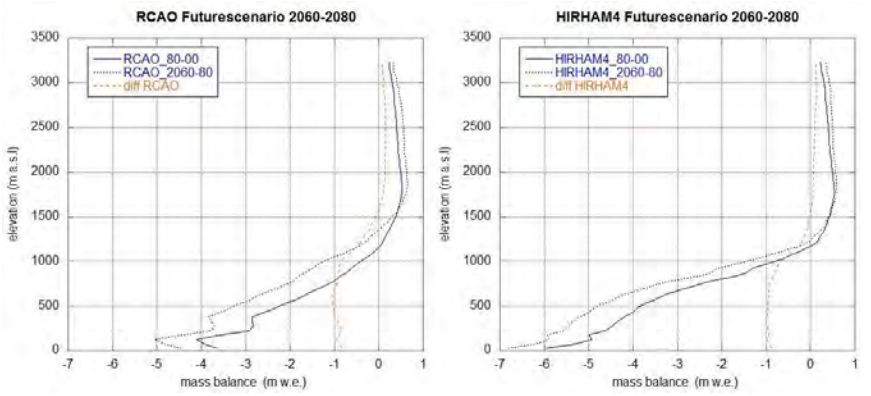

Figure 5.5. Simulations of glacier mass balance as a function of elevation for the Paakitsoq area near the western margin of the Greenland Ice Sheet calculated using bias-corrected RCAO (left panel) and HIRHAM4 (right panel) RCM downscaling of global climate simulations with the ECHAM5 GCM. The dotted orange curves show the difference between the years 2060–2080 and 1980–2000.

5.4.2 Storbreen, Southern Norway

Storbreen (61°34' N, 8°8' E) is a small glacier (5 km²) in the Jotunheimen mountain massif in central southern Norway. Measurements of winter balance (b_w) and summer balance (b_s) have been carried out since 1949. An automatic weather station (AWS) has been operated in the ablation zone of the glacier since September 2001 providing a near-continuous series of meteorological parameters and surface energy balance. Analysis of the first five years of data revealed that variations in temperature and reflected shortwave radiation (albedo) explained most of the inter-annual variation in melt, whereas the seasonal mean incoming shortwave radiation was remarkably constant between the years (Andreassen *et al.*, 2008). Within the CES project, a mass balance model was applied and tested for Storbreen (Andreassen and Oerlemans, 2009). The model was calibrated and validated with data from the AWS. The model included parameterisation of snow albedo and was forced by temperature and precipitation data from weather stations outside the glacier.

Results revealed that modelled and observed b_w and b_s values compared well for the period 1949–2006. Although discrepancies occurred in some years, the mass balance model was able to reproduce the main characteristics of b_w and b_s. Climate sensitivity calculations suggested that a 1°C warming must be compensated by a 30% increase in precipitation to avoid mass deficit and that the day of maximum b_w and minimum b_s will be greatly influenced by warming. Model results indicated that warming of 1 (3) °C will increase the length of the ablation season by ~20 (~50) days. The model sensitivities to ice and firn albedo will increase in a warmer climate due to earlier removal of the snow pack and thus an extension of the ice and firn melt periods.

5.4.3 Iceland

Ice-volume and runoff simulations were carried out with coupled mass-balance/ice-flow models and with mass-balance and hydrological models coupled to volume–area glacier-scaling models. Figure 5.6 shows changes in the geometry of the Langjökull and Hofsjökull ice caps in central Iceland simulated with a dynamic ice-flow model until the end of the 21st century for the climate change scenario based on the DMI HIRHAM dynamic downscaling (for a description of the methodology used in these simulations, see Guðmundsson *et al.*, 2009). This simulation indicates a ~30% reduction in the volume of Langjökull and ~20% for Hofsjökull by 2050.

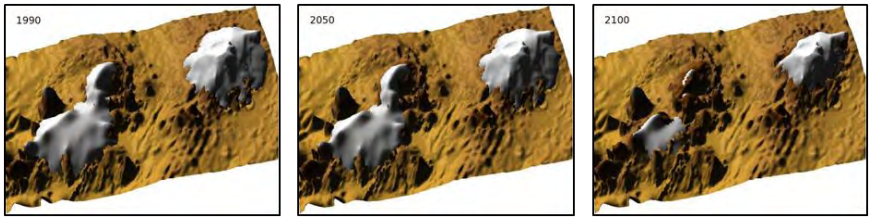

Figure 5.6. Simulations of the Langjökull and Hofsjökull ice caps in central Iceland for climate forcing as specified by the ECHAM5/DMI-HIRHAM4 dynamically downscaled climate change scenario. This scenario falls near the middle in the set of 13 scenarios shown in Figure 5.3. The panels show the initial spin-up state assumed to be valid for 1990 (left) and the simulated ice cap geometries at 2050 (centre) and 2100 (right).

Figure 5.7 shows ice-volume and runoff changes for Langjökull and Hofsjökull for all 13 Icelandic GCM- and RCM-based climate change scenarios. The temperature and precipitation changes specified by the scenarios are also shown. Before 2010, the model is forced with records of observed temperature and precipitation. The results corresponding to the CSIRO_MK35 GCM model stand out with very large interannual to decadal runoff variations that may be untrustworthy as mentioned before. During the first half of the 21st century, the other simulations show substantial future variations in runoff superimposed on a rising trend and a slow reduction in ice volume. The runoff changes fluctuate close to ~1 m/y for the first decades after 2010 for both Langjökull and Hofsjökull, rising to ~2 m/y for Hofsjökull and 2–4 m/y for Langjökull near the middle of the century. The reason for this difference in the response of the two ice caps is that the lower altitude distribution of Langjökull leads to an amplified response. In spite of the annual fluctuations, the simulated runoff changes are almost always positive and their magnitude is such that increased glacier runoff will be substantial for watersheds with only 10% glacier coverage or even less.

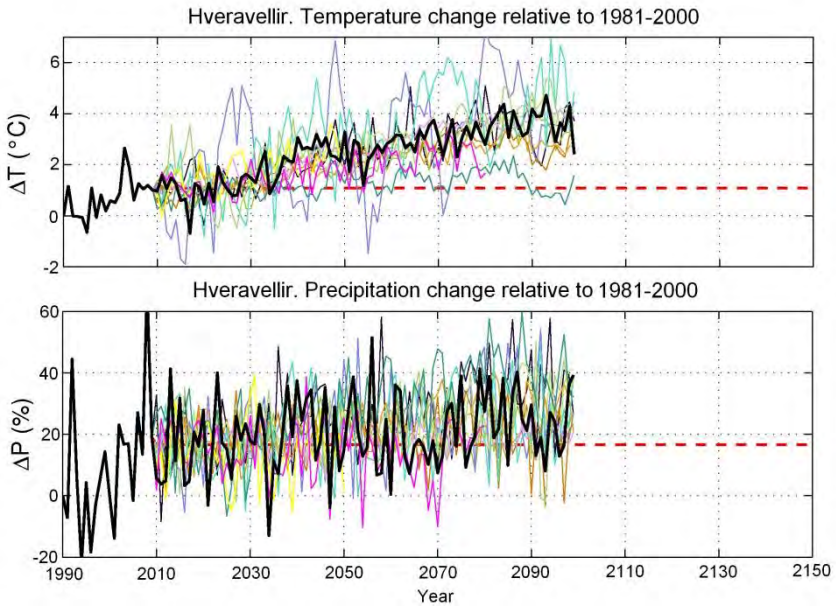

Climate change scenario:

- Present day (2000-2009) climate
- DMI-HIRHAM5-ECHAM5
- BCCR-BCM2
- CCCMA-CGCM31
- CSIRO-MK35
- MIROC32-Medres
- MPI-ECHAM5
- MRI-CGCM232a
- NCAR-CCSM3
- UKMO-HadCM3
- UKMO-HadGEM1
- MIUB-Echo-G
- MetNo-HIRHAM5-HAD
- SMHI-RCA3

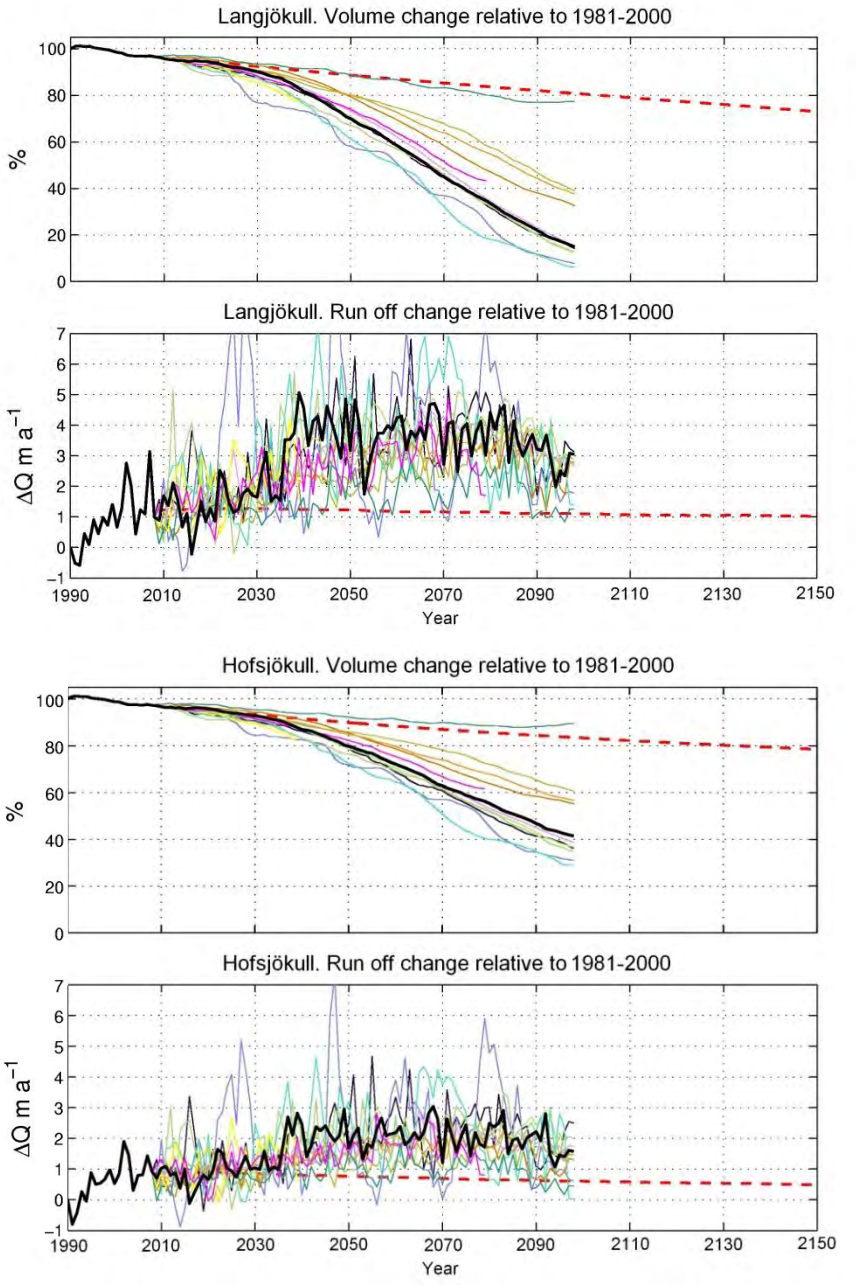

Figure 5.7. Simulated changes in ice volume and glacier runoff for the Langjökull and Hofsjökull ice caps in Iceland for 13 climate change scenarios deduced for the Hveravellir meteorological station. Top panel: Changes in temperature and relative changes in precipitation with respect to the average of the period 1981–2000. The averages of the period 2000–2009 are indicated with red dashed lines to indicate the changes that have already taken place. Centre and bottom panels: Simulated changes in ice volume and glacier runoff for Langjökull and Hofsjökull. The changes are for technical reasons with respect to the period 1981–2000 but this is very similar to the CES reference period 1961–1990. Red dashed lines show the results of simulations where the future climate is maintained at the 2000–2009 average.

5.4.4 Norway

Figure 5.8 shows ice-volume and runoff changes for Midtdalsbreen for three climate projections from the ENSEMBLES project with the A1B emission scenario used in CES project for Norway. Runoff from the glacier and total runoff from the catchment are shown separately. Before 2005, the coupled mass-balance/flow-line glacier model is forced with records of observed temperature (Bergen/florida) and precipitation (Bulken). During the first 20 years, the simulations shows substantial interannual runoff variations with no trend except for the results based on MetNo-HIRAM-HadCM3 that stand out with a rising trend and a fast reduction in ice volume. The runoff from the glaciated part fluctuates close to ~2.8 m/y for the first decades after 2005, rising to ~3.8 m/y near the middle of the century and continues to increase to ~4–5 m/y at the end of the century. The runoff increase from the ice-covered area is both related to increasing temperature, and a result of the progressive lowering of the ice surface. Considering total runoff from the catchment, the picture is different in the latter half of the century. The runoff from the catchment fluctuate close to ~2.5 m/y for the first decades after 2005, rising to ~3.6 m/y near the middle of the century and decreases during the latter half of the century. The decreasing runoff in the latter half of the century is due to a decrease in the glacier component of the total runoff that is a consequence of the reduction in glacier area associated with the reduction in ice volume. This shows that it is important to take dynamic glacier changes into account in order to obtain realistic estimates of melt water runoff from initially ice-covered areas in long integrations for a warming climate.

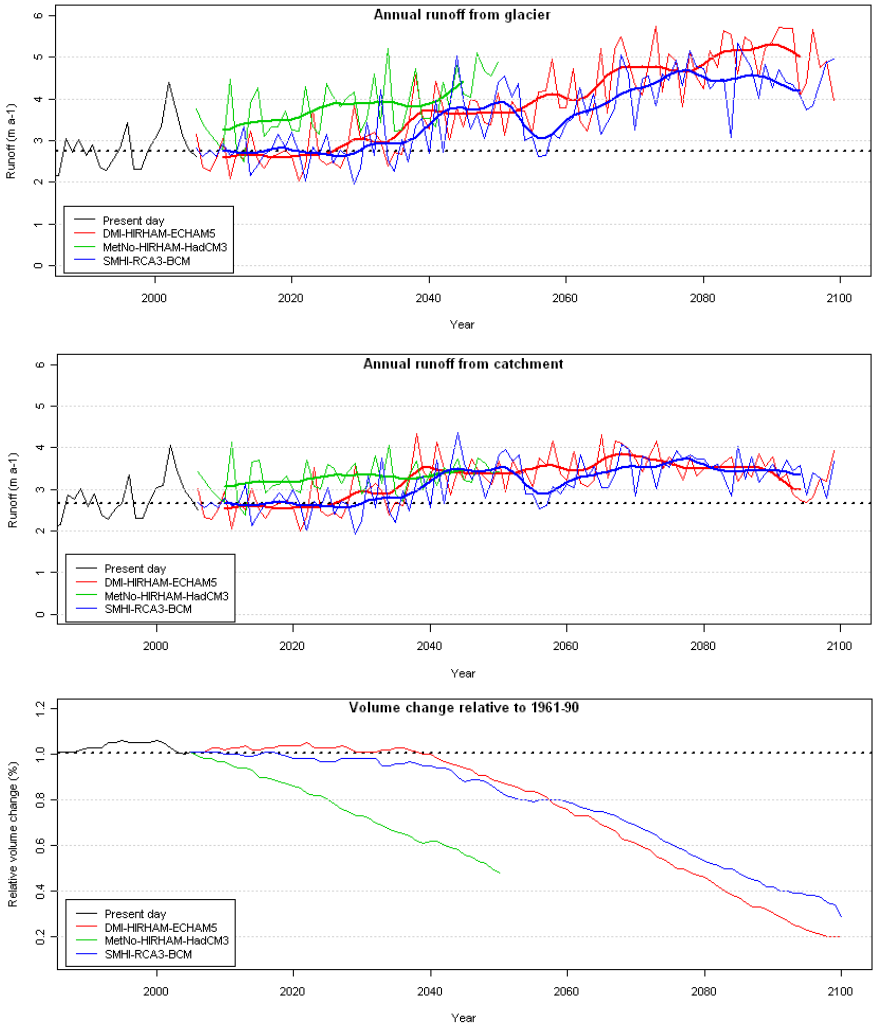

Figure 5.8. Simulated changes in glacier runoff and ice volume for the Midtdalsbreen outlet glacier in Norway for the three CES climate change scenarios for Norway. Changes in runoff from glaciated areas (upper), total runoff from catchment (middle) and relative volume change with respect to 1961–1990 (lower). The averages of the period 1961–1990 are indicated with black dashed lines to indicate the changes with respect to the CES baseline period. The runoff series are smoothed by Gaussian low-pass filters removing variations on smaller time-scales than a decade (thick lines).

Two partly glacier-covered watersheds in Norway, Nigardsbrevatn and Fønnerdalsvatn, were modelled with the HBV hydrological model coupled to a volume–area glacier-scaling model that was developed as a part of the CES project (Jóhannesson, 2009). This model makes it possible to carry out simple runoff modelling of drainage basins with many glaciers without detailed mass balance and dynamic modelling of each glacier. Long hydrological simulations of such watersheds need to take into account the limited ice volume stored in the glaciers, and preferably also the progressive lowering of the ice surface and the reduction in glacier area that are associated with a reduction in ice volume. The current versions of the Swiss WaSiM and the Norwegian HBV models effec-

tively assume an inexhaustible reservoir of ice with an unchanged altitude distribution, which may lead to an unrealistic contribution of melt water from initially ice-covered areas in long integrations for a warming climate. Figure 5.9 shows an example of the results for Nigardsbrevatn for the three CES climate change scenarios, both with and without the glacier-scaling model. It is seen that the results with and without the glacier-scaling model are not much different during the initial decades of the future simulation but as the ice volume is reduced the results start to diverge and have become noticeably different around 2050. By the end of the 21st century the difference between simulations with and without the glacier-scaling model is greater than the inter-model difference corresponding to the different scenarios.

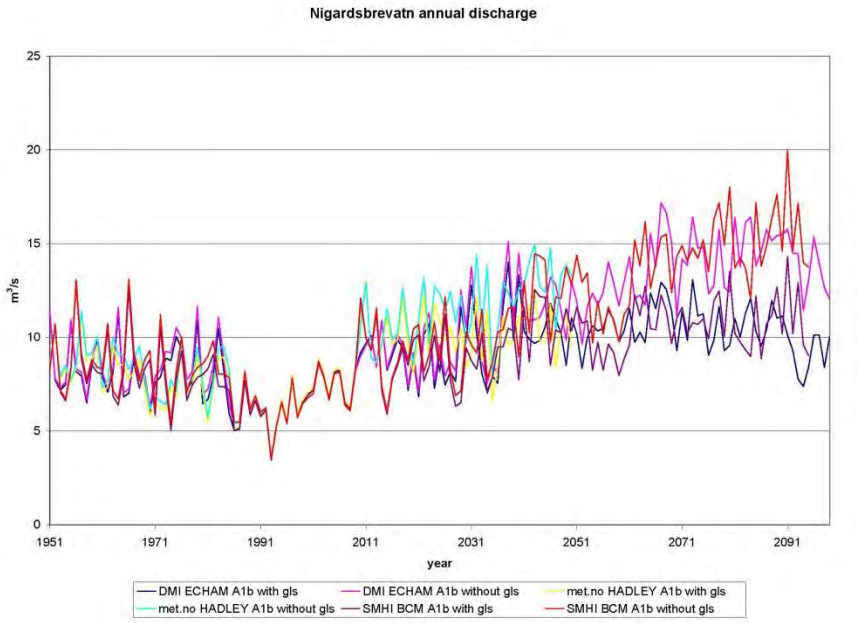

Figure 5.9. Simulated discharge from the partly ice-covered Nigardsbreen/Nigardsbrevatn watershed in Norway using the HBV hydrological model coupled to a volume–area glacier-scaling model for three climate change scenarios. Results from simulations with and without the glacier-scaling model are shown.

5.5 Comparison of future projections

Coupled mass-balance/ice-dynamic or mass-balance/glacier-scaling modelling was carried out within the CES project for three ice caps in Iceland, a glacier and two partly glacier-covered watersheds in Norway and two glaciers in Sweden, in each case for several different climate change scenarios. Figure 5.10 shows the simulated variation of ice volume with time for all these simulations to the end of the 21st century (some of the simulations end before 2100 because the corresponding climate scenarios do not extend up to 2100). It is seen that most of the glaciers have lost more than half of their volume by the end of the 21st

century for most of the climate scenarios. Simulations were also carried out for all glaciers in Iceland and Scandinavia with a lumped model based on volume–area scaling using 10 GCM-based A1B climate change scenarios (Radić and Hock, 2011) showing a somewhat larger range of variation depending on the choice of scenario. The simulated glacier response depends crucially on the employed scenarios and on the methodology used to implement them in glacier mass balance models so that ice loss by the end of the 21st century varies by an order of magnitude between scenarios for simulations of the same glacier.

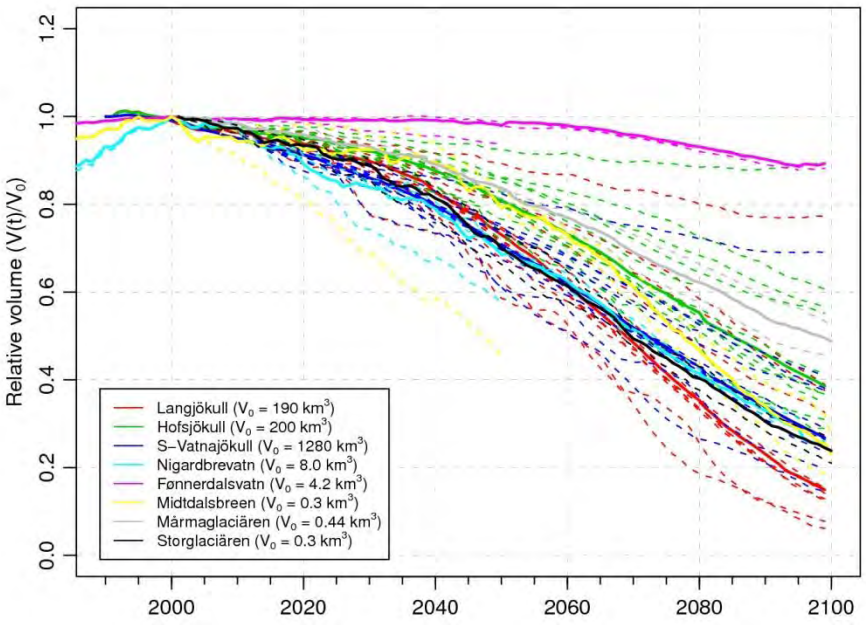

Figure 5.10. Relative changes in ice volume simulated with coupled mass-balance/ice-dynamic or mass-balance/glacier-scaling models three ice caps in Iceland (Langjökull, Hofsjökull and S-Vatnajökull), one glacier (Midtdalsbreen) and two partly glacier-covered watersheds (Nigardsbrevatn and Fønnerdalsvatn) in Norway and two glaciers in Sweden (Storglaciären and Mårmaglaciären). The dashed lines show the results of individual similations and thick, solid curves of the same colour show the median of all scenarios for the corresponding glacier.

5.6 Conclusions

The results of the CES project largely confirm the main results obtained in the earlier assessments including the CE and CWE projects. These results may be summarised as follows:

- Most glaciers and ice caps in the Nordic countries, except the Greenland ice sheet, are projected to essentially disappear in the next 100–200 years
- Runoff from ice-covered areas in the period 2021–2050 may increase by on the order of 50% with respect to the 1961–1990 baseline. About half of this change has already taken place in Iceland

- There will be large changes in runoff seasonality and in the diurnal runoff cycle and, in some cases, changes related to migration of ice divides and subglacial watersheds
- The dynamic response of the glaciers, that is the retreat of the ice margin and the thinning of the ice, has little effect on the modelled runoff changes in the short term but this becomes important in the second half of the 21st century
- The runoff change may be important for the design and operation of hydroelectric power plants and other utilisation of water
- There is a large uncertainty associated with differences between the climate development as modelled by different GCMs and RCMs. Most GCMs and RCMs still have spatial resolutions that are far coarser than needed for realistic mass balance modelling, making it necessary to apply special downscaling techniques and bias corrections in the glaciological modelling

The results show that substantial changes in ice volumes and glacier runoff may be expected in the future and that the glaciers are already considerably affected by human-induced climate changes. Glacier changes and runoff variations in the next few decades will nevertheless be much affected by natural climate variability as they have been in the past and predictability is, in addition, limited by scenario-related uncertainties.

5.7 References

Ahlstrøm, A. P., Mottram, R. H., Nielsen, C., Reeh, N., Andersen, S.B. (2008). Evaluation of the future hydropower potential at Paakitsoq, Ilulissat, West Greenland. Copenhagen, GEUS, Technical Report 2008/37.

Andreassen, L.M. (2009). Storbreen blir mindre. *Klima*, 4, 18–19.

Andreassen, L.M., van den Broeke, M.R., Giesen, R.H., Oerlemans, J. (2008). A five-year record of surface energy and mass balance from the ablation zone of Storbreen, Norway. *Journal of Glaciology*, 54 (185), 245–258.

Andreassen, L.M. and Oerlemans, J. (2009). Modelling long-term summer and winter balances and the climate sensitivity of Storbreen, Norway. *Geogr. Ann*., 91 A (4), 233–251.

Björnsson, H., Sveinbjörnsdóttir, Á.E., Daníelsdóttir, A. K., Snorrason, Á, Sigurðsson, B.D., Sveinbjörnsson, E., Viggósson, G., Sigurjónsson, J., Baldursson, S., Þorvaldsdóttir, S., Jónsson, T. (2008). Hnattrænar loftslagsbreytingar og áhrif þeirra á Íslandi – Skýrsla vísindanefndar um loftslagsbreytingar (Global climate change and their effect on Iceland – A report of a expert committee on climate change. In Icelandic.). Reykjavík, The Ministry for the Environment. 118 pp.

Crochet, P., Jóhannesson, T., Jónsson, T., Sigurðsson, O., Björnsson, H., Pálsson, F., Barstad, I. (2007). Estimating the spatial distribution of precipitation in Iceland using a linear model of orographic precipitation. J. *Hydrometeorol*., 8 (6), 1285–1306.

Döscher, R., Wyser, K., Meier, H.E.M., Qian, M., Redler, R. (2010). Quantifying Arctic Contributions to Climate Predictability in a regional coupled Ocean–Ice–Atmosphere Model. *Climate Dynamics,* 34 (7–8), 1157–1176, doi: 10.1007/s00382-009-0567-y.

Engen-Skaugen, T. (2007). Refinement of dynamically downscaled precipitation and temperature scenarios. *Climatic Change,* 84, 365–382, doi: 10.1007/s10584-007-9251-6.

IPCC (2007). Climate Change 2007: The Physical Science Basis. Contribution of Working Group I to the Fourth Assessment Report of the Intergovernmental Panel on Climate Change. Solomon, S., D. Qin, M. Manning, Z. Chen, M. Marquis, K. B. Averyt, M. Tignor and H. L. Miller, Jr., (*eds*). Cambridge University Press, Cambridge, UK, and New York, NY, USA, 996 pp.

Jóhannesson, T., Crochet, P., Sigurðsson, O. (2007). Use of glacier mass-balance measurements to estimate precipitation and model parameters in hydrological simulations for mountainous regions. In: Hock, R., T. Jóhannesson, G. Flowers and G. Kaser (eds.), *Abstract volume for Workshop on Glaciers in Watershed and Global Hydrology Obergurgl, Austria, 27–31 August 2007*, 42–43.

Jóhannesson, T., Aðalgeirsdóttir, G., Björnsson, H., Crochet, P., Elíasson, E.B., Guðmundsson, S., Jónsdóttir, J.F., Ólafsson, H., Pálsson, F., Rögnvaldsson, Ó., Sigurðsson, O., Snorrason, Á., Sveinsson, Ó.G.B., Thorsteinsson, T. (2007). Effect of climate change on hydrology and hydro-resources in Iceland. Reykjavík, National Energy Authority, Rep. OS-2007/011.

Jóhannesson, T., Aðalgeirsdóttir, G., Björnsson, H., Crochet, P., Elíasson, E.B., Guðmundsson, S., Jónsdóttir, J.F., Ólafsson, H., Pálsson, F., Rögnvaldsson, Ó., Sigurðsson, O., Snorrason, Á., Sveinsson, Ó.G.B., Thorsteinsson, T. (2007). Veður og orka. Loftslagsbreytingar og áhrif þeirra á vatnafar og orkuframleiðslu (An executive summary in Icelandic of the report OS-2007/011: Effect of climate change on hydrology and hydro-resources in Iceland). Reykjavík, National Energy Authority.

Jóhannesson, T. (2009). A simple (simplistic) method to include glaciated areas with a limited ice volume in the WaSIM and HBV models. Icelandic Meteorological Office, memo TóJ-2009/01.

Jóhannesson, T. (2010). Sviðsmynd um loftslagsbreytingar á Íslandi fyrir jökla- og vatnafræðilega líkanreikninga í CES og LOKS verkefnunum (Climate change scenarios for glaciological and hydrological simulations in the CES and LOKS projects). Icelandic Meteorological Office, memo ÚR-TóJ-2010-02.

Koenigk, T., Döscher, R., Nikulin, G. (2011). Arctic future scenario experiments with a coupled regional climate model. *Tellus* A, 63, 69–86, doi:10.1111/j.1600-0870.2010.00474.x.

Machguth, H. and Ahlstrøm, A.P. (2010). Ice sheet surface mass balance at Paakitsoq, West Greenland, derived from future scenario regional climate model data. Copenhagen, GEUS, Technical Report.

Nawri, N. and Björnsson, H. (2010). Surface air temperature and precipitation trends for Iceland in the 21st century. Icelandic Meteorological Office, report 2010-005.

Radić, V. and Hock, R.. (2006). Modeling future glacier mass balance and volume changes using ERA-40 reanalysis and climate models: A sensitivity study at Storglaciären, Sweden. *J. Geophys. Res.,* 111, F03003, doi:10.1029/2005JF000440.

Radić, V. and Hock, R. (2011). Regional differentiated contribution of mountain glaciers and ice caps to future sea-level rise. *Nature Geoscience*, doi: 10.1038/NGEO1052.

Schuler, T. V., Crochet, P., Hock, R., Jackson, M., Barstad, I., Jóhannesson, T. (2008). Distribution of snow accumulation on the Svartisen ice cap, Norway, assessed by a model of orographic precipitation. *Hydrological Processes,* 22 (19), 3998–4008.

Smith, R. B. and Barstad, I. (2004). A linear theory of orographic precipitation. *J. Atmos. Sci.,* 61, 1377–1391.

Peer-reviewed publications resulting from work carried out during (or in conjunction with) the CES project, but not referenced in the chapter.

Aðalgeirsdóttir, G., Guðmundsson, S., Björnsson, H., Pálsson, F., Jóhannesson, T., Hannesdóttir, H., Sigurðsson, S. Þ., Berthier, E. (2011). Modelling the 20th and 21st century evolution of Hoffellsjökull glacier, SE-Vatnajökull, Iceland. *The Cryosphere,* 5, 961–975, doi:10.5194/tc-5-961-2011.

Crochet, P. (2007). A study of regional precipitation trends in Iceland using a high quality gauge network and ERA-40. *J. Climate*, 20(18), 4659–4677.

Crochet, P., Jóhannesson, T., Sigurðsson, O., Björnsson, H., Pálsson, F. (2008). Modelling precipitation over complex terrain in Iceland. *In*: Sveinsson, Ó. G. B., S. M. Garðarsson and S. Gunnlaugsdóttir (*eds.*), *Northern hydrology and its global role: XXV Nordic hydrological conference, Nordic Association for Hydrology, Reykjavík, Iceland August 11–13, 2008*. Reykjavík, Icelandic Hydrological Committee.

Guðmundsson, S., Björnsson, H., Magnússon, E., Berthier, E., Pálsson, F., Guðmundsson, M.T., Högnadóttir, Th., Dall, J. (2011). Glacier mass balance response to regional warming, deduced by remote sensing on three ice caps in S-Iceland. *Polar Research*, 30, 7282, DOI: 10.3402/polar.v30i0.7282

Guðmundsson, S., Björnsson, H., Jóhannesson, T., Aðalgeirsdóttir, G., Pálsson, F., Sigurðsson, O. (2009). Similarities and differences in the response of two ice caps in Iceland to climate warming. *Hydrology Research*, 40 (5), 495–502.

Hock, R., Flowers, G., Jóhannesson, T., eds. (2008). *Glaciers in Watershed and Global Hydrology*. Special Issue of *Hydrological Processes*, 22 (19), 3887–4021.

6. Modelling Climate Change Impacts on the Hydropower System

*Sten Bergström, Johan Andréasson, Noora Veijalainen, Bertel Vehviläinen, Bergur Einarsson, Sveinbjörn Jónsson, Liga Kurpniece, Jurate Kriaučiūnienė, Diana Meilutytė-Barauskienė, Stein Beldring, Deborah Lawrence and Lars A. Roald **

*Details on author affiliations are given in the Appendix

6.1 Introduction

The work of the Hydropower-Hydrology group of CES has focused on hydropower production and dam safety studies based on ensembles of up-to-date regional climate scenarios. The model interface between climate models and hydrological models has been improved and uncertainties have been explored. An improved methodology to cope with impacts on lake and river regulation in a changing climate has also been studied, in particular for large lakes. Finally, a comparison of Nordic design flood standards under today's and future climate conditions has been carried out.

The work of the CES Hydropower Hydrology group has to a high degree been based on national research programmes in individual countries, supplemented by support from CES. Therefore, the different studies may have somewhat different focus and are often based on different methodologies and databases. So is, for example, the selection of regional climate scenarios different between national programmes. This fact has to be borne in mind when comparing results.

6.2 Methods

The use of ensembles of regional climate scenarios is an overarching strategy within CES. But in the case of hydrology and water resources the interface between models is another strategic issue. Due to systematic climate model errors, some form of adjustment is generally required in the raw climate model output before use in hydrological simulations. This is necessary to obtain realistic and credible hydrological results. So far three methods have been developed and used; the so called *Delta-*

change method, the *Distribution Based Scaling* (DBS) approach, and an *Empirical adjustment method.*

6.2.1 The Delta-change method

The Delta-change method is the most widely used technique for hydrological impact studies. It is based on the assumption that the relative change between a control simulation and a simulation of the future climate can simply be superimposed upon the observed time series used as input to the hydrological model. The change is normally expressed as percent for precipitation and as degree Celsius for air temperature. The method has the advantage of being simple to use but it has been criticized for not handling all the modelled changes in statistics properly, such as number of rainy days, long term annual fluctuations and extremes. Some of these signals are washed out by a too simplistic interface between models. The Delta-change method has been standard in many previous studies of climate impacts on hydropower such as the ones in the CE-project (Bergström *et al.*, 2007).

The Delta-change method can be combined with a temperature dependant temperature change to take into account the different changes in different parts of the temperature distribution (Andréasson *et al.*, 2004). In this method, the temperature change is calculated as a seasonal linear function of the temperature in the control period, estimated based on the daily RCM temperatures. The monthly temperature changes can then be scaled to match the original monthly changes in temperature in the scenario. This was used as part of the delta-change method in the calculations in Finland.

The delta-change method was also used in a modified version in Iceland. The delta-changes scenarios were given as differences for each future month with respect to expected values for temperature and precipitation in 2010 estimated by statistical AR (auto-regressive) modelling of past records. The monthly internal variability from the climate models is preserved by this methodology and account is taken of the inertia of the climate and the warming that has taken place in Iceland in recent years and decades (see further description in Chapter 5.2 and in Jóhannesson, 2010).

6.2.2 Distribution Based Scaling (DBS)

The Distribution Based Scaling (DBS) approach (Yang *et al.*, 2009) was developed to overcome the drawbacks of the Delta-change method. In the DBS approach, two primary meteorological variables, precipitation (P) and temperature (T), from climate model projections are adjusted before being used for hydrological simulations. Observed daily P and T time series for a reference period are used as a base to derive the respective scaling factors for the P and T outputs from the corresponding time period of

the climate projection. The function of the scaling factors is to adjust output from the regional climate model to make it statistically comparable to observations, in terms of mean and standard deviation. The scaling factors are then applied to the climate projection as it extends into the future. This correction assumes that the biases of the climate model are systematic and constant for the entire climate projection.

For precipitation, two separate gamma distributions are implemented. One gamma distribution is for low-intensity rainfall events, and the other for the extremes. The lower gamma distribution represents precipitation up to the 95th percentile of total precipitation events; the upper distribution represents events above the 95th percentile. The gamma distribution is a two-parameter distribution with the shape parameter, α, and the scale parameter, β. The product of $\alpha\beta$ describes the mean value of the studied data set, and $\alpha\beta^2$ represents the variance. Both mean and variance are calculated for RCM raw output and observations respectively. The deficit in mean and ratio in variance can, therefore, be used as indices of the resulting improvement from applying the DBS approach.

Compared to precipitation, adjusting daily temperature is less complex. It is described by a Gaussian distribution with mean, μ, and standard deviation, σ. The distribution parameters are smoothed over the reference period using a 15-day moving window. Separate distribution parameters are calculated for precipitation days and non-precipitation days to take into account the dependence between P and T. As with precipitation, the resultant scaling factors are subsequently applied to the climate projections.

6.2.3 The Empirical adjustment method

An empirical adjustment technique (Engen-Skaugen, 2007), is used in Norway to refine daily RCM output to better reflect local conditions. RCM output for temperature is height corrected for individual stations, and output for precipitation during a control period is corrected relative to observed monthly data. Further empirical adjustment of both precipitation and temperature are applied to RCM output for the future scenario period, based on residuals representing the variability of daily precipitation or temperature. The method preserves the relative changes in mean values and in the standard deviation based on daily values, between the control and future periods, as simulated by the RCM.

6.2.4 Evapotranspiration

Evapotranspiration change is often subject to less attention than temperatures and precipitation when impacts on water resources due to climate change are modelled. But evapotranspiration maybe an equally important factor as precipitation change in certain areas. Attempts have been made to extract changes in evapotranspiration from climate mod-

els, but the most commonly used technique is to simply assume a proportionality to air temperature changes. This is the technique used in all studies within the CES-project.

6.2.5 The hydrological model

Most studies in the Nordic and Baltic countries are carried out by use of some variant of the HBV-hydrological model (Bergström, 1995). The exception is the group from Iceland, which uses the WASIM model due to its need for a better groundwater description than HBV can offer. There are different national standard versions of HBV, which have developed over time to meet the needs of the specific country.

6.3 Uncertainty and ensembles

The use of ensembles of regional climate scenarios visualises the unavoidable uncertainty in simulation of future conditions for hydropower production and safety. In the CES-project as many as 20 different climate scenarios have been used in some cases. But there are other sources of uncertainty as well such as choice of technique in the interface between the climate models and the hydrological model, choice of hydrological model and its calibration. It is of utmost importance that these uncertainties are communicated properly to decision makers.

6.3.1 An example from the border between Norway and Sweden

One way of illustrating the uncertainty caused by differences in the regional climate simulations is by presenting diagrams like in Figure 6.1. It shows the development of the 100-year inflow flood in the Höljes basin in upper Klarälven in Sweden (named Trysilelva in Norway). Figure 6.1 is based on 16 regional climate scenarios and a continuous frequency analysis carried out in a moving window of 30 years. The interface between the climate models and the hydrological model is based on the Distribution Based Scaling approach. The frequency analysis is based on the Gumbel distribution function.

In Figure 6.1 each regional climate scenario has a unique colour code. Note that some of these only extend until 2050. As can be seen uncertainties are large even though the tendency of declining 100-year floods is clear in this case. The wide range of the obtained results brings up the critical issue of which of regional scenarios to choose in an impact analysis. This question is still unsolved.

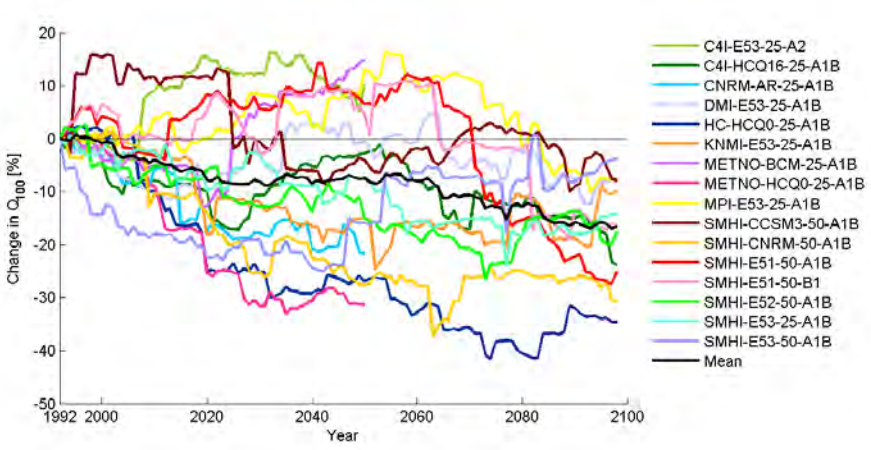

Figure 6.1. The development of the 100-year inflow flood in the Höljes basin in upper Klarälven in Sweden (named Trysilelva in Norway) based on an ensemble of regional climate scenarios and a continuous frequency analysis carried out in a moving window of 30 years. Altogether 16 scenarios were available for the period until 2050 and 12 for the remaining part of the century.

6.3.2 A Lithuanian example

In Lithuania, catchment-scale modeling of climate change impact on the Merkys river runoff was carried out. The simulations were based on scenarios from two global climate models (ECHAM5, HadCM3), three emission scenarios for greenhouse gases (A2, A1B, B1) and the Delta-change approach for transferring the climate change signal to a meteorological station. A simulation of the river runoff in the 21st century was made using the HBV hydrological model (Kriaučiūnienė *et al.*, 2009). During the century, runoff is projected to decrease by 30–50% according to the different scenarios but there are significant uncertainties (Figure 6.2).

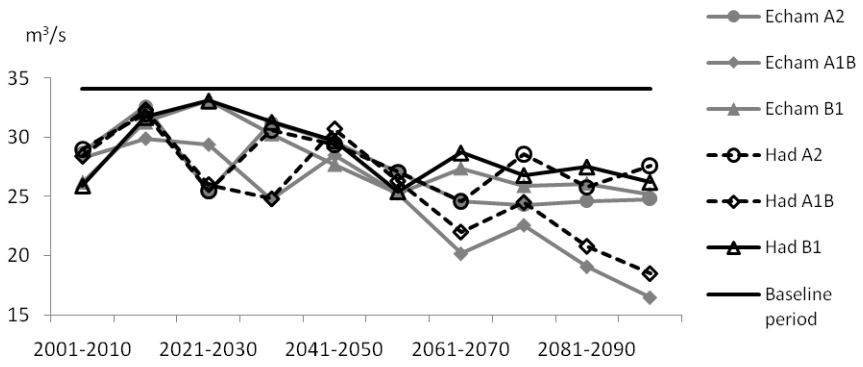

Figure 6.2. Change in the discharge of the Merkys river according to six different climate scenarios for the period 2001–2100.

Further analysis of the uncertainty in the modelling of climate change impacts was carried out by a separation of the effects of the hydrological model parameter set, the emission scenario and the global climate model used in the simulations. The study used the GLUE (Generalized Likelihood

Uncertainty Estimation) method (Beven and Binley, 1992; Ratto and Saltelli, 2001), which uses the accumulated difference between the calculated and the observed discharge, Δh, as a criterion for the goodness-of-fit. The average of Δh was calculated separately for emission scenarios and global climate models for each decade under consideration.

The period of 1975–1984 was selected for calibration and validation of the hydrological model by manual calibration of 16 of its parameters. The GLUE method was applied to the six most important parameters out of these 16. They were: β – soil moisture parameter; *cfmax* – snow melting factor; *FC* – maximum storage of the soil moisture reservoir; *k4* – base flow recession parameter; *perc* – ground water percolation (upper to lower zone); *sfcf* – snowfall correction factor. The remaining parameters were left unchanged after the manual calibration. All together 1000 sets of values of the parameters *sfcf, FC, cfmax, β, k4* and *perc* were generated using a Monte Carlo method and discharge was generated. In the output Δh varied between 10 and 200 mm. In the estimation of uncertainty of the model parameters, two Δh values were selected: (1) the average Δh obtained when river discharges are simulated according to 1000 parameter sets (120 mm); and (2) average Δh of the 10 best-fit parameter sets according to the GLUE function (31 mm).

The uncertainty analysis was performed by comparing the respective impacts of emission scenarios and global climate models with the results of the hydrological model expressed by Δh for every decade of the 21st century.

The results showed that simulated runoff was most sensitive to the selected emission scenario. For example, the air temperature in the Merkys catchment area at the end of the century can differ by up to 2.2°C depending on which emission scenario is used. The choice of a global climate model had much less influence on the results. The calibration process reduced the influence of model parameters on the uncertainty of simulated of river runoff from 23% to 7%.

6.4 Hydropower production

National studies on the impacts of climate change on hydropower production have been carried out in most of the Nordic and Baltic countries. Some of this work was made in co-ordination with CES and is presented below.

6.4.1 A Finnish example

The Finnish Watershed Simulation and Forecasting system (WSFS) was used to simulate changes in discharge and hydropower potential in the five largest and most important hydropower producing rivers in Finland. Simulations were carried out for the period 2021–2050 (Figures 6.3 and 6.4), using the Delta-change method. The WSFS includes a HBV-type con-

ceptual watershed model developed and operated at the Finnish Environment Institute and used for operational forecasting and research purposes in Finland (Vehviläinen *et al.,* 2005). Two scenarios produced an average increase of 5–10% in annual discharge relative to the control period and a clear increase in winter runoff. The scenarios differed from each other especially during summer, when one scenario produced a decrease in discharge while the other indicated no change from the control period. Spring runoff peaks occurred earlier in both scenarios, but while a slight increase in average peak discharge was produced by one scenario, the other produced a clearly smaller and earlier peak discharge.

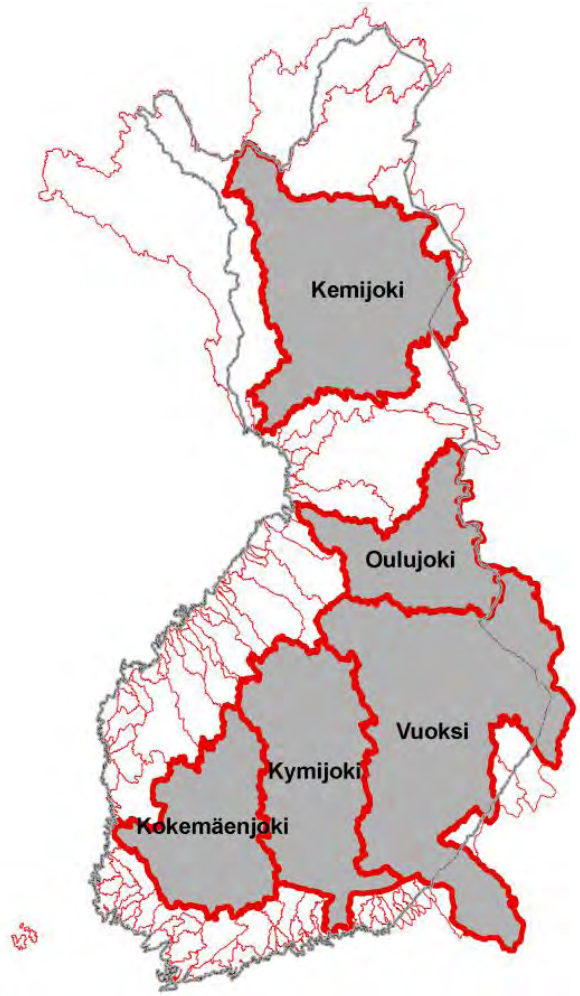

Figure 6.3. Watersheds of the five largest and most important hydropower producing rivers in Finland.

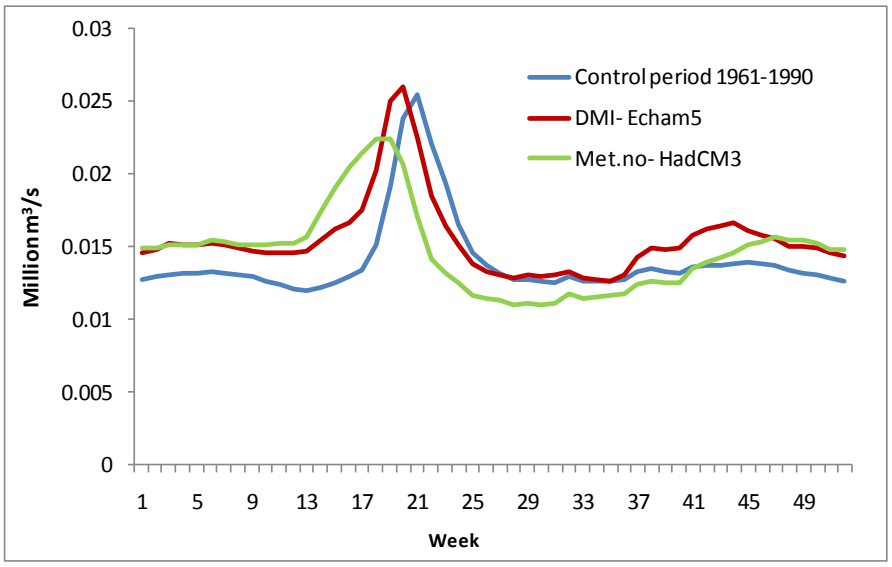

Figure 6.4. Sum of average weekly discharges (million m³/s) in the five largest rivers of Finland (see Figure 6.3) in the control period 1961–1990 and calculated for 2021–2050 using two scenarios (DMI-Echam5 and Met.no-HadCM3).

6.4.2 An Icelandic example

To investigate the effect of climate change on the hydrological regime in Iceland and the implications for the hydropower industry, projections of river discharge in the period 2021–2050 have been made for two watersheds using the WASIM hydrological model (Figure 6.5). One of the watersheds has a 10% glacier cover while the other one has none (Einarsson and Jónsson, 2010a).

The runoff projections are based on thirteen climate change scenarios (Nawri and Björnsson, 2010; Jóhannesson, 2010), ten derived from GCM model runs prepared in connection with the IPCC 2007 report and three based on RCM downscalings recommended by the CES climate scenario group (Kjellström, 2010). To account for changes in temperature and precipitation, monthly delta changes with respect to the period 1981–2000 for each future year are applied repeatedly to a single past base year. By this method, monthly variability from the climate scenario runs is preserved. As the runoff modelling depends on the selection of base year, three different base years were used, each close to the mean of the baseline periods 1961–1990 and 1981–2000 in their climatic characteristics.

In the present study the groundwater module of WASIM has been implemented for the first time in hydrological modelling of watersheds in Iceland (Einarsson and Jónsson, 2010b). This is an important step forward because bedrock in large areas of the country is porous and has high hydraulic conductivity, making groundwater flow an important part of the runoff from many watersheds. The results are presented in Figure 6.6. Average warming for both watersheds between the reference period and the scenario period is on the order of 2°C. A precipitation increase averaging 20% is predicted for the partly glacier covered wa-

tershed and an average increase of 3% is predicted for the other one. As glacier melt is affected by increasing temperatures this causes an average increase of 40% in the runoff for the glacier covered watershed and an average runoff increase of 3% for the non-glaciated one. The timing of maximum snowmelt is predicted to occur approximately one month earlier for both watersheds and the magnitude of the mean annual maximum snowmelt is predicted to decrease by 5–70%.

The period of considerable snow cover is predicted to diminish from 7 months annually to 5 months for the Austari Jökulsá catchment and from 7 to 3 months for the Sandá catchment. Mean annual maximum snow thickness is predicted to decrease by 5–80%. This results in increased average winter flow and more evenly distributed seasonal discharge to the benefit of hydropower development on these rivers. For the partly glacier covered watershed, runoff from the glacier will increase substantially and the duration of glacier runoff is predicted to increase by nearly two months. The increase of annual glacier melt, assuming unchanged glacier geometry, is predicted to be in the range from 75–150% depending on the climate scenario. This leads to increased hydropower potential for partly glacier covered watersheds during the period in which past precipitation stored in the glaciers is released.

Compared to the period 1961–1990 a warming of about 1°C has already been observed for the watersheds during the period 2000–2009, causing considerable discharge changes in the same direction as the predicted future changes.

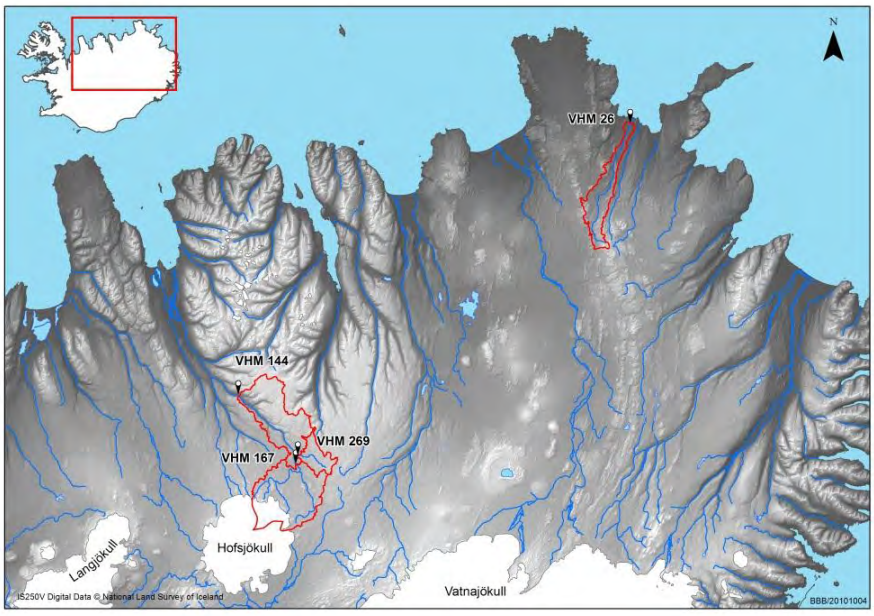

Figure 6.5. Location of the partly glacier covered watershed of the river Austari Jökulsá (VHM144) and the non-glacier covered watershed of the river Sandá in the Þistilfjörður district (VHM26).

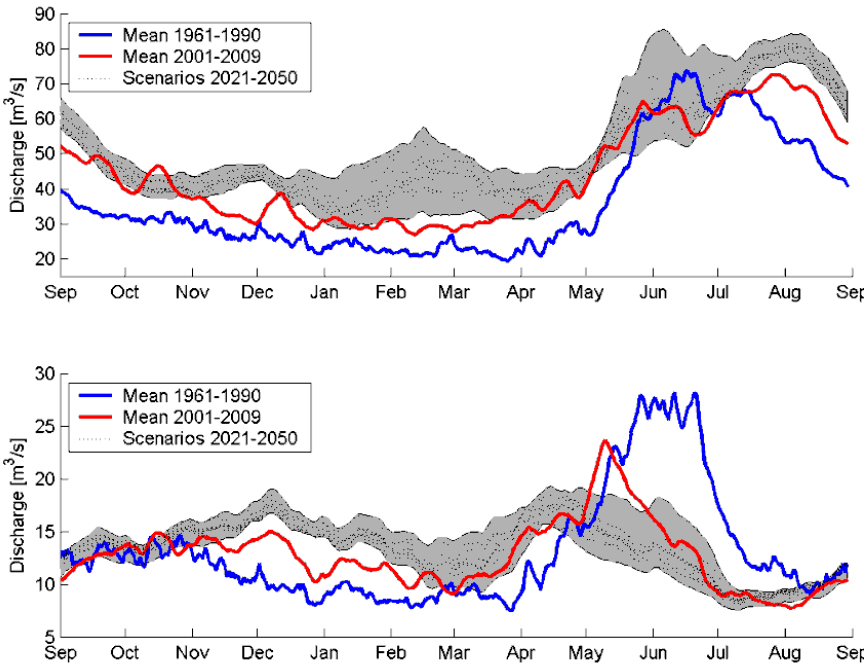

Figure 6.6. Observed and predicted discharge for the partly glacier covered watershed of Austari Jökulsá (top) and for the non-glacier covered watershed of Sandá (bottom).

6.4.3 A Latvian example

The largest hydropower plants in Latvia produce approximately 50% of the electricity used in the country. The HBV model was used in climate change impact studies for the Plavinas hydropower plant on the Daugava River and the Aiviekstes hydropower plant on the Aiviekste River. The simulation of future (2021–2050) climate conditions was based on results of the three climate models DMI-HIRLAM-ECHAM5, MetNo-HIRLAM-HadCM3 and SMHI-RCA3-BMC, employing the SRES A1B emission scenarios. The climate model results were downscaled using a statistical downscaling method (Sennikovs and Bethers, 2009).

According to the scenarios and the hydrological simulation the annual runoff will increase by 19–27%. The most remarkable increase was found for the winter (DJF) season (30–70%). All scenarios predict a decrease in runoff for the period April–May (Figure 6.7).

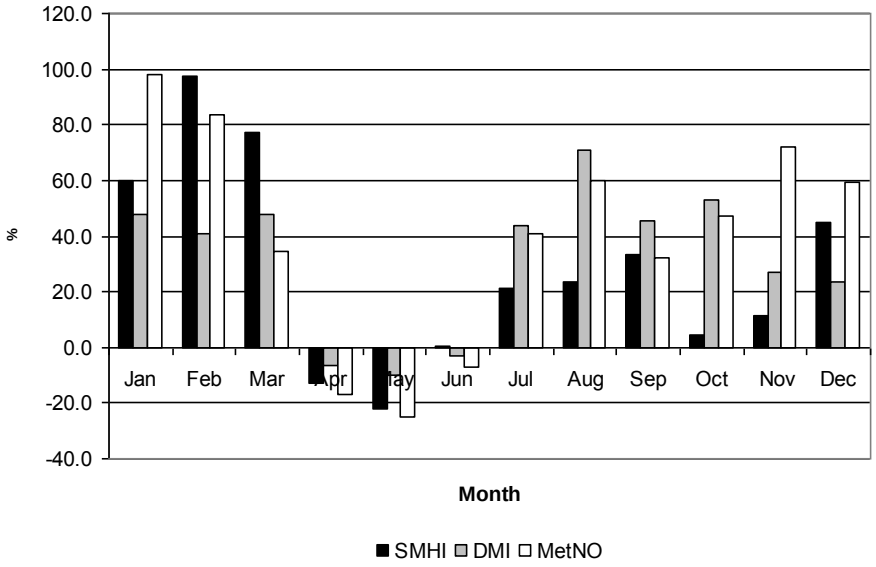

Figure 6.7. Percentage changes in monthly runoff from 1961–1990 to 2021–2050 for the Aiviekste hydropower plant in Latvia, according to 3 climate scenarios: DMI-HIRLAM-ECHAM5, MetNo-HIRLAM-HadCM3, SMHI-RCA3-BCM.

6.4.4 A Lithuanian example

Presently, hydropower comprises only 2.2% of the total energy production in Lithuania but is expected to increase in importance in the future. The Kaunas hydropower plant on the river Nemunas produces some 359.0 GWh, while 84 small hydropower plants produce about 65 GWh. The volume and seasonal distribution of runoff in the Nemunas river are thus of particular importance in the context of the CES project.

The climate change impact on hydrological processes in the Nemunas river basin was estimated using the A1B, A2 and B1 emission scenarios and the two global climate models ECHAM5 and HadCM3. Temperature and precipitation simulations from the regional climate model were downscaled by the Delta-change approach. The climate scenarios were then used as input data in the HBV hydrological model and climate change impacts were calculated for every decade of the period of 2011–2100 (Figure 6.8). The results were compared with the baseline period which was 1975–1984 in this specific national project (Kriaučiūnienė et al., 2008).

As shown in Figure 6.8, the average annual runoff is projected to decrease with the exception of the period 2011–2020 during which a small increase is predicted. According to all emission scenarios, the river runoff will increase in winter, because of higher temperatures and less stable snow cover. Spring runoff will decrease for the same reason. The runoff shows a tendency to decrease in summer and in autumn (Meilutytė-Barauskienė *et al.*, 2010).

The projected decrease in runoff in the river Nemunas will have a great impact on the energy production of the Kaunas hydropower plant

during the 21st century. The analysis of the seasonal runoff distribution shows that energy production will increase in winter and decrease in spring, summer and autumn. According to the simulations, the average energy production will decrease between 7 and 26% during the period 2001–2100 in comparison with the baseline period.

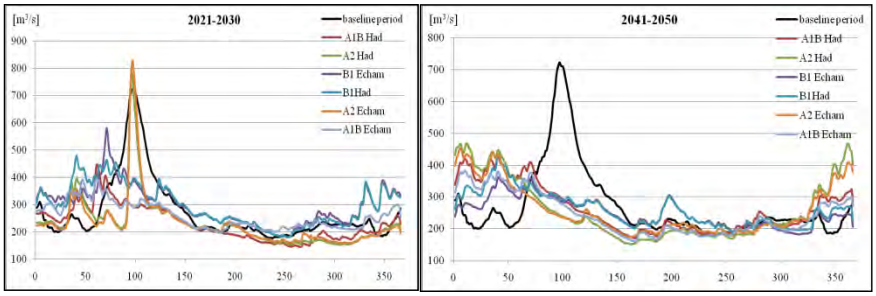

Figure 6.8. Simulated changes of seasonal runoff in the river Nemunas in Lithuania for the periods of 2021–2030 and 2041–2050 according to six climate scenarios, in comparison with the baseline period 1975–1984.

6.4.5 A Norwegian example

Three climate projections from the ENSEMBLES project assuming the A1B emission scenario for greenhouse gases were used for studying the impacts of climate change on hydrological processes in Norway: The Max-Planck Institute ECHAM5 model downscaled by the Danish Meteorological Institute using the HIRHAM5 regional climate model; the Hadley Centre HadCM3 model downscaled by the Norwegian Meteorological Institute using the HIRHAM regional climate model; and the Bjerknes Centre BCM model downscaled by the Swedish Meteorological and Hydrological Institute using the RCA3 regional climate model.

Figure 6.9 shows changes in mean annual runoff from the control period 1961–1990 to the projection period 2021–2050 for maps with 1 by 1 km² grid cells for all of Norway. The projected increase in runoff is generally substantial. The maps were produced by a spatially distributed version of the HBV hydrological model (Beldring *et al.*, 2003) with precipitation and temperature input from the three climate projections downscaled to the grid cells of the hydrological model on a daily time step, using an empirical adjustment procedure developed by Engen-Skaugen (2007). The purpose of this method is to reproduce the statistical properties of daily precipitation and temperature data with spatial resolution 1 by 1 km² for the control period 1961–1990, based on spatial interpolation of observed meteorological data. The applicability of this procedure for hydrological modelling was verified by Beldring *et al.* (2008). Although hydropower production depends on a number of factors, including the design of reservoirs and hydropower plants, reservoir operation strategies, distribution of floods and droughts and energy demand, these maps still present a view of the change in inflow to hydropower reservoirs for different regions.

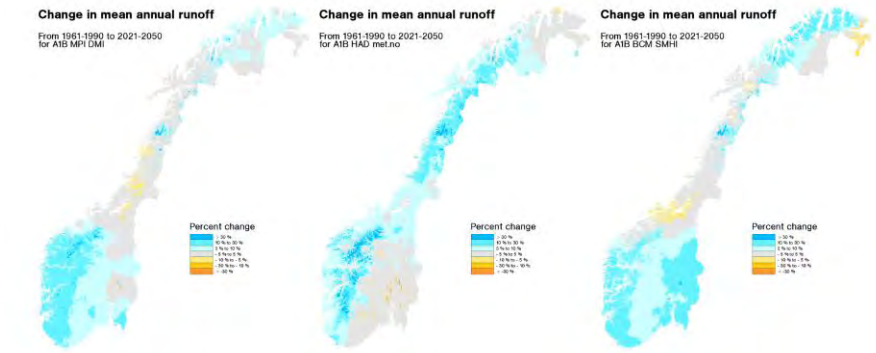

Figure 6.9. Percent change in mean annual runoff from 1961–1990 to 2021–2050 for climate projections A1B/Max-Planck Institute ECHAM5/Danish Meteorological Institute/HIRHAM5 (left), A1B/Hadley Centre HadCM3/Norwegian Meteorological Institute/HIRHAM (centre), and A1B/Bjerknes Centre BCM/Swedish Meteorological and Hydrological Institute/RCA3 (right).

6.5 Regulation of lakes and rivers

A great number of the rivers and lakes in the Nordic and Baltic countries are regulated for water management, flood protection and hydropower production. The rules are often set by some legal rules or decrees, which may date back several decades or more. The decree for the largest one, Lake Vänern, was, for example, adopted as early as in 1937 based on the knowledge and on the climate conditions of those days. As a warmer climate may make old regulation roles obsolete, the question of adjustment of these have been studied within the CES-project, in particular by the Finnish team at SYKE.

6.5.1 A Finnish example

More than 300 lakes in Finland are regulated for hydropower, flood protection and recreational purposes. Lake regulation requires a legal regulation permit, which in many cases includes upper and lower regulation limits for water levels. Often these limits include a mandatory lowering of water levels at certain set dates in spring to make room for the snowmelt flood. Temperature increases projected by climate change scenarios will, however, change the seasonality of runoff and cause spring floods to decrease and occur earlier. Many of the current regulation permits will no longer function properly in these changed conditions and as much as half of the regulation permits may need revision due to climate change (Silander *et al.*, 2006).

The Finnish Environment Institute's Watershed Simulation and Forecasting System (WSFS) (Vehviläinen *et al.*, 2005) was used to simulate the impacts of climate change on hydrology and lake regulation (Veijalainen *et al.* 2010a). The simulations were performed in several lakes in 12 watersheds in different parts of Finland with an ensemble of

climate scenarios for 2010–39, 2040–69 and 2070–99, using the control period 1971–2000. The observed temperatures and precipitations of the control period were changed using the Delta-change approach.

Different regulation practices were simulated in the WSFS by use of operating rules, whereby a specific water level at a certain time of the year corresponds to known outflow. In the reference period the operating rules corresponded on average to the current regulation practices. The climate change simulations were carried out with the similar operating rules as in the reference period and additionally with modified regulation. The modified operating rules took the changed climate with shorter and wetter winters better into account and assumed milder and earlier lowering of water levels during winter and spring. Figure 6.10 shows an example from Lake Höytiäinen where the current regulation limits are broken during spring with the modified regulation to avoid low water levels in summer.

The results show that changes of runoff cause the current regulation practices with a winter and spring lowering of water levels to function poorly on many lakes. In large lakes in southern and central Finland, the largest challenges in the future will be autumn and winter floods and occasional summer dryness. To adapt to these changes and to decrease the negative effects of climate change, many of the regulation practices and limits have to be changed (Figure 6.10). In northern Finland, the changes in seasonality are smaller, since snowmelt floods remain the largest floods and, therefore, the changes required in regulation practices are less dramatic.

The new regulation permits and limits should be flexible enough to function properly in a variety of conditions. Winters with large amounts of snow will still occur even in southern and central Finland during 2010–39, which means that storage space for spring snowmelt floods may still be required. On the other hand, winters with low snow accumulation and large runoff will become more common and the new regulation practices should take this into account. Decreasing and earlier spring floods and longer and warmer summers increase the risk of low water levels in summer and early autumn, and therefore the lakes should be high enough before summer.

The mild winters of 2006–2008 already demonstrated that in southern Finland some of the regulation permits are not suitable for warmer conditions. Therefore, it is important to assess the suitability of the current regulation permits and practices in future conditions to avoid situations where unsuitable regulation will aggravate problems caused by climate change.

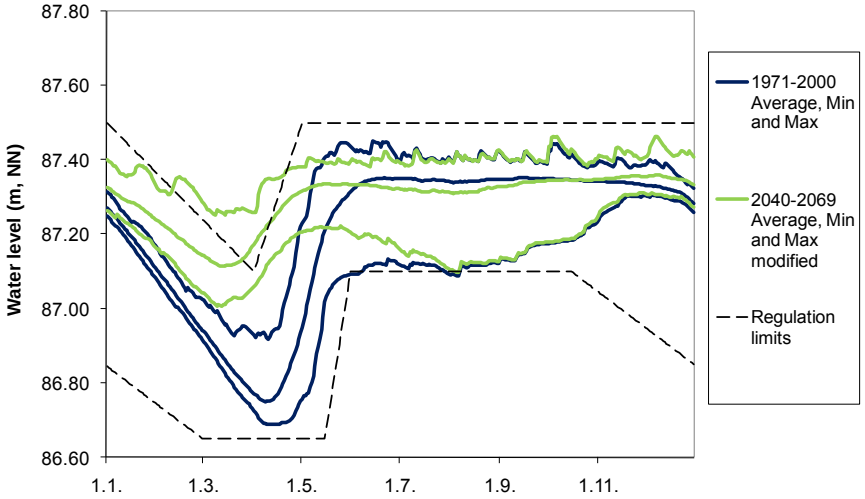

Figure 6.10. Average, minimum and maximum water levels in Lake Höytiäinen within the Vuoksi watershed in eastern Finland. Shown are data from the reference period 1971–2000 and a projection for 2040–69 assuming the modified regulation rules. The climate scenario used is an average from 19 global climate models employing the A1B emission scenario.

6.6 Extreme floods and dam safety

Design flood determination is one of the most important questions in scientific hydrology. The situation is now even more delicate due to the prospect of global warming, creating new challenges for the hydroelectric power industry. Large investments are made to upgrade dams to comply with the current safety requirements. At the same time, it is realised that the hazards associated with global warming cannot be ignored. However, existing regional climate scenarios continue to vary over a wide range, especially in the case of extreme precipitation within areas as small as a catchment area. This calls for special care in the interpretation of climate modelling results from a dam safety point of view. It is also recognized that new climate calculations will most likely appear as science advances and a new attitude must be developed by the dam owners to deal with this moving target. A new dimension has arrived in dam safety philosophy and work.

The fundamental questions asked are:

- What will be the combined effects on dam safety of more irregular winters, altered snow conditions, altered precipitation and altered evaporation?
- How is the best use to be made of scenarios from meteorological climate models in order to calculate the effects on design floods?
- What is the magnitude of the uncertainty in scenarios?

The national standards for analysis of dam safety differ widely between the Nordic and Baltic countries. But normally both the 100-year flood and a more extreme design value are of interest depending on the classification of the dams. In the following sections, both these aspects are addressed. An intercomparison is also carried out between Norway, Sweden and Finland and is presented separately in section 6.7.

6.6.1 Changes in the 100-year floods in Finland

Climate change impacts on 100-year floods in Finland by 2010–2039 and 2070–2099 were estimated to gain a general overview on national scale impacts (Veijalainen *et al.*, 2010b). These results can be used to assess dam safety on lower risk dams and in planning flood risk assessments for the EU flood directive.

Changes in floods were evaluated at 67 sites in different part of Finland with runoff-areas ranging from 86 to 61,000 km^2. The hydrological simulations were performed with a HBV-type conceptual hydrological model within the Watershed Simulation and Forecasting System (WSFS) (Vehviläinen *et al.*, 2005). Altogether 20 climate scenarios from both global and regional climate models and with different emission scenarios were used with the delta change approach. The 100-year floods in the reference period 1971–2000 and in 2010–2039 and 2070–2099 were estimated with frequency analysis using the Gumbel distribution.

According to the results, the 100-year floods in Finland will decrease on average by 8–22% in 2070–2099 compared to the reference period, but variation between different sites and hydrological regions will be significant (Figure 6.11). In northern and central Finland, where snowmelt-floods are the largest floods, annual floods will decrease or remain unchanged due to decreasing snow accumulation in winter. On the other hand, increased precipitation especially in autumn and winter will result in increasing floods in large central lakes and their outflow rivers in central Finland. Changes in snow accumulation and melt and their importance in flood generation explain the changes in flood behaviour. A significant shift is predicted to take place in the seasonal distribution of runoff and floods with increasing magnitude of autumn and winter floods and decreasing magnitude of spring floods, especially in southern and central Finland. Scenarios imply that floods will decrease at most sites, but an increase is predicted in some of the most important flood hazard regions with high potential damages.

The results demonstrate that even within a relatively small area like Finland, the impacts of climate change on floods can vary substantially due to regional differences in climatic conditions and watershed properties. Important explanatory variables in the changes of floods include many hydrological and climatological characteristics such as the timing of floods, importance of snowmelt-floods, snow water equivalent, winter temperature, latitude, lake percentage and watershed size. These varia-

bles can explain most of the average changes at different sites and their explanatory power improves when applied separately to different hydrological regions. The uncertainties included in flood and climate change studies are, however, still considerable and in many sites the range produced by the 20 climate scenarios was large.

6.6.2 Changes in the 100-year floods in Norway

The three recommended CES climate projections (Kjellström *et al.*, this volume) and the hydrological modelling strategy described in the subsection *A Norwegian example* in section 4 of this chapter, were used for studying the impacts of climate change on 100 year floods in the 21st century in Norway.

Runoff changes in Norway are strongly linked to changes in the snow regime. Snow cover will be more unstable and all three scenarios indicate increase in winter and autumn runoff in areas where the snow cover has a major impact on runoff in the control climate. These results are caused by the combined effects of higher temperature and more precipitation in winter in the scenario climate. Reduced snow cover leads to smaller snow melt floods, while increased precipitation where a larger proportion falls as rain will increase rain floods, and possibly also combined snow melt and rain floods (Beldring *et al.*, 2008).

Figure 6.12 and Figure 6.13 illustrate the long term variability of 100-year floods for two Norwegian catchments based on the Gumbel distribution using running 30 year periods. The Tora catchment is located at elevations 717–2006 m a.s.l. in a mountain region in the north-western part of southern Norway, while catchment Gryta is located at elevations 163–438 m a.s.l. in the forest region in the south-eastern part of southern Norway. Due to the large precipitation increase in western Norway, the high elevation catchment Tora will experience an increase in 100-year floods caused by the effect of more severe combined snowmelt and rain floods. The 100-year floods in the catchment Gryta will not increase to the same extent because the precipitation increase projected for south-eastern Norway is moderate, and there will be a shift in the flood regime towards less influence of snowmelt floods.

The results for the two catchments shown in Figure 6.12 are similar to those obtained in an investigation of projected changes in the 200-year flood in 115 catchments distributed throughout Norway (Lawrence, 2010). In that study, catchments located in western Norway and along much of the coastal zone throughout Norway have the largest projected increases in the magnitude of the 200-year flood, whereas more inland catchments dominated by snowmelt floods are less vulnerable to this change. There is, however, considerable uncertainty, particularly associated with projections for catchments in areas where snowmelt dominates flooding (Lawrence and Haddeland, 2010).

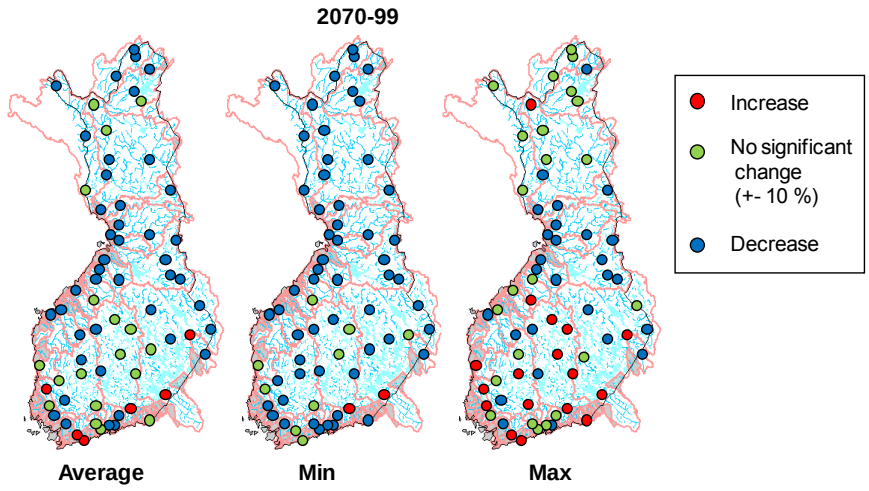

Figure 6.11. The average, minimum and maximum changes in 100-year floods at 67 study sites in Finland. Results for the period 2070–99 are compared to the control period 1971–2000.

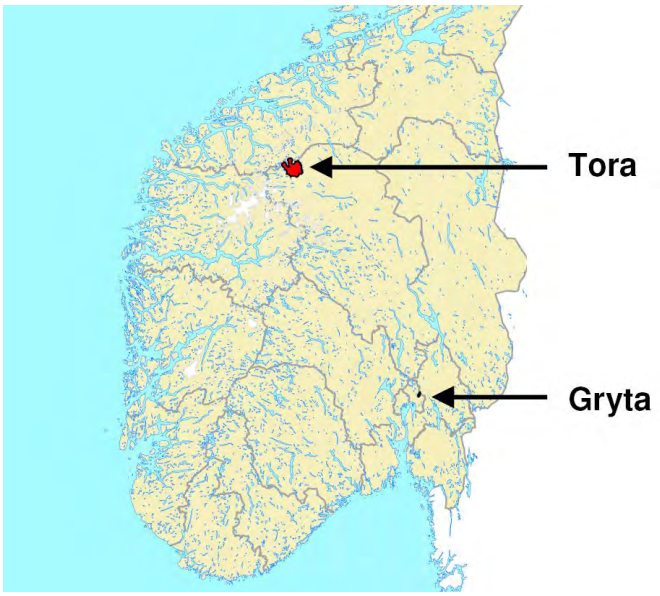

Figure 6.12. The catchments Tora (263 km²), located in a mountainous region in the north-western part of southern Norway (top) and Gryta (7 km²), located in a forest region in the south-eastern part of southern Norway (bottom). Both are used in this study to exemplify changes in 100-year floods.

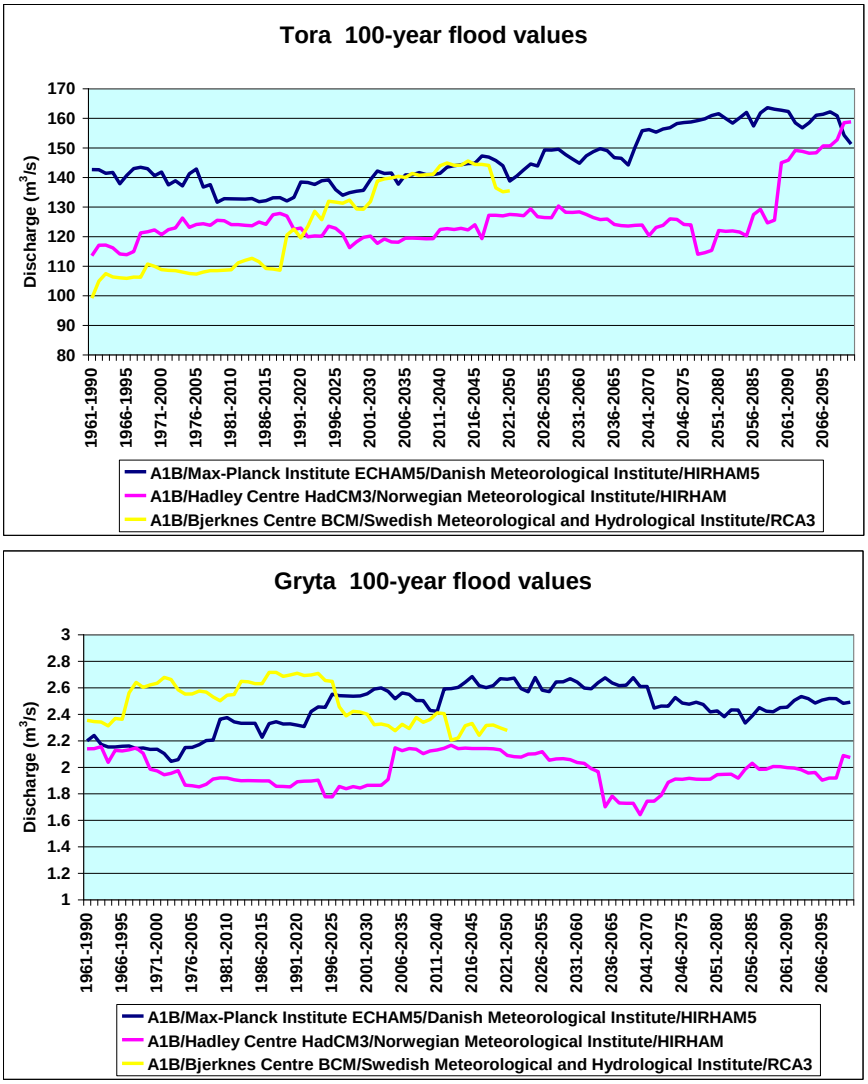

Figure 6.13. 100-year flood values based on data for running 30 year intervals for the climate projections A1B/Max-Planck Institute ECHAM5/Danish Meteorological Institute/HIRHAM5, A1B/Hadley Centre HadCM3/Norwegian Meteorological Institute/HIRHAM, and A1B/Bjerknes Centre BCM/Swedish Meteorological and Hydrological Institute/RCA3. See locations of the Tora and Gryta catchments in Figure 6.12.

6.6.3 Changes in the 100-year floods in Sweden

Analysis of the 100-year flood is an essential component in the Swedish Guidelines for Design Flood Determination for Dams (Svensk Energi *et al.*, 2007), in particular for less significant dams. Therefore, nationwide climate change impact studies have been made as a foundation for discussion on adaptation strategies. One example of such a simulation is shown in Figure 6.1, but altogether 1001 such simulations are now available nationwide. The results in the form of interpolated maps showing mean change from the reference period 1963–1992 to the scenario period 2021–2050, based on 16 regional climate scenarios and the Distribution Based Scaling (DBS) approach (see section 3) are shown in

Figure 6.14. The frequency analysis is based on the Gumbel distribution function and a moving 30-year window technique.

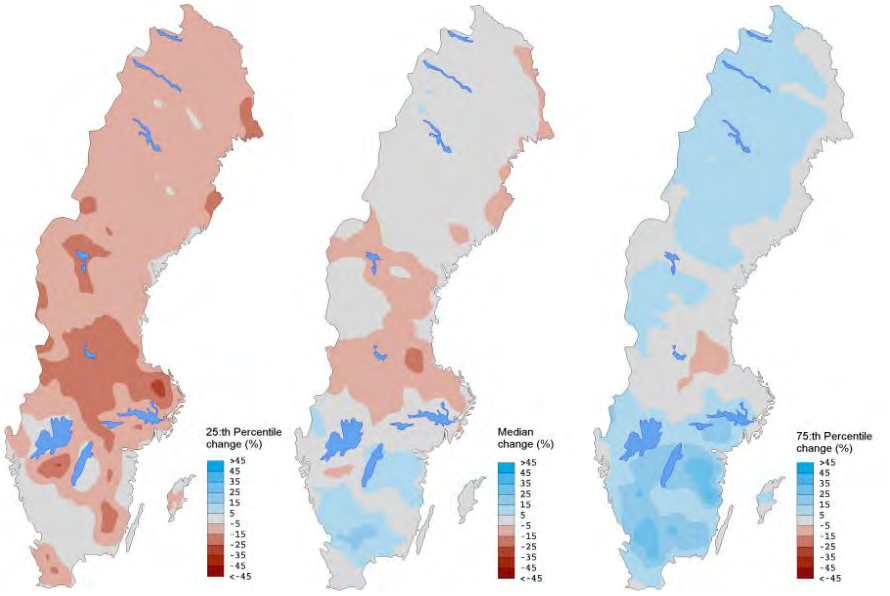

Figure 6.14. Analysis of the median change and percentiles of the change for the 100-year flood in Sweden (%) from the period 1963–1992 until the period 2021–2050. The results are based on 16 regional climate scenarios and the Distribution Based Scaling (DBS) approach in 1001 river basins.

The map in the middle of Figure 6.14 shows that median impacts on the 100-year floods in Sweden are quite variable. In the centre of the country, they tend to go down, mainly due to decreasing snowmelt floods in spring, while rain-fed floods in the south show the opposite tendency. The two percentile maps show, however, that the span of possible outcomes is great when all of the 16 regional climate scenarios available are used.

6.6.4 Impacts on design floods for high hazard dams in Norway

For Norwegian high hazard dams, the flood that a dam must be able to withstand without failure is the probable maximum flood. This inflow flood is calculated by a hydrological model with probable maximum precipitation input and a contribution from snowmelt that depends on the time of the year when maximum precipitation is expected to occur. The probable maximum inflow flood is routed through the reservoir and the outflow flood and reservoir water level is determined. The initial conditions of the hydrological model with respect to soil moisture and groundwater storage and the water level of the reservoir are selected to be as unfavourable as possible with respect to minimization of flood magnitudes and reservoir level.

Results for two Norwegian reservoirs with dams are presented in Figure 6.15. The catchment area of one of the reservoirs is located at elevations between approximately 900 and 1950 m a.s.l. in a mountain region in the north-western part of southern Norway, the other reservoir catchment area is located at elevations between approximately 300 and 550 m a.s.l. in a forest region in the south-eastern part of southern Norway. In both catchments, probable maximum precipitation occurs during autumn. The flood calculations that have been approved for these reservoirs and dams were used as the basis for this study.

In order to determine the projected change in probable maximum precipitation for durations of 6, 24, 48 and 72 hours for the catchments draining to these reservoirs, the results from a study by the Norwegian Meteorological Institute (Engen-Skaugen and Førland, 2010) were applied. Probable maximum precipitation was determined for the control climate 1961–1990 and the future climate 2021–2050, using the A1B emission scenario and the Max-Planck Institute ECHAM5 model downscaled by the Danish Meteorological Institute with the HIRHAM5 regional climate model. In this study, the data was downscaled to a spatial resolution of 1x1 km^2 on a daily time step using the empirical adjustment procedure developed by Engen-Skaugen (2007).

To modify the snowmelt contributions to the probable maximum inflow floods, snowmelt for the autumn with the same duration as the approved flood calculations and a return period of 30 years was determined based on HBV model simulations. The relative change in probable maximum precipitation based on the results from the Norwegian Meteorological Institute and the absolute change in daily snowmelt with the return period 30 years were used to modify the flood calculations that have been approved for these two reservoirs and dams. All other conditions in the approved flood calculations were kept unchanged.

Figure 6.15 shows the inflow flood based on probable maximum precipitation input with contribution from snowmelt, and the subsequent outflow flood after routing through the reservoir for the two sites. The high mountain catchment will experience both a large increase in probable maximum precipitation and the amount of snowmelt. These results are caused by the combined effects of more precipitation and higher temperature in the autumn in the projected climate, while temperatures still remain below the freezing point for sufficiently long periods to allow snow to accumulate. The lowland forested catchment on the other hand, will experience a minor increase in probable maximum precipitation and a decline in the amount of snowmelt. Although precipitation will increase in the projection period in the lowland catchment, these changes are moderate. Higher temperatures will reduce the snow storage in the autumn with an impact on the amount of snowmelt.

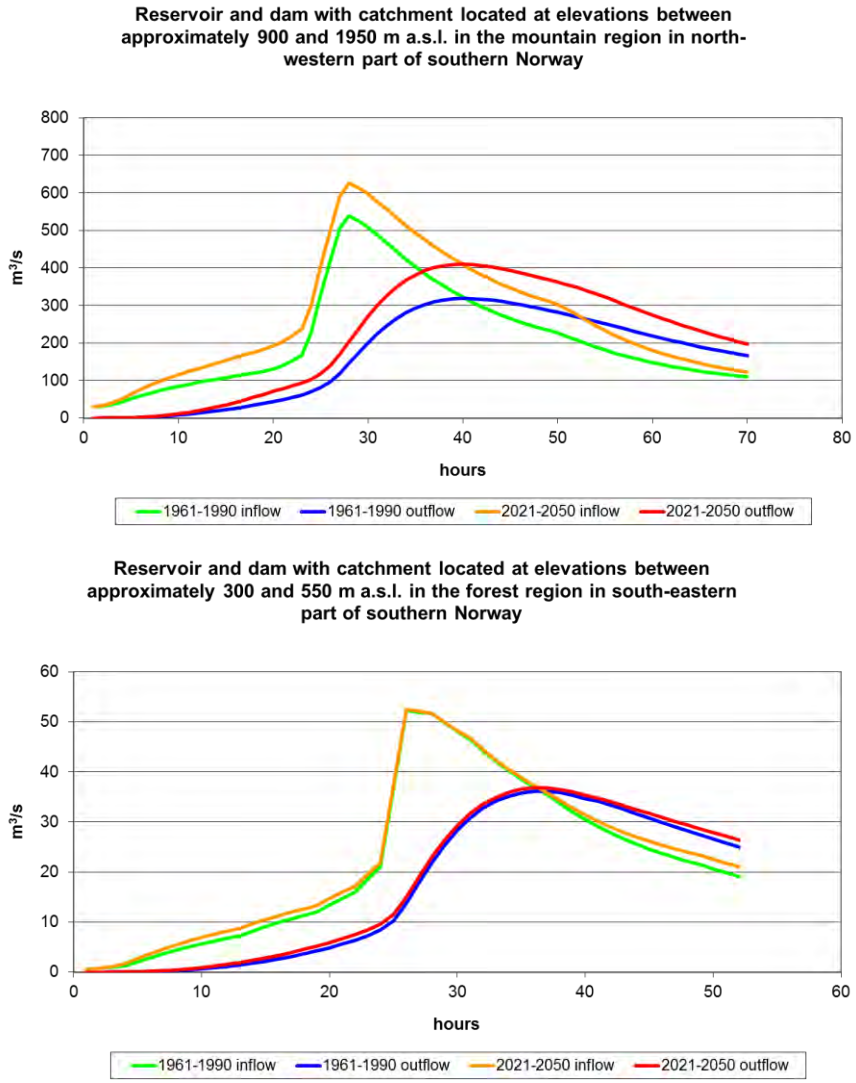

Figure 6.15. Inflow flood based on probable maximum precipitation input with contribution from snowmelt, and the subsequent outflow flood after routing through a reservoir. Reservoir and dam with catchment located at elevations between approximately 900 and 1950 m a.s.l. in a mountain region in the north-western part of southern Norway (top). Reservoir and dam with catchment located at elevations between approximately 300 and 550 m a.s.l. in a forest region in the south-eastern part of southern Norway (bottom).

6.6.5 *Impacts on design floods for high hazard dams in Sweden*

The simulation scheme for design flood determinations in Sweden was developed in the 1980s when it became obvious that the criteria then in use were obsolete. In a recent new edition of the guidelines (Svensk Energi *et al.*, 2007) it is prescribed that climate change shall also be considered in the design studies. This has led to a research project with the aim to analyse possible impacts of climate change on the design floods and to find means to account for climate change in future design studies.

A number of drainage basins and dams, relevant for the power industry and the mining industry, have been selected for the studies of climate change impacts on design floods. In these basins, floods are calculated using the available regional future climate scenarios. Focus for the design studies in a changing climate is on the first half of the 21st century, but simulations are also made until the year 2100.

Figure 6.16 shows one example of simulations for the Seitevare dam in upper River Luleälv in the far north of the country. Shown are changes in the major components of a design simulation for high hazard dams (Design Flood Category I, according to Swedish guidelines). The end result is represented by the bars to the far right denoted *"Design W"*. They show impacts on the design level of the reservoir according to the regional climate scenarios.

Results so far show that global warming may have great significance for dam safety, flood risks and the production of hydroelectric power in Sweden. The milder and more unstable winters in the future also means that there is a risk that spill will be released more often. This affects both dam safety and the lives of those who live along the rivers. Higher winter flows are at the same time beneficial to the production of hydroelectric power.

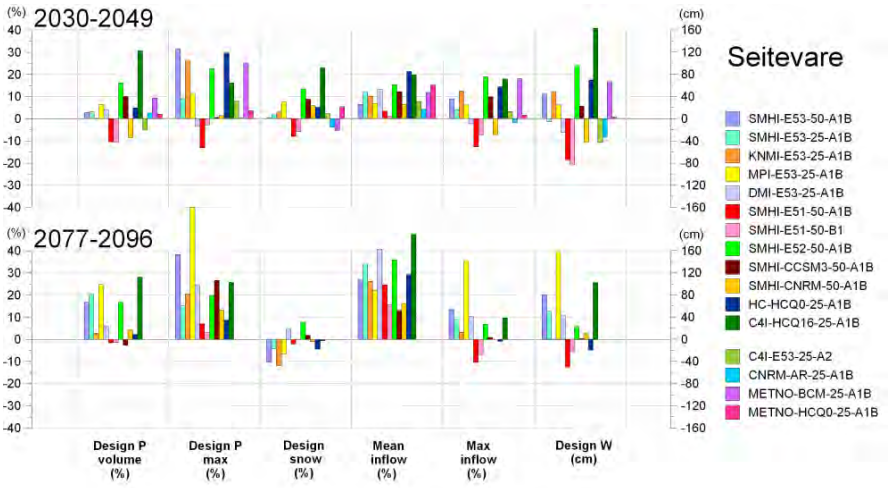

Figure 6.16. Changes in the main components of a design flood simulation for the Swedish high hazard dam Seitevare, based on several regional climate scenarios. Shown are design precipitation (Design P), design snowpack (Design snow), and calculated mean and max inflow according to the Swedish guidelines for design flood determination. "Design W" denotes changes in the design level of the reservoir.

6.7 A Nordic intercomparison of design flood standards

Various methods for estimating the magnitude and likelihood of low frequency, extreme flooding are used in analyses for evaluating dam safety in the Nordic countries. Within the CES project, a comparison of the methods currently used in Finland, Norway and Sweden was undertaken. This comparison particularly considered the application of these methods in an assessment of climate change impacts, based principally on the CES climate scenarios.

All three countries use a combination of flood frequency analyses and design flood simulations to meet requirements for assessing flood risks under the current climate for assessing the safety of reservoirs and dams of various risk classes (Working group for the Dam safety Code of Practice, 1997; Svensk Energi *et al.*, 2007; NVE, 2009). The comparison, therefore, considered a) flood frequency analyses, as applied to simulated daily discharge series from hydrological models based on input data from climate scenarios, and b) design flood simulations, based on similar input climate data, further processed according to the requirements for the procedure in each country.

In all cases, input precipitation and temperature series for the simulations cannot be taken directly from RCM output, but must be further adjusted to local conditions prior to use in hydrological modelling. This is done by applying the Delta-change method, the DBS approach, or the Empirical adjustment procedure.

The procedures used for this adjustment vary between the Nordic countries, as do the source RCMs for which adjusted data are available. The comparison presented here, therefore, considers the question: Given the methods and data currently available in practice in each of the three countries, how similar are the estimates of the impact of climate on large magnitude, low frequency flooding, which are derived from the various procedures? Two transboundary catchments were used for the comparison: Tana River at Polmak (Finland and Norway) and Muonio River at Muonio (Sweden and Finland). In addition, comparisons between Norwegian and Swedish methods were made based on two catchments located in a similar area near the boundary: Nybergsund (Norway) and Höljes (Sweden). All four catchments are located in areas where seasonal snowmelt makes a significant contribution to annual maximum flows.

6.7.1 100-year floods

The 100-year flood was used as the common basis for comparing results based on flood frequency analysis. In this application, flood frequency analysis was undertaken on simulated (rather than historical) daily data, and the Gumbel extreme value distribution was used for estimating re-

turn periods. Estimated changes in the 100-year flood between a reference period and the CES 2021–2050 scenario period are given in Table 6.1 for each of the catchments. The different estimates for the individual catchments are in general consistent in terms of the projected sign of the expected change. In most cases, a decrease is projected, due to changes in snow storage leading to a decrease in the contribution of snowmelt to peak flows.

There are, however, significant differences between the results for the different scenarios for each catchment. In addition, projections based on the Delta-change method tend to indicate larger decreases than with the bias correction type methods used in Norway and Sweden, and in some cases, increases in the magnitude of the 100-year flood are projected. The estimated percentage change also varies considerably with the particular 30-year period evaluated, as the fit of the extreme value distribution is sensitive to individual events. This variation was previously illustrated in Figure 6.1 for the Höljes catchment for each of the 16 scenarios considered for the period 1992–2100.

Table 6.1. Percentage change in the 100-year flood for catchments used in the comparison of Nordic design flood standards.

	Polmak (14157 km^2)	Muonio (9259 km^2)	Nybergsund (4420 km^2)	Höljes (6001 km^2)
SYKE (Finland)[1]				
DMI-Echam5	–15	–12		
Met.no-Hadley	–17	–11		
SMHI-BCM	–22	–12		
NVE (Norway)[2]				
DMI-Echam5	–10/+33		–33/–2	
Met.no-Hadley	–26/–12		–24/+5	
SMHI-BCM	–35/–30		–13/–2	
SMHI (Sweden)[3]				
DMI-Echam5		–5		–1
Met.no-Hadley		–11		–31
Median of 16		–3		–6
Maximum of 16		+11		+15

[1]SYKE calculations are based on reference period 1961–1990 as compared with 2021–2050. The delta change method was used to adjust P,T data from RCMs.

[2] NVE calculations are based on reference period 1961–1990 as compared with 2021–2050. Two methods are used to adjust P,T data: Delta change (first number given) and empirical adjustment (second number). Values given are the median based on simulations with 25 different HBV parameter sets.

[3]SMHI calculations are based on reference period 1963–1992 as compared with 2021–2050. The DSB method was used to adjust P,T data. Results are also given for the median of 16 scenarios representing differing GCM/RCM combinations.

6.7.1 Design floods for high hazard dams

The methods used in each country for simulating design floods were also used to estimate possible changes in the design flood between reference and future periods. Finland and Sweden use a design precipitation based approach in which the design flood is produced by combining the design

precipitation with other critical weather and catchment conditions (Svensk Energi *et al.*, 2007; Veijalainen and Vehviläinen, 2008).

In the method used in Finland for estimating extreme floods, design precipitation is combined with 30 years weather data to find the most critical timing of the design precipitation, which produces the largest flood (Veijalainen and Vehviläinen, 2008). This flood is considered to be the design flood and it should have a return period of approximately 5000–10000 years, which corresponds to the design criteria for high hazard dams in Finland (Working group for the Dam safety Code of Practice, 1997). The method is based on the Swedish design flood calculation method for large dams (Svensk Energi *et al.*, 2007), but the Swedish guidelines have been modified to be better suited for the Finnish conditions and dam safety rules. The design floods for 2021–2050 were simulated by changing the temperature and precipitation of the 30 year period using the delta-change approach and three different climate scenarios and changing the design precipitation according to two projections. The delta change approach also includes a temperature dependant component in the temperature change (Andréasson *et al.*, 2004) to take into account the different changes in different parts of the temperature distribution. The projections for design precipitation change by 2021–2050 were estimated seasonally based on the daily RCM data. The "smaller" change in design precipitation was the average change from eight RCM scenarios and the "larger" change was the 90th percentile of the same scenarios.

Design flood estimations for the probable maximum flood in Norway are usually based on the application of an event-based simulation using a simple three-parameter hydrological model, PQRUT (described in NVE, 2009). This model is run on an hourly timestep and uses estimates for the probable maximum precipitation (PMP) (e.g. Førland and Kristoffersen, 1992) as input. A snowmelt contribution can also be added to the input, but in practice, for catchments as large as those considered here, the application of a full HBV model is more suitable for simulating snow storage and release. Therefore, for the purposes of this comparison, two methods were applied to the Norwegian catchments: 1) an event-based hourly simulation using PQRUT; and 2) an application of HBV with a daily timestep, in which the PMP sequence was used to replace the input precipitation for a 20-day period during the snowmelt season each year. Estimates for PMP for the scenario data were calculated from gridded scenario data (adjusted from RCMs using the empirical adjustment method) by the methods described in Alfnes (2007).

A comparison of the results obtained for the different catchments using the various methods is given in Table 6.2. The results for Polmak and Muonio estimated by SYKE highlight the differences resulting from the use of a design precipitation reflecting the average of eight scenarios *vs*. the more extreme case representing the 90th percentile of the range of scenarios. This is further illustrated in Figure 6.17, which displays the simulations with the largest and smallest changes in peak discharge,

relative to the design flood for the control period. The results for Polmak and Nybergsund (Figure 6.18) calculated by NVE emphasise the impact of including changes in patterns of snowmelt in the simulation of the probable maximum flood (PMF). In those cases, the small positive changes reported for the event-based PQRUT simulations directly reflect the increases in estimated PMP for all three scenarios in these catchments. The HBV modelling for Polmak, however, points towards a decrease in the PMF for two of the scenarios, and the estimated changes are very similar to those obtained by SYKE using the average (i.e."smaller") value for the design precipitation sequence.

Table 6.2. Percentage changes in the design flood for high hazard dams for catchments used in the comparison of Nordic design flood standards.

	Polmak (14157 km^2)		**Muonio (9259 km^2)**		**Nybergsund (4420 km^2)**		**Höljes (6001 km^2)**
SYKE (Finland)1	Design precip. Smaller	Design precip. larger	Design precip. smaller	Design precip. Larger			
DMI-Echam[5]	–7	–1	–12	–2			
Met.no-Hadley	–8	+1	–10	–3			
SMHI-BCM	–10	–3	–11	–4			
NVE (Norway)[2]	PQRUT	HBV			PQRUT	HBV	
DMI-Echam[5]	+5	+6			+3	+11	
Met.no-Hadley	+10	–10			+2	–7	
SMHI-BCM	+8	–10			+3	+8	
SMHI (Sweden)[3]							
DMI-Echam[5]							–2
Met.no-Hadley							–21
Median of 16							–5
Maximum of 16							+15

- [1]SYKE calculations are based on reference period 1961–1990 as compared with 2021–2050. The delta change method was used to adjust P,T data from RCMs. Results are for design precipitation estimated from eight scenarios where "smaller" refers to the use of the average of the 8 scenarios, and "larger" to the use of the 90th percentile
- [2] NVE calculations are based on reference period 1961–1990 as compared with 2021–2050.PQRUT simulations only consider changes in PMP for a single 480-hour event. HBV modelling simulates the entire period and the 480-hour PMP event is used to replace the input precipitation for 20 days during the snowmelt period
- [3]SMHI calculations are based on reference period 1971–1990 as compared with 2030–2050. Results are also given for the median and maximum of 16 scenarios representing differing GCM/RCM combinations

A comparison between the two methods applied by NVE for Nybergsund are illustrated in Figure 6.18 for one scenario. In this case, the PQRUT model again indicates a small increase in the magnitude of the peak flow, whereas a decrease is projected based on the HBV model, which includes changes in snow storage and melting between the two scenario periods. Overall, the absolute magnitude of the peak flow tends to be larger for

simulations based on PQRUT. This is due to the simplicity of the PQRUT model, which is based on three parameters estimated from regional empirical formulas, generated for use in catchments generally much smaller than those considered here. The changes in the design flood estimated by SMHI for Höljes show some agreement with those obtained for Nybergsund, in that the results obtained by NVE are all within the range of the 16 simulations undertaken for Höljes. Values for Höljes, however, generally suggest a decrease in the design flood, whereas five of the six estimates for Nybergsund indicate a small increase.

The comparison of the methods suggests that differences in the climate scenarios considered, the methods used for adjusting RCM output to a local scale, and whether or not and by which methods changing patterns of snowmelt are taken into account, all contribute to differences in design flood estimates between the three countries. The results indicate that the delta change approach generally produces larger decreases for snow and flood magnitudes than the use of direct bias corrected daily RCM data. This is mainly due to larger increases in high winter temperatures in this method, which lead to smaller amounts of snow accumulation. However, even with the same method and model and in the same catchment, different climate scenarios can produce markedly different results.

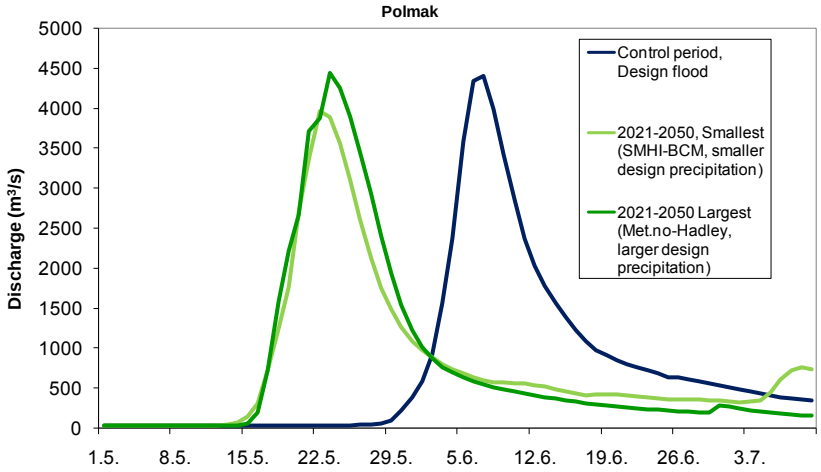

Figure 6.17. The design flood in Polmak in the control period 1961–1990 and in the smallest and largest design floods in 2021–2050. The smallest design flood is produced with the smaller change in design precipitation and SMHI-BCM scenario and the largest design flood with the larger change in design precipitation and Met.no-Hadley scenario.

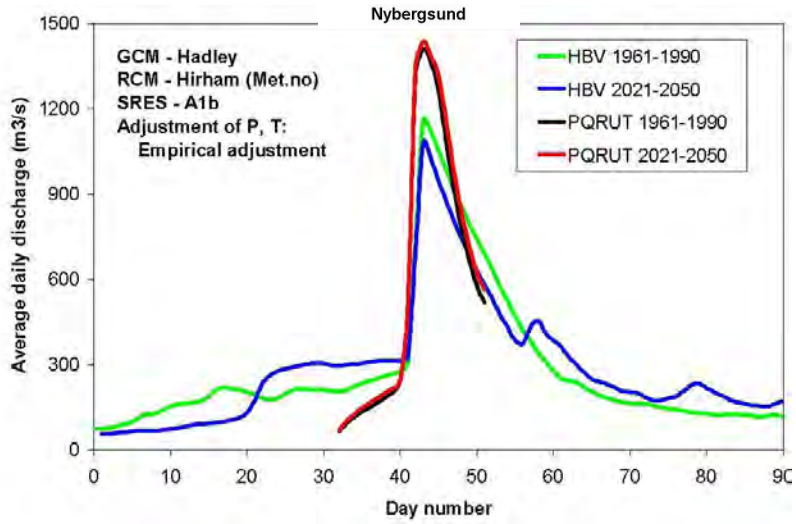

Figure 6.18. Comparison of estimation of the probable maximum flood (PMF) using the PQRUT model with 20-day probable maximum precipitation (PMP) sequence and the HBV model with the PMP sequence and full snow storage and melting routines. The comparison is based on one climate scenario. Results for other scenarios are given in Table 6.2.

6.8 Discussion and conclusions

There is little doubt that the Nordic and Baltic hydropower systems will be affected strongly by a changing climate. Production volumes will change differently from one region to another and seasonalities will alter as winters are becoming milder and wetter. The results also show that there is considerable uncertainty as regional climate scenarios vary greatly and the chosen methodologies, for example in the downscaling of climate simulations, have different effects on both volumes of water and floods.

The hydrological simulations have generated a large amount of data on projected changes of runoff for the Nordic-Baltic region. The results show that the potential for hydropower production will generally increase, although water shortage may become a problem in some locations for the summer season. Given earlier snowmelt and reduced snow storage, the occurrence of large snowmelt floods is likely to become more seldom. The combined effect of increase in the rainfall intensities, number of rainfall events and total rainfall volume will most likely provide conditions that may be expected to yield larger rain floods.

There are many sources of uncertainties in the hydrological impact projections; in the climate modelling, the method used for transferring the climate change signal to meteorological station sites and in the hydrological modelling. The hydrological climate change projections presented in this report are based on climate projections from several different combinations of emission scenarios for greenhouse gases, global climate models, regional climate models and methods for transferring

the climate change signal to hydrological models. Nevertheless, a comparison between the annual and seasonal hydrological projections shows general similarities.

The difference between different climate scenarios is particularly large when it comes to impacts on design floods. The floods can either increase or decrease depending on how changing precipitation patterns interact with modified snowmelt conditions. It is, therefore, crucial to use more than one climate scenario in this type of studies. One key finding is also that the national guidelines for determination of design floods show different sensitivity to simulated climate change. This needs more attention since there is a growing demand for climate impact studies in dam safety analysis.

The CES-project has demonstrated that the choice of regional climate scenarios is a crucial factor in any impact study. So far this choice has been rather arbitrary. In some cases the simple strategy has been to use those scenarios which for the time being are easily available. This means that the used ensemble of scenarios is not a systematic mix of global climate models, emission scenarios, regional models and in a few cases, initial conditions. For future work more attention has to be given to this issue so that the used ensemble of regional climate scenarios is as unbiased as possible and covers a reasonable spread of future developments. It is certainly a challenge to provide such an ensemble of regional climate scenarios and to develop an adaptation strategy that can handle the fact that the output from the ensembles will always represent a moving target.

The model simulations have not considered land use or vegetation changes caused by climate change or human transformation of the land surface. However, it is likely that changes in land cover may interact with climate, leading to different projections of future hydrological conditions due to feedback effects involving the land surface and the atmosphere. The uncertainty of hydrological climate change impact simulations increases due to the lack of consideration of possible land use and vegetation changes.

Evaporation is an important part of the hydrological cycle. On average, approximately one third of the precipitation falling in the Nordic countries is lost to the atmosphere as evaporation, while the remaining fraction discharges to the ocean. The hydrological model calculates potential evaporation using a temperature index approach for the control and projection climates. Although this is a common parameterisation procedure in hydrological models, it may not be valid under changed climate conditions as transpiration from plants depends on several factor like wind, humidity, radiation and ambient air CO_2 concentration which may influence the feedback between the land surface and the atmosphere. Neither does transpiration depend linearly on temperature. However, the effects of these changes are uncertain.

6.9 Acknowledgments

The Finnish research on climate change and hydrology has been financed by the Finnish Ministry of Agriculture and Forestry (WaterAdapt-project) and the Finnish Academy (The Future of Floods in Finland-project). The Icelandic study was carried out as a part of the project "Loftslagsbreytingar og áhrif þeirra á Orkukerfi og Samgöngur" (LOKS) funded by the National Power Company of Iceland, the National Energy Fund of Iceland, the Ministry of Industry and the National Energy Authority. The research on climate change impacts on water resources in Norway has received support from Norwegian Water Resources and Energy Directorate and Energy Norway, formerly Norwegian Electricity Industry Association. The Swedish research on climate change and design floods is financed by the Swedish dam safety authority (Svenska Kraftnät) and the power industry via Elforsk.

The Lithuanian authors would like to thank Dr. Egidijus Rimkus and Dr. Justas Kažys at Vilnius University for climate scenarios data for the Lithuanian territory and Marco Ratto for help using the GLUE technique.

The regional climate scenarios for this work have been provided by the ENSEMBLES project in co-operation with the CES scenario group and the Rossby Centre at SMHI.

6.10 References

Alfnes, E. (2007). Ekstremnedbør beregnet fra serier med gridbasert areanedbør. (Extreme precipitation estimated from series with grid-based areal precipitation). Met.no Report 1/2007, 22 pp.

Andréasson, J., Bergström, S., Carlsson, B., Graham, L., Lindström, G. (2004). Hydrological change – climate change impact simulations for Sweden. *Ambio*, 33, 228–234.

Beldring, S., Engeland, K., Roald, L.A., Sælthun, N.R., Voksø, A. (2003). Estimation of parameters in a distributed precipitation-runoff model for Norway. *Hydrology and Earth System Sciences*, 7, 304–316.

Beldring, S., Engen-Skaugen, T., Førland, E.J., Roald, L.A. (2008). Climate change impacts on hydrological processes in Norway based on two methods for transferring regional climate model results to meteorological station sites. *Tellus* 60A, 439–450. doi: 10.1111/j.1600-0870.2008.00306.x

Bergström, S. (1995). The HBV model In: *Computer Models of Watershed Hydrology*. Water Resources Publications, Highlands Ranch, Colorado, 443–476.

Bergström, S., Jóhannesson, T., Aðalgeirsdóttir, G., Andreassen, L. M., Beldring, S., Hock, R., Jónsdóttir, J. F., Rogozova, S., Veijalainen, N. (2007). *Hydropower*. In: *Impacts of Climate Change on Renewable Energy Sources - Their role in the Nordic Energy system.* Report Nord 2007:003. Fenger, J. (ed.).

Beven, K.J. and Binley, A.M. (1992). The future of distributed models: model calibration and uncertainty prediction. *Hydrological processes*, 6, 279–298.

Einarsson, B. and Jónsson, S. (2010a). The effect of climate change on runoff from two watersheds in Iceland. Reykjavík, Icelandic Meteorological Office, Report 2010-016.

Einarsson, B. and Jónsson, S. (2010b). Improving groundwater representation and the parameterization of glacial melting and evapotranspiration in applications of the WaSiM hydrological model within Iceland. Reykjavík, Icelandic Meteorological Office, Report 2010-017.

Engen-Skaugen, T. (2007). Refinement of dynamically downscaled precipitation and temperature scenarios. *Clim. Change,* 84, 365–382. DOI:10.1007/s10584-007-9251-6

Engen-Skaugen, T. and Førland, E.J. (2010). Future change in return values and extreme precipitation at selected catchments in Norway, Met.no Report 2010.

Førland, E.J. and Kristoffersen, D. (1989). Estimation of extreme precipitation in Norway. *Nordic Hydrology,* 20, 257–276.

Jóhannesson, T. (2010). Sviðsmynd um loftslagsbreytingar á Íslandi fyrir jökla- og vatnafræðilega líkanreikninga í CES og LOKS verkefnunum. (Climate change scenarios for Iceland for glaciological and hydrological modelling in the CES and LOKS projects). Icelandic Meteorological Office, Memo-TóJ-2010-02.

Kjellström, E. (2010). Deliverable 4.3: Report on user dialogue and analysis of regional climate scenarios for northern Europe. The CES-project, technical report, final version delivered 15 April 2010.

Kriaučiūnienė, J., Meilutytė-Barauskienė, D., Rimkus, E., Kažys, J., Vincevičius, A. (2008). Climate change impact on hydrological processes in Lithuanian Nemunas river basin. *Baltica,* 21 (1–2), 51–61. ISSN 0067-3064. 2008,

Kriaučiūnienė, J., Šarauskienė, D., Gailiušis, B. (2009). Estimation of uncertainty in catchment-scale modeling of climate change impact (case of the Merkys River, Lithuania). *Environmental Research, Engineering and Management,* 47 (1), 30–39. ISSN 1392–1649.

Lawrence, D. (2010). Hydrological projections for changes in flood frequency under a future climate in Norway and their uncertainties. *In: Hydrology: From Research to Water Management (Ed. by Apsite, E., Briede, A. Klavins, M)* Proceedings of the XXVI NHC, NHP Report No. 51, 203–204.

Lawrence, D. and Haddeland, I. (2010). Uncertainty in hydrological modelling of climate change impacts in four Norwegian catchments. *Hydrology Research* (In press).

Meilutytė-Barauskienė, D., Kriaučiūnienė, J., Kovalenkovienė, M. (2010). Impact of Climate Change on Runoff of the Lithuanian Rivers. In: *Modern climate change models, statistical methods and hydrological modelling.* LAP LAMBERT Academic Publishing. 2010. 68 p.

Nawri, N. and Björnsson, H. (2010). Surface air temperature and precipitation trends for Iceland in the 21st century. Reykjavik, Icelandic Meteorological Office. Report 2010-005.

NVE (2009). Retningslinjer for flomberegninger til § 5–7 i forskrift om sikkerhet ved vassdragsanlegg. (Guidelines for flood estimation). Norwegian Water Resources and Energy Directorate.

Ratto M. and Saltelli, A. (2001). GLUEWIN User Manual, In Model assessment in integrated procedures for environmental impact evaluation: software prototypes, Dec. 2001, IMPACT Project (SCA, DG-IST, 1999-11313), Deliverable 18.

Sennikovs, J. and Bethers, U. (2009). Statistical downscaling method of regional climate model results for hydrological modeling. 18th World IMACS / MODSIM Congress, Cairns, Australia 13–17 July 2009 http://mssanz.org.au/modsim09

Silander, J., Vehviläinen, B., Niemi, J., Arosilta, A., Dubrovin, T., Jormola, J., Keskisarja, V., Keto, A., Lepistö, A., Mäkinen, R., Ollila, M., Pajula, H., Pitkänen, H., Sammalkorpi, I., Suomalainen, M., Veijalainen, N. (2006). Climate change adaptation for hydrology and water resources. FINADAPT Working Paper 6, Finnish Environment Institute Mimeographs 335, Helsinki.

Svensk Energi, Svenska Kraftnät, SveMin (2007). Swedish Guidelines for Design Flood Determination for Dams – New edition 2007.

Vehviläinen, B., Huttunen, M., Huttunen, I. (2005). Hydrological forecasting and real time monitoring in Finland: The watershed simulation and forecasting system (WSFS). In: *Innovation, Advances and Implementation of Flood Forecasting Technology*, conference papers, Tromsø, Norway, 17–19 Oct 2005.

Veijalainen, N., Dubrovin, T., Marttunen, M., Vehviläinen, B. (2010a). Climate change impacts on water resources and lake regulation in the Vuoksi watershed in Finland. *Water Resources Management,* 24 (13), 3437–3459.

Veijalainen, N., Lotsari, E., Alho, P., Vehviläinen, B., Käyhkö, J. (2010b). National scale assessment of climate change impacts on flooding in Finland. *Journal of Hydrology,* 391, 333–350.

Veijalainen, N. and Vehviläinen, B. (2008). The effect of climate change on design floods of high hazard dams in Finland. *Hydrology Research,* 39 (5–6), 465–477.

Working group for the Dam safety Code of Practice (1997). Patoturvallisuusohjeet. (Dam Safety Code of Practice). Publications of Ministry of Agriculture and Forestry 7/1997. Ministry of Agriculture and Forestry. Helsinki. 90 p.

Yang, W., Andréasson, J., Graham, L.P., Olsson, J., Rosberg, J., Wetterhall, F. (2010). Distribution-based scaling to improve usability of regional climate model projections for hydrological climate change impacts studies. *Hydrology Research*, 41 (3–4), 211–229. doi: 10.2166/nh.2010.004

Peer-reviewed publications resulting from work carried out during (or in conjunction with) the CES project, but not referenced in the chapter.

Jónsdóttir, J. F. (2008). A runoff map based on numerically simulated precipitation and a projection of future runoff in Iceland. *Hydrological Sciences Journal*, 53, 100–111.

Olsson, J., Yang, W., Graham, L.P., Rosberg, J., Andréasson, J. (2011). Using an ensemble of climate projections for simulating recent and near-future hydrological change to lake Vänern in Sweden. *Tellus,* 63A, 126–137.

Veijalainen N., Lotsari, E., Alho, P., Vehviläinen, B., Käyhkö, J. (2010). National scale assessment of climate change impacts on flooding in Finland. *Journal of Hydrology*, 391, 333–350.

7. Wind power

*Niels-Erik Clausen, Xiaoli Guo Larsén, Sara C. Pryor and Martin Drews**

*Details on author affiliations are given in the Appendix

7.1 Introduction

Despite the economic crisis in recent years causing a slump in the renewable energy sector in the last quarter of 2008 and throughout 2009 due to a lack of investment capital, wind energy continued its growth. There was a 35% increase in total installed wind energy capacity in 2009, and the average growth during the last five years is 36% (BTM Consult, 2010). The strongest growth rates in 2009 were seen in firstly China and secondly in the USA, with China more than doubling its installed capacity in 2009, advancing to a second place in cumulative installed capacity after the USA. For the second year running, more wind power was installed than any other power generating technology, accounting for 39% of total new electricity-generating installations. In terms of CO_2 emission, Europe's installed wind energy in 2009 helped avoid emission of 106 million t of CO_2 per year, equivalent to removing 25% of all cars in the EU off the roads (EWEA, 2010).

All operating offshore farms except one are situated in northern Europe, i.e. in Denmark, the UK, Sweden, the Netherlands, Germany, Ireland and Belgium. Since September 2009, Norway has a single prototype floating turbine in operation (2.3 MW). By the end of 2009, the offshore market corresponds to 2.7% of the total European wind capacity (2063 MW of installed capacity) and in 2010 1000 MW of newly installed offshore wind capacity in European waters are expected, thus making up around 10% of Europe's annual new wind installation.

The amount of wind power in the Nordic countries at the end of year 2010 was: Denmark 3800 MW, Sweden 2163 MW, Finland 197 MW and Norway 448 MW. Wind power is currently not utilized in Iceland. The production of wind power is expected to grow significantly both on land and offshore in the Nordic region in coming years.

Wind is caused by global and local differences in air temperature and pressure. The most important parameter for wind power is the wind in the lowest part of the atmosphere. Local winds depend on the surface characteristics: terrain, type of surface and nearby obstacles and are always superimposed upon the larger scale wind systems. When larger scale winds are light, local winds may dominate the wind patterns. Thus

changes in global, regional or local temperature fields, in local vegetation and in other factors will affect the wind climate.

The impact of climate change on the average wind speed has been reported earlier (Fenger *et al.*, 2007; Pryor and Barthelmie, 2010). In this chapter, the impact on the extreme wind in the form of the 50-year wind as well as on the so-called strong wind is reported. The extreme wind is an important design parameter for structural design of wind farms on land as well as offshore but also for other infrastructure, e.g. bridges and buildings. Strong wind speeds are important for e.g. the planning of operation and maintenance of wind farms and may occur once or twice a year.

When focussing on rare events like the 50-year wind derived from highly spatially resolved climate projections we face a number of challenges. Thus a major contribution within the CES project has been both to assess possible future wind climates, and also to assess the sources and magnitudes of uncertainties. Further, given that wind climates over the CES domain exhibit high year-to-year and decade-to-decade variability due to natural (or inherent) climate variability, we also sought to quantify how anthropogenically-forced climate change due to increased greenhouse gas forcing might compare with natural variability (see Pryor and Schoof, 2010 and Pryor *et al.,* 2010).

7.2 Extreme wind speeds

Analyses of the Regional Climate Model output from the CES project were conducted with three principal foci;

- To examine possible changes in extreme wind speeds at 10 m.
- To estimate the extreme winds at wind turbine hub height (100 m), and to examine evidence for possible evolution of those extreme wind speeds
- To provide an assessment of strong wind statistics (herein we use the 99th percentile wind speed, but other work has included analysis of the 90th and 95th percentile wind speed (Clausen *et al.*, 2009; Pryor and Schoof, 2010))

In keeping with the Wind Turbine Design standards we use the 50-year return period wind speed as the primary metric of extreme wind speeds. Within the CES project, we also quantified possible changes in wind gust magnitudes, the inter-annual variability of the wind resource and the directional frequency of intense wind speeds (for information regarding these parameters, see Pryor and Schoof, 2010 and Pryor *et al.*, 2010).

In light of high inherent (or internal) variability of wind climates over the study region we seek to examine possible trends in extreme wind climates in the context of natural variability. Thus we examine differ-

ences in extremes in two different temporal windows and examine longer-term tendencies up to the end of this century.

7.3 Model and data

The analysis is based on scenario runs from HIRHAM5 (Christensen *et al.*, 2006), in accordance with the latest reports from the ENSEMBLES project and Pryor *et al.* (2010). HIRHAM5 has a good representation of wind climate. The results used here are from two runs of HIRHAM5, one with the boundary conditions from ERA-40 for the control period 1958–2000 and one with a single set of lateral boundary conditions from ECHAM5 for the A1B scenarios for the period 1951–2099. In the A1B scenario, the greenhouse gas emissions increase until the middle of the 21st century, followed by a decrease until 2099 (Nakićenović and Swart, 2000). The details of these data are given in Table 7.1. The horizontal resolution is about 25 km with a model time step of 10 min. Data for 10 m are saved hourly while data used for the analysis in 100 m height are saved 6-hourly. We also use the reanalysis data ERA-40 for reference.

Table 7.1. Description of the model simulations used for analysis.

Data	Description	Temporal resolution	Horizontal resolution	Period	Heights (m)
HIRHAM5-ERA40	HIRHAM5 runs with forcing from ERA-40	6 hourly	25 km	1958–2000	10, 34, 155
HIRHAM5-ECHAM5	HIRHAM5 runs with forcing from ECHAM5	6 hourly 1 hourly	25 km	1951–2099	34, 155 10
ERA-40	Reanalysis data from ECMWF	6 hourly	250 km	1958–2000	10 m

7.4 Methods

The outputs from HIRHAM5-ECHAM5 represent the past and future projections at a given greenhouse gas emission, while the outputs from HIRHAM5 with forcing from the reanalysis data ERA-40 are assumed to represent the "reality". Thus the results from HIRHAM5-ECHAM5 for the control period, here 1958–2000 (period I), are calibrated through a comparison with results from HIRHAM-ERA40. Accordingly we gain knowledge about the uncertainty in the A1B scenario, first in the control period and then extend this knowledge for the future scenarios.

In order to estimate the winds at the hub height, here defined as 100 m, we use the modeled winds from the two lowest model levels, about 34 m and 155 m, and apply the logarithmic wind law to obtain the winds at 100 m. Since we are only dealing with the strongest winds here, the neutral stability condition is a reasonable assumption. Unfortunately, the winds at 34 and 155 m are saved only every 6 hours. This will intro-

duce an underestimation (bias) of the extreme winds. However, the effects of temporal and spatial resolution will be discussed in a separate section below, where recipes for correcting these effects are introduced and the bias is estimated.

The extreme winds are calculated in terms of the 50-year wind at 10 and 100 m height. The Annual Maximum Method is used. It can be shown that if the tail of the wind distribution is exponential, then the extreme winds have an accumulated probability $F(U)$ that is double-exponential (Gumbel, 1958):

$$F(U) = \exp(-\exp(-\alpha(U - \beta)))$$

From a record of n years (here 43 years for period I, 50 years for period II and 49 years for period III), the annual maximum winds are sorted in ascending order: $U_{max,i}$ where $i = 1, \ldots, n$. We use the above $F(U)$ function to make a fit to $U_{max,i}$ and thus extrapolate the samples beyond the record length to T years. The T-year period is related to $F(U)$ through the following expression

$$T = (1 - F(U_T))^{-1}$$

Thus the T-year wind can be obtained through the above two expressions:

$$U_T = -\alpha^{-1} \ln \ln \frac{T}{T-1} + \beta \approx \alpha^{-1} \ln T + \beta$$

The coefficients α and β are obtained with the Probability-Weighted-Moment procedure (Abild, 1994):

$$\alpha = \frac{\ln 2}{2b_1 - \overline{U_{max}}} \text{ and } \beta = \overline{U_{max}} - \frac{\gamma_E}{\alpha}$$

where $\overline{U_{max}}$ is the mean of $U_{max,i}$, $\gamma_E \approx 0.577216$ is Euler's constant and b_1 is calculated from

$$b_1 = \frac{1}{n} \sum_{i=1}^{n} \frac{i-1}{n-1} U_{max,i}$$

The uncertainty of U_T can be calculated from the uncertainty on α and β and is expressed as:

$$\sigma(U_T) = \frac{\pi}{\alpha} \sqrt{\frac{1 + 1.14k_T + 1.10k_T^2}{6n}}$$

with

$$k_T = -\frac{\sqrt{6}}{\pi}\left\{\ln\ln\left(\frac{T}{T-1}\right) + \gamma_E\right\}$$

This uncertainty reflects the quality of the fitting with the Gumbel distribution. The 95% confidence interval is calculated as 1.96 $\sigma(U_T)$, see details of derivation in e.g. Abild (1994).

7.5 Results

The results are presented below for 10 m height and 100 m height respectively. The parameters used in the two sections are shown in Table 7.2 below.

Table 7.2. Parameters for used for analysis of model simulations

Height over terrain	10 m	100 m
Domain	Northern Europe (0–35°E; 50–70°N)	Europe (-10–35°E; 30–70°N)
Temporal resolution	hourly	6-hourly
Temporal window	1961–1990; 2036–2065	1958–2000; 2001–2050; 2051–2099

7.5.1 Examination of extreme wind speeds at 10-m

Estimates of the 10-m extreme wind speed U_{50} derived from the two HIRHAM5 simulations of the historical period 1961–1990 are highly correlated (r = 0.95), indicating that the ECHAM5 driving fields show a high degree of agreement with the reanalysis data and thus validating use of these simulations for developing climate projections. Further, when the extreme wind speed estimates are compared to those from the high-quality research station at Westermarkelsdorf in northern Germany, the results (Table 7.3) indicate that the estimates of U_{50} derived from HIRHAM5 with both lateral boundary conditions lie within the uncertainty bounds computed from the observations. A further, but more qualitative comparison can be made with return 50-year period wind speed estimates derived from estimates derived from 10-minute average wind speeds measured between 1958 and 1986 for a site in eastern Denmark (Abild *et al.,* 1992). The observations pertain to a 74 m height and were used to derive a U_{50} estimate of 36.6 m s^{-1}, with $\sigma(U_T)$ = 1.1 m s^{-1} (Abild *et al.,* 1992). Using the power law to vertically extrapolate this gives an estimate of U_{50} at 10-m of about 27.5 m s^{-1}. HIRHAM5 simulations within ERA-40 for 1961–1990 give an estimate for hourly average wind speeds in the grid-cell containing the observational station of 22.1 m s^{-1}, while the simulations within ECHAM5 for 1961–1990 give an hourly average estimate for the grid-cell containing the observational station of 21.6 m s^{-1}. These comparisons were conducted to examine the ability of the HIRHAM model to capture the primary features and magnitude of the extreme wind climate. The good agreement found with observations provides confidence in the climate projections presented herein.

Table 7.3. Extreme wind U_{50} (and 1.96 $\sigma(U_{50})$) (m s^{-1}) estimated for 1961–1990 using in situ data from the Westermarkelsdorf meteorological station (54.55°N, 11.10°E) and output for the closest grid- cell (centered at 54.53 °N, 11.28 °E) from HIRHAM5 simulations nested in ECHAM5 and ERA-40.

	U_{50} (m s^{-1})	95% confidence interval (m s^{-1})
Westermarkelsdorf	26.62	3.69
HIRHAM5/ERA-40	28.31	3.81
HIRHAM5/ECHAM5	24.34	1.80

When U_{50} estimates generated from HIRHAM5 output for each 30-year period in the 140-year duration simulation are compared with estimates for 1961–1990 and the 95% confidence intervals computed therein, the majority of grid cells exhibit no significant change. During the mid-21st century period (2036–2065), approximately 10% of computed grid cells exhibit higher extreme wind speeds than during the 1961–1990 period, indicating a weak tendency towards increased extreme wind speeds in the future. However, for the greater part of the study domain and for most of the 21st century, the U_{50} estimates lie within the historical variability. By the end of the 21st century, the fraction of grid cells exhibiting higher U_{50} estimates than during the control period is close to 0.2 (i.e. nearly 20% of grid cells) (Figure 7.1), with a maximum increase in wind speed magnitude of approximately +15% (Figure 7.2). There is tremendous variability in the number of grid cells from the HIRHAM5 simulations that exhibit higher and lower values of U_{50} in periods subsequent to 1961–1990. It may also be worthy of note that while there is a general tendency towards grid-cells indicating increased U_{50}, there are future time periods during which grid cells that had moved beyond the control period estimate return to within the envelope of U_{50} for the control period (e.g. periods starting in the 1990's and again in the 2040's (Figure 7.1)). This behavior may indicate substantial quasi-periodic internal variability within the modeled climate system.

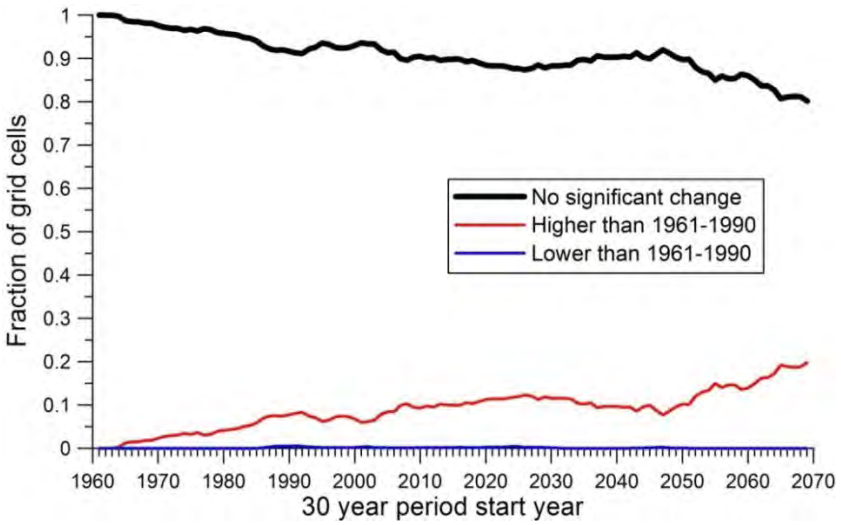

Figure 7.1. Fraction of the total number of grid cells over the study domain that exhibits a U_{50} from a given 30-year period that is higher or lower than the 95% confidence intervals on the U_{50} estimate from 1961–1990. Also shown is the fractional number of grid cells for which the U_{50} from a given 30-year period is within the 95% confidence intervals on the 1961–1990 estimate.

The spatial pattern of projected changes in extreme wind speed is highly irregular and variable with the period used. However, one region that appears to exhibit consistent evidence for increased U_{50} in the HIRHAM5 extends from the southwest of the domain across the central Baltic Sea, and thus covers areas of current or proposed wind energy installations (Figure 7.2).

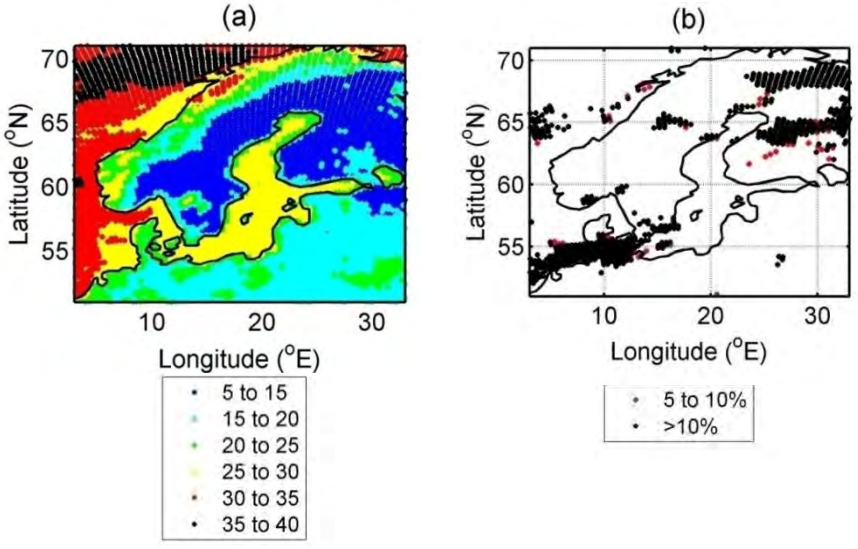

Figure 7.2 (a)50-year return period wind speed (U_{50}) (m s^{-1}) estimates derived for 1961–1990 using output from HIRHAM5, and (b) Difference in U_{50} (in %) computed using HIRHAM5 output from simulations within ECHAM5 (run 3) for 2036–2065 versus 1961–1990. The differences are shown as a percent change from the 1961–1990 estimates. Differences are only shown if statistically significant (i.e. if the U_{50} from the future period lies beyond the 95% confidence intervals for 1961–1990).

7.5.2 *Examination of extreme wind speeds at wind turbine hub-height*

In the following results are presented from the analysis of climate change impact on extreme wind at 100 m above the terrain, corresponding to the hub height of a modern wind turbine. The parameters used are described in Table 7.4 below.

Table 7.4. Description of the 50-year wind at 100 m from HIRHAM5 with different forcing and different periods, all 6h values.

Parameter	Forcing	Period
$U_{50,ERA,I}$	forcing of ERA-40	(control) period I, 1958–2000
$U_{50,ECH,I}$	forcing of ECHAM5	(control) period I, 1958–2000
$U_{50,ECH,II}$	forcing of ECHAM5	period II, 2001–2050
$U_{50,ECH,II}$	forcing of ECHAM5	period III, 2051–2099

The 50-year winds at 100 m, U_{50}, from the control period are shown in Figure 7.3a ($U_{50,ECH,I}$) and Figure 7.3b ($U_{50,ERA,I}$). The results are instantaneous values but saved every 6 hours. This temporal resolution leads to underestimation of the 50-year wind but it does not affect our analysis of the spatial distribution of U_{50}, nor does it affect the discussion of climate change in U_{50}. The quality of Gumbel fitting at most of the grid points can be considered satisfactory because the ratio $\sigma(U_{50})/U_{50}$ is mostly less than 6%, both for HIRHAM5-ECHAM5 and HIRHAM5-ERA40.

The difference between $U_{50,ECH,I}$ and $U_{50,ERA,I}$ is presented in Figure 7.3c as the absolute difference ($U_{50,ECH,I} - U_{50,ERA,I}$) and as the percentage difference $100*((U_{50,ECH,I} - U_{50,ERA,I})/U_{50,ERA,I})$ (%) in Figure 7.3d. It seems that for most part of the Scandinavian countries, i.e. the upper-center part of the entire domain, HIRHAM5-ECHAM5 is in good agreement with HIRHAM5-ERA40, the difference in U_{50} lying mostly within 10%. Over most of Denmark, HIRHAM5-ECHAM5 yields 5–10% lower extreme winds than HIRHAM5-ERA40. For areas south of latitude about 50°N and east of longitude about 30°E, results from $U_{50,ECH,I}$ are overall more than 10% higher than those from $U_{50,ERA,I}$ and more than 20% higher in a considerable part of the domain, as evident from Figure 7.3d. This suggests that for these areas the ECHAM5 model tends to over-predict extreme winds.

The future scenario is divided into two parts following the pattern of greenhouse gas emission, 2001–2050 (period II) and 2051–2099 (period III). There is a few years difference in the data length for the three time periods but the influence from this is small regarding its effect in the calculation of the 50-year wind U_{50}.

The 50-year winds at 100 m for the period II and III from HIRHAM5-ECHAM5 are plotted in Figure 7.4. In comparison with the control period the wind patterns look quite similar and the difference is mostly within 5% over the entire domain. Regions displaying a larger difference are distributed irregularly within the domain, see Figure 7.5a for comparison between period I and period II and Figure 7.5b for comparison between period I and period III. However, for most part of Denmark, the model scenario suggest that the extreme winds will increase up to 20% by 2050, but slightly less by 2099.

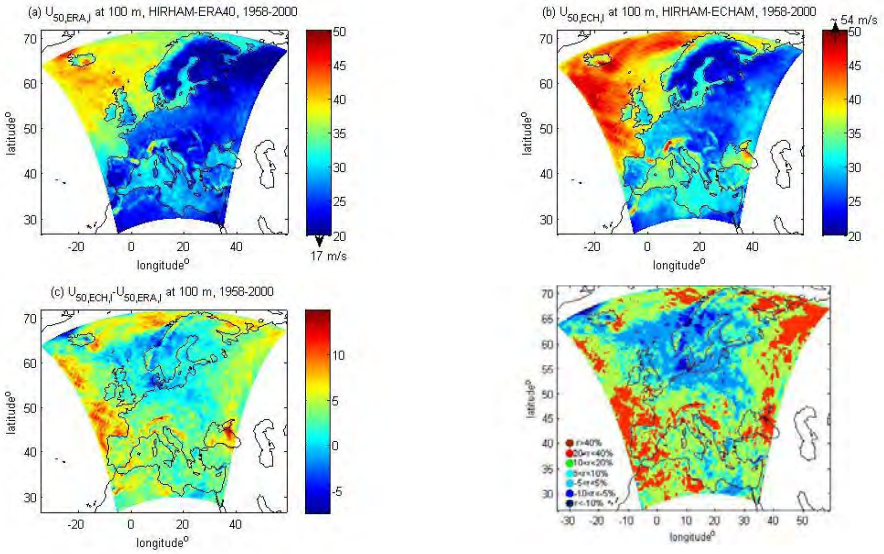

Figure 7.3. Spatial distribution of the 50-year wind at 100 m in the control period 1958–2000, (a) from HIRHAM5- ERA40 $U_{50,ERA,I}$ and (b) HIRHAM5- ECHAM5 $U_{50,ECH,I}$. Below the differences, absolute (c) $U_{50,ECH,I} - U_{50,ERA,I}$. and relative (d) $100((U_{50,ECH,I} - U_{50,ERA,I})/U_{50,ERA,I})$ (%).

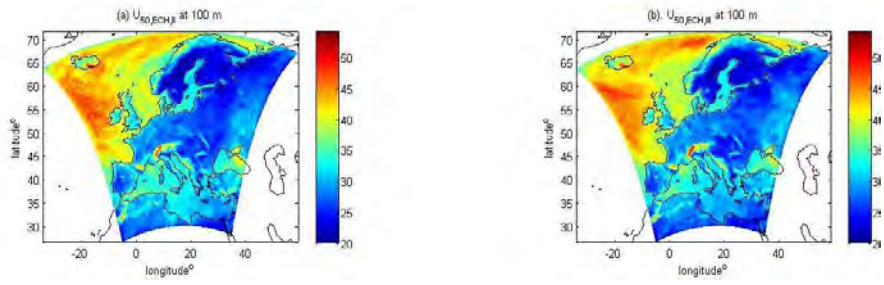

Figure 7.4. (a) Spatial distribution of the 50-year wind at 100 m for period II, 2001–2050, from HIRHAM5-ECHAM5 $U_{50,ECH,II}$; and (b) for the period 2051–2099 from $U_{50,ECH,III}$.

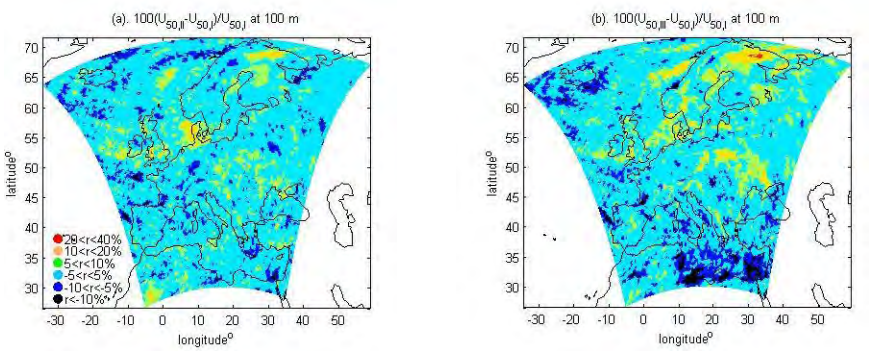

Figure 7.5. (a) Spatial distribution of differences in the 50-year wind between the control period and period II 2001–2050 from HIRHAM5-ECHAM5; (b) Spatial distribution of difference in the 50-year wind between the control period and period III 2051–2099.

7.6 Trend of strong winds

The trend of the strongest winds reflects the long term climatological variation. Two parameters were used to describe the strong winds, the yearly maximum wind speed and the 99th -percentile of the wind speed at 34 m. The 99th-percentile of winds is the value below which 99 percent of the winds may be observed. In the following, only results of the 99th-percentile wind speed analysis are shown. In Wind Engineering, due to lack of long term measurements, it has been accepted as a good approximation to use a data set as long as 10 years to calculate the 50-year wind (Mann *et al.,* 1998). For a period of 50 years, if there is no trend, it does not make a statistical difference which period to use for the calculation of the 50-year wind. If there exists a significant positive trend, then it is critical which period is used, because the last 10 years will give larger 50-year wind than the first 10 years.

The trend is defined in terms of the regression coefficient a as in

$$y = ax + b$$

where x is the list of the 99th-percentile wind speeds at 34 m.

The spatial distributions of a for the 99th-percentile of the wind speed at 34 m are presented in Figure 7.6. All four plots suggest that over most part of the domain the overall trend is small, with $|a| < 0.03$. In the northern-half part of the domain, HIRHAM5-ERA40 results indicate a slight increase of the 99th-percentile wind during the control period with $0.01 < a < 0.03$. A few areas display a stronger increasing trend with $a > 0.03$, i.e. parts of the N-Atlantic Ocean, the south-east part of the Baltic Sea and the western part of Jutland in Denmark.

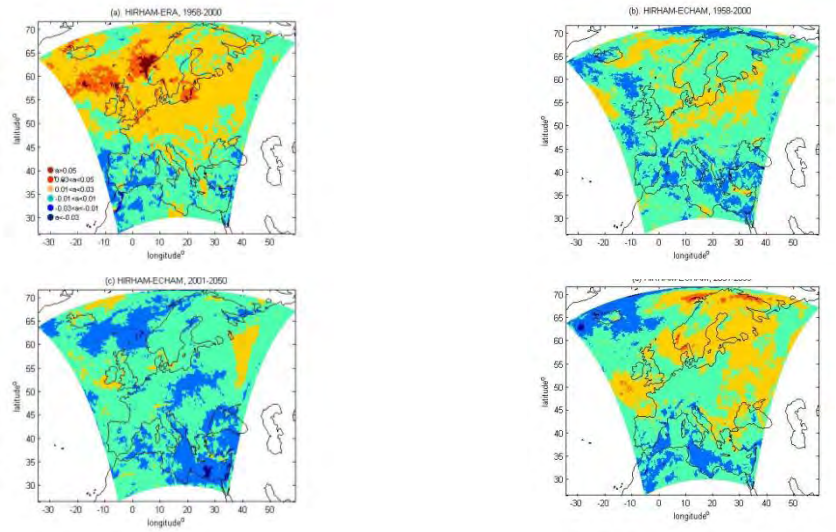

Figure 7.6. Spatial distribution of the regression coefficient a as an indication for a trend in the 99th-percentile of the wind speeds at 34 m. (a) from HIRHAM5-ERA40, control period; (b) from HIRHAM5-ECHAM5, control period; (c) from HIRHAM5-ECHAM5, period II; (d) from HIRHAM5-ECHAM5, period III.

7.7 Effects of temporal and spatial resolution

The effect of temporal and spatial resolution is a common issue when validating the modeled values or when comparing simulations from models of different resolutions. According to the IEC standard (IEC 1999), the 50-year winds at turbine sites should be referred to as 10 min values at hub height. In this report, we have a spatial resolution of 25 km for all regional climate models but the temporal resolutions include 1 hour as averaging time (winds at 10 m) and 6 hours as disjunctive sampling interval (winds at higher model levels).

The effect of temporal resolution, both as averaging time and disjunctive sampling interval, is modeled in Larsén and Mann (2006) by assuming the time series to be a Gaussian process. Thus, values of different and/or coarser temporal resolutions can be converted to the same and finer resolution as 10 min averages. Without correcting the spatial resolution, the 6-hour disjunctive values will lead to an underestimation of about 19% in the peak factor $\frac{U_{max}-\bar{u}}{\sigma}$, where $\bar{u}$ and σ are the mean and standard deviation of the wind speed, which with typical values of $\bar{u}$ and σ corresponds to about 14% in u_{max} for mid-latitude sites.

Winds simulated with meso-scale models are smeared in comparison with point measurements, due to the spatial resolution. This is reflected as flattened wind variance in the mesoscale range. As shown in Larsén *et al.* (2011), the variance in this range is important in contributing to the peak factor and therefore the extreme wind. Although the mean winds from the simulations could be reasonable, the lack of the variance leads to underestimation of the extreme winds.

Larsén *et al.* (2011) developed an approach to take the tails of the spectrum (here in the meso-scale range, from 2 day^{-1} to the 72 day^{-1}, i.e. 10 min) into account. The peak factor was derived as a function of the variance m_0 and second order moment of the spectrum m_2. As a result, the smoothing effect due to the mesoscale resolution on the peak factor is about 15% for the particular case here, namely HIRHAM5-ECHAM5, 10 m winds of 25 km and 1 hour resolution. This, with σ = 3 ms^{-1}, and $\bar{u}$ in the range of 4 to 8 ms^{-1}, corresponds to an underestimation in the extreme wind of 10% to 12%.

7.8 Summary

The extreme wind with a return period of 50 years (U_{50}) is an important design parameter for wind turbines, while strong winds are more important for the operation and maintenance of an offshore wind farm. The importance of strong winds is twofold: Firstly, during the planning period, the developer must compare potential wind farm sites and different operation and maintenance strategies; secondly, in the daily planning of maintenance, strong winds influence decision-making concerning ship travel to the wind farm. Strong winds are important as they occur much more frequently than extreme winds (e.g. wind speeds >17 ms^{-1} occur 3–4 days per year at 10 m height in the Fehmern Belt between Denmark and Germany).

In this work, two scenario runs from HIRHAM5 have been analysed. The first scenario run utilized the boundary conditions from the European Center for Medium-range Weather Forecasts (ECMWF) reanalysis data, ERA40, representing the historical period and the second used ECHAM5 boundary conditions for the A1B emission scenario for the period 1951–2099.

For the historical period, the estimates of the extreme wind U_{50} as derived from the two HIRHAM scenario runs above showed a good agreement over most of the Scandinavian countries. Over Denmark the HIRHAM-ECHAM5 run gives values 5–10% lower than the ERA40 run, while for regions south of 50°N and east of 30ºE the ECHAM5 run generally gives higher values than the ERA40 run.

The analysis shows that the natural variability of the extreme wind in Northern Europe (0–35°E; 50–70°N) is large and that projected extreme wind in more than 80% of all grid cells of the domain remains within the 95% confidence interval of the U_{50} estimate for the period 1961–1990. Those grid cells that exhibit a significant change at the end of this century generally show an increased extreme wind speed U_{50}.

For the middle of this century, the spatial analysis of Northern Europe shows that the 50-year wind speed U_{50} (at 10m) generally remains within the 95% confidence intervals. The southern part of Denmark as

well as parts of Finland and a few other areas show increases > 10% (corresponding to 2.5–3.5 ms^{-1}).

The results for 100 m height are analyzed over a larger spatial domain in Europe (30–70°N) and show likewise no significant change in U_{50} in a majority of the grid cells by the middle of the century. As found in the 10 m data, an area near Denmark shows increases >10%. Towards the end of the century an increasing number of grid cells displays increases in the 50-year wind larger than the natural variability.

Concerning strong winds at 100 m height, the analysis over Europe in general shows small trends for most parts of the domain. This is confirmed by an analysis at 10 m height for Northern Europe where the preliminary conclusion is that the changes by the middle of this century as well at the end of the century remain within the 95% confidence intervals for 1961–1990 data (Pryor, 2009). The numbers listed above are based on data of their original temporal and spatial resolutions, namely 25 km, 1-hourly for the 10 m statistics and 6-hourly for the 100 m statistics.

7.9 Acknowledgments

This work is financially supported by the Nordic Energy Research and by the energy sector in the Nordic countries (Climate and Energy Systems; Risks, Potential and Adaptation) and the Danish PSO project 2009-1-10240.

7.10 References

Abild, J., Andersen, E.Y., Rosbjerg, D. (1992). The climate of extreme winds at the Great Belt, Denmark. *Journal of Wind Engineering and Industrial Aerodynamics,* 411 (3), 521–532.

Abild J. (1994). Application of the wind atlas method to extremes of wind climatology. Technical report Risoe-R-722 (EN). Risø DTU, Roskilde, Denmark.

BTM Consult (2010). World Market Update 2009.

Christensen O.B., Drews, M., Christensen, J.H., Dethloff, K., Ketelsen, K., Hebestadt, I., Rinke, A. (2006). The HIRHAM regional climate model version 5b. DMI.

Clausen, N.-E., Pryor, S.C., Larsén, X.G., Hyvönen, R.,Venäläinen, A., Suvilampi, E., Kjellström, E., Barthelmie, R. (2009). Are we facing extreme winds in the future? Proc. EWEC 16–19 March 2009.

EWEA (2010). Wind energy factsheets from www.ewea.org accessed October 2010.

Fenger, J., ed. (2007). Impacts of climate change on renewable energy sources: Their role in the Nordic energy system. Nord 2007:003, Nordic Council of Ministers, Copenhagen. 190 pp.

Gumbel, E.J. (1958). Statistics of Extremes. Columbia University Press. New York.

IEC 61400-1 Ed. 2 (1999). Wind turbine safety system – part I: Safety requirements.

Larsén, X.G. and Mann, J. (2009). Extreme winds from the NCEP/NCAR reanalysis data. *Wind Energy*, DOI: 10.1002/we.318, 12, 556–573.

Larsén, X.G. and Mann, J. (2006). Effects of disjunct stride and averaging time on maximum wind speeds. *Journal of Wind Engineering and Industrial Aerodynamics,* 94, 581–602.

Larsén, X.G., Ott, S., Badger, J., Hahmann, A., Mann, J., Clausen, N. (2011). Recipe for correcting the effect of mesoscale resolution on the estimation of extreme winds. In: *Scientific Proceedings* (on-line) in European Wind Energy Conference and Exhibitions, Brussels, March 2011.

Mann J., Kristensen, L., Jensen, N.O. (1998). Uncertainties of extreme winds, spectra and coherence. In: Larsen and Esdahl, eds., *Bridge Aerodynamics*, ISBN 9054109610. Rotterdam, Balkerma.

Nakićenović, N. and Swart, R., eds. (2000). Special Report on Emissions Scenarios. A Special Report of Working Group III of the Intergovernmental Panel on Climate Change. Cambridge University Press, Cambridge, United Kingdom and New York, NY, USA. 599 pp.

Pryor S.C., Barthelmie, R.J., Clausen, N.E., Drew, M., MacKellar, N., Kjellström, E. (2010). Analyses of possible changes in intense and extreme wind speeds over northern Europe under climate change scenarios. *Climate Dynamics (accepted subject to minor revisions)*.

Pryor, S.C. and Schoof, J.T. (2010). Importance of the SRES in projections of climate change impacts on near-surface wind regimes. *Meteorologische Zeitschrift,* 19, 267–274.

Pryor, S.C. and Barthelmie, R.J. (2010). Climate change impacts on wind energy: A review. *Renewable and Sustainable Energy Reviews,* 14, 430–437.

Pryor, S.C. (2009). Extreme and intense winds. Presentation at the Fehmern Belt workshop on climate scenarios. May 2009.

Peer-reviewed publications resulting from work carried out during (or in conjunction with) the CES project, but not referenced in the chapter.

Pryor S.C. and Schoof J.T. (2010). Importance of the SRES in projections of climate change impacts on near-surface wind regimes. *Meteorologische Zeitschrift*, 19 (3), 267–274.

Pryor S.C. and Barthelmie R.J. (2010). Climate change impacts on wind energy: A review. *Renewable and Sustainable Energy Reviews*, 14, 430–437.

8. Forest biomass for fuel production – potentials, management and risks under warmer climate

*Seppo Kellomäki, Ashraful Alam and Antti Kilpeläinen**

*Details on author affiliations are given in the Appendix

8.1 Introduction

The EU is committed to reduce its greenhouse gas emissions by 20% and also raise the share of renewable energies (including biofuels) to 20% by 2020 (EC, 2008), which will most likely increase the utilisation of various sources of bioenergy including forest biofuels (energy biomass). This policy will affect energy production in the Nordic and Baltic countries and as an example, Finland has already taken important steps to promote and increase the share of energy biomass. The Finnish "National Forest Programme 2015" aims to increase the use of energy biomass from 3.4 million m^3 in 2006 to 8–12 million m^3 by 2015 (Finnish Ministry of Agriculture and Forestry, 2008) and a recent "National Climate and Energy Strategy" (2008) approved by the Finnish Government aims to increase the share of renewable energy to 38% by 2020, in line with the level proposed by the EC.

A large-scale harvesting of energy biomass will raise the question how sustainable the energy systems based on biomass are and what are the climatic and management effects on energy biomass production and utilisation. In addition, the production of energy biomass needs fossil energy and enhances the emissions of greenhouse gases, thus negating the benefits of the production. In this context, carbon and energy input calculations are needed for evaluating the environmental burden and the contribution of forests and energy biomass to reduce emissions and storage of carbon in the forest ecosystem.

Finnish forests are of the boreal type, where forest growth is mainly limited by low temperature, a short growing season and limited availability of nitrogen (Linder, 1987; Kellomäki *et al.*, 1997; Mäkipää *et al.*, 1998a, b). Low temperatures reduce the decomposition rate of organic matter, which limits the availability of nitrogen in the soil. Furthermore, a short growing season slows down the process of succession due to the

lack of optimal growing conditions, resulting in a longer rotation period (time until the final felling is done). Therefore, in changing climatic conditions, characterized by an increase in temperature and carbon dioxide (CO_2) concentration in the atmosphere and changes in precipitation patterns, it is expected that boreal forests will respond in a complex manner in the future.

In Finland, increases in annual mean temperature and changes in precipitation patterns are expected in the near future (Kjellström *et al.*, 2011). Furthermore, CO_2 concentration in the atmosphere may be doubled by the end of the century (Jylhä *et al.*, 2004; Carter *et al.*, 2005; Ruosteenoja *et al.*, 2005). These changes are likely to increase the growth of forests directly through intensified physiological processes in trees due to elevated temperature and CO_2 concentration, but also through longer growing seasons and mineralization of nitrogen. Increased sequestration and accumulation of carbon in forest biomass could also affect species composition in the long run (e.g. Kellomäki *et al.*, 2008; Garcia-Gonzalo *et al.*, 2007). The unique characteristics of the boreal forest ecosystems make them particularly susceptible to future climate change.

In addition to changing climatic conditions, forest management practices, e.g. the intensity and timing of thinning, also affect the growth and development of a forest by redistributing the available resources for the remaining trees after management intervention. Thinning in young stands yields energy biomass (small-sized trees), provides more growing space for the remaining trees and accelerates the accumulation rate of carbon in the growing stocks. Timber (sawlog and pulpwood) and energy biomass (logging residues i.e. the stem tops, branches, roots and stumps) are produced in older stands during commercial thinning and final felling. These forest productions vary widely depending on the species, site fertility and climatic conditions. Generally, these factors are used to develop forest management recommendations for scheduling the timing and intensity of thinning. However, increased growth under warmer climate could affect the currently recommended practice of managing forests. Thus, the changing climate would necessitate the modification of the business-as-usual management in order to fully utilise the positive effects of climate change, such as increased forest productivity and carbon sequestration in the forest ecosystem.

In addition, as the traditional way of managing forests has been to produce timber in Finland and other Nordic countries, management solely aiming to produce timber may not necessarily be appropriate for the joint production of energy biomass, timber and carbon stocks in the forest ecosystem. Novel forest management practices are, therefore, needed in order to enhance the possibility of climate change mitigation in the context of energy biomass production.

Based on the above mentioned issues, the general objective of this study was to investigate the production of energy biomass along with timber, and carbon sequestration and storage in forest ecosystems in

Finnish conditions. The effects of climate change and forest management on these factors were studied based on several climate scenarios and by changing current forest management recommendations. In addition, CO_2 emissions in management operations per unit of energy (kg CO_2 MWh^{-1}) for energy biomass were calculated by using an emissions calculation tool. This approach reveals not only the production potential of energy biomass, but also facilitates assessment of the role of forests in climate change mitigation and fossil fuel substitution. This kind of comprehensive assessment also helps to compare energy biomass with other bioenergy sources and evaluate different policies for climate change mitigation in forest management.

8.2 Materials and methods

8.2.1 General approach

The study was conducted by using an ecosystem model (Sima) (Kellomäki *et al.*, 1992, 2008; Kolström, 1998), which simulates forest growth and development according to the implemented forest management and a given climate scenario. In addition, an emission calculation tool was developed and it was used together with Sima for assessing the CO_2 emissions of the management operations in the production chain, such as harvesting and transportation. The production chain was covered from seedling production in a nursery, proceeds through management and harvest, and ends up in the yard of a power plant (chipped biomass for energy), a pulp mill (pulpwood) or a sawmill (saw logs).

The Sima model was run for a 90-year period and the obtained results were used as an input for the emission calculation tool. In the model, energy biomass was produced, integrated with timber, in energy biomass thinning (EBT) (small-sized trees) and final fellings (FF) (branches, large roots, stumps, tops of the stem). Two climate scenarios (current (i.e. unchanged) and changing climate) were utilised with varying forest management regimes. Forest management regimes were varied by increasing initial stand density (ISD) and thinning thresholds from current forest management recommendations. By doing this, energy biomass and timber production as well as carbon stocks were studied jointly with the related emissions.

Comparisons focused on either the effect of climate or effect of thinning regimes under the current and the changing climatic conditions. To be able to assess the effect of climate change, corresponding thinning regimes under the changing climate were compared with the current climate. The effect of thinning was compared only with the current thinning and this was done for the current and changing climatic conditions.

8.2.2 Sima model

In the utilised model, the dynamics of the forest ecosystem are assumed to be determined by the dynamics of the number and mass of trees as regulated by their regeneration, growth and death. All these processes are related to the availability of resources, which are in turn regulated by the dynamics of the gaps in the canopy of the tree stand. The model is parameterised for Scots pine (*Pinus sylvestris* L.), Norway spruce (*Picea abies* L. Karst.), silver birch (*Betula pendula* Roth), downy birch (*Betula pubescens* Ehrh), aspen (*Populus tremula* L.) and grey alder (*Alnus incana* Moench., Willd.) growing between the latitudes N 60° and N 70° and longitudes E 20° and E 32° within Finland. The model utilises an area of 100 m^2 with a one-year time step.

Four environmental subroutines are utilised in the model describing the site conditions that affect the growth and the development of forests, i.e. temperature, light, moisture and availability of nitrogen. Temperature controls the geographical thresholds and annual growth response of each species and their ecotypes included in the study. Simultaneously, competition for light controls tree growth and it is dependent on tree species and their height distributions. The effect of soil moisture is described through the number of dry days, i.e. the number of days per growing season with soil moisture equal to or less than that of the wilting point specific for soil types and tree species. Soil moisture indicates the balance between precipitation, evaporation and drainage. The availability of nitrogen is controlled by the decomposition of litter and soil organic matter and it is dependent on the quality of litter, soil organic matter, and evapotranspiration.

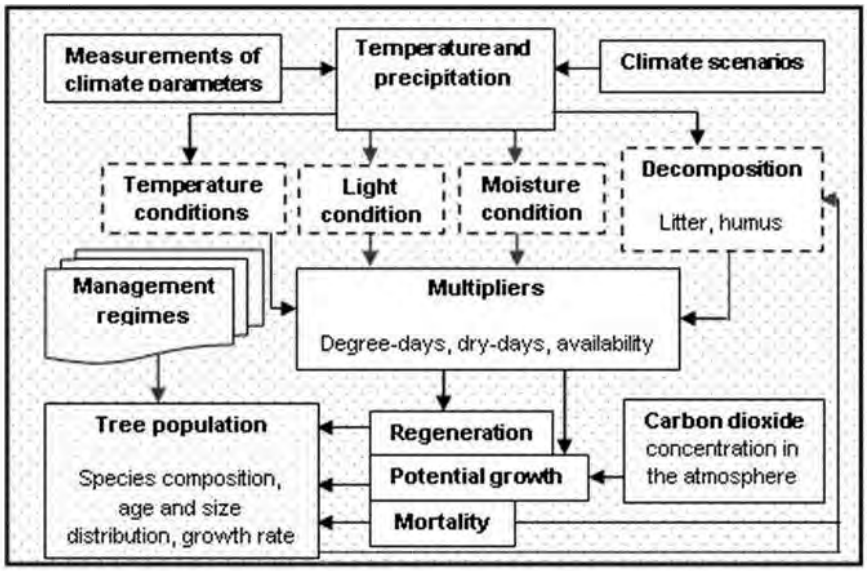

Figure 8.1. Outline of the Sima model.

The environmental subroutines are linked to demographic subroutines by multipliers (M); i.e. $G = G_o \times M_1...M_n$, where G is growth and/or regeneration, G_o is growth and/or regeneration in optimal conditions meaning that there is no shading and no limitation of soil moisture and supply of nitrogen, and $M_1...M_n$ are multipliers for different environmental factors (Figure 8.1). In addition, in the case of growth, the values of G_o are assumed to be related to the maturity of the tree (diameter of tree) and the prevailing atmospheric CO_2. Furthermore, the parameterisation of the growth response is also species-specific. The data for the G_o calculation are based on the simulations of a physiological growth and yield model applying the same methodology as Matala *et al.* (2005). In these simulations, the growth of a single tree with an ample supply of water and nitrogen was calculated under varying atmospheric CO_2 concentrations and under no shading in Finnish conditions.

In the model, mortality is determined by factors that are either age-dependent or age-independent. Age-dependent mortality is a stochastic event depending on the maximum age of a tree. In the case of age-independent mortality, the probability of tree death at a certain moment increases with decreasing diameter growth due to competition from other trees. After dying, trees are eliminated from among the living trees and immediately converted to litter, which is linked directly to a decomposition subroutine and included in the nitrogen cycle.

8.2.3 Sample plot data

The data utilised in this study was based on the Finnish National Forest Inventory (Tomppo *et al.*, 2001; Korhonen *et al.*, 2001; Tomppo, 2006). The measurements in the inventory were done from systematically located rectangular or L-shape clusters, each cluster containing 10–18 sample plots. The distance between the clusters varied from 6 km in the southernmost part of the country to 10 km in Lapland (northern Finland) (Figure 8.2). For our study, data from one sample plot from each cluster was used to represent variables such as tree species, diameter at breast height (usually measured at 1.3 meter from the ground level), site type, location and temperature sum. The simulations included only sample plots in upland mineral soil sites (Figure 8.2).

Figure 8.2. Dots show sample plots, thick line separates southern and northern Finland and number indicates different forestry centres in Finland (South: 1–10; North: 11–13).

8.2.4 Site type

Species composition differs among the site classes over the whole of Finland. Scots pine is mostly dominating the less fertile sites i.e. *Vaccinium* and *Cladonia*, while Norway spruce, together with birch, is dominating the most fertile sites, i.e. *Oxalis-Myrtillus*. However, the medium site class, *Myrtillus*, is suitable for (or a mixture of) Norway spruce, birch and Scots pine.

8.2.5 Forest management and climate scenarios

In the simulations, management includes EBT, commercial thinning, FF and regeneration. The thinning rules followed those currently recommended for the different tree species, site types and regions of Finland (southern and northern Finland separately) (Tapio, 2006). Whenever a given upper threshold for the basal area (cross section area of stems of all trees in unit stand) was encountered at a given dominant height, commer-

cial thinning was triggered (Figure 8.3). Thinning was done from below (mostly smaller/suppressed trees were removed), to such a level that the remaining basal area after thinning was reduced to the expected value at a given dominant height. As recommended by Tapio (2006), EBT was done when a dominant tree height of between 8–14 metres was reached. The remaining basal area threshold after EBT was also determined by following the site- and species-specific recommended number of trees.

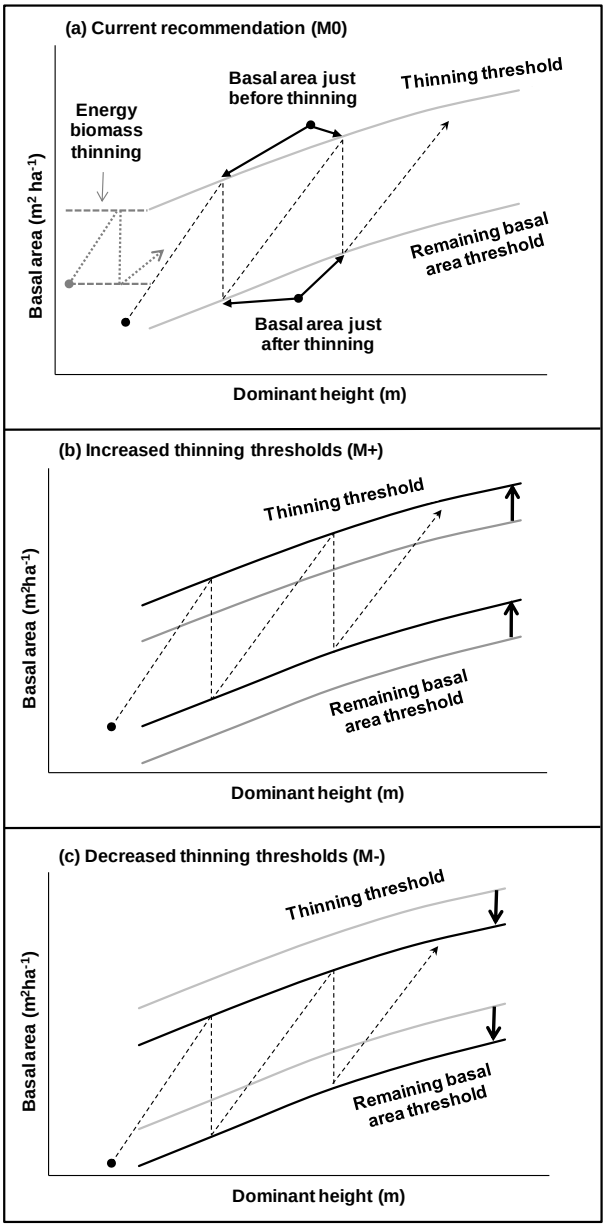

Figure 8.3. Principles defining the thinning regime based on development of dominant height and basal area, considered as current thinning regimes (panel a). Before the commercial thinning, energy biomass was harvested at energy biomass thinning (EBT) and followed the site- and species-specific recommendation. Thinning regimes were changed in terms of increased (panel b) and decreased (panel c) thinning thresholds, where grey lines show the limit used in current recommendation. The thresholds for EBT were similar for all the thinning regimes applied.

The modified management regimes were constructed by means of relative increase (M+) or decrease (M–) of both the thinning thresholds (when thinning is done and remaining basal area after thinning) compared with current recommendation (M0) (see Figure 8.3). In addition, an ISD, varying from 2000 to 4000 trees ha^{-1}, was used in the analysis of emissions calculations per unit of energy for energy biomass. Including timber production, all the management regimes produce energy biomass at EBT and FF. The thresholds for EBT were always similar for current thinning and increased basal area thinning thresholds, but with decreased thinning thresholds, the species-specific stem numbers were decreased but kept within the recommendation of Tapio (2006).

The climate data, utilised in the simulations, are provided by the Finnish Meteorological Institute. Projections are averages of responses calculated using nineteen global climate models, where variables such as minimum and maximum temperature, precipitation, solar radiation, air pressure, snow depth, soil moisture and wind velocity have been analysed (Ruosteenoja *et al.*, 2007; Ruosteenoja and Jylhä, 2007). The grid for current climate (1961–1990) was 10×10 km, whereas the model used in this study applied a 50×50 km grid. The climate change scenarios were produced for three tri-decadal periods, i.e. near-term, 1991–2020, mid-term, 2021–2050 and long-term, 2070–2099 and used the grid size of 50×50 km. In the climate scenario, CO_2 concentration was estimated to rise from the 1990 level of 367 ppm to 545 ppm by 2050. Temperatures were projected to increase by about 3 °C over the whole of Finland. In winter, warming was strongest in the north, while in summer the more pronounced warming would be in the south of the country. Precipitation was estimated to increase by about 10% by 2050. The climate scenario utilised in this impact study differed little compared to that projected and reported in Kjellström *et al.* (2011). At 50^{th} percentiles, Kjellström *et al.* (2011) estimated that temperature would increase over 2 °C and precipitation would increase by 5% during 2021–2050 in Finland and other Nordic countries compared to 1961–1990.

8.2.6 Emission calculations

In the emissions calculation, CO_2 emissions from the management, during the whole production chain in the forest production system, were included. This includes production and transportation of seedling, site preparation and planting, management operations (thinnings and harvesting), chipping and transportation of biomass to the manufacturers' gate as well as all the related commuter traffic and transportation of machinery necessary to conduct the operations (Figure 8.4). The energy inputs required for each of the processes were analysed and calculated by assuming 0.857 kg l^{-1} C content of fuel, to obtain the value in kg CO_2 MWh^{-1}. Wood density of 400 kg m^{-3} was utilised in the calculation, while

C content in dry biomass was assumed to be 50%. The functional unit for this study was determined as 1 ha of forest managed for 80 years.

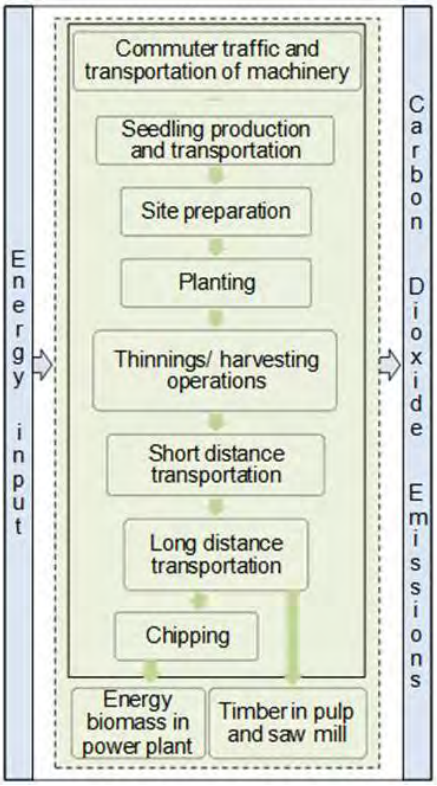

Figure 8.4. Diagram of forest production system boundary.

The performance and consumption parameters of the machines used in the production were collected from available sources (Table 8.1). In the emission calculation, harvested energy biomass and timber were transported an average distance of 70 km utilising 40 tonnes of transportation capacity. However, the truck load size was smaller, being 25 tons, for stump transportation. A constant coefficient of 0.70 was used for determining driving with an empty truck for the return trip. Energy biomass chipping was done in the power plant yard by a drum chipper. In the system, average commuter traffic was assumed to be 50 km and fuel consumption for a passenger car was 0.07 l km^{-1}. Average values for drum chipper and seedling transportation from nursery to the forests were assumed. However, emissions from the manufacturing and maintenance of the machines have not been included in the calculation.

Table 8.1. Parameters utilised in the emission calculation.

Phases	Productivity	Fuel consumption
Forest establishment		
Seeding production		237.54 MJ seedling–1
Seedling transportation (50 km)		0.40 l km–1
Site preparation	0.91 ha h–1	18.20 l h–1
Transportation of Scarifier	12.10 km ha–1	0.54 l km–1
Forest operations		
Thinning by harvester	8.20 m3 h–1	12.00 l h–1
Final felling by harvester	17.20 m3 h–1	12.00 l h–1
Stump removal (excavator)	13.00 m3 h–1	15.00 l h–1
Forwarder and harvester transportation	0.16 km m–3	0.54 l km–1
Biomass transportation and chipping		
Forwarding (thinning)	11.80 m3 h–1	8.50 l h–1
Forwarding (final felling)	15.90 m3 h–1	8.50 l h–1
Long distance transportation (truck)		
Transportation capacity: 40/25 tons		0.54 l km–1
Chipping (drum chipper)	150.00 m3 h–1	60.00 l h–1
Commuter traffic (50 km)		0.07 l km–1

8.3 Results

8.3.1 Effects of climate and thinning on energy biomass production

In general, the energy biomass production at EBT (small-sized trees) increased over time both for current (i.e. unchanged 1961–1990 climate) and changing climate in the whole of Finland. During the first period (1991–2020), neither increased basal area thinning thresholds, compared with current thinning regime, nor climate change, did affect the energy biomass production at EBT. During the second period (2021–2050) increased basal area thresholds did not affect the energy biomass production at EBT, but climate change increased energy biomass production at EBT. During the last period (2070–2099), climate change increased the energy biomass production at EBT but increased basal area thresholds increased the energy biomass production at EBT only under changing climate (Figure 8.5).

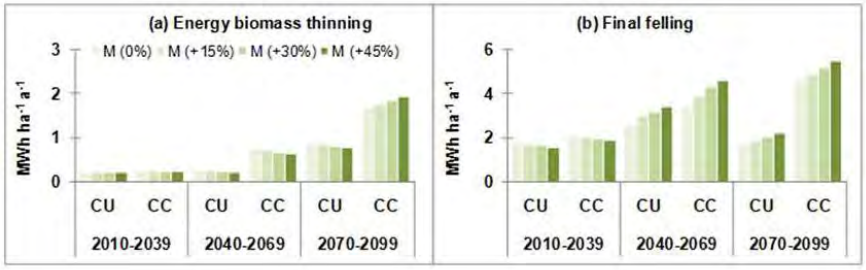

Figure 8.5. Effects of climate change (changing climate "CC" compared to current climate "CU") on energy biomass production (MWh ha^{-1} a^{-1}) at energy biomass thinning (EBT) (panel a) and final felling (FF) (panel b) in three 30-year periods (1991–2020, 2021–2050, 2070–2099) under varying thinning regimes for whole of Finland. M(0%) represents current thinning regime. The scale of the EBT (panel a) is smaller than that of FF (panel b).

The energy biomass production at FF (branches, large roots, stumps and tops of the stem) was higher during the second period (2021–2050) compared with first period (1991–2020) under both current and changing climate but it was highest during the third period (2070–2099) under climate change. During the first period (1991–2020), increased basal area thinning thresholds, compared with the current thinning regime did not affect the energy biomass production at FF under current and changing climate, but climate change increased the production at FF. During the second and last period, both climate and increased thinning thresholds enhanced the energy biomass production at FF (Figure 8.5).

8.3.2 Effects of climate and thinning on timber production and carbon stocks

In general, the changing climatic conditions increased timber production (i.e. sawlog and pulpwood) and carbon stocks in the forest ecosystem (trees and soil) in all the three periods (1991–2020, 2021–2050, 2070–2099) (Figure 8.6). Moreover, increased thinning thresholds compared with current thinning also enhanced carbon stocks in all periods and timber only during the second period for both current and changing climate. However, during the first period (1991–2020), increased thinning thresholds reduced timber production both under current and changing climate. In both climatic conditions, increased thinning thresholds did not have a major effect during the last period (2070–2099).

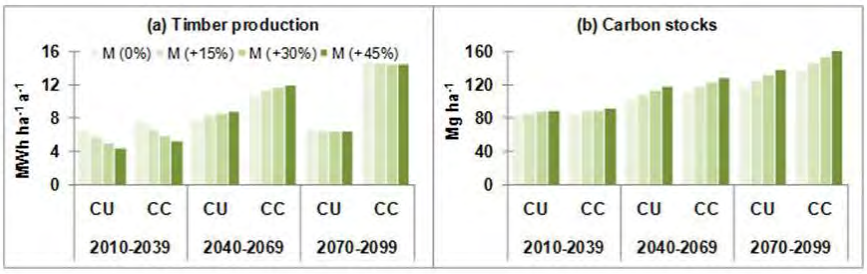

Figure 8.6. Effects of climate change (changing climate "CC" compared to current climate "CU") on timber production (MWh ha^{-1} a^{-1}) (panel a) and Carbon stocks (Mg ha^{-1}) (panel b) in three 30-year periods (1991–2020, 2021–2050, 2070–2099) under varying thinning regimes for whole of Finland. M(0%) represents current thinning regime.

8.3.3 Energy biomass production and CO_2 emissions under varying thinning and initial stand density

In general, increased initial stand density enhanced energy biomass recovery at EBT for both Scots pine and Norway spruce. However, the emissions per unit of energy (kg CO_2 MWh^{-1}) for energy biomass production for Scots pine were higher than that for Norway spruce.

For Scots pine, increased basal area thinning thresholds, compared to current thinning, enhanced energy biomass production (up to 14%) and decreased CO_2 emissions (up to 6%) at the *Myrtillus* site (Figure 8.7). The opposite results were found for decreased thinning thresholds for the same species at the same site. At the *Vaccinium* site, increased thinning thresholds had a similar pattern to the *Myrtillus* regarding energy biomass production and CO_2 emissions, except for 2000 ISD, where energy biomass production was reduced slightly compared to the current thinning regime.

For Norway spruce, decreased thinning thresholds compared with current thinning at the *Oxalis-Myrtillus* and *Myrtillus* sites had a similar effect as on Scots pine, i.e. reduced energy biomass production and increased emission to produce per energy unit of energy biomass (Figure 8.7). The only exception was found at the *Oxalis-Myrtillus* site with 2000 ISD, where energy biomass and CO_2 emissions were both lower. However, up to a 20% increase in thinning thresholds, compared to current thinning, did not show any major changes in energy biomass and CO_2 emissions, but a 30% increase of thresholds enhanced the energy biomass production and reduced CO_2 emissions for both sites and ISDs.

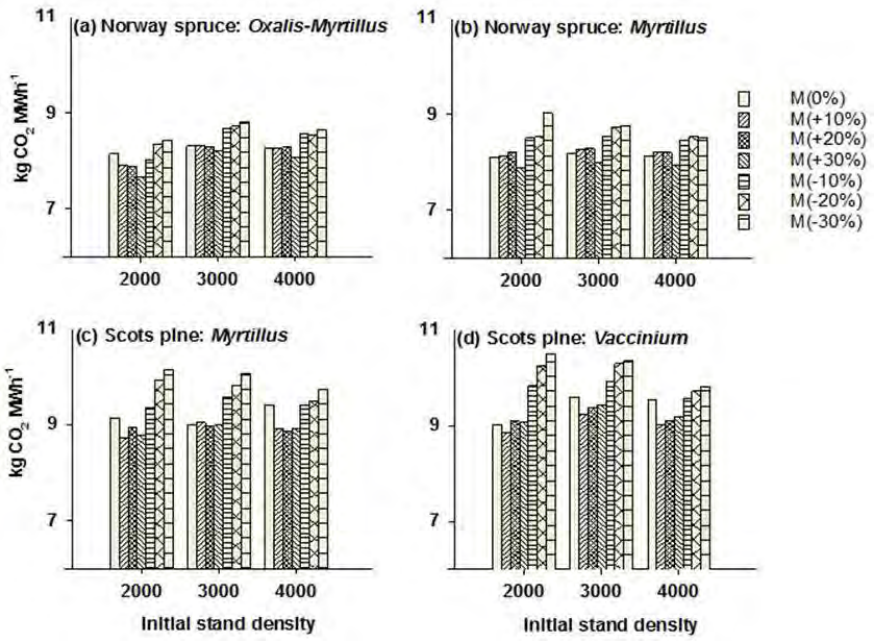

Figure 8.7. Effect of management regimes on CO_2 emissions per MWh of energy biomass (kg CO_2 MWh^{-1}) for Norway spruce at the Oxalis-Myrtillus (panel a) and Myrtillus (panel b) sites and Scot pine at Myrtillus (panel c) and Vaccinium (panel d) sites between 2000–4000 initial stand density (ISD).

8.4 Discussion

The objective of this study was to investigate the potential production of energy biomass as well as timber and carbon stocks in forest ecosystems in Finnish conditions. The effects of climate change (increase in temperature, precipitation and CO_2 concentration in the atmosphere) and forest management on these factors were studied based on the recent climate scenarios and by changing current forest management recommendations. In addition, management related CO_2 emissions for the production of energy biomass were studied. However, risks, for example related to insect attacks, wind throw, forest fires, and frost damage related to climate change were not included in the analysis.

The results show that, compared with current climate, forest production is expected to increase considerably in Finland under future climatic conditions. The largest relative changes were found in northern Finland, although the absolute values were higher in southern Finland (data not shown here). This is in line with other studies, which have also found a corresponding increased production under the future climatic conditions in Finland (e.g., Briceño–Elizondo *et al.*, 2006; Garcia–Gonzalo *et al.*, 2007; Talkkari, 1996).

Under current climate and the current thinning regime, the production of energy biomass at FF (ca. 6.6 Tg a^{-1} or 33 TWh a^{-1}) during the first period (1991–2020) had lower values than those estimated by

Hakkila (2004), Asikainen *et al.* (2008) and Kärkkäinen *et al.* (2008). This might be a result of the different cutting scenarios, logging residues components and their recovery at varying thinning stages. Thus, results from those studies may not directly be comparable with our findings. For example, low quality timber as energy biomass raw material and energy biomass extraction (logging residues) in all the commercial thinnings, were not considered in this study as was done by Kärkkäinen *et al.* (2008). However, estimated total energy biomass potential found in this study may be affected by practical limitations, so that the results should be considered as theoretical potentials (Table 8.2).

Table 8.2. Effects of climate (changing climate compared to current climate) and thinning (changing regime compared to current regime) on annual energy biomass production and fossil fuel substitution potential (TWh[1]) over the simulation period in Finland derived at energy biomass thinning (EBT) and final felling (FF). M (0%) represents currently recommended thinning thresholds.

Thinning regimes	Under current climate			Under climate change		
	EBT	FF	Total	EBT	FF	Total
M (0%)	8.7	40.4	49.1	17.8	67.5	85.4
M (+15%)	8.7	43.9	52.6	18.1	72.8	90.9
M (+30%)	8.4	46.4	54.8	18.4	76.4	94.8
M (+45%)	8.1	48.7	56.8	19.0	80.3	99.3

The potential production of energy biomass at FF was higher in southern Finland compared with northern Finland, which might be due to the effect of timber production in those regions (Figure 8.5, result was shown for whole Finland). In contrast, energy biomass production at EBT was higher in northern than in southern Finland. These dissimilarities in production were mainly the result of variation in forest structure and growth potential in southern and northern Finland. Currently, in the south, the forests are dominated by young stands, while, in the north, stands are more mature or close to that stage (Peltola, 2007). Therefore, with the development of the forests both in northern and southern Finland, the energy biomass production was enhanced in the second (2021–2050) and third (2070–2099) periods compared with the first period (1991–2020).

The concurrent analyses of energy biomass, timber and carbon stocks showed that an increase in these parameters was possible during the second period (2021–2050), in which they increased with increased basal area thinning thresholds. In the case of timber and carbon, this is in good agreement with the findings of Briceño–Elizondo *et al.* (2006), Garcia–Gonzalo *et al.* (2007), and Thornley and Cannell (2000), who concluded that management with higher tree stocking, but also with continuous canopy cover and fewer disturbances throughout the rotation could give maximum production of timber and carbon stocks. How-

[1] Conversion factor: 19.23 GJ/t (energy biomass thinning) and 19.00 GJ/t (final felling) at 20% moisture content of biomass. 1 GJ = 0.2778 MWh.

ever, Seely *et al.* (2002) suggested a trade-off between ecosystem carbon storage capacity and timber production, which was found also in this study during the first and last periods. Nevertheless, in all cases, increased thinning thresholds enhanced carbon stocks in the forest ecosystem under current and changing climate, as could be expected due to an increase in growing stocks.

In this study, all the CO_2 emissions calculated for the forest establishment phase (seedling production and transportation, site preparation, scarifier transportation and commuter traffic) were included in the energy biomass production chain and thus the result could be an overestimation of the energy input required for energy biomass production. However, this study found that it was possible to concurrently increase energy biomass production and reduce management related CO_2 emissions (kg CO_2 MWh^{-1}) if thinning thresholds are increased from the current recommendations. In general, the emission for energy biomass production of Norway spruce was lower than that of Scots pine, as can be expected owing to the former producing higher mass of crown mass though utilising similar amount of input energy. This study found that one unit of fossil energy could roughly produce 30–40 units of biomass-based energy. The estimated emissions for the whole energy biomass production chain were about 7.7–10.5 kg CO_2 MWh^{-1} depending on management, sites and species, slightly higher compared with the values reported by Wihersaari (2005). The discrepancy might be due to the differences between the studies regarding the system boundary settings, selection of species and their growth potential, utilised site type, and assumed energy and moisture content in the biomass. Nevertheless, both studies showed that utilisation of biomass-based energy could avoid a considerable amount of greenhouse gases when coal and energy biomass carbon neutrality are assumed.

8.5 Conclusions

This study concluded that the expected 21st century climate changes and their impacts, i.e. elevated temperature and precipitation, a longer growing season and a concurrent increase in CO_2 levels, could increase energy biomass production in Finland. Energy biomass production can also be enhanced by increasing both initial stand density (ISD) and basal area thinning thresholds compared with the current forest management recommendation. In addition, a concurrent increase in energy biomass and timber production as well as carbon stocks in either of the climate scenarios considered would be possible if thinning was performed at a higher thinning thresholds level than in the current recommendation. Moreover, increased thinning thresholds reduced management related CO_2 emissions for the energy biomass production. For a holistic approach, however, emissions related to ecosystem processes (e.g. decom-

position) should also be included in the analysis. Such a comprehensive approach would give new insights for ecologically sustainable energy biomass production related to the carbon balance of the forest production system and climate change mitigation options of boreal forests.

8.6 References

Asikainen, A., Liiri, H., Peltola, S. (2008). Forest energy potential in Europe (EU27). http://www.metla.fi/julkaisut/workingpapers/2008/mwp069.pdf. Cited December 2009.

Briceño–Elizondo, E., Garcia–Gonzalo, J., Peltola, H., Kellomäki, S. (2006). Carbon stocks and timber yield in two boreal forest ecosystems under current and changing climatic conditions subjected to varying management regimes. *Environmental Science and Policy,* 9, 237–252.

Carter, T.R., Jylhä, K., Perrels, A., Fronzek, S., Kankaanpää, S. (2005). FINADAPT scenarios for the 21st century: alternative futures for considering adaptation to climate change in Finland. FINADAPT Working Paper 2, *Finnish Environment Institute Mimeographs* 332, Helsinki. 42 pp.

Climate and Energy Strategy in Finland (2008). Government Report to Parliament 6 November 2008. http://www.tem.fi/files/20587/Climate_Change_and_Energy_Strategy_2008_summary.pdf. Cited December 2009.

EC (2008). Proposal for a directive of the European parliament and of the council on the promotion of the use of energy from renewable sources. Com (2008) 19 final, Brussels, Belgium.

Finnish Ministry of Agriculture and Forestry (2008). Finland's National Forest Programme 2015 http://www.mmm.fi/en/index/frontpage/forests/nfp/documents_reports.html Cited March 2009.

Garcia-Gonzalo, J., Peltola, H., Zubizarreta-Gerendiain, A., Kellomäki, S. (2007). Impacts of forest landscape structure and management on timber production and carbon stocks in the boreal forest ecosystem under changing climate. *Forest Ecology and Management,* 241, 243–257.

Hakkila, P. (2004). Developing technology for large-scale production of forest chips. Wood Energy Technology Programme 1999–2003. *National Technology Agency* 6, p 99.

Jylhä, K., Tuomenvirta, H., Ruosteenoja, K. (2004). Climate change projections for Finland during the 21st century. *Boreal Environmental Research,* 9, 127–152.

Kärkkäinen, L., Matala, J., Harkonen, K., Kellomäki, S., Nuutinen, T. (2008). Potential recovery of industrial wood and energy wood raw material in different cutting and climate scenarios for Finland. *Biomass and Bioenergy,* 32, 934–943.

Kellomäki, S., Väisänen, H., Hänninen, H., Kolström, T., Lauhanen, R., Mattila, U., Pajari, B. (1992). SIMA: a model for forest succession based on the carbon and nitrogen cycles with application to silvicultural management of the forest ecosystem. *Silva Carelica,* 22, 85.

Kellomäki, S., Karjalainen, T., Väisänen, H. (1997). More timber from boreal forests under changing climate? *Forest Ecology and Management,* 94, 195–208.

Kellomäki, S., Peltola, H., Nuutinen, T., Korhonen, K.T., Strandman, H. (2008). Sensitivity of managed boreal forests in Finland to climate change, with implications for adaptive management. *Philosophical Transactions of the Royal Society,* 363, 2341–2351.

Kjellström, E., Räisänen, J., Engen–Skaugen, T., Rögnvaldsson, Ó., Ágústsson, H., Ólafsson, H., Nawri, N., Björnsson, H., Ylhäisi, J., Tietäväinen, H., Gregow, H., Jylhä, K., Ruosteenoja, K., Shkolnik, I., Efimov, S. Jokinen P., Benestad, R. (2011). Climate Scenarios. *In*: T. Thorsteinsson and H. Björnsson, eds., *Climate Change and Energy*

Systems: Impacts, Risks and Adaptation in the Nordic and Baltic Countries. Nordic Council of Ministers 2011 (this volume).

Kolström, M. (1998). Ecological simulation model for studying diversity of stand structure in boreal forests. *Ecological Modelling,* 111, 17–36.

Korhonen, K.T., Tomppo, E., Henttonen, H., Ihalainen, A., Tonteri, T., Tuomainen, T. (2001). Pohjois–Karjalan metsäkeskuksen alueen metsävarat ja niiden kehitys 1966–2000 (Forest resources and their development in the area of Forestry Center Pohjois–Karjala 1966–2000). *Metsätieteen aikakauskirja,* 3B, 495–576 (in Finnish).

Linder, S. (1987). Response of water and nutrition in coniferous ecosystem. In Schulze, E.D. and Zwölfer, H., eds., Potentials and limitations of ecosystem analysis (pp 180–222). Springer Verlag, Berlin, Germany.

Matala, J., Ojansuu, R., Peltola, H., Raitio, H., Kellomäki, S. 2005. Introducing effects of temperature and CO_2 elevation on tree growth into a statistical growth and yield model. *Ecological Modelling,* 181, 173–190.

Mäkipää, A., Karjalainen, T., Pussinen, A., Kukkola, M. (1998a). Effects of nitrogen fertilization on carbon accumulation in boreal forests: model computations compared with the results of long-term fertilization experiments. *Chemosphere,* 36, 1155–1160.

Mäkipää, A., Karjalainen, T., Pussinen, A., Kukkola, M., Kellomäki, S., Mälkönen, E. (1998b). Applicability of a forest simulation model for estimating effects of nitrogen deposition on a forest ecosystem: test of the validity of a gap-type model. *Forest Ecology and Management,* 108, 239–250.

Peltola, A. (2007). Metsätilastollinen vuosikirja (Finnish Statistical Yearbook of Forestry). Finnish Forest Research Institute. 436 pp (in Finnish).

Ruosteenoja, K., Jylhä, K., Tuomenvirta, H. (2005). Climate scenarios for FINADAPT studies of climate change adaptation. FINADAPT Working Paper 15, *Finnish Environment Institute Mimeographs* 345, Helsinki. 32 pp.

Ruosteenoja, K. and Jylhä, K. (2007). Temperature and precipitation projections for Finland based on climate models employed in the IPCC 4th Assessment Report. In: Third International Conference on Climate and Water, Helsinki, Finland, 3–6 September 2007.

Ruosteenoja, K., Tuomenvirta, H., Jylhä, K. (2007). GCM-based regional temperature and precipitation change estimates for Europe under four SRES scenarios applying a super-ensemble pattern-scaling method. *Climatic Change*, 81, 193–208.

Seely, B., Welham, C., Kimmins, H. (2002). Carbon sequestration in a boreal forest ecosystem: results from the ecosystem simulation model, FORECAST. *Forest Ecology and Management,* 169, 123–135.

Talkkari, A. (1996). Regional predictions concerning the effects of climate change on forests in southern Finland. *Silva Fennica,* 30, 247–257.

Tapio (2006). Hyvän metsänhoidon suositukset (Recommendations for forest management). Metsätalouden kehittämiskeskus Tapio, Metsäkustannus Oy, p 100 (in Finnish).

Thornley, J.H.M. and Cannell, M.G.R. (2000). Managing forests for wood yield and carbon storage: a theoretical study. *Tree Physiology,* 20, 477–484.

Tomppo, E., Henttonen, H., Ihalainen, A., Tonteri, T., Tuomainen, T. (2001). Etelä–Savon metsäkeskuksen alueen metsävarat 1966–2000 (Forest resources in the area of Forestry Center Etelä–Savo 1966–2000). Metsätieteen aikakauskirja, 2B, 309–388 (in Finnish).

Tomppo, E. (2006). The Finnish National Forest Inventory. In Kangas A, Maltamo M (Eds.) Forest Inventory – Methodology and Application. Springer, Netherlands, pp 179–194.

Wihersaari, M. (2005). Greenhouse gas emissions from final harvest fuel chip production in Finland. *Biomass and Bioenergy,* 28, 435–443.

Peer-reviewed publications resulting from work carried out during (or in conjunction with) the CES project, but not referenced in the chapter.

Alam, A., Kilpeläinen, A., Kellomäki, S. (2008). Impacts of thinning on growth, timber production and carbon stocks in Finland under changing climate. *Scandinavian Journal of Forest Research*, 23, 501–512.

Alam, A., Kilpeläinen, A., Kellomäki, S. (2010). Potential energy wood production with implications to timber recovery and carbon stocks under varying thinning and climate scenarios in Finland. *BioEnergy Research*, 3, 362–372.

Alam, A., Kilpeläinen, A., Kellomäki, S. (2011). Impacts of initial stand density and thinning regimes on energy wood production and management-related CO_2 emissions in boreal ecosystems. *European Journal of Forest Research,* doi 10.1007/s10342-011-0539-8.

9. The Nordic Power System in 2020. Impacts from changing climatic conditions

*Joar Styve, Birger Mo and Ove Wolfgang**

*Details on author affiliations are given in the Appendix

9.1 Introduction

The objective of this study is to identify and quantify changes in generation of and demand for electricity in the Nordic region as a result of changing climatic conditions. In the analysis, we simulate the operation of a given electricity system using present and predicted climate data. Main focus is on the NordPool market, i.e. the single financial energy market for Norway, Sweden, Finland and Denmark. The situation in Iceland is discussed separately in Chapter 10. The results show how generation, demand, and transmission characteristics, for a fixed system configuration, respond to expected changes in temperatures and inflow to hydropower reservoirs. The present climate is represented by observed weekly inflow, temperature and wind speed for the period 1961–1990. The future climate is represented by model generated inflow and temperature for the period 2021–2050, from the models "DMI-HIRHAM-Echam5" and "met.no-HIRHAM-HadCM3" (from now on referred to as Echam and Hadam), using the emission scenario "A1B" defined by IPCC (Nakićenović and Swart, 2000). The system model represents the electricity system in 2020, and is based on forecasts of production – and transmission capacities, electricity demand, input fuel costs, and CO_2-quota prices.

Simulations have been carried out using SINTEF Energy Research's EMPS-model[2]. Most major players in the NordPool market apply the EMPS-model for market analysis. The model is also used for hydro scheduling and investment planning (generation and transmission). The EMPS-model simulates the balance between supply and demand in a geographically distributed electricity market, for a selec-

[2] EMPS is the acronym for EFI's Multi-area Power-market Simulator. EFI is now a part of SINTEF Energy Research.

tion of historical weather years. The electricity system model is given exogenously, and EMPS does not account for investment in new production or transmission equipment during the simulation period. For a more detailed description of the model, see (Wolfgang *et al.*, 2009).

9.2 Modelling the Nordic power system

9.2.1 Climatic variables

Inflow data, provided by the hydrological modelling group, are used as input to rivers and reservoirs in the EMPS-model. The received data were distributed to the hydropower system model according to geographical location. The inflow series were prepared to comply with EMPS format requirements by scaling the observed inflow in the reference period with the relative change between the hydrological models' reference period and the climatic scenario period.

Temperature data were used as input for demand predictions in the EMPS-model, as the usage of electricity for heating purposes is significant in the Nordic countries. Temperature forecasts were given for six major Nordic cities. The temperature series were prepared to comply with EMPS format requirements by scaling the observed temperature in the reference period with the absolute change between the hydrological models' reference period and the climatic scenario period.

9.2.2 Electricity system model

The electricity system is modeled as the current system modified with expected changes for 2020. The system is divided into 23 areas, reflecting major transmission constraints and hydrological diversity. The model contains 110 thermal power plants in the Nordic countries, described by capacity and marginal cost. Marginal costs are calculated on basis of predictions for fuel – and CO_2-quota prices, combined with efficiency and fuel input parameters for each individual power plant. Expected capacity development towards 2020 is based on Eurelectric's statistics report (Eurelectric 2009). The model includes 1108 hydropower modules with a detailed description of reservoirs, discharge and relevant constraints. Electricity prices in continental Europe are given exogenously.

9.2.3 Capacities

The production capacities in the Nordpool countries for the model of the 2020 system are shown in Table 9.1. Major changes from today's system include:

- Finnish nuclear capacity increases by 3.2 GW.
- Swedish thermal capacity decreases by 1.5 GW.
- Swedish and Finnish wind capacity increases by respectively 4.4 and 1.3 GW.

Table 9.1. Expected generation capacity in 2020 (GW).

	Nuclear	Thermal	Hydro	Wind	Sum
Denmark	0.0	8.9	0.0	5.6	14.5
Sweden	10.0	6.2	16.4	6.0	38.7
Finland	5.9	10.8	3.4	1.5	21.5
Norway	0.0	1.5	29.5	1.7	32.6
Sum	**15.9**	**27.3**	**49.3**	**14.8**	**107.3**

9.2.4 Electricity consumption

Assumptions regarding electricity demand in 2020 have been based on Eurelectric's 2009 statistics report where predictions about future consumption were made; Norway, 142.7 TWh yr^{-1}, Sweden, 144.0 TWh yr^{-1}, Finland, 101.3 TWh yr^{-1}, and Denmark, 38.2 TWh yr^{-1}. The annual consumption data have been further manipulated to match the observed seasonal consumption pattern throughout the year.

9.2.5 Transmission

The transmission system for 2020 is based on various predictions (Statnett, 2009; Baltso, 2009; Nordel, 2008), combined with a subjective assessment of what might be a likely outcome. Changes include a 2000 MW connection between western and central Norway (Aurskog – Fardal), an upgrade to 2500 MW between western Denmark and Germany, a 1400 MW connection from southern Norway to Germany, and a 600 MW connection from southern Sweden to the Baltic area.

9.2.6 Production costs and export/import prices

An important input parameter in the EMPS system simulations is the marginal production cost for thermal generation, which was modeled exogenously. The main cost components are input fuel- and CO_2-quota prices. Individual marginal costs were estimated using forecast fuel and CO_2-quota prices for 2020 combined with each power plant's efficiency parameters.

Another important parameter is the export and import price to areas outside the model, in this case continental Europe. These prices are also given exogenously in the EMPS-model. Export and import prices were estimated by calculating average marginal production costs in Germany for gas-based units, using 2020 predicted fuel and CO_2 prices. Based on observed hourly spot prices in Germany in 2008, we calculated the relative relationship between day, night and weekend prices. Under the assumption that gas represents the marginal production technology during

daytime, the price relationship was applied to the average marginal production cost for German gas units to obtain a consistent 2020 estimate for prices during night and weekend. These prices were used to represent export and import prices to all the connected continental European countries, after adjustments to account for transmission losses.

9.3 Results

9.3.1 Inflow

Table 9.2 shows the simulated average annual reservoir inflow, measured in TWh, for the reference period (1961–1990) and for future conditions (2021–2050). Average annual inflow for the Nordpool area in the reference scenario, using observed climatic variables from 1961 to 1990, is 214.9 TWh. With the inflow given by the Echam scenario, using predicted climatic variables for 2021–2050, the inflow increases to 240.7 TWh (by 12.0%). The equivalent inflow in the Hadam scenario is 238.3 TWh (10.8% increase). In Echam, the inflow increases by 18.0 TWh (44.8%) during winter and 7.8 TWh (4.5%) during summer. The major part of the increase in winter inflow comes from Norway, where the increase is 12.8 TWh (59.3%), while the equivalent increase in Sweden is only 4.3 TWh (30.3%). The increase in summer inflow is similar in all countries, and ranges from 3.0% to 6.9%. In Hadam, the seasonal change pattern is stronger. Inflow increases by 35.6 TWh (88.6%) during winter, but decreases by 12.2 TWh (7.0%) during summer. Again, Norway with a 24.9 TWh (115.3%) increase in winter inflow is the most influential contributor, as Sweden's corresponding increase is only 9.6 TWh (67.6%). The decrease in summer inflow ranges between 8.3% in Norway and 4.6% in Sweden. Figure 9.1 illustrates the average annual inflow for all countries and scenarios in TWh per year.

The analyses also indicate that monthly maximum and minimum runoff have increased as well, implying an increased winter flood risk, particularly during winter periods.

Table 9.2. Regional average annual inflow (TWh).

	Reference			Echam			Hadam		
Area	**S**	**W**	**Year**	**S**	**W**	**Year**	**S**	**W**	**Year**
East Norway	46.1	9.4	55.6	48.1	15.4	63.5	43.4	20.5	63.9
West Norway	33.2	6.2	39.3	36.0	9.7	45.7	30.2	12.9	43.1
Central Norway	11.7	2.8	14.5	11.3	4.1	15.4	10.3	5.5	15.8
North Norway	16.5	3.2	19.7	15.4	5.2	20.6	14.8	7.6	22.4
Sum Norway	**107.6**	**21.6**	**129.1**	**110.8**	**34.4**	**145.2**	**98.7**	**46.5**	**145.2**
North Sweden	44.1	7.8	51.9	46.4	10.3	56.7	42.0	14.4	56.4
Central Sweden	9.3	2.9	12.2	10.5	3.7	14.2	9.0	5.0	14.1
South Sweden	3.4	3.4	6.9	3.8	4.5	8.3	3.2	4.4	7.5
Sum Sweden	**56.8**	**14.2**	**70.9**	**60.7**	**18.5**	**79.2**	**54.2**	**23.8**	**78.0**
Finland	10.3	4.5	14.9	11.0	5.3	16.3	9.7	5.5	15.1
Nord Pool area	174.7	40.2	214.9	182.5	58.2	240.7	162.5	75.8	238.3

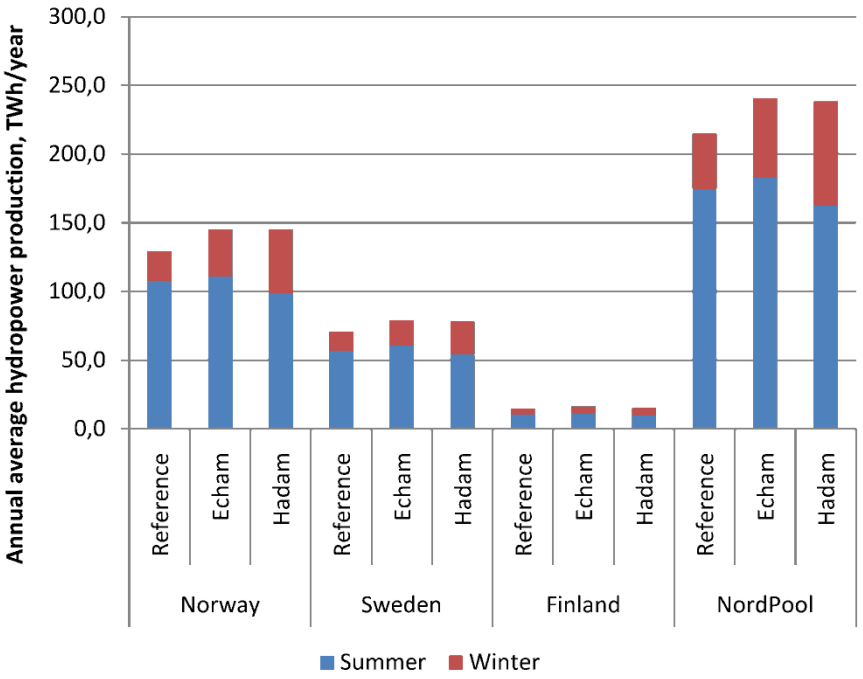

Figure 9.1. Average annual inflow (TWh yr^{-1}) in the NordPool countries.

9.3.2 Hydropower production

Table 9.3 shows the average annual simulated hydropower production in TWh for all scenarios. In Echam, the increase in NordPool hydropower production amounts to 20.7 TWh (10.3%), while for Hadam, the increase is 18.9 TWh (9.4%). The increase in production is not equal to the potential increase from greater inflow as more water will induce more spillage. In addition, the seasonal change for production does not follow the seasonal change in inflow, or in other words, the strong increase in winter inflow does not imply a corresponding increase in winter production. Instead, we see that the production increase is distributed relatively evenly throughout the year. Production throughout the year is shown in Figure 9.2.

Table 9.3. Average annual hydropower production (TWh).

	Reference			Echam			Hadam		
	S	W	Year	S	W	Year	S	W	Year
Norway	51.5	69.7	121.1	57.6	77.1	134.7	56.1	78.1	134.2
Sweden	29.2	37.6	66.9	32.9	40.1	73.1	32.9	39.8	72.7
Finland	6.9	6.9	13.8	7.5	7.3	14.7	6.6	7.2	13.8
Nord Pool	87.6	114.2	201.8	98.0	124.5	222.5	95.6	125.1	220.7

Table 9.4 shows the average annual simulated spillage in TWh for all scenarios. Spillage in the winter season increases relatively more than summer spillage, however, spillage during summer remains the largest component in total average annual spillage.

Table 9.4. Average annual spillage (TWh).

	Reference			Echam			Hadam		
	S	W	Year	S	W	Year	S	W	Year
Norway	6.6	1.1	7.8	7.8	2.3	10.1	6.6	3.8	10.4
Sweden	3.0	0.9	3.8	4.3	1.5	5.8	3.2	1.9	5.1
Finland	0.9	0.1	1.1	1.3	0.3	1.5	1.0	0.3	1.3
Nord Pool	10.6	2.2	12.7	13.4	4.1	17.5	10.8	6.0	16.8

Figure 9.2 shows averages for simulated inflow, reservoir level and production for each week of the year. Under the climate scenarios, greater winter inflow and smaller spring floods are observed. Together with higher winter temperatures, which result in less winter demand and a slightly earlier spring flood, this contributes to diminished seasonal variation in reservoir level. The increase in hydropower production is more or less evenly distributed over the year.

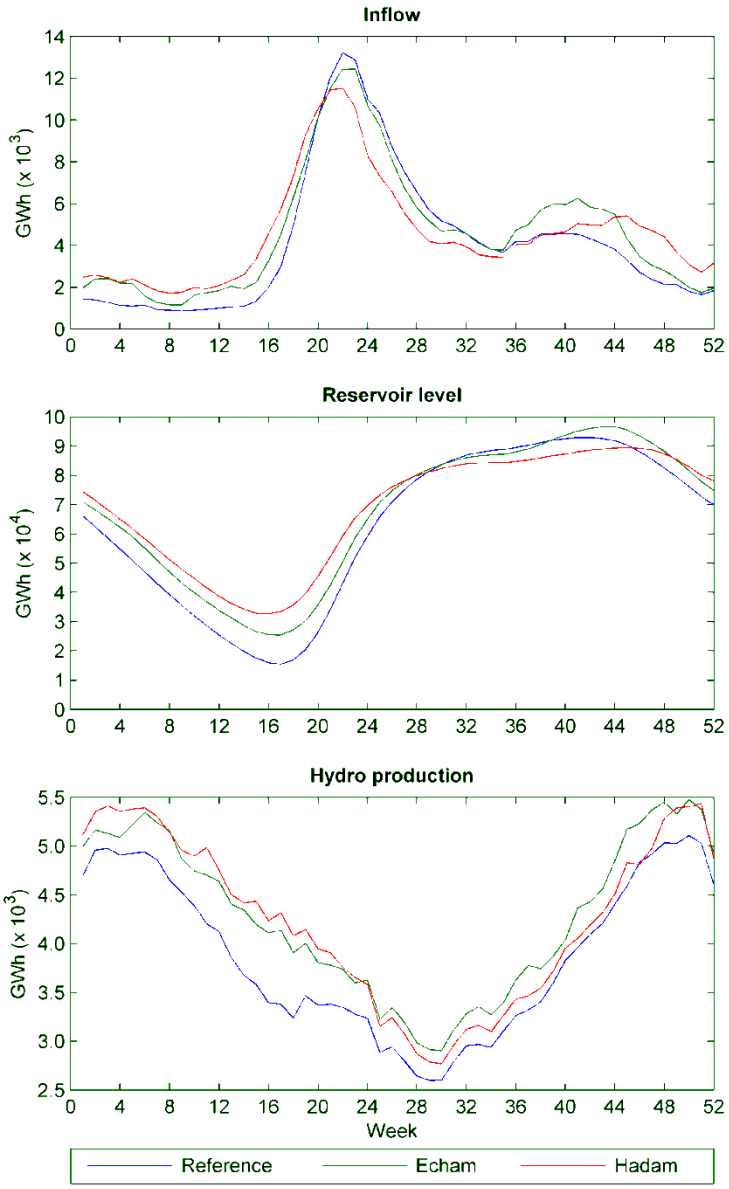

Figure 9.2. Hydropower properties for the NordPool area.

Table 9.5 shows the simulated average annual thermal power production in TWh, for all scenarios. In the reference scenario, simulated thermal production is 197.3 TWh. Due to increased hydropower production, this is reduced by 14.8 TWh (7.5%) in Echam, and 15.5 TWh (7.9%) in Hadam. The largest reductions take place in Finland and Denmark where the production is reduced by 6.6–7.1 TWh and 5.4–5.6 TWh, respectively. Also here we find that the reduction is evenly distributed between summer and winter.

Table 9.5. Average annual thermal power production (TWh).

	Reference			Echam			Hadam		
	S	W	Year	S	W	Year	S	W	Year
Norway	0.8	2.5	3.3	0.6	1.5	2.1	0.6	1.3	1.9
Sweden	47.0	46.5	93.5	45.8	46.3	92.1	45.7	46.2	91.9
Finland	31.9	37.5	69.4	28.8	33.9	62.8	29.1	33.3	62.3
Denmark	14.6	16.5	31.1	10.9	14.7	25.5	11.5	14.2	25.7
Sum	**94.3**	**103.0**	**197.3**	**86.2**	**96.3**	**182.5**	**86.9**	**94.9**	**181.8**

9.3.3 Demand

The average annual demand for electricity in the NordPool area is 432.8 TWh in the reference case. In the Echam scenario, demand is reduced by 8.4 TWh (1.9%), while for Hadam, the reduction is 11.0 TWh (2.5%).

9.3.4 Power trade between countries

Table 9.6 shows projections for net energy export in comparison with the reference period. All countries (excluding Finland) increase their net export to continental Europe. The hydro-dominated systems (Norway and Sweden) also increase their net export to other NordPool countries. Total net export increases for the hydro-dominated systems while Denmark and Finland reduce their total net export. All countries but Finland are net exporters in the climate scenarios.

Table 9.6. Average annual net export (TWh/year).

	Reference			Echam			Hadam		
	S	W	Year	S	W	Year	S	W	Year
Norway	-7.0	-7.0	-14.0	0.1	0.9	1.0	-1.2	2.6	1.4
Sweden	20.9	8.4	29.3	24.4	12.3	36.8	24.4	13.1	37.5
Finland	-7.0	-9.9	-16.9	-8.4	-11.0	-19.5	-9.0	-11.5	-20.6
Denmark	4.0	5.1	9.1	0.2	3.2	3.4	0.8	2.7	3.5
Sum	**10.9**	**-3.4**	**7.5**	**16.3**	**5.4**	**21.7**	**15.0**	**6.9**	**21.8**

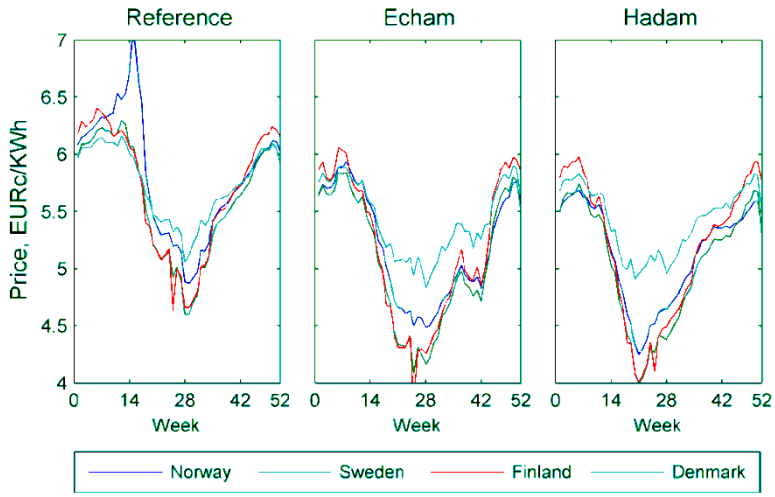

Figure 9.3. Average weekly electricity price over the year (EURc/kWh).

9.3.5 *Electricity prices*

The electricity prices are projected to decrease in all NordPool countries. Figure 9.3 shows the average weekly electricity price for all simulated years in EURc/kWh. Each country's price is the average of all the inherent area prices. The lower prices are mainly due to higher supply from increased inflow combined with lower demand due to higher temperatures. The Danish price levels do not decrease as much as in the other countries. This is mainly due to Denmark's high level of thermal production combined with a strong transmission capacity to Germany.

9.3.6 *Energy balances*

Table 9.7, accompanied by Figure 9.4, shows the average annual simulated energy balance in TWh for all scenarios. Main findings are increased hydropower production, decreased thermal power production, and decreased demand for all countries in the climate scenarios.

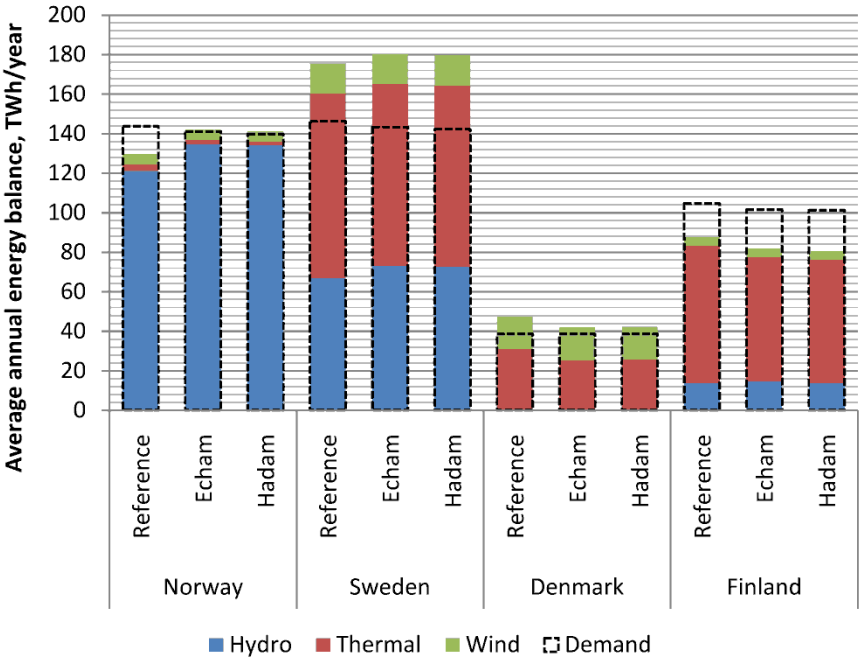

Figure 9.4. Average annual energy balance, (TWh/year).

Table 9.7. Average annual energy balances (TWh).

Reference	Hydro	Thermal	Wind	Net Import	Demand
Norway	121.1	3.3	5.2	14.0	143.6
Sweden	66.9	93.5	15.0	-29.3	146.1
Denmark	0.0	31.1	16.5	-9.1	38.5
Finland	13.8	69.4	4.5	16.9	104.6
NordPool	201.8	197.3	41.2	-7.5	432.8
Echam	**Hydro**	**Thermal**	**Wind**	**Net Import**	**Demand**
Norway	134.7	2.1	5.2	-1.0	141.0
Sweden	73.0	92.1	15.0	-36.8	143.3
Denmark	0.0	25.5	16.5	-3.4	38.6
Finland	14.7	62.8	4.5	19.5	101.5
NordPool	**222.5**	**182.5**	**41.2**	**-21.7**	**424.4**
Hadam	**Hydro**	**Thermal**	**Wind**	**Net Import**	**Demand**
Norway	134.2	1.9	5.2	-1.4	139.8
Sweden	72.6	91.9	15.0	-37.5	142.1
Denmark	0.0	25.7	16.5	-3.5	38.6
Finland	13.8	62.3	4.5	20.6	101.2
NordPool	**220.7**	**181.8**	**41.2**	**-21.8**	**421.8**

9.3.7 CO_2 emissions

Average annual CO_2 emission from the NordPool area is 43.0 million tonnes in the reference scenario (Table 9.8). This estimate includes the direct emission from power production in each country, and the indirect effect of exporting and importing electricity to continental Europe. When electricity is imported from continental Europe to NordPool, the induced CO_2 emission can be credited to the NordPool area. When electricity is exported from NordPool to continental Europe, the avoided CO_2 emission in Europe can be credited to the NordPool area. Under the climate scenarios (Table 9.8), the direct CO_2 emission from the NordPool area goes down by 10.6–11.0 Mtonne (ca. 24%). Including the effects from trade with continental Europe, the equivalent decrease is 24.5 Mtonne (57%). About 60% of the reduction comes from the second order effect through trade with continental Europe.

Table 9.8. Average annual CO_2-emission from power production (Mtonne/year).

	Reference	Echam	Hadam
Norway	1.4	1.1	1.0
Sweden	5.1	4.4	4.4
Finland	14.7	9.1	8.7
Denmark	24.0	20.0	20.1
Sum	**45.2**	**34.6**	**34.2**
Import from Europe	14.7	8.5	8.7
Export to Europe	-16.9	-24.5	-24.6
Sum, adjusted for Europe	**43.0**	**18.5**	**18.4**

9.4 Concluding remarks

This analysis has modeled how the NordPool electricity system will respond to predicted changes in climatic conditions. The average annual inflow to reservoirs will increase by 12–13% compared to current conditions. A significant part of this increase stems from more inflow during the winter season. The inflow increase will result in more hydropower production. The modified seasonal distribution of inflow will decrease variations in both inflow and reservoir levels over the year. The predicted average daily temperature is expected to increase by 1–2°C. Also here we find that temperatures increase more during the winter. Warmer winters reduce the electricity demand in the traditional high-load period, which further contributes to less variation in reservoir levels. Due to the increase in inflow, parts of the thermal power production will be substituted by hydropower production. Combined with the reduction in demand, NordPool will have an excess supply of electricity. This leads to reduction in imports and increases exports from/to continental Europe. Electricity prices are expected to decrease. The reduction in thermal production leads to a 10 Mtonne reduction of CO_2-emissions in the NordPool area. By including the effects from trade with continental Europe, an additional reduction of 14 Mtonne CO_2 is projected to occur.

9.5 References

Baltso, Nordel, PSE Operator SA (2009). Market based analysis of interconnections between Nordic, Baltic and Poland areas in 2025.

Eurelectric (2009). Statistics and prospects for the European electricity sector.

Nordel (2008). Nordic grid master plan.

Statnett (2009). *Statnetts nettutviklingsplan.* Statnett.

Wolfgang, O., Haugstad, A., Mo, B., Gjelsvik, A., Wangensteen, I., Doorman, G. (2009). Hydro-reservoir handling in Norway before and after deregulation. *Energy* 34 (10), 1642–1651.

Nakićenović, N. and Swart, R., eds. (2000). Special Report on Emissions Scenarios. A Special Report of Working Group III of the Intergovernmental Panel on Climate Change. Cambridge University Press, Cambridge, United Kingdom and New York, NY, USA, 599 pp.

10. Hydropower in Iceland. Impacts and Adaptation in a Future Climate

*Óli Grétar Blöndal Sveinsson, Úlfar Linnet and Elías B. Elíasson**

*Details on author affiliations are given in the Appendix

10.1 Introduction

All of the largest hydroelectric power stations in Iceland are fed by glacial rivers. Over the last few decades some changes have been observed in both the volume and the seasonal distribution of river flows and further changes are expected in future climate. These changes will have impacts on the utilization and operation of existing power stations and should also be taken into account in the design of new ones. In order to be prepared for these changes, Landsvirkjun (The National Power Company) has analyzed the operation of its hydroelectric system with different expected "stationary" flow scenarios in the period 2010 to 2050.

10.2 Runoff model and flow scenarios

A conceptual rainfall-runoff model is used to create five different flow scenarios which are based on perceived trends in historical measurements and prediction of future climate trends. The expected trends in future climate are derived from Nordic projects on climate, water and energy systems 2002–2010 and from IPCC reports. Temperature trends were estimated to be 0.75 °C per century in the period 1950–1975, 1.55 °C per century from 1975 to 2000 and 2.35 °C per century after 2000. Within the year these trends were seasonally distributed according to the interpretation by meteorologists of climate model results of future expected changes. With these estimated trends historical climate measurements from 1950 to 2005 were transformed into the future by adding the total change from the time of measurements to the target time. In this manner five different temperature scenario series, one for each year; 2010, 2015, 2025, 2035 and 2050 were created. Similar methods were used for precipitation and glacier area-volume-elevation curves. Using these transformed measurements as input for the runoff model, the five different "stationary" flow scenarios were created.

10.3 Results and discussion

Analysis of these scenarios shows that potential energy in the total river flows to Landsvirkjun's power system is expected to have increased by 20% (2.8 TWh) in 2050. The major part of this increase is explained by added runoff in glacial rivers, ranging from 27% to 84% for individual rivers. There are also differences in the seasonal flow pattern. Spring comes early causing earlier snowmelt, flow is lower in early summer but in late summer glacier melt is significantly higher. Small winter floods occur more often. Changes in direct runoff rivers and spring fed rivers are much smaller, around 5% for most rivers.

The current production system is not designed to meet these changes in runoff and will, in 2050, only be able to utilize 38% of the increase, equal to a production increase of 8.5% (0.8 TWh), see Fig. 10.1. This proportion is low compared with the present utilization of more than 85% of the potential energy in the river flows. There are a number of reasons for this drop. Iceland has a hydrodominant system with a 30% share of geothermal energy and negligible thermal (diesel/gas) production capacity. As a result, Landsvirkjun's hydroelectric stations function as base load stations with the peak load being only 15% higher than the base load. This means that the utilization of the stations is high, 6570 h yr^{-1} compared to a worldwide mean of 3854 h yr^{-1} (Energy Information Administration international statistics database, 2006). This has resulted in a design with sufficient but little additional reservoir capacity and limited extra power that will be exceeded if flow increases as predicted.

The results of this study are being used for more detailed analyses of possible redesign and upgrades of current power stations and revaluation of future projects that have been proposed. The increase in production has been estimated by simulating the power system with new or altered design using these flow scenarios. The results have yielded valuable information for decision-making regarding future investment

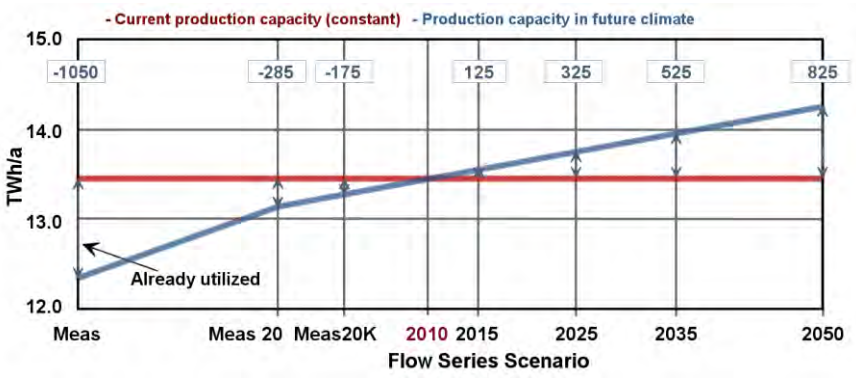

Figure 10.1. Possible production increase in warming climate. Meas, Meas20 and Meas20K are flow scenarios based only on historical measurements. Numbers in boxes show difference between current (2010), future and past production capacity.

10.4 References

Fenger, J., ed. (2007). Impacts of climate change on renewable energy sources: Their role in the Nordic energy system. Nord 2007:003, Nordic Council of Ministers, Copenhagen. 190 pp.

IPCC Fourth Assessment Report (2007). The Synthesis Report (SYR): Summary for Policymakers (SPM).

Elíasson, E. B. and Jóhannsson, S. (2009). Global Warming: Landsvirkjun's Production Capacity from Present to 2050. Landsvirkjun's Internal Report (in Icelandic).

11. The effects of climate change on power & heat plants – assessing the risks and opportunities

*Jaana Keränen, Riitta Molarius, Jari Schabel, Jenny Gode, Edward James-Smith, Noora Veijalainen and Kirsti Jylhä **

*Details on author affiliations are given in the Appendix

11.1 Introduction

It is important for decision makers to acknowledge and consider the impacts of climate change on Nordic renewable energy resources with regards to strategies for energy production and distribution. There is a need to produce information based on risk assessments for investors through short-term studies which take into account both the impacts of changing climate on power production and the uncertainties of these impacts. Since the life-time of power plant investments is usually less than 40 years, there is seldom a need for a longer planning period in an economic study. Private investors also tend to focus more on the near future because of the interest rate and because of the larger uncertainty surrounding the distant future. Recognising and identifying risks associated with changes in weather patterns is an important step towards planning of new infrastructure investments and mitigating potential damage to existing power production, transmission and distribution systems.

The goal of this study was to assess the climate associated risks and opportunities of power and heat production systems in the Nordic countries for the next 20–30 years. The increased uncertainty of the future renewable resources with respect to climate change is a key issue for the energy sector. While the companies obviously aim to minimise negative impacts, it must be remembered that it is also possible that some features of renewable resources may create new opportunities for the power plants in the future. Moreover, changes in the seasonal and geographical circumstances may affect the productivity of current power plants. Disturbances in production due to extreme events such as floods, droughts, storms, increased wave heights, etc. must also be taken into account. Uncertainty translates into riskier decisions at all levels within

the sector including operational and market issues, short-term responses, and investments.

This study focused on managing the risks and opportunities at the operational level with a view to preventing adverse effects on current power and heat plants and production due to climatologic changes. The method being used can also be used to support decision-making about new construction projects and power and heat plants while considering their geographical situation.

The risk and opportunity management tool is targeted at decision makers in power companies, which makes it possible to analyse the potential climate change related risks especially associated with power plants. It is intended to be used as a first step in the strategy for identifying not only potential risks due to climate change, but also the associated opportunities for power companies.

11.2 Methods

The use of formal risk assessment procedures across different industrial areas has increased. A formal analysis has become a symbol of efficient information use, rational decision-making and a willingness to carry out actions (Heikkilä *et al.*, 2009). Formal analysis utilisation has four different purposes: information purposes, communication, to direct and focus the attention and symbolic reasons (Langley, 1989). The implementation of formal analysis can be seen to address several purposes and needs at the same time.

The basic premise behind developing the risk and opportunity assessment framework was to integrate climate scenarios with the technical risk assessment traditions. The industrial safety standard of risk analysis for technological systems (IEC 60300-3-9, 2000) was chosen to provide a structure for the desired risk analysis process since it is already widely applied, for instance, in the process industry. A structured risk analysis process is general in its nature so it may be exploited across many industries and applied to many types of systems. An overview of the general risk assessment procedure is presented in Figure 11.1.

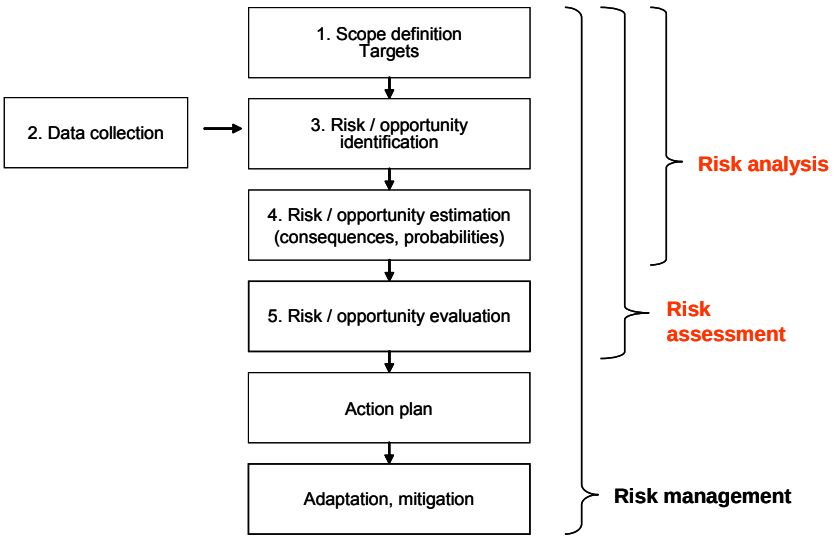

Figure 11.1. A modified risk analysis process based on a risk analysis standard (IEC 60300-3-9, 2000).

The risk analysis process includes the following steps: scope definition, data collection, risk/opportunity identification and risk/opportunity estimation. Risk/opportunity evaluation is a part of decision-making in which decision makers judge the tolerability of risks and distinguish between potential risk reduction or avoidance actions (IEC 60300-3-9, 2000). Action plan implementation enables continual improvement in risk management and establishes an organisation's adaptation and mitigation actions in practice.

Risk analysis relies on the use of historical meteorological and hydrological data as well as on future climate scenarios. In the work reported here, climate modelling and scenarios were initially provided by Finnish case studies conducted by the Finnish Meteorological Institute (FMI) and the Finnish Environment Institute (FEI). The Swedish case study utilised data created by the Swedish Meteorological and Hydrological Institute (SMHI), while the Danish study exploited data provided by the Danish Meteorological Institute (DMI) and the Norwegian case study made use of data created by the Norwegian Meteorological Institute. The climate scenarios examined in the different case studies were partially based on global climate models.

The approach utilises brainstorming-based risk identification methods like "What-if?" analysis to create a shared understanding among participants in the risk analysis about possible future events. A "What-if?" analysis is a structured brainstorming method for determining what things can go wrong and for determining the likelihood of, and consequences of, those situations occurring (Dougherty, 1999). The answers to these questions form the basis for making judgments regarding the acceptability of those risks and determining a recommended course of action for those risks deemed to be unacceptable.

Two tools to aid data collection during the brainstorming session were developed. The first one, known as a functional model, divides the power production and distribution process into three parts: *Energy source*, *Power plant* and *Distribution*. During the *Energy source* examination, climate change effects on the utilised energy source and its aspects, such as catchment area or collection area, are studied. The *Power plant* study highlights future changes associated with the actual power plant, such as technique and maintenance. The final element, *Distribution*, allows the study of aspects and changes in the transmission and distribution network, like future changes in seasonal energy consumption needs. Each part can be affected in a specific way due to the changing climate and it therefore makes sense to examine the parts separately. And in any studied case, one should specifically decide to which extent the possible risks and opportunities are examined. An example of a functional model for a hydropower plant is shown in Figure 11.5.

Another tool, known as the *Seasonal plan*, helps to generate an overview of the seasonal issues by incorporating all relevant climate scenario data and information on typical seasonal actions for the power plant and the different periods of energy production. The seasonal plan helps to determine how climate change could affect a power plant's typical seasonal practices and routines. An example of seasonal plan for a biomass-based power plant is shown in Figure 11.6.

The subsequently identified risks and opportunities are then all documented in a Risk/Opportunity Table (R/O Table), which is the main documentation tool within the developed method (Figure 11.2). All necessary information from different sources – such as knowledge from climate scenarios and results from the risk/opportunity identification sessions – shall be recorded to the R/O Table. Also, all possibilities to control or reduce the identified risks, as well as benefits from similarly identified opportunities, which arise during the risk/opportunity identification sessions, should be documented to the R/O Table.

The risk estimation contains two steps that deal with the definition of the risk/opportunity consequences and uncertainty. The uncertainty is associated with the likelihood that a risk or an opportunity remains after the prevention or enhancement actions have been enforced. The likelihood classification can be expressed in various ways and can be customised according to the specific case. The risk/opportunity consequences will typically be discussed in parallel with risk/opportunity identification.

Scenarios and phenomena	Likelihood of the phenomena	Energy source (e.g. catchment area, peat or biomass production area)	Power / Heat plant	Distribution network	Risk reduction / control / potential	Likelihood of the consequences to the energy production	Consequence category
Phenomena according to regional scenario of future climate, hydrological model or wind model	Probability according to IPCC 2007	The consequences of the phenomena to energy source and its usability	The consequences of the phenomena to the power plant	The consequences of the phenomena to the distribution network	The operations which will be done to protect against the phenomena and its consequences	Likelihood according to own ranking	Consequence category according to own ranking
Scenario 1: warmer climate							
Phenomena: 1.1 higher temperature, especially during winter	Very likely, the probability that the next decade is warmer is 90%	Increasing water capacity	Hot weather decreases the lifetime of transformers	Increased electrical resistance affects energy losses	Increased turbine capacity	Very likely	

Figure 11.2. A sample overview of the "R/O Table" (Molarius et al., 2010).

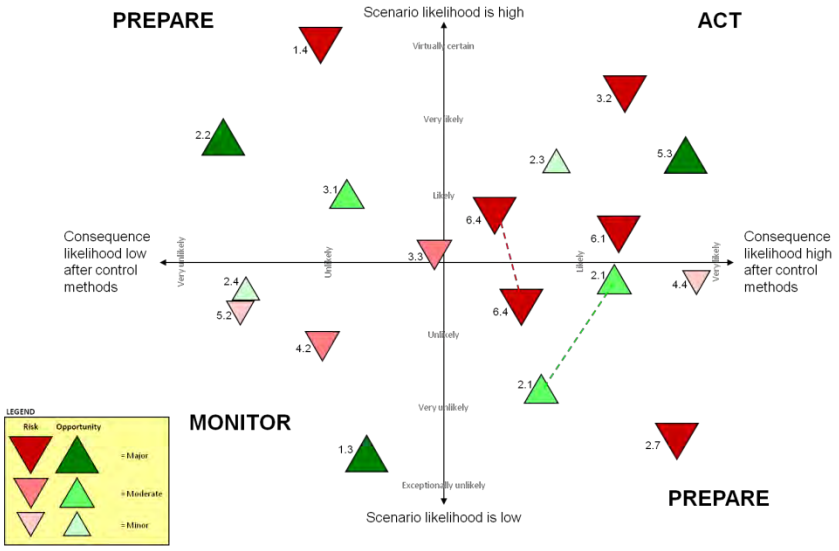

Figure 11.3. The representation in a quadrant diagram helps to prioritise the action plans needed to manage future risks (Keränen et al., 2010).

Finally, the results of the risk/opportunity analysis are represented visually in a quadrant diagram of the kind displayed in Figure 11.3. The symbols (triangles) used in the diagram aim to portray each identified risk or opportunity – "up-pointing" (green) triangles represent opportunities and the "down-pointing red triangles" are associated with risks. The size (and shade of colouring) indicate the strength of the identified issue – with the darker shades signifying they are major issues, down to the lighter shades for the minor issues. The main idea behind the diagram is to provide a readily interpretable overview of the highlighted risks and opportunities in relation to the likelihood of the examined scenarios and the likelihood of the risks and opportunities identified. The different quadrants of the diagram (Act, Prepare and Monitor) provide both an overview of the results and also helps decision-makers to define the significance and order of the action plans made to minimise or promote identified risks and opportunities. With the aid of this visual summary it is also possible to represent the risk analysis results in an effective and balanced way for other stakeholders.

11.3 Risk assessment case studies

The risk assessment framework was tested in six case studies. Four of the case studies were hydropower plants (two in Finland and two in Norway) and two were biomass fired CHP (combined heat and power) plants, one in Finland and one in Sweden (Figure 11.4). After various case study examinations, the improved risk assessment method and its suitability for wind power and distribution network cases was also discussed and estimated. The risk assessment framework was also evaluat-

ed from an economics-emphasised risk assessment viewpoint (Linnerud, 2009a; Linnerud, 2009b).

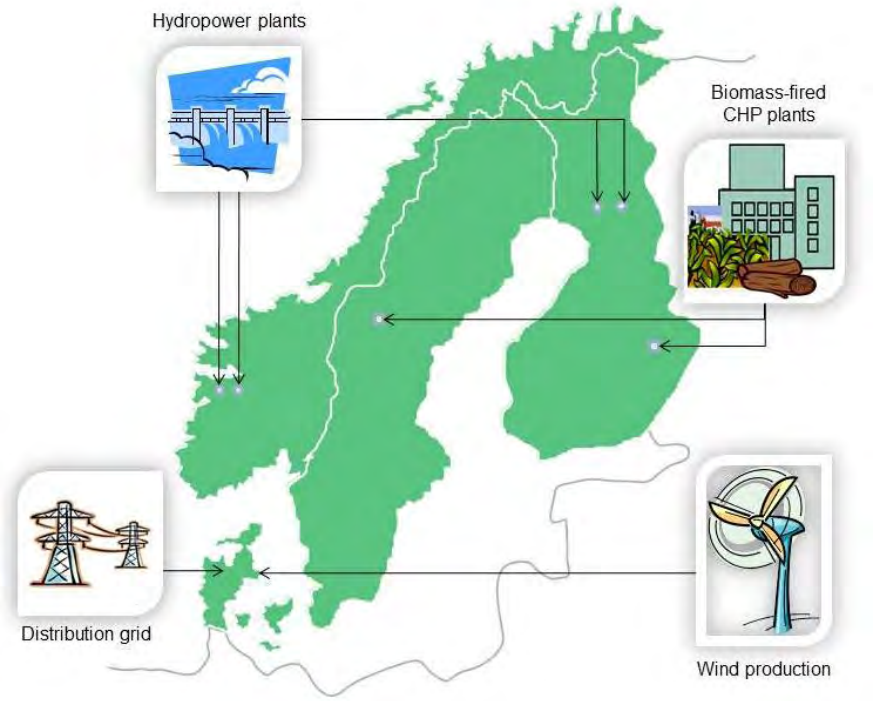

Figure 11.4. The Risk Assessment Framework was developed and applied in various installations in the Nordic countries.

The implementation method was quite similar in each case study examination. Before the risk assessment sessions, the climate change scenarios for the studied power plant operations, together with other background information related to the future circumstances, such as hydrological scenarios for a catchment area, were prepared. At the beginning of the risk assessment session, the gathered meteorological information was introduced and major impacts of future changes were documented as keywords within the seasonal plan. Also the power plant's annual routines, such as maintenance operations, were documented to the seasonal plan. The risk and opportunity identification was carried out during the session and the results were documented to the R/O Table. Identified risks and opportunities were then evaluated and the final results were presented in the quadrant diagram. All suggestions to control or change the identified impacts, that is, to minimise negative risks or maximise possible opportunities, were also documented to the R/O Table.

11.4 Hydropower plants case studies

11.4.1 Finnish case study description

In the Finnish case study two hydropower plants in Northern Finland on the catchment area of Kemijoki, the largest river in Finland, were examined. The catchment area of this 550 km long river is about 51,000 km^2. Although the greatest flood flow was about 5000 m^3s^{-1} (in 1973), the average flow is about 500 m^3 s^{-1}. The twenty hydropower plants along the river produce about 1000 MW, about one tenth of Finland's energy need (Molarius *et al.*, 2008).

The Seitakorva hydropower plant is located by the outlet of the lake Kemijärvi. The lake is regulated by the power plant and the water level of the lake ranges between 142 and 149 metres above sea level according to the regulation guideline. The plant has an installed effect of 130 MW and an average yearly production of 506 GWh.

The Valajaskoski power plant is located 15 km downstream of the city of Rovaniemi in the Kemijoki river basin. Upstream of the Valajaskoski power plant the unregulated river Ounasjoki joins the river Kemijoki which increases the likelihood of the flood in the river basin and also for the city of Rovaniemi. The plant has an installed effect of 101 MW and an average yearly production of 365 GWh.

11.4.2 Scenarios (Finland)

In the Finnish case study, the climate scenarios were based on two global climate models: ECHAM4/OPYC3 and HADAm3H. The hydrological scenarios for the studied catchment area were developed by the FEI's Watershed Simulation and Forecasting System (WSFS). The WSFS is a conceptual hydrological model, used for operational flood forecasting and for research purposes. The system is based on a watershed model, which is originally the HBV (rainfall-runoff) -model, and simulates the hydrological cycle using standard meteorological data. The model simulates the entire land area of Finland (Vehviläinen *et al.*, 2005; Vehviläinen & Huttunen, 1997). The main inputs of the model with regards to the CES-project were the monthly precipitation and temperature data.

The hydrological scenarios represented flow changes during two 40-year periods, the reference period 1961–2000 and future period 2010–2049. The hydrological scenarios utilised in the risk assessment process included the annual average, the minimum and the maximum of incoming flows for the two studied hydropower plants. They also included the annual average, the minimum and the maximum water level stated for the regulated reservoir situated in the catchment area. In addition, the hydrological scenarios also represented six individual great flood years or very dry years, based on the simulated extreme wet or dry period.

Based on climate models and hydrological scenarios, the average temperature will increase, especially during the winter. Precipitation will also increase, together with an increase in autumnal and winter flooding. In the future the actual flow peak is expected to take place earlier in the spring. Extreme weather events, like heavy rain or heavy snow, are also expected to increase (Jylhä *et al.*, 2009).

11.4.3 Risk identification

The experts who participated in the risk assessment sessions were able to draw on a wide range of knowledge about the hydropower companies. For instance, the company experts were responsible for the plant's operational work, real estate, production planning, development work, risk management, environmental issues, water resources, security issues and maintenance of the electricity grid. Hence, it was possible to obtain a comprehensive view of future changes, risks and opportunities.

All three parts of a power plant's functional model (Figure 11.5) were studied. However, the energy source and some units of the power plants were examined in more detail than the distribution network. As the distribution of electricity was not a part of the company's business, only a cursory examination was conducted.

Figure 11.5. The functional model provides an overview of those functions of the examined power plant which are to be taken into account in the risk analysis process (Molarius et al., 2010).

11.4.4 Risk estimation

The risk estimation was carried out with the help of a three-level risk-consequence classification. The actual classification varied in the different case studies and was established and confirmed by the current case-study risk assessment group. The identified risks could be estimated monetarily (associated costs or income) by the power plant company. Depending on the organisation level in which the costs are managed and the associated decision-making is performed, the consequences were divided into minor, moderate and major levels.

11.4.5 Results (Finland)

The hydrological scenarios showed that the effects of climate change can be expected to be rather steady in the studied catchment area of the Finnish case study. Thus, most of the identified risks were also estimated to be minor. The most significant risks, which might require new operational actions, planning and guidelines, were related to the autumn or winter time flooding increase which might mobilise ice flow – the ice could then pack within the dam structures. In the worst case, the ice masses could roll over the dam barriers and the integrity of the dam could thus also be endangered. The regulation operations of reservoir lakes can become more complicated as the wintertime weather circumstances become more unstable. In such cases the reservoir's water level control might in fact require new regulating guidelines. A concern arose with regards to initiating application actions for renewing authority guidelines, as they should consider also the time-consuming regulatory process. Nevertheless, opportunities were also identified. An earlier and longer-lasting spring could not only extend the spring-time flood, but also reduce the anticipated flood peak. It is in fact easier to control hydropower plants in such circumstances, and the company may be able to realise significant economic benefits by reducing the amount of by-pass flow.

11.4.6 Norwegian case study description

The Norwegian case study hydropower plants (Mel and Åskåra I), are located in the county of Sogn and Fjordane in the Western part of Norway. Both power plants draw water from reservoirs and their drainage basins include glaciers. Mel uses water from four reservoirs in Vetlefjordvassdraget. The drainage basin includes part of the glacier Jostedalsbreen. Water from three smaller magazines is transported in tunnels to Nedre Svartevassvatn reservoir which is regulated between 815 and 883 metres above sea level. When there is overflow, the excess water may cause flooding of farmland down in the valley. The installed power of the Mel plant is 52 MW and the average yearly production is 212 GWh (Linnerud, 2009a).

Åskåra I uses water from the reservoir Store Åsgårdsvatn which is regulated between 614 and 697 metres above sea level. The drainage basin includes the glacier Ålfotbeen. The drainage basin is characterised by gravels and smooth rock slopes which quickly leads the water to Store Åsgårdsvatn. Thus, compared with Mel, the reservoir filling will vary more directly with the amount of rain. The installed power of this plant is 116 MW and the average yearly production is 535 GWh (Linnerud, 2009a).

11.4.7 Scenarios (Norway)

In the Norwegian case study, the climate scenario information was mainly based on the results of the REGCLIM research programme, in which

climate change in the Nordic countries was studied. The results are quite similar to those from the Finnish case study, indicating increased temperatures, increased and more intense precipitation, and increased and more intense wind during the scenario period. Snow cover extent and glacier cover are expected to decrease. Overall, there will be changes in the seasonal flood patterns, with increasing occurrence of autumn and winter flooding. (Linnerud, 2009a).

11.4.8 Results (Norway)

The Norwegian study highlighted the following case-specific risks: Generally, more rainfall means increased production for hydropower companies. On the other hand, more volatile weather conditions require changes in optimal seasonal production patterns and may increase the risk of overflow. Extreme rainfall and extreme wind will reduce access to reservoirs and networks and potentially damage installations. If the glaciers disappear or are heavily reduced in volume, the power plant loses reservoir capacity (Linnerud, 2009a).

11.5 Biomass-based CHP plants case studies

11.5.1 Finnish case study description

The biomass-based CHP (combined heat and power) plant, which was the subject of this case study, is located in the southern part of Finland, where it produces heat for the nearby city area and electricity for the national grid. The plant uses various fuel fractions such as peat, wood, logging waste and also small quantities of reed canary grass. The maximum harvesting and transport distance between the power plant and the biomass collection area is about 100 km. The power plant company buys all fuel fractions from subcontractors and does not itself actually own any part of the fuel supply. Oil is needed as an emergency fuel. The volume of different fuel fractions varies from year to year depending on the harvesting conditions, for example. The ratio of peat and wood must, however, be maintained within a specified range in order to prevent corrosion damage to the power plant boiler.

A significant amount of critical infrastructure and other built environment (e.g. hospitals, health centres and elderly people's homes) are connected to the district heating grid, and essential heat energy supply needs to be maintained at all times – especially with respect to the changing future climate.

11.5.2 Scenarios

The goal of the analyses was to examine what kind of changes, threats and opportunities in a CHP power plant's fuel purchase, transport and storage regime, plant operations and energy transmission network might be encountered due to changing climatic conditions. In the Finnish case study, the short-term climate forecasts and long-term climate projections data utilised in the risk assessment process were prepared by FMI (Jylhä *et al.*, 2009). Meteorological data was extracted from the results of the ACCLIM project, which produced results consistent with the CES project climate scenarios results. The ACCLIM data were chosen for this case study because they represented the latest knowledge of climate change affects on the Finnish climate at the time of this study.

The knowledge of biofuels' (e.g. peat, wood, logging waste and reed canary grass) growth, availability and storage aspects, and the expected changes in the future, utilised during the risk assessment session were provided by the forest science experts from the University of Eastern Finland.

Based on the reference climate models, future temperatures will increase. The winter will become shorter and the growing season will lengthen. Precipitation is also expected to increase, although the biomass growth is unable to fully exploit the increased precipitation because of simultaneous increased evaporation. Snow cover will be reduced. Exceptional weather phenomena might increase, but as the statistical uncertainty needs also to be taken into account, accurate predictions for at least the next few decades might be difficult.

11.5.3 Risk identification

The risk identification sessions were carried out by the power plant's representatives, the forest science expert and the risk analysis expert. The seasonal circumstances and their changes in the future were compiled to the seasonal plan, as shown in Figure 11.6. This seasonal plan was then used as a checklist within the brainstorming session.

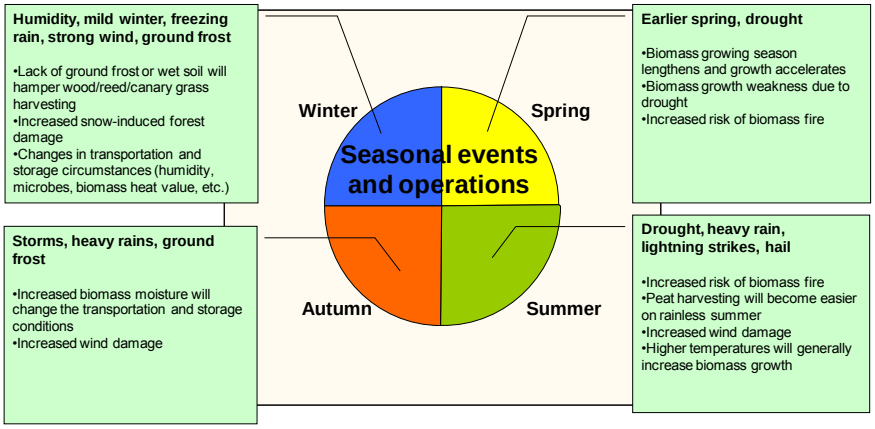

Figure 11.6. The seasonal plan tool is a type of future-oriented tool. It helps portray climate scenario information as keywords according to changing seasonal circumstances.

11.5.4 Risk estimation

In the Finnish case study, the risk/opportunity estimation was done by applying a three-level consequence classification, which was refined during the brainstorming session. The classification was based on the risks' impacts on the power plant's heat energy production and distribution to the clients.

The consequences of the risk were estimated to be minor, if they caused the following disturbances to the energy production or distribution:

- a momentary shortage of heat energy production,
- a lack of domestic hot water, or
- a short-term temperature drop in an apartment

The consequences were estimated to be moderate, if:

- the buildings, which are connected to district heating network, are cooling, or
- normal water-systems' pipe systems cooling poses a freezing risk to the district heating network

The consequences were estimated to be major if:

- the energy transfer is interrupted for at least 1 hour, or
- so-called critical buildings (e.g. hospitals, health clinics, nursing homes, elderly people's homes) need to begin evacuation actions

11.5.5 Results

Increased precipitation can result in the increased moisture content of fuel fractions, which decreases the biomass's fuel heat value and the efficiency of the power plant. On the other hand, increased biomass growth with regard to increased bioenergy potential is considered to be a major opportunity.

In the future, heating demands on district heating areas might decrease due to increasing temperatures, which will result in a need for changes in power plants' combined heat and electricity production. In order to maintain the heat production at the current level, further development of the grid might be needed or new business opportunities might be sought. It is supposed that energy demand estimations will be more difficult to assess, if the amount of extreme weather events increases. Extreme weather events like heavy rain or snow and strong wind already directly disrupt the electricity distribution network (e.g. through fallen trees, etc.). If the maintenance of the district heating grid is facilitated by increased temperatures and reduced ground frost due to presumption of warmer climate, the grid maintenance risks may increase in the future. The identified power plant's operation risks included, for example, shortened operating life of electrical equipment and increased cooling demand due to the expected temperature rise.

Identified risks related to fuel supply included, for example, peat harvesting long-term interruptions because of either a very dry or wet period, difficulties in canary grass or wood-based biomass harvesting as a result of the loss of ground frost, and the increased biomass's moisture content negative influence on storage, transport and combustion processes.

The heat energy users of the public buildings in the district heating network may need to develop adaptation strategies. It is particularly important that the heat energy supply is guaranteed, even in changing climate circumstances. At the same time, the increasing demand for cooling in a warmer climate – especially for maintaining a healthy indoor climate (in e.g. hospitals) – will also need to be considered. Interference-free biomass fuel supply is important, although alternative fuels can be used as emergency fuels. Both the texture of biomass fuel fractions (e.g. possible increased moisture) and circumstances of biomass storages (e.g. moisture increases the number of harmful microbes, and drought increases the risk of fire) may vary as a result of changing climate. To ensure the availability of biofuel purchase, transport and storage it might be necessary to re-examine the storage locations and capacities.

11.5.6 Swedish case study description

The Swedish case study (Gode, 2010) utilised climate scenarios developed by the Rossby Centre, SMHI, commissioned by the Governmental investigation on climate impact and vulnerability. The most relevant climate

parameters, and their change, were deemed to be increased temperature, precipitation and wind. The increasing temperature will most likely result in a decrease in heating demand, an increased cooling demand, and an extended vegetation season and decreased ground frost. Increased precipitation is expected to be expressed by more rain, but less snow. Future changes in wind strength in Sweden are uncertain, but for the purpose of the risk assessment, a moderate increase in wind speed was anticipated.

11.6 Distribution grid case studies

Risks associated with future climate change may place new and greater demands on ensuring the security of the electricity supply in the Nordic countries. The transmission and distribution networks transport electricity from generation units to the end user. These networks stretch to the farthest corners of the Nordic region supplying electricity to consumers and are often exposed to climatic conditions that can seriously affect the supply of electricity from generator to consumer.

11.6.1 Danish case study description

Two Danish distribution companies, SEAS-NVE and NOE tested the risk assessment framework in order to identify the risks for distribution companies in a changing climate and to identify how the tools could be improved for use by the grid companies. Structured interviews were conducted in which the risk management tool was basically applied as a questionnaire; moving through it point by point with the interviewee. Each distribution company was represented by a representative of the senior management with responsibility for making decisions for new investments and operation and maintenance strategies. In addition to the two distribution companies, the Danish Energy Association, the umbrella organisation for Danish grid companies, was consulted for input on the risk assessment framework and climate risks facing the grid companies (James-Smith, 2010).

11.6.2 Scenarios

Danish climate scenarios, provided by DMI, were used in the desktop studies to identify potential climate associated risks. These were supplied to the distribution companies during the interviews as distribution companies do not generally develop climate scenarios of their own.

According to DMI simulations of three climate scenarios for Denmark[3], climate change is expected to result in both rising winter temperatures (2–3°C) and rising summer temperatures (1–3°C). The precipitation amounts will continuously increase in the winter. The frequency and duration of droughts and heat waves are projected to increase in the summer. In the summer, the precipitation will decrease, whereas downpours are expected to become heavier (Jørgensen *et al.*, 2006). In extreme situations of surge, an increase in the maximum sea level (0.45–1.05 m) is estimated. It is also expected that an increase in the average wind velocity (1–4%) will occur. The maximum storm strength is expected to increase both on land and over the ocean (up to 10%).

11.6.3 Risk identification

In these two case studies, a series of risks that may affect distribution networks in the future were identified. Both of the case studies generally showed that distribution networks in Denmark were already well prepared for most of the risks associated with climate change.

In Denmark it is expected that higher levels of precipitation and the increased risk of flooding could be problematic and could increase the risk of disturbances in electricity supply on some level due to water seeping into electrical installations. Both case study organisations had already experienced increased outages due to flooding of distribution boxes, resulting from increased downpours or tidal surges because of stronger storms. Re-establishment of the supply cannot be made before the electrical installations are dried, which typically takes several days. The case studies indicated that adaptation measures are already in place for these issues in the form of elevated distribution boxes in areas prone to flooding. Distribution boxes in areas prone to flooding are being mapped and either replaced or elevated.

In the case studies, increased corrosion of transformers due to salt spray being blown further inland was also identified as a new and serious problem due to changing weather patterns. Some transformer stations in the high voltage systems are vulnerable to flooding, and to reduce the risk, embankments are typically established around the transformer stations. Transformers are also sensitive to higher air temperature and technical lifetime could be reduced if long periods of high temperatures become more common in summer.

The case studies emphasised the significant influence of power generating and consumption patterns in the power grid. Increased deployment of distributed generation, generally in the form of wind turbines, imposes

[3] One of the scenarios is based on the EU objective that the global temperature may not rise more than 2 °C. The other two scenarios are based on IPCC's A2 and B2 emissions scenarios (IPCC, 2007).

increased pressure on existing infrastructure. Both case studies concluded that distribution grids were no longer dimensioned according to demand, but rather to production from distributed generation. The case studies underlined the sensitivity to changes in wind power production, since the number of wind turbines is one of the most important factors for dimensioning the power grid. Increasing wind speeds, the occurrence of stronger, more frequent storms and further expansion of wind turbine deployment could place more pressure on existing infrastructure. This is especially relevant in winter and during the months in autumn and spring when maintenance is usually carried out, because the capacity of the grid is reduced when maintenance occurs. Both cases also identified climate policy to be a concern for distribution companies. For historical reasons, the grid in Denmark is not dimensioned at the lowest level to supply households with electricity for heating purposes. If demand for electric heating and electric cars were to increase, new investments would most likely be necessary. A rapidly increasing demand for electricity amongst households, as well as the deployment of more wind turbines, poses a risk when dimensioning distribution grids in the future.

11.6.4 Risk estimation

Technical and economic changes in the form of increased energy demand and increased levels of wind power are expected to have a much larger impact on distribution networks in Denmark than will changes in climate patterns. Both case studies identified climate policy and policy induced changes to be a significant risk factor in power generation and consumption patterns. Moreover, with regards to the wind power itself, only a small part of the foreseen increase in energy demand and supply of wind power is expected to be directly attributable to climate change.

11.6.5 Results

The distribution networks in Denmark are already well prepared for most of the physical risks presented by the changing climate. Most of the overhead lines have been replaced by underground cables, which greatly reduces many weather related risks. Currently, about 90% of the electrical distribution lines (up to 20 kV) are cable laid, and within 10 years it is expected that cables will have replaced all overhead lines sensitive to storms.

The high voltage transmission lines are largely overhead lines, and they are already dimensioned to withstand increased storm strength and precipitation. The transmission system also has a high level of redundancy, which allows electricity to be rerouted if a transmission line is damaged. An increasing risk associated with the replacement of overhead transmissions lines by underground cables, however, is typically highlighted in cases of flooding and drought in relation to

the fact that high voltage cables need to be able to divert heat to the surrounding soil. If the ability of the soil to absorb heat is reduced by drought or flood, the transmission cable may not be able to function at full capacity or at all.

Some technical risks associated with water seeping into the distribution boxes and salt corrosion of transformers were identified. A major concern for distribution companies appears to be climate policy that influences the demand patterns and the levels of distributed generation on distribution grids – increasing the risk for both under- or over-dimensioning current grid extensions and reinforcements, and making investments in future transmission and distribution infrastructure a significant challenge.

11.7 Discussion and conclusions

According to the series of case studies, the implementation of the risk assessment framework provides useful discussion and insightful opinions about forthcoming changes and circumstances for which the power plants need to be prepared. The developed method is valuable for the companies to study the upcoming phenomena and trends and furthermore evaluate the order and intensity of action plans needed.

One of the most challenging issues for users is the need to ensure that necessary information is available from climate scenarios and environmental models, like hydrology models and snow and ice models, etc. for the risk assessment process. As expert knowledge and data was available from the other groups of the CES-project, this was not an especially significant issue for the case studies. However, it was nevertheless also observed that the climate and environmental information needs to be sufficiently clear in order to ensure that misunderstandings are avoided. Expert participation is not always possible during the risk analysis process and thus the information needs to be readily available for utilisation and analysis by non-experts.

The case studies highlighted the value of the seasonal plan tool. As climate phenomena are strongly seasonal by their nature, it is valuable to have a visual summary of occurring phenomena listed by seasons. The seasonal plan supports the analyses of changes in climate and power plant operations during the year and provides shared knowledge for the risk and opportunity identification.

Another developed tool which was identified as being extremely valuable was the quadrant diagram, which manages to show at a glance the results of the risk analysis process. It does not show any detailed information about the identified risks or opportunities, but instead not only shows the estimated magnitude of every identified risk/opportunity, but also classifies the urgency of any suitable actions for each specific risk/opportunity and thus supports their pri-

oritisation in associated action and adaptation plans. The diagram is especially useful for representing the risk analysis results to decision makers or other stakeholders in an efficient and compact way.

Both risks and opportunities were identified in the case studies. In the hydropower cases in Finland, increased production due to moderate flow growth and longer-term springtime flow was identified as a major opportunity. Identified risks included, for instance, an increase in autumn or wintertime flow which might mobilise ice flow. In the worst case, the ice masses could create hazardous situations and endanger the safety and integrity of dams. In Norway the hydropower production was estimated to be more profitable due to increased rainfall. On the other hand, the risk of overflow might also increase and, for instance, various network installations may become more vulnerable. Biomass-based CHP plants were estimated to benefit from a longer growing season and a subsequent increase in biomass growth. In the future, heating demands on district heating areas could be expected to decrease due to higher temperatures, which will in turn necessitate changes in the power plants' heat and electricity production. In Denmark, the case study showed that the Danish networks are reasonably well prepared for the physical risks presented by climate change. A majority of the electrical distribution lines are now underground cable lines, which greatly reduces the vulnerability to weather related risks. Although a significant portion of the risks and opportunities were identified based on examined scenarios, climate change as a phenomenon is exceedingly uncertain and it would be difficult to claim that all the risks and opportunities associated with climate change had been identified.

The usability of the developed risk assessment method could be further improved by enhancing the financial risk dimension in the process. In her study Linnerud (Linnerud, 2009a) highlighted the risk definition of Modern Portfolio theory and the Capital Asset Pricing Model. According to the Capital Asset Pricing Model theory, the risk of the investment is measured as the investment's contribution to the standard deviation of a well diversified portfolio. Thus, investments which tend to be strongly pro-cyclical are seen as risky, while investments which tend to be weakly related to the changes in the rest of the economy are seen as less risky. Since, for instance, hydro companies may be positively affected by the changing climate, the economy as a whole may lose, as the risk of investing in the power sector may be seen as small or even negative.

Energy conversion and future energy decisions are complex issues in which many different viewpoints need to be considered, and it is not only the actual climate change that is demanding the attention of decision makers. For instance, biomass based CHP plants need to adjust their fuel supply and operations according to political decisions of the government's financial support and tax definition policy.

And last but not least, for CHP plants the future energy demand depends not only on climate conditions but also to a great extent on energy efficiency improvement implementation, population growth, and the customer's choice of heating systems, amongst a raft of other issues. Therefore, any analysis of future CHP demand must also attempt to take those factors into account.

11.8 Acknowledgments

The risk assessment working group is grateful for the valuable contributions from case study participants – especially with regards to the associated feedback to the development of the risk assessment framework. Climate scenario data and modelling expertise and knowledge from the respective Nordic meteorological and environmental institutes was also very much appreciated.

11.9 References

Dougherty, T.M. (1999). Risk Assessment Techniques. In: *Handbook of Occupational Safety and Health.* Second Edition, L. Diberardinis, ed., John Wiley and Sons, Chapter 6, 127–178.

Gode, J. (2010). Test and evaluation of a risk/opportunity assessment procedure – Case study of a Swedish biomass fired CHP plant. IVL Rapport B1948. Swedish Environmental Research Institute.

Heikkilä, A.-M., Murtonen, M., Nissilä, M., Rouhiainen, V. (2009). Quality of risk assessment and its implementation. In V. Rouhiainen, ed., *Scientific activities in Safety & Security*. VTT Technical Research Centre, Espoo, Finland, 66–67.

IEC 60300-3-9 (2000). Dependability management. Part 3: Application guide. Section 9: Risk analysis of technological systems. Finnish Electrotechnical Standards Association.

IPCC (2007). Climate Change 2007: Synthesis Report. An Assessment of the Intergovernmental Panel on Climate Change.

James-Smith, E. (2010). Using the CES risk assessment framework in the distribution sector. *Conference on Future Climate and Renewable Energy: Impacts, Risks and Adaptation.* Oslo. Norwegian Water Resources and Energy Directorate. pp.58–59.

Jørgensen, A., Christensen, O., May, W. (2006). Klimascenarier for Danmark. Danish Meteorological Institute. Copenhagen.

Jylhä, K., Ruosteenoja, K., Räisänen, J., Venäläinen, A., Tuomenvirta, H., Ruokolainen, L., Saku, S., Setola, T. (2009). The changing climate in Finland: estimates for adaptation studies. ACCLIM project report 2009. Finnish Meteorological Institute. Reports 2009:4. ISBN 978-951-697-700-6 (pdf). (*in Finnish – Abstract, extended abstract and captions for figures and tables also in English).*

Keränen, J., Kilpelainen, A., Gode, J., Molarius, R., Schabel, J. (2010). Case study – using the CES risk assessment framework in the biomass and wind power sectors. Conference on Future Climate and Renewable Energy: Impacts, Risks and Adaptation. Oslo: Norwegian Water Resources and Energy Directorate. pp.60–61.

Langley, A. (1989). In search of rationality: The purposes behind the use of formal analysis in organisations. *Administrative Science Quarterly*, 34 (4), 598–631.

Linnerud, K. (2009a). Test and evaluation of a climate risk assessment procedure. Case study: The Norwegian hydro power company SFE. CICERO, University of Oslo. Report 2009:3. Feb.2009. 44 p. ISSN:0804-4562.

Linnerud, K. (2009b). How to improve the risk assessment procedure to better reflect a financial perspective to risk. CICERO. 11 p. (*project internal report*)

Molarius, R., Wessberg, N., Keränen, J., Schabel, J. (2008). Creating a climate change risk assessment procedure – Hydropower plant case, Finland. XXV Nordic Hydrological Conference – Northern Hydrology and its Global Role (NHC-2008) Reykjavík, Iceland. 11–13 August 2008.

Molarius, R., Keränen, J., Schabel, J., Wessberg, N. (2010). Creating a climate change risk assessment procedure: Hydropower plant case, Finland. *Hydrology Research* 41 (3–4) 282–294.

Vehviläinen, B. and Huttunen, M. (1997). Climate change and water resources in Finland. *Boreal Environ. Res.,* 2, 3–18.

Vehviläinen, B., Huttunen, M. Huttunen, I. (2005). Hydrological forecasting and real time monitoring in Finland: the watershed simulation and forecasting system (WSFS). In*: Innovation, Advances and Implementation of Flood Forecasting Technology*, Conference Papers, Tromsø, Norway, 17–19 October 2005.

Appendix 1

The Climate System: A 2011 update

The coverage in this section is partly based on a Nordic report written by Rummukainen *et al.* (2010), who reviewed advances in studies of the physical climate system since the publication of the IPCC Fourth Assessment Report, AR4 (IPCC, 2007). Updates based on data and information presented on the webpages of key climate data centers are included as well.

A1.1 Greenhouse gas concentrations

Ranked by their contribution to the terrestrial greenhouse effect, the following greenhouse gases are the most important: Water vapour (H_2O) contributes 36–72%, carbon dioxide (CO_2) 9–26%, methane (CH_4) 4–9% and ozone (O_3) 3–7% (Kiehl *et al.*, 1997). The range in contributions reflects absorption overlaps between gases at particular radiation frequencies and indirect radiative effects that have not been fully quantified (Isaksen *et al.*, 2011). Current concentrations of major greenhouse gases (2010 values, excluding H_2O), changes since the pre-industrial era and the corresponding increased radiative forcing are given in Table A1. Trends in CO_2, CH_4, N_2O and CFCs are shown in Figure A1.

Figure A1 displays globally averaged data showing changes in greenhouse gases since 1979. The CO_2 concentration continues to increase, with a growth rate of 1.94 ppm/year after 1995 (as compared with 1.43 ppm/year before 1995). The growth rate of methane declined from 1983 until 1999 and the CH_4 burden was nearly constant from 1999 to 2006, but has continued to increase since 2007. Warm temperatures in the Arctic in 2007 and increased precipitation in the tropics in 2007 and 2008 are believed to cause the recent increase (Dlugokencky *et al.*, 2009). Nitrous oxide continues to increase at a relatively uniform growth rate, while radiative forcing from the sum of observed CFC changes ceased increasing in about 2000 and is now declining (Montzka *et al.*, 2011).

Table A1. Current and pre-industrial concentrations of the most important greenhouse gases[*] and their contributions to changes in the radiative balance of the atmosphere[**].

GAS	Pre-1750 tropospheric concentration	Recent tropospheric concentration	% increase since 1750	Increased radiative forcing (W/m^2)
Carbon dioxide (CO_2)	280 ppm	388.5 ppm	35%	1.76
Methane (CH_4)	700 ppb	1870/1748 ppb	260%	0.50
Nitrous oxide (N_2O)	270 ppb	323/322 ppb	30%	0.17
Tropospheric ozone (O_3)	25 ppb	34 ppb	36%	0.35
CFC-11 (CCl_3F)	0	241/239 ppt	–	0.063
CFC-12 (CCl_2F_2)	0	534/532 ppt	—	0.17

[*] Source: Carbon Dioxide Information Analysis Center, http://cdiac.ornl.gov/pns/current_ghg.html and references given there. The recent CO_2 concentration (388.5 ppm) is the 2010 average taken from globally averaged marine surface data given by the US National Oceanic and Atmospheric Administration Earth System Research Laboratory, web site: http://www.esrl.noaa.gov/gmd/ccgg/trends/index.html#global. For methane, nitrous oxide and the CFCs, the first value in a cell represents Mace Head, Ireland, a mid-latitude Northern-Hemisphere site, and the second value represents Cape Grim, Tasmania, a mid-latitude Southern-Hemisphere site. Recent values given for these gases are annual arithmetic averages based on monthly background concentrations for October 2009 through September 2010. [ppm = parts per million; ppb = parts per billion; ppt = parts per trillion].

[**] Changes (since 1750) in radiative forcing represent changes in the rate per square meter, at which energy is supplied to the atmosphere below the stratosphere.

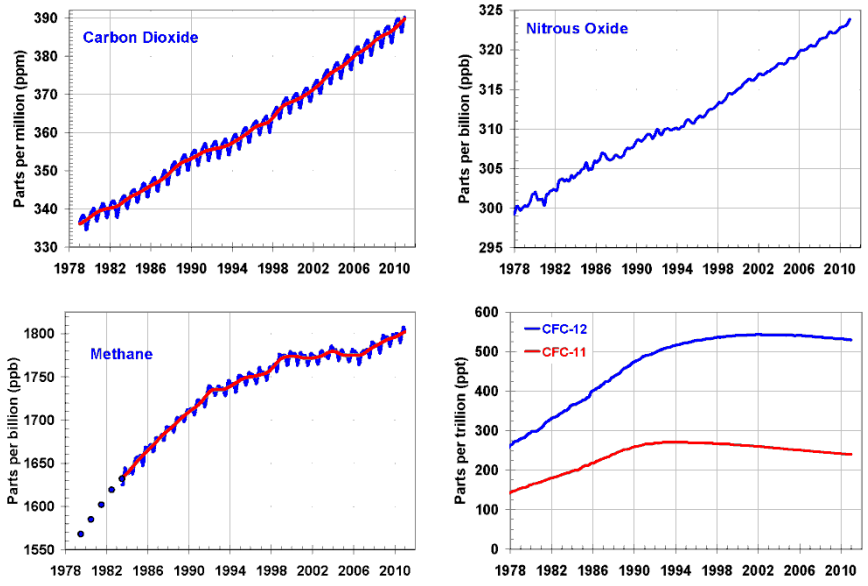

Figure A1. Global average abundances of the greenhouse gases carbon dioxide, methane, nitrous oxide, CFC-12 and CFC-11. Data from the NOAA global air sampling network since the beginning of 1979. These gases account for about 96% of the direct radiative forcing by long-lived greenhouse gases since 1750. Source: http://www.esrl.noaa.gov/gmd/aggi/

A1.2 Atmospheric warming

The global warming trend that commenced in the mid-1970s slowed after 2005, but 2010 was equal third warmest year on record (with 2003), exceeded only by 1998 and 2005. According to data prepared by the Climate Research Unit (CRU), University of East Anglia, the period 2001–2010 was 0.44°C above 1961–90 mean and 0.20°C warmer than the 1991–2000 decade. After 1998, the next nine warmest years in the global instrumental temperature series are all in the decade 2001–2010, with 2008 being the sole exception (Brohan et al., 2006 – with updates to the data set until 2010, see link in caption to Figure A2).

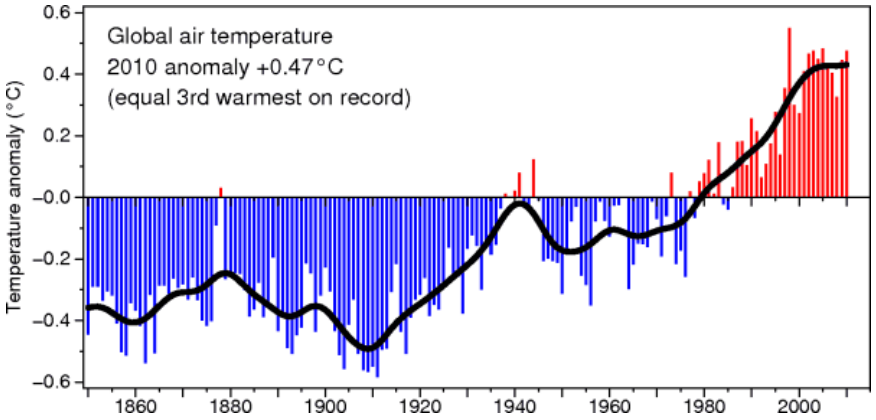

Figure A1.2. The combined global land and marine surface temperature record from 1850 to 2010. Source: Climate Research Unit, University of East Anglia, UK. http://www.cru.uea.ac.uk/cru/info/warming/

A1.3 Sea-level changes

Mean sea-level rose by 17 cm during the 20th century and satellite altimetry data showed a steady sea-level rise averaging 3.2 mm/year from the early 1990s until 2009. A 6 mm drop in sea level in 2010 has been attributed to intensified continental rainfall across the globe, resulting from a strong Pacific El Nino/La Niña shift during that year. The Multivariate ENSO Index reversed again in 2011 and mean sea level is expected to start rising again in the wake of this reversal (see http://www.jpl.nasa.gov/news/news.cfm?release=2011-262).

In IPCC's 4th Assessment Report, projections of sea level change from 1990 to 2095 spanned the range 0.18–0.59 m, depending on the emission scenario. Thermal expansion of sea water would be expected to account for 70–75% of this rise (IPCC, 2007). These results did not take into account a rapid increase in the discharge of ice from ice sheets, which had then been observed in many outlet glaciers in Greenland. A

recent review concluded that "global sea level rise could significantly exceed 1 m by 2100" (Overpeck and Weiss, 2009).

A1.4 Glaciers and ice sheets

Significant advances have been made since AR4 in estimating mass changes in the ice sheets in Antarctica and Greenland. In AR4, altimetry measurements were reviewed both from Greenland and Antarctica. The results indicate thinning due to increased melting on the margins of the ice sheets, but also of thickening in the interior due to increased accumulation. Results from the GRACE satellite mission indicate that the Greenland Ice Sheet has lost 230±30 Gt of ice per year in the period 2002–2009 and Antarctica 143±73 Gt ice per year (Wouters *et al.*, 2008; Velicogna, 2009). These ice losses correspond to 1.1±0.2 mm/year of the global mean sea level rise in the period. Acceleration in the velocity of outlet glaciers in Greenland was discussed in AR4. Later research has documented the extent of this phenomenon (Stearns and Hamilton, 2007) and a connection to warming sea waters has also been implicated (Holland *et al.*, 2008).

A new comprehensive survey of cryospheric changes in the Arctic reveals that nearly all glaciers and ice caps in the Arctic have shrunk over the past 100 years. The rate of ice loss increased over the past decade in most regions. Total loss of ice from glaciers and smaller ice caps in the Arctic probably exceeded 150 Gt per year in the past decade, which is comparable in magnitude to the estimated amount lost from the Greenland Ice Sheet (SWIPA, 2011).

A1.5 Sea-ice conditions

Data issued in October 2011 indicate that this year's minimum in sea-ice extent was the second lowest in the satellite record, which started in 1979. The average minimum sea-ice extent over the period 1979–2010 was $6.29*10^6$ km^2, whereas the preliminary 2011 value was $4.33*10^6$ km^2. The record low in 2007 was marked by a combination of weather conditions that favored ice loss (clearer skies, wind patterns, warm temperatures), whereas more typical weather patterns have been observed in 2011 along with continued warmth over the Arctic. This supports the idea that the Arctic sea ice cover is continuing to thin.

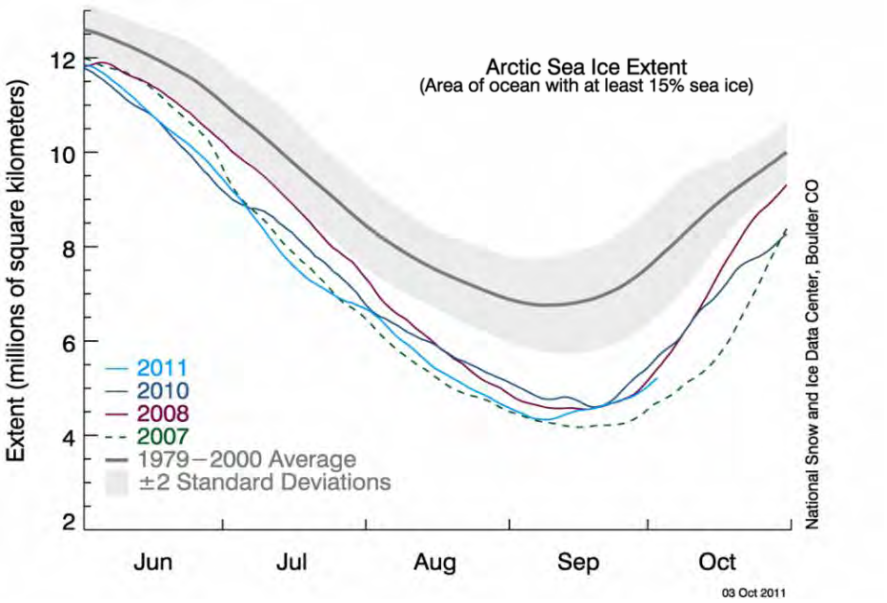

Figure A1.3. Daily Arctic sea ice extent as of September 13, 2011, along with daily ice extents for the previous three lowest years for the minimum ice extent. The 2011 minimum in sea-ice extent is only slightly higher than the record minimum in 2007.

Source: http://www.nsidc.org/arcticseaicenews/

A1.6 Arctic amplification

Serreze *et al.* (2009) presented evidence that surface-based Arctic amplification of global warming has been occurring within the last decade. Satellite-derived summer sea-surface temperatures over the Arctic Ocean (Steele *et al.*, 2008) indicated substantial warming over areas from which sea-ice cover had retreated. Moreover, it was found that recent autumn warming, which also affects the overlying atmosphere, is stronger in the Arctic than in lower latitudes. The effects of Arctic amplification on the atmospheric circulation are not well understood, but the loss of sea ice cover may lead to changes in storm tracks and rainfall patterns over Europe or the American West. Analysing the effects of Arctic amplification on the terrestrial Arctic snowpack, Ghatak *et al.* (2010) found a correlation between increasing snow cover over Siberia during fall and early winter and decreasing September Arctic sea ice over the Pacific sector. Research on Arctic amplification has recently been reviewed by Serreze and Barry (2011).

A1.7 References

Brohan, P., Kennedy, J.J., Harris, I., Tett, S.F.B., Jones, P.D. (2006). Uncertainty estimates in regional and global observed temperature changes: a new dataset from 1850. *J. Geophys. Res.,* 111, D12106, doi:10.1029/2005JD006548.

Dlugokencky, E.J., Bruhwiler, L., White, J.W.C., Emmons, L.K., Novelli, P.C., Montzka, S.A., Masarie, K.A., Lang, P.M., Crotwell, A.M., Miller, J.B., Gatti, L.V. (2009). Observational constraints on recent increases in the atmospheric CH_4 burden. *Geophys. Res. Lett.*, 36, L18803, doi:10.1029/2009GL039780.

Ghatak, D., Frei, A., Gong, G., Stroeve, J., Robinson, D. (2010). On the emergence of an Arctic amplification signal in terrestrial Arctic snow extent, *J. Geophys. Res.*, 115, D24105, doi:10.1029/2010JD014007.

Holland, D.M., Thomas, R.H., de Young, B., Ribergaard, M.H., Lyberth, B. (2008). Acceleration of Jakobshavn Isbræ triggered by warm subsurface ocean waters. *Nature Geoscience*, 1, 659–664, doi:10.1038/ngeo316.

Isaksen, I.S.A., Gauss, M., Myhre, G., Katey, M., Anthony, W., Ruppel, C. (2011). Strong atmospheric chemistry feedback to climate warming from Arctic methane emissions. *Global Biogeochemical Cycles*, 25 (2). doi:10.1029/2010GB003845.

Kiehl, J.T. and Trenberth, K.E. (1997). Earth's Annual Global Mean Energy Budget. *Bull. Am. Met. Soc.,* 78 (2), 197–208.

Montzka, S. A., Dlugokencky, E. J., Butler, J. H. (2011). Non-CO_2 greenhouse gases and climate change. *Nature*, 476, 43–50.

Overpeck, J.T and Weiss, J.L. (2009). Projections of future sea level becoming more dire. *Proc. Natl. Acad. Sci.*, 106, 21461–21462. doi:101073/pnas.0912878107.

Rummukainen, M., Raisainen, J., Björnsson, H., Christensen, J.C. (2010). *Physical Climate Science since IPCC AR4*. TemaNord 2010:549. Nordic Council of Ministers, Copenhagen 2010. 88 pp.

Serreze, M.C., Barrett, A.P., Stroeve, J.C., Kindig, D.N. , Holland, M.M. (2009). The emergence of surface-based Arctic amplification. *The Cryosphere*, 3, 11–19, 2009.

Serreze, M.C. and Barry, R. (2011). Processes and impacts of Arctic amplification: A research synthesis. *Global and Planetary Change*, 77, 85–96.

Stearns, L.A. and Hamilton, G.S. (2007). Rapid volume loss from two East Greenland outlet glaciers quantified using repeat stereo satellite imagery. *Geophys. Res. Lett.*, 34, L05503. doi:10.1029/2006GL028982.

Steele, M., Ermold, W., Zhang, J. (2008). Arctic Ocean Surface Warming Trends Over the Past 100 Years. *Geophys. Res. Lett.,* 35, L02614, doi:10.1029/2007GL031651.

SWIPA (2011). *Snow, Water, Ice and Permafrost in the Arctic*. Executive Summary of Assessment Report. 16 pp. Available at: http://www.amap.no/swipa/

Velicogna, I. (2009). Increasing rates of ice mass loss from the Greenland and Antarctic ice sheets revealed by GRACE. *Geophys. Res. Lett.*, 36, L19503.

Wouters, B., Chambers, D., Schrama, E.J.O. (2008). GRACE observes small-scale mass loss in Greenland. *Geophys. Res. Lett.*, 35, L20501. Doi:10.1029/2008GL034816

Appendix 2

Project participants

Scientists who contributed to the material published in this book are listed below. Information on additional contributors to the CES project can be found on the CES webpage at http://en.vedur.is/ces and in Pikkarainen (2010) – see reference list at the end of Chapter 1.

Co-workers in the Information Management Working Group (Chapters 1 and 2 & editorial group)

Árni Snorrason (Project Manager), Icelandic Meteorological Office (IMO)
Halldór Björnsson, IMO
Jórunn Harðardóttir, IMO
Stefanía G. Halldórsdóttir, HugurAx Software Solutions
Tómas Jóhannesson, IMO
Thorsteinn Thorsteinsson, IMO

Co-workers in the Climate Scenarios Working Group (Chapter 3)

Erik Kjellström (Principal investigator), Rossby Centre of the Swedish Meteorological and Hydrological Institute
Jouni Räisänen, University of Helsinki
Torill Engen-Skaugen, Norwegian Meteorological Institute
Ólafur Rögnvaldsson, Institute for Meteorological Research
Hálfdán Ágústsson, Institute for Meteorological Research
Haraldur Ólafsson, University of Iceland; Icelandic Meteorological Office
Nikolai Nawri, Icelandic Meteorological Office
Halldór Björnsson, Icelandic Meteorological Office
Jussi Ylhäisi, University of Helsinki
Hanna Tietäväinen, Finnish Meteorological Institute
Hilppa Gregow, Finnish Meteorological Institute
Kirsti Jylhä, Finnish Meteorological Institute
Kimmo Ruosteenoja, Finnish Meteorological Institute
Igor Shkolnik, Voeikov Main Geophysical Observatory, St. Petersburg
Sergey Efimov, Voeikov Main Geophysical Observatory, St. Petersburg
Pauli Jokinen, Finnish Meteorological Institute
Rasmus Benestad, Norwegian Meteorological Institute
Martin Drews, Danish Meteorological Institute
Jens Hesselbjerg Christensen, Danish Meteorological Institute

Co-workers in the Statistical Analysis Working Group (Chapter 4)

Deborah Lawrence (Principal investigator), Norwegian Water Resources and Energy Directorate
Rebecca Barthelmie, Indiana University; Risø DTU National Laboratory for Sustainable Energy
Philippe Crochet, Icelandic Meteorological Office
Göran Lindström, Swedish Meteorological and Hydrological Institute
Tatjana Kolcova, Latvian Environment, Geology and Meteorology Centre
Jurate Kriauciunienè, Lithuanian Energy Institute
Søren Larsen, National Environmental Research Institute, Denmark
Sara Pryor, Indiana University; Risø DTU National Laboratory for Sustainable Energy
Alvina Reihan, Tallinn University of Technology
Lars A. Roald, Norwegian Water Resources and Energy Directorate
Hanna Tietäväinen, Finnish Meteorological Institute
Donna Wilson, Norwegian Water Resources and Energy Directorate

Co-workers in the Hydropower - Snow and Ice Working Group (Chapter 5)

Tómas Jóhannesson (Principal investigator), Icelandic Meteorological Office
Guðfinna Aðalgeirsdóttir, Danish Climate Centre, Danish Meteorological Institute
Andreas Ahlstrøm, Geological Survey of Denmark and Greenland (GEUS)
Liss M. Andreassen, Norwegian Water Resources and Energy Directorate
Stein Beldring, Norwegian Water Resources and Energy Directorate
Helgi Björnsson, Institute of Earth Sciences, University of Iceland
Philippe Crochet, Icelandic Meteorological Office
Bergur Einarsson, Icelandic Meteorological Office
Hallgeir Elvehøy, Norwegian Water Resources and Energy Directorate
Sverrir Guðmundsson, Institute of Earth Sciences, University of Iceland
Regine Hock, Uppsala University; University of Alaska
Horst Machguth, Geological Survey of Denmark and Greenland (GEUS)
Kjetil Melvold, Norwegian Water Resources and Energy Directorate
Finnur Pálsson, Institute of Earth Sciences, University of Iceland
Valentina Radić, University of British Columbia
Oddur Sigurðsson, Icelandic Meteorological Office
Thorsteinn Thorsteinsson, Icelandic Meteorological Office

Co-workers in the Hydropower - Hydrology Working Group (Chapter 6)

Sten Bergström (Principal investigator), Swedish Meteorological and Hydrological Institute
Johan Andréasson, Swedish Meteorological and Hydrological Institute
Noora Veijalainen, Finnish Environment Institute
Bertel Vehviläinen, Finnish Environment Institute
Bergur Einarsson, Icelandic Meteorological Office
Sveinbjörn Jónsson, Icelandic Meteorological Office
Liga Kurpniece, Latvian Environment, Geology and Meteorology Centre
Jurate Kriaučiūnienė, Lithuanian Energy Institute
Diana Meilutytė-Barauskienė, Lithuanian Energy Institute
Stein Beldring, Norwegian Water Resources and Energy Directorate
Deborah Lawrence, Norwegian Water Resources and Energy Directorate
Lars A. Roald, Norwegian Water Resources and Energy Directorate

Co-workers in the Wind Power Working Group (Chapter 7)

Niels-Erik Clausen (Principal investigator), Risø DTU National Laboratory for Sustainable Energy
Xiaoli Guo Larsén, Risø DTU National Laboratory for Sustainable Energy
Sara C. Pryor, Indiana University; Risø DTU National Laboratory for Sustainable Energy
Martin Drews, Danish Meteorological Institute

Co-workers in the Bio-fuels Working Group (Chapter 8)

Seppo Kellomäki (Principal investigator), University of Eastern Finland
Ashraful Alam, University of Eastern Finland
Antti Kilpeläinen, University of Eastern Finland

Co-workers in the Energy Systems Analysis Working Group (Chapters 9 and 10)

Birger Mo (Principal investigator), SINTEF Energy Research
Joar Styve, SINTEF Energy Research, Norway
Ove Wolfgang, SINTEF Energy Research
Óli Grétar Blöndal Sveinsson, Landsvirkjun (National Power Company), Iceland
Úlfar Linnet, Landsvirkjun
Elías B. Elíasson, Landsvirkjun

Co-workers in the Risk Analysis Working Group (Chapter 11)

Jaana Keränen, VTT Technical Research Centre of Finland
Riitta Molarius, VTT Technical Research Centre of Finland
Jari Schabel (Principal investigator), VTT Technical Research Centre of Finland
Jenny Gode, IVL Swedish Environmental Research Institute
Edward James-Smith, Ea Energy Analyses, Copenhagen
Noora Veijalainen, Finnish Environment Institute
Kirsti Jylhä, Finnish Meteorological Institute

Nordic Council of Ministers

Ved Stranden 18
DK-1061 København K
www.norden.org

Climate Change and Energy Systems

Impacts, Risks and Adaptation in the Nordic and Baltic countries

Renewable energy sources contribute 16% of the global energy consumption and most nations are working to increase the share of renewables in their total energy budget, to reduce the dependence on fossil fuel sources. Most Nordic and Baltic countries have already surpassed the target set for EU countries by 2020, to produce 20% of energy use from renewables like hydropower, solar energy, wind power, bio-energy, ocean power and geothermal energy.

This publication presents results from a comprehensive research project that investigated the effects of projected future climate change on hydropower, wind power and bioenergy in the Nordic and Baltic countries, with focus on the period 2020–2050.

The research group investigated historical climate, runoff and forest growth data and produced climate scenarios for the region based on global circulation models. The scenarios were used as input in models forecasting changes in glacial meltwater production, basin-wide runoff, mean wind strength, extreme storm and flooding events and energy biomass production.

Although the uncertainty in modelling results translates into increased risks for decision-making within the energy sector, the projected climate change is predicted to have a largely positive impact on energy production levels in the region, and energy systems modelling projects increased export of energy to continental Europe by 2020.

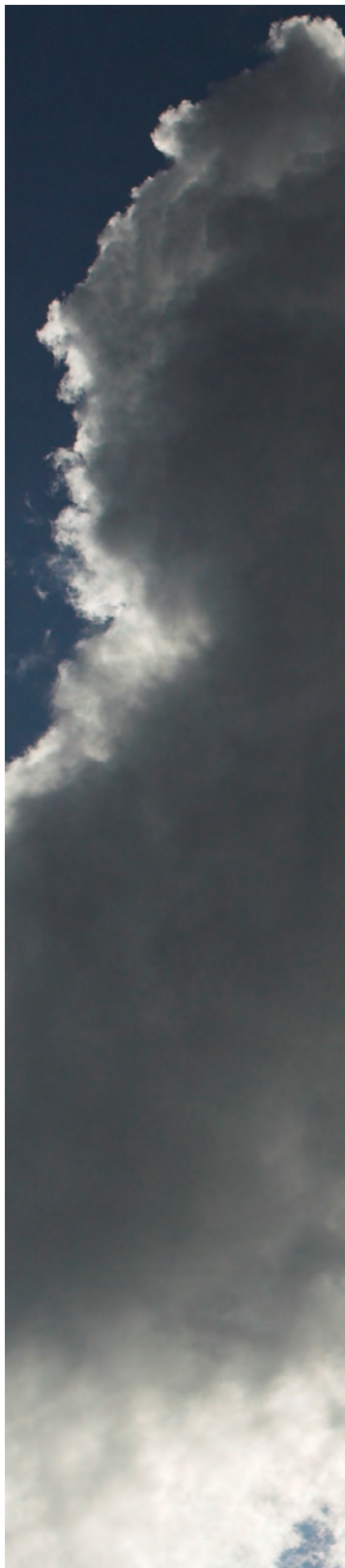

TemaNord 2011:502
ISBN 978-92-893-2190-7